ENGINEERING GEOLOGY AND GEOTECHNICAL INVESTIGATION OF HIGHWALL STABILITY OF THE PROPOSED CYPRESS OPENCAST MINE MT WILLIAM FAULT ZONE, CYPRESS NORTH BLOCK UPPER WAIMANGAROA

A thesis
Submitted in partial fulfilment
Of the requirements for the degree of
Master of Science in Engineering Geology
University of Canterbury
By

Te Ngere Russell Pehi

Department of Geological Sciences
University of Canterbury, Christchurch, New Zealand

June 2004

Frontispiece.

Frontispiece: Turmoil in the skies over Westport.

Abstract

The objective of this thesis was to develop a comprehensive understanding of the geotechnical nature of the proposed Cypress North Block Opencast Coalmine highwall in the Mt William Range east of present mine operations at Stockton Opencast. An investigation was undertaken to gather information on the rock material and rock mass properties of the Basement, Brunner Coal Measures, and Kaiata Mudstone stratigraphic units that would make up the composition of the proposed highwall. The specific aims of the thesis were to identify the distribution of rock types and the locations and orientations of mappable defects such as faults, joints, shears, and crush zones. The stratigraphic units are subdivided into their respective geotechnical units based on physical, and mechanical intact rock material parameters.

The basement lithologies comprised of interfingered layers of Greenland Group metasediments and intrusive Berlins Porphyry granite/granodiorite. These were divided into 3 geotechnical units where analyses of the rock parameters were determined. These units (Berlins Porphyry, Greenland Group hornfels, & mixed basement) returned mean values of low porosity (n= 0.8-2.3%), and slake durability index results (I_{d2} =99.0-99.6% retained), and high friction angles (40.6-44.5º), dry densities (2657-2666Kg/m^3), and moderate UCS (78.8 -136.6MPa), tensile splitting strength (5.1 - 6.2 MPa), and cohesion values (6.38MPa).

The Brunner Coal Measures are an alternating sedimentary sequence of massive sandstones, laminated sandstones, siltstones, mudstones, and coal that were divided into 5 geotechnical units. Due to a lack of samples recovered from the two drillholes (DH 1694 and DH 1717) that penetrated this layer limited results were returned. Testing was constrained to the coarse-medium grained lithology which showed high porosities (n=7.9%), and slake-durability index results (I_{d2}=94.0% retained), and moderate friction angles (33.2º), and dry densities (2411Kg/m^3), and low strength characteristics with UCS intact rock strength (15.3MPa), tensile splitting strength (1.32MPa), and cohesion (2.1MPa).

The Kaiata Mudstone is a marine sedimentary layer comprised of a massive silty mudstone which a gradational contact with the BCM, this unit was therefore divided into 2 geotechnical units. Due to the same constraints outlined above for the BCM testing was constrained to the massive silty mudstone lithology which showed the highest porosities (n=9.9%), and greatest variability in slake-durability index results (I_{d2}=34.2-94.5% retained), and the lowest friction angles (18.6º), dry densities (2.377t/m^3), and UCS intact rock strength (9.9MPa), as well as low tensile splitting strength (1.47MPa), and cohesion (3.0 MPa).

Scanline survey traverses were conducted along exposed areas of the Mt William Range adjacent to the Cypress North Block basin in an attempt to correlate the downhole data within the basement unit, as well as interpret discontinuity properties along the proposed highwall development. This was achieved by recording the rock mass properties and developing a kinematic analysis within the basement lithographies. The rock mass properties determined were; defect type, dip and dip direction, persistence, aperture, nature of infilling, defect roughness, and spacing.

Joints are typically steeply dipping with mean joint set orientations in the northern region of the ridge JS1 76°/041°, JS2 89°/261°, JS3 79°/118° (dominant set), JS4 47°/106°(where present), and JS5 85°/174°. Joint set in the southern section of the surveyed area had mean orientations of JS1 78°/025°, JS2 70°/245°, JS3 84°/285°, JS4 43°/106°, and JS5 79°/161°.

Structural domains were developed within the ridge crest using interpretation of the scanline survey and kinematic analysis to constrain the boundaries (along with physical and mechanical properties),- with respect to both highwall orientation and the Mt William Fault. The fault is the major through going structure that is surmised to be the controlling factor for defect formation propagation through the basement lithologies (and Tertiary sediments). These were further classified on the potential mode of failure after kinematic stability analysis was performed on the joints sets. Potential toppling failure on joints was found to be the dominant failure mode within the projected highwall orientation.

Table of Contents

LIST OF FIGURES

LIST OF TABLES

LIST OF APPENDICES

(all appendices are made available through the CD insert)

ACKNOWLEDGEMENTS

First and foremost, I would like to thank Solid Energy New Zealand Ltd who provided me with this project, and financial assistance throughout its duration. In particular I would like to thank Kane Inwood, for going out of your way to help with fieldwork, providing invaluable comments and project direction, and for providing field assistance. I would also like to thank the rest of the staff at the Westport office for there accommodation afforded me for the duration of my fieldwork. Thank you to Adrian Field for his assistance and friendship for the duration of my stay at Westport and on going help. Thank you to Richard Mould for reviewing my thesis chapters on behalf of Solid Energy. Thank you to David Bell (University of Canterbury) for agreeing to supervise me on this project and provide critical reviews of written work, and discussion on project organization and content. Thank you also to Jocelyn Campbell for assistance and discussion on the structural aspects of the project.

Many thanks to the staff in the Department of Geological Sciences who have assisted with this research project: Especially Cathy Knight and Arthur Nicolas for instructing me on the use of the various equipment in the Rock Mechanics Laboratory and putting up with my numerous requests on them, John Southward for help with computer and printer problems I have encountered as well as comic relief.

Last of all I would like to thank my family whose moral support, especially my older sister (who is also completing her thesis), and financial assistance helped me out of a few tight spots, and all my friends who have kept me sane through and provided me with support and understanding, and a special thanks to Kim for putting up with me through thick and thin and reminding me (in the stressful times) that there is always another tomorrow and that you can change that tomorrow for the better.

CHAPTER *1*

1. INTRODUCTION.

1.1 Project Formulation

Cypress North Block is located east of the existing coal mining Stockton operations and is set to be the first of a series of opencast mines scheduled for the Upper Waimangaroa Sector (figure 1.1). Solid Energy New Zealand Ltd is proposing to use the Cypress North block to set up of the initial infrastructure needed for the Upper Waimangaroa project with a long term goal to extend the existing operation at Stockton by supplementing coal production. The design incorporates the setting up of a highwall along the western side of the Mt William range and stripping the over burden, mainly comprised of sulphur-rich Kaiata Mudstone and highly disturbed basement (Berlins Porphyry) to access the gently dipping (8-12°) coal seams which terminate at the contact with the Mt William Fault. The orientation of the highwall, and the mode of extraction, will be dependant on the rock mass characteristics (defects, joint sets) and any design facets will have to incorporate these structural flaws.

The major focus of the thesis is to develop a greater understanding of the geotechnical issues affecting the proposed opencast mine through investigation of the proposed highwall area. Previous work in the area has developed a general understanding of the structural geology with numerous holes having been drilled throughout the basin that led to a knowledge base for both coal quality and a good stratigraphic overview of the lithologies present. To further the geotechnical and geological understanding a new series of drillholes was commissioned comprising 5 exploratory drillholes and a further 5 coal quality drillholes.

Determination of the physical and mechanical properties is paramount to the successful development of any highwall design, and to this end a series of laboratory tests were carried out from 5 exploratory holes. The testing regime incorporated unconfined

compressive strength (UCS), triaxial, porosity/density, Brazilian, and slake durability index determination. As a result detailed information was available collected on both the intact rock strength and rock mass characteristics of the Kaiata Mudstone, Brunner Coal Measures, and Berlins Porphyry to be exposed at the mine site.

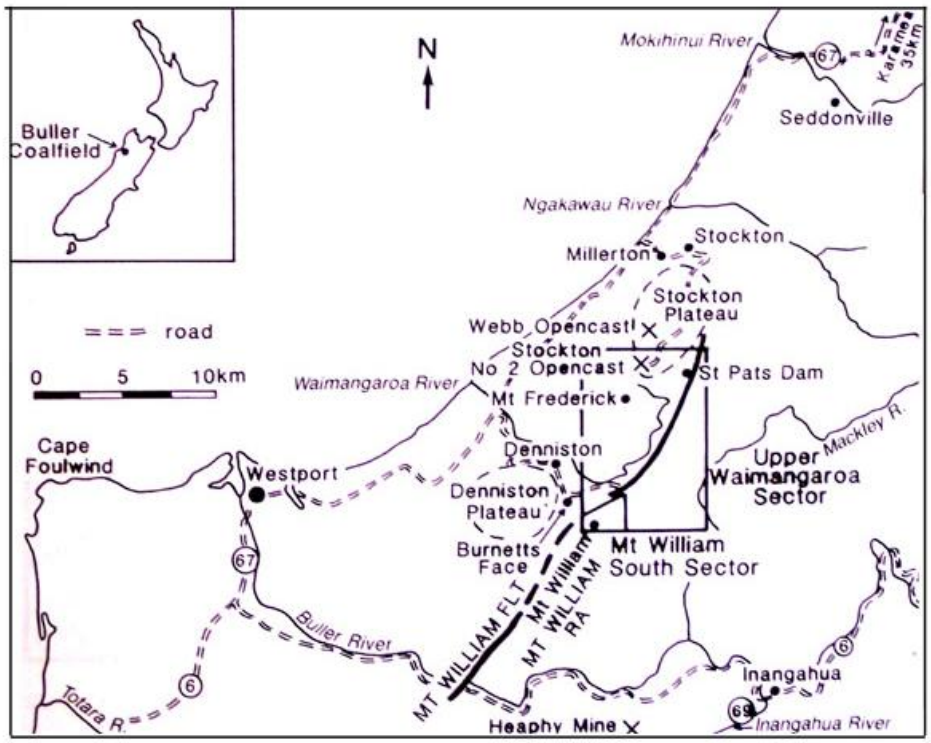

Figure 1.1 Location of Buller Coalfield

Scanline surveys were undertaken along the Mt William range in order to investigate the location, orientation, persistence, and frequency of faults and joint sets associated with the disruption of the Berlins Porphyry unit due to interaction with respect to the Mt William Fault Zone (MWFZ). Distribution of the rock types (granite and hornsfel) and the nature of their contacts is at best speculation, and therefore interpretation of the available data due to the intermittent nature of the defects provides only a generalized understanding which can be updates once more specific details are ascertained as the high wall is excavated.

Information collected through this study will help in the development of the final slope design along the Mt William Range with respect to the orientation and overall safe

design. Constraints on the mine development reside in both the economic value of the recoverable coal as well as the geotechnical properties and will dictate the final positioning of the highwall.

1.2 Thesis Objectives

The general objectives of the project are as follows:-

- To examine and test properties of intact rock in overburden strata associated with proposed highwall of the Cypress North Mine.
- To carry out engineering geological mapping of the proposed site along the MWFZ using existing topographical base maps to record rock mass defects.
- To carry out kinematic analysis of selected proposed pit slopes and to determine potential failure modes, in particular toppling failure and sliding.
- To evaluate geotechnical implications for mine development through the MWFZ, and any feasible failure within the high walls.
- To recommend a monitoring programme to identify problem areas ahead of mining due to excavation.

1.3 Location and Mining History

1.3.1 Location of Field Area

Cypress North Block is situated in the Upper Waimangaroa Sector (16 kms northeast of Westport) due east of Mt Frederick and the present operations at Stockton Opencast Mine, West Coast, South Island of New Zealand (Figure 1.1). Cypress North is in the northern section of a north-east / southwest trending Upper Waimangaroa Basin. The basin is bounded on its eastern extent by the Mount William Range and on its western extent by a series of stepping normal faults, at the base of Mt Frederick (Figure 1.3). Cypress North consists of several gently eastward dipping coal seems terminating in the contact between the BCM and the MWFZ. Access at present consists of a 30-45 min track

from the end of the old St Pats Dam road, or a 5 minute helicopter ride from the base of Mt Frederick. Haul road access will be extended with the commencement of mining operations.

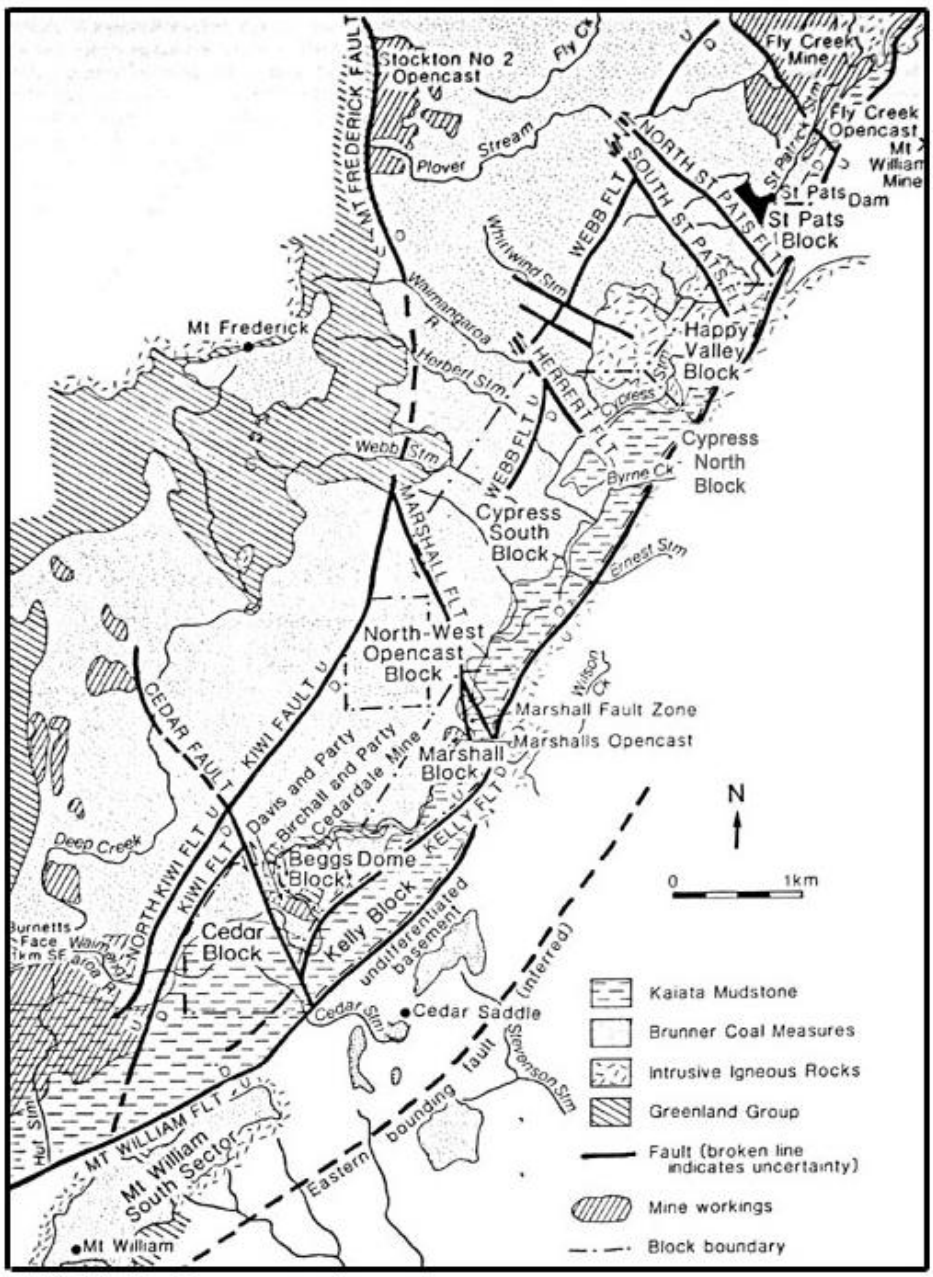

Figure 1. 2 Block Divisions of Upper Waimangaroa Sector (modified from Barry and Macfarlan, 1988)

1.3.2 Site Description

Situated on the southeast margin of the Stockton Plateau, at a base surface elevation of 696 metres, the coal-bearing BCM outcrops in the east, and with a gentle dip gives way

to Kaiata mudstone which outcrops along the upper western face of the Mt William Range rising to a maximum elevation of 844 meters in the west. Vegetation varies as the mire-like conditions suit tussock floras which then change to dense weather-stunted native bush on the majority of the ridge with upper slopes being exposed highly weathered basement. Drainage from the basin comprises the St Patrick Stream extending northward, and Cypress Stream flowing southward. The exceptionally high rainfall (6+ metres per annum) and rapid runoff, mean temperatures range between 4-17°C (2004 NIWA).

1.3.3 Mining History

Coal was initially discovered in the Buller Coalfield by Heaphy and Brunner in 1846, and mining began in the 1860s. Large scale mining began at Banbury Mine at Denniston Mine, Denniston Plateau, in 1878 and production peaked between 1908 and 1916 with an output between 700 000 and 800 000 tonnes per annum until mining finally ceased in 1968. Following the initial large scale operations at Denniston, Stockton and Webb opencast mines were established in 1908, and with the introduction of the aerial ropeway production grew steadily to 300 000 tonnes per annum in the early 1990's. The shortening of the ropeway in 2001, and the introduction of better extraction methods has seen production increase to 1 800 000 million in 2003 with plans to increase it further in 2004-5. Several smaller mines have been established at various times within the Upper Waimangaroa; Fly Creek Mine (underground and opencast), Millerton Mine, Mt William Mine, Davis and Party, Birchall and Party, Cedardale Mine, and Marshalls Opencast. All were on a smaller scale and produced only a few thousand tonnes of coal per annum locations of which are shown in figure 1.2.

1.4 Regional Geology – Buller Coal Field

1.4.1 Stratigraphy

The Buller Succession is made up three main stratigraphic units, Kaiata Mudstone, Brunner Coal Measures, and Basement (table 1.1), each of which is then separable into

specific lithologies. Throughout the Coalfield the BCM outcrops predominantly, with thicknesses rarely exceeding 70 metres (Coote 1991), and rests unconformably on pre-Tertiary basement rocks comprised of Ordovician Greenland Group Hornfels and Cretaceous Berlins Porphyry intrusives (Bowen 1964). The present extent of Kaiata Mudstone is minimal and present only in topographical lows as other areas have eroded down to the indurated coarse quartz sandstone of the BCM.

1.4.2 Basement

The Karamea Batholith comprises two difference phases, a fine-grained phase characterised by large quartz phenocrysts in a fine matrix, often altered to chlorite and sericite; and a coarse biotite granite phase, the former being the more prevalent of the two with the latter only being intersected in a few drillholes (L&M 1986). Granitoids from the Karamea Batholith form the Paparoa Range to the east of the Mount William Fault. The batholith is divided into two suites, but is dominated by the Karamea Suite (Carboniferous and Devonian) which is observed intruding on the Greenland group (Nathan 1986) along the length of the Mt William Range immediately to the east of the MWFZ.

FORMATION/GROUP	LITHOLOGY		
Not differentiated	River gravel, marine sand and gravel, local dune sand.	Hawera Series	Holocene
	Raised terraces of river gravel overlying marine sand and gravel.		Upper Pleistocene
REGIONAL UNCONFORMITY			
Blue Bottom Group	Sandstone up to 1,500m thick.	Sw-T	Miocene
UNCONFORMITY			
Nile Group	Calcareous mudstones and limestones.	Lwh - Lw	Oligocene
Kaiata Formation	Dark coloured, micaceous siltstone up to 200m or more thick in east. Sandy interbeds especially near base; Torea Breccia member near Papahaua Overfold.	Ak - Ar	
Brunner Coal Measures	Quartzose sandstones, grits and conglomerates; mudstones, shales and bituminous coal seams; 40 - 60m thick in west, 15 - 30m in east, 270m near Mt. Rochfort.	Ab - Ak	Eocene
REGIONAL UNCONFORMITY			
Hawks Crag Breccia	Greywacke and granite breccia	Mid - Cretaceous	
Karamea Batholith	Porphyrite granite and associated rocks intruded by Berlins Porphyry (Cretaceous)	Lower Cretaceous; Carboniferous - Permian	
Greenland Group	Greywacke and argillite locally metamorphosed to biotite hornfels and schist near granite intrusions.	Ordovician	

Table 1.1 Stratigraphic Columns for the Buller Region (Fergusson, CoalCorp Feb 1995)

The Greenland Group Sandstone metasediments (Nathan 1976) typically consist of light grey to greenish grey greywacke and argillite, with a chloritic matrix (L&M 1986). In the southern and middle areas of the sector the Greenland group, near Berlins Porphyry intrusives, has a speckled texture, and the degree of alteration appears to be greater. In the northernmost part of the block biotite Hornfels is incorporated with the intrusives. The group represents the oldest rocks of the Buller coalfield, being Upper Ordovician in age ($495^{\pm}11$ Ma).

1.4.3 Tertiary Formations

Kaiata Mudstone is the highest stratigraphic unit preserved on the Stockton Plateau and can be separated into down into two major lithologies, massive micaceous siltstone displaying sandy interbeds near the basal contact with the BCM. Thicknesses of the mudstone in the Upper Waimangaroa vary considerable with the thickest deposit (+200 metres) observed in the south of the sector as it wedges out against the Mt William Range. The Kaiata Formation is a massive dark olive grey calcareous mudstone that incorporates a sandy component near the basal contact. These sandy units are either dark olive/grey muddy sandstone to sandy mudstone, or light yellow-brown arkosic sandstone interbedded with carbonaceous mudstone. The depositional setting is an expanding shallow transgressional marine environment with poor circulation (Nathan et al., 1986). The Kaiata sediments in the Buller coalfield are relatively homogenous throughout due to the extensive depositional environment of the basin. Erosion has now all but removed the upper part of the sequence with only minimal traces found on the Stockton Plateau.

Brunner Coal Measures represents the most widespread unit in the Buller coalfield. The initial sedimentary unit was laid down uncomfortably in the Paparoa Trough over deeply weather basement rocks in the early to mid Eocene. The BCM is a fluviatile sequence of highly quartzose coarse grained sandstones, mudstones, shales, coal, and conglomerate derived from the underlying basement. The sequence is typically 70-130 m thick, but reaches 200m+ in old major fluvial channel which separates the Stockton and upper Waimangaroa sectors.

Coal seams in the Upper Waimangaroa are litho stratigraphic equivalents of both the Mangatini and Matipo seams found at Stockton, as both Sectors accumulated coal at the same time, more or less, in which case the seams can be assigned the same stratigraphic status (Titheridge 1992). However a direct correlation is not necessarily correct or obvious, as depositional controls, such as rate of subsidence of respective tilt blocks, affected the seam sequence in the Upper Waimangaroa.

The Upper Waimangaroa Sector is marked by west to east thickening which indicated the shape of the basin is asymmetrical and covers an area 9 kilometres long and 2-3 kilometres wide. The degree of seam splitting associated with the BCM indicates a dynamic depositional setting which is contrasted to relatively stability of the Stockton Sector. The Brunner Coal Measures in the Buller coalfields typically display normal and strike-slip faulting (Kennedy, 1988) which controlled the deposition regime.

The coal from the Upper Waimangaroa valley is high volatile A Bituminous rank found the length of the Sector with a change to High volatile B south of Beggs Dome. Petrographic evidence suggests that most of the coal accumulated in peat swamps and in low energy meandering streams/tidal estuaries, dominated by reed and small herbaceous vegetation, and generally lacking trees (Nathan, 1986). Vitrinite reflectance of coal in the Upper Waimangaroa averages at 0.60 which relates back to the coal quality (Norgate et al 1997).

1.4.4 Quaternary Deposits

Colluvial deposits occur below fault and erosional scarps forming talus cones and aprons (landslides and rockfalls) through the dry erosion under major fault scarps. The soils in the Buller comprise organic-rich Pakahi deposits, and often include a mixture of broken down highly weathered Kaiata mudstone and basement rock lithologies. Alluvial deposits are minimal on the plateau as a result of high rainfall. These deposits are limited to thin lenses in the major streams, as frequent flooding sees most sediment in the minor creeks washed away.

1.4.5 Depositional Environment

The history of the depositional environment of the BCM is controlled by structural deformation associated with the Paparoa Trough (Buller Coalfield) has been and the topic of debate for many years. It is commonly accepted that sedimentation of the last 80 Ma in the trough was controlled by subsidence in a north-northeast trending half-graben, in which there is much thicker succession of coal measures than elsewhere. Intense sub aerial

weathering from the Late Cretaceous to the mid Eocene saw the development of a widespread peneplain surface (Nathan et al., 1986).

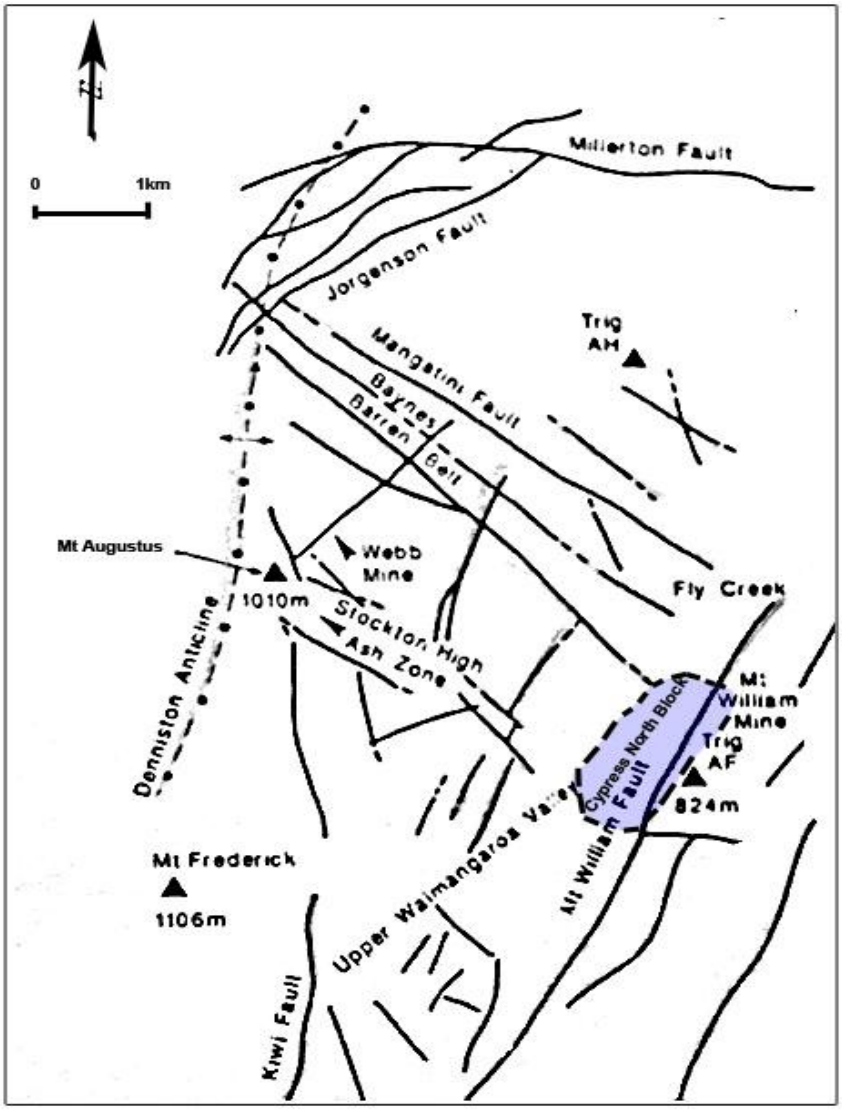

Figure 1.3 Fault trends in the Buller Coalfield (Titheridge 1993)

Deposition of the BCM in the Eocene shows a clear relationship between faulting and unit thickness, indicating that faults (figure 1.3) were active during this period. Different rates of subsidence associated with different orientations of the half-graben tilt block had a profound effect on the distribution and rate of sedimentation. Burial depths associated with sedimentation showed unit thicknesses up to 4000 metres (includes marine units) occurring in the deepest parts of the tilted hanging block walls (Titheridge, 1993).

Depth of burial and geothermal interaction due to extensive faulting, which increased the geothermal gradient, resulted in the formation of very high rank coals in the BCM.

Marine transgression then initiated the formation of the Kaiata Mudstone unit. This unit formed an effective impermeable layer over the BCM (a hydrocarbon cap) under which the coal seams maturated. The actively subsiding Paparoa Basin formed in the Late Eocene with successive deposition of the Nile group through the Oligocene and the Blue Bottom Group through the Miocene (Table 1.1). The regional extensional regime was reversed through a period of compression in which the Paparoa Trough was inverted. This caused the majority of the Kaiata Mudstone to be absent from the Buller Succession as severe erosion due to tremendous rainfall as seen the less durable mudstone stripped back to the more indurated coarse quartz sandstone of the BCM. As a result of the change into a compressional regime, in the late Miocene, the originally normal trending faults experienced reversals in directions, with a predominance of reverse thrust and strike slip faulting (Laird 1968).

The inversion of the Paparoa Trough has seen the once deeply buried BCM exposed to the surface through uplifting associated with the Kongahu Fault in the west (Laird, 1968). The Kongahu Fault forms the western extent of the Buller Coalfield and is bounded on the eastern extent by the Mt William Fault (Figure 1.4).

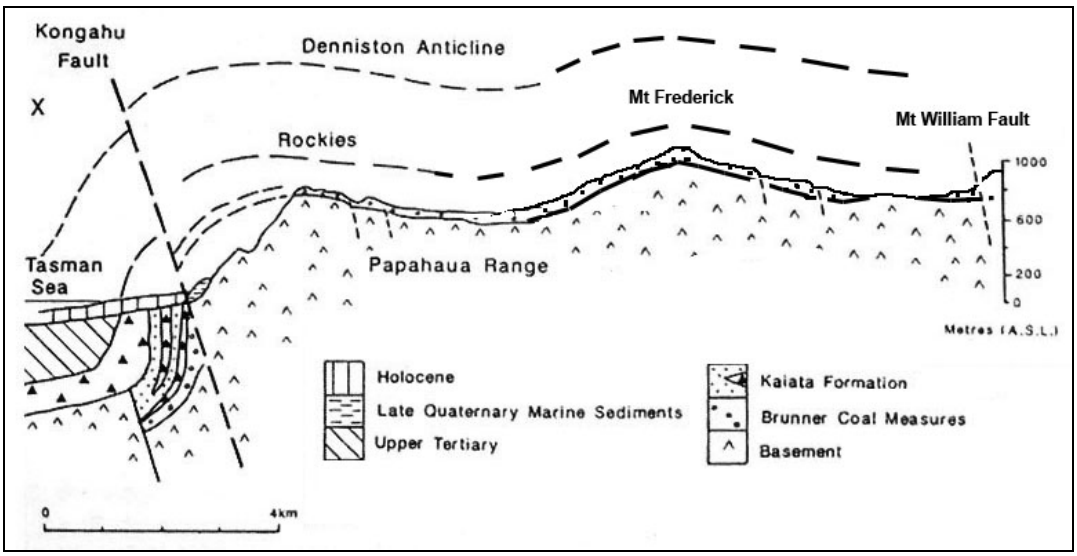

Figure 1.4 Cross Section of the Buller Coalfield (modified from Titheridge 1993)

1.5 Cypress North Block Geology

The geology of the Cypress North Basin mimics that seen along the length of the Upper Waimangaroa with gently dipping Tertiary units that terminate against the Mt William reverse fault. Interpretation of the basin geology was developed from a series of four cross sections and interpretation of existing and recently commissioned drillhole logs (Appendix 5 – CD insert). Three of the four cross sections are positioned in a west–east trend across the basin, and the fourth in a north-south trend along the length of the basin. Cross sections used for the interpretation of the basin structure are outlined in figure 1.6 (Map Pocket).

1.6 Stratigraphy of Cypress North Basin

Interpretation of the stratigraphic units below has been derived from the drillhole logs for the five exploratory holes. DH 1694 and DH 1717 are situated in the tertiary units found in the basin and intersect the coal bearing BCM. DH 1697, DH 1698, and DH 1715 are situated in the basement lithologies found along the Mt William range above the MWFZ. The core log for each of the five drillholes has been logged by Adrian Field and has been provided in the appendix (5).

1.6.1 Basement

Basement rocks in the Cypress North block consist of a mixture of Berlins Porphyry and altered Greenland Group metasediments. They are exposed on the Mt William range, east of the MWFZ, and along the western margin of the basin. In DH 1697, DH1698 and DH 1715 they comprise of medium grained biotite granites, granodiorite and microgranodiorite, containing xenoliths of biotite Hornfels derived from Greenland Group sediments. Interaction with the MWFZ has left the metasediment highly fractured with the granite slightly less so but also highly fractured. A mixed sequence of Greenland Group and Berlins Porphyry is also worthy of note. Alteration in the Greenland Group during the cooling of the Berlins Porphyry sees the interfingering and amalgamation of the two

lithologies. The combination of the two lithologies, although generally thin, represents an increase of strength in the units.

1.6.2 Brunner Coal Measures

The Brunner Coal measures found in the Cypress North Block basin tend to be relatively thin seams with respect to the Buller Coalfield, with thicknesses of 30 m uniformly the length of the basin. The composition of the measures along the basin mimic the same pattern found elsewhere on the Buller Coalfield, with a sequence of; massive medium to very course quartz conglomerate sitting unconformably on basement, Coal (M1, M2, M3 seams) interfingered with both fine laminated carboniferous sandstone and laminated carboniferous mudstone, then a graduated sequence of fine grained heavily bioturbated sandstone to coarse sandstone to granule conglomerate,.

The initial tertiary unit is a massive medium to very coarse quartz conglomerate is well indurated and consists of predominantly light grey brown sub-rounded to rounded greywacke, quartz, and argillite. The unit is moderately weak to strong with a creamy matrix of white quartz grit with minor weathered feldspar and biotite. These are interpreted as channel deposits on the peneplain, which is the initial surface for sedimentary deposition seen in the Paparoa Trough.

The laminated carbonaceous sandstone in located in between the coal seams and represent a hiatus in the peat mire growth. The hiatus is the result of a higher energy depositional environment resulting in greater volume of sediments (unfavourable to peat mire growth). This lithographic unit is interfingered with bands of weaker silty mudstone and carbonaceous/coal layers (described below).

The next unit is a fine laminated carbonaceous mudstone similar to the laminated sandstone (described above). This unit also represents a hiatus in the depositional environment required for peat mire growth with a greater percentage of fines from a lower energy system then the previous unit. The mudstone is dark brown in colour and is moderately weak.

The fine-grained heavily bioturbated sandstone unit is located towards the top of the BCM succession. This unit is a moderately strong, indurated to well indurated, fine quartz and minor feldspar, with occasional carbonaceous and coal laminations, and micaceous partings. Increased lamination between fine sandstones and siltstones become more prominent with increased fining downwards.

The last unit in the BCM is coarse sandstone to granule conglomerate consisting of massive quartz grit lithofacies. This represents the dominant unit within the coal measures (apart from the coal seams) comprising of well indurated to very well indurated, dark grey/brown, angular to sub rounded quartz, with minor bioturbation observed. This unit has a gradational contact with the fine-grained bioturbated sandstone unit.

1.6.3 Kaiata Mudstone

The Kaiata Mudstone in the basin is represented by a moderately weak to moderately strong hard marine mudstone which is generally weakly calcareous in the upper part of the sequence. The mudstone tends to be dark coloured, with silty fine sand interbeds near the base (4m) of the stratigraphic unit. Interaction with the fault zone has left some sections highly jointed with associated crush zones. Bedding is not always apparent in Kaiata mudstone (but becomes obvious on laboratory testing), with increased dip observed in drillhole core samples positioned near the fault zone. The increase in dip has been interpreted as an upturn in the stratigraphic unit due to uplift displacement of the Mt William Fault.

1.7 Structure of Cypress North Basin

The structure of the Cypress North basin is dominated by the influences of the basement relief. In the west the relief has been significant with whirlwind rise effectively restricting the development of the M1 seam group north of the Marshall Fault Zone (figure 1.5). In the east the relief is dominated by the Mt William Reverse Fault terminating the Tertiary sediment abruptly with a 120 upthrow to the west (L&M 1986). During deposition

of the Tertiary sediments the Mt William Fault had a normal component that was reversed during the transition from a compressional regime into an extensional one. The Basement rocks encountered in the Mt William Range are dominated by highly fractured Greenland Group metasediments and Berlins Porphyry intrusives. The Greenland Group encountered within DH 1697, DH 1698, and DH 1715 tends to be biotite hornsfel.

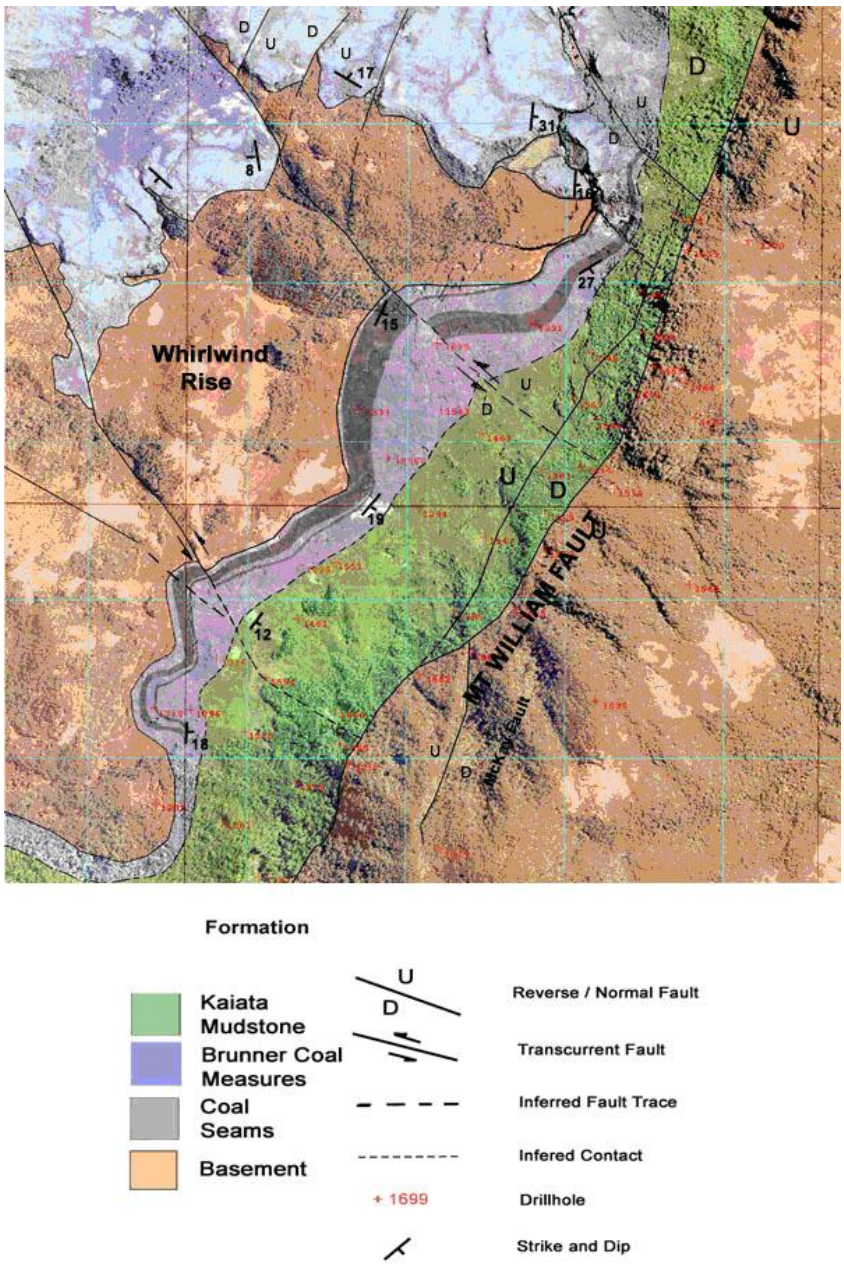

Figure 1.5 Geological Interpretation of Cypress Basin

Both the Tertiary units within the Cypress North Basin (Kaiata and BCM) mimic the trends observed the length of the Upper Waimangaroa Sector, with gentle dips towards the east wedging out against the MWFZ. The thickness of this wedge increases to the south of the basin with variation to the thickness of Kaiata Mudstone. The mudstone increases from 50m in the north of the basin to 90 m in the south and in contrast there is little too no increase in the BCM.

1.8 Investigation Methodology

1.8.1 Literature Review

The literature review consisted of collating existing information pertaining to the geology of the Stockton/Mt William/Upper Waimangaroa Sector such as mining history, existing drillholes, climate, and geomorphology. The sources of the information included published reports and papers, unpublished data, aerial photos, and published and unpublished maps of geological and geotechnical data. The literature review provided an overview of the general geology in the area and the extent of the initial investigations along the Mt William Range.

It also highlighted the need for further investigation in the area to build up a more appreciable understanding of specific problems pertaining to mining along a fault zone. Specifically, it highlighted the need to develop an understanding of the homogeneity of the rock mass perpendicular to the Mt William Fault Zone, along which any highwall would be situated. (Figure 1.5)

1.8.2 Determination of Rock Material Parameters

Information available on rock material strengths of the three stratigraphic units in the Upper Waimangaroa Sector that comprise the proposed highwall are limited to UCS and Point load testing carried out by Brown (L&M 1986) and further and more comprehensive study of the rock materials is required. Any testing will have to incorporate

variations in the lithologies in these units. Previous field studies initiated with Laird 1968 and then further developed upon by L&M 1986, Barry 1988, Kennedy 1988, and Coote 1991 of the these stratigraphic units showed that there were a number of geotechnical units present, with the Kaiata Mudstone separated into two main lithologies, Brunner Coal Measures (BCM) into five main lithologies, and Basement separated into disturbed Greenland Group Hornsfel (GG) and Berlins Porphyry (BP) all requiring rock material parameters. A laboratory programme was then devised to determine a separate set of properties of each geotechnical unit. The programme included porosity-density and slake-durability tests to ascertain the durability of any high wall structure, and uniaxial, Brazilian and triaxial compression testing to determine strength characteristics. These results will be used to determine the parameters of any high wall design as well as an initial assessment of the break down of overburden material on freshly exposed pit slope surfaces and long-term breakdown in overburden stock piles.

1.8.3 Determination of Rock Mass Properties

Rock mass properties are also required in any design aspects of the proposed highwall, and combined with the rock material properties can be used to develop a Factor of Safety (FOS). The information is then used to identify the best orientation of the highwall to minimize failure due to instability. The rock mass properties are sourced from the outcropping of the basement (GG and BP) along the Mt William Range and have been determined from 12 separate scanline surveys conducted parallel to the MWFZ. Sites for the scanline were determined by the excavation of shallow gully features at the suggestion of Kane Inwood (Solid Energy Engineering Geologist). Thereafter statistical analysis was conducted to determine the relationship of joint and defect sets across the ridge crest and the effect of the rotation in MWFZ. Properties determined were limited to visible sections observed in the excavated creek beds and included defect type, defect orientation, aperture, roughness, defect infilling, and where appropriate, persistence, aperture, wavelength, and amplitude.

1.8.4 Highwall Stability Analysis using Kinematic Analysis of Defect Planes Associated with the Mt William Range

The kinematic analysis of the potential failure modes associated with the proposed highwall has been assessed using scanline data. The plausible modes of failure associated with highwall instability include planar, wedge, and toppling failures. The prediction on whether particular failures modes will daylight was ascertained by proposing different orientations with regards to highwall design, both of slope orientation and slope angle, to determine the best overall stability of the highwall. General characterisation of the deformation along the eastern side of the MWFZ will help establish overall structural domains by grouping joint and defect sets with similar orientations or properties. Based on the orientation of the MWFZ specific structural defects may then be described and correlated, providing a general identification of plausible failure.

Structural deformation in the basement rock is the result of several periods of both extension and compression, and in its current configuration is susceptible to geotechnical changes over relatively small areas both laterally and vertically. Localized information will still be assessed to identify any possible minor localized failures with respect to lateral components. Vertical assessment is limited to correlating surface observations with existing drill hole logs, therefore an ongoing assessment as features are exposed during mining will insure that weaknesses in the rock mass that may affect the overall safety are addressed.

1.9 Thesis Format

This thesis has been separated into 5 chapters, with the first and the last acting as an introduction and summary respectively. Chapter one provides a thesis background, objectives, investigation methodology, geological history and site geology. Chapter Five provides a summary of the middle three chapters outlining findings and recommendations.

Chapter Two, titled Rock Material Characteristics, focuses on rock material characterisation, starting with a geotechnical description of the three stratigraphic layers and their respective lithologies which will comprise the proposed highwall. Laboratory testing is focused on determining physical and mechanical properties of the 3 stratigraphic units that have been described at the beginning of the chapter.

Chapter Three, titled Rock Mass Properties, focuses on interpreting discontinuity data collected from scanline surveys conducted along the Mt William Range adjacent to the MWFZ. From the scanline surveys prominent defect joint sets, defect orientation, persistence, defect infilling and consistency, wavelength and amplitude, and distribution are identified and described for the disrupted Berlins Porphyry comprised of Greenland group and Granite.

Chapter Four, titled Highwall Stability Analysis of Geotechnical Hazards and Mining Implications, is a study of the potential instability due major defects present in the proposed highwall. Detailed kinematic analysis of the mean joint/defect sets projected on stereographic plots to determine potential failures. Kinematic checks performed were for planar sliding, wedge failure, and toppling failure. The establishment of structural domains based on the results of the kinematic checks, and the locality of the faults, and defects with similar rock mass properties.

CHAPTER 2

Rock Material Characterisation

2.1 Introduction

In the design of any effective rock slope a number of factors need to be taken into consideration to limit the economic consequences and address safety issues associated with instability. One of the keys factors to be derived from this characterisation on the rock material is the reduction of the amount of waste rock which has to be excavated in recovering an ore body (Hoek & Bray 1977). The initial step is to establish accurate descriptions of the intact rock material properties which will comprise the face of the proposed highwall. In doing this the engineering geological model can be derived from a laboratory programme for the various lithologies associated with the Kaiata Mudstone, Basement Rock, and to a limited extent Brunner Coal Measures.

Due to the nature of the sampling regime more focus is directed to the units that comprise the majority of the highwall, both during stripping and the final wall orientation. These comprise a Tertiary sedimentary unit (the Kaiata mudstone), which will potentially comprise up to 70+ metres of the temporary highwall, and basement rock, which will comprise the majority of the final highwall design potentially making up 120 metres of the vertical component (figures 1.6 map pocket). The BCM due to the overall thickness and lack of viable samples, over the 10-15 metres of alternating lithologies and coal, will need to be extrapolated from existing data and the already substantial understanding from the Stockton opencast development. The laboratory tests selected have been broken down into those that define the physical properties, and those that define the intact rock mechanical properties.

The physical property tests selected were Porosity, Density, and Slake-Durability. The strength and deformation characteristics of a rock are determined primarily by the magnitude of effective stress, which is in turn affected by a variety of intrinsic properties such as grain size and porosity that control the overall strength of the rock material

(Vutukuri et al., 1974). Porosity is one of these intrinsic properties as the presence of interconnected pores, in the fabric of the rock decreases its strength and increases its deformability (Kowalski, 1966). Porosity-Density was therefore chosen to provide an insight into the variation in the intact physical properties of the selected stratigraphic units.

The Slake-Durability testing was selected as it simulates the effect of long term weathering of the samples. Through a series of wetting and dry cycles the test gives an indication of probable long term effects of breakdown of stripped overburden material as well as the effect of weather on the rock face material. This is particularly important in the case of the Kaiata formation as this unit contains a high percentage of sulphur which when exposed to oxygen oxidises to form Sulphuric Acid (H_2SO_4) which if introduced into the local hydrological cycle can cause damage (via Acid Mine Drainage) to the local eco-system.

The tests selected in determining the intact rock mechanical properties were; Unconfined Compression Strength testing (UCS), Triaxial Compression, and Brazilian tests (splitting tensile). The UCS tests define the compressive strength (σ_1) of the rock samples under atmospheric conditions (i.e. σ_3=0). The Triaxial tests use simulated insitu horizontal compression (σ_3) to derive the compressive strength of the rock samples at depth. These define the strength classification and characterisation of the intact rock sample. From these values the Mohr strength envelope may be determined, along with the internal angle of friction and cohesion.

The methods in ISRM (1981) were followed for all the laboratory programmes with all samples prepared to meet the relevant specifications. Testing was carried out using facilities provided in the Rock Mechanics Laboratory, Civil Engineering Department, University of Canterbury, Christchurch, New Zealand. ISRM methods for each of the laboratory tests are outlined in appendix 2(CD insert).

Basin lithologies were mostly defined by analysis of the drill core log records (DHs 1694, 1697, 1698, 1715, and 1717), as surface outcropping was limited to the more indurated rock lithologies and was predominantly altered after long exposure to weathering

in the fault controlled escarpment. During the laboratory programme each of the stratigraphic units was divided into their appropriate lithographies using engineering geological descriptions which followed Bell & Pettinga (1983). The lithologies for the Kaiata formation (the highest stratigraphic unit found within the sector) were divided into massive micaceous siltstones and fine grained sandy interbeds (near basal contact); The BCM was divided, using drillhole logs (appendix 5 – CD insert), into Coarse Sandstone to Granule conglomerate, fine grained heavily bioturbated sandstone, laminated carbonaceous mudstone, fine laminated carboniferous Sandstone, Coal (M1, M2, M3 seams), and massive medium to very coarse quartz conglomerate; and the Basement separated into Greenland Group Metasediments and Berlins Porphyry.

Variations were observed both laterally and vertically through both the BCM and the basement units, with the Kaiata mudstone proving the most homogeneous stratigraphic unit. The anisotropic nature of the BCM tends to be more prevalent through vertical variation, with the sedimentary litho structures dictated by depositional controls which were relatively uniform laterally along the length of the Mt William Range. The basement units tend to be the least predictable of the stratigraphic units with variations in composition and lithotypes both vertically and horizontally due to the intrusive nature of the Berlins Porphyry.

Samples of core were selected for testing from a new series of exploratory drillholes used to fill in gaps in existing drillhole coverage. The numbers of samples varied from location to location as closeness to the MWFZ and location of intrusive bodies gave large sections of core log with negligible RQD (<10% intact samples greater then 100mm) from which intact samples were few. The BCM was the greatest effected with only two drillholes penetrating this stratigraphic layer and intermittent interfingered layers of coal and sandstone/mudstone saw minimal returns in the form of samples. Also due to the intrusive nature of the granite into the Greenland Group greywacke, occurrence of intact rock samples of the biotite hornfels sandstone unit was also minimal.

2.2 Geotechnical Units Associated with Proposed Highwall

2.2.1 Engineering Geological Descriptions

The following units are described geotechnically using Bell & Pettinga's (1983) Engineering Geological Field Description for Rock Material (appendix 1 – CD insert). The division of these units was based on analysis of the drill core log and descriptions provided by Solid Energy (Adrian Field attending geologist). In increasing depth below the surface these descriptions are as follows:

Kaiata Mudstone

- **Unit 1.1** Slightly weathered, moderately weak, dark olive grey, massive, micaceous mudstone
- **Unit 1.2** Slightly weathered, moderately weak – moderately strong, dark olive grey, finely layered, sandy siltstone, interbedded with carbonaceous mudstone.

Brunner Coal Measures

- **Unit 2.1**: Moderately weathered, moderately strong, light greenish brown, massive, Coarse Sandstone, with minor bioturbation
- **Unit 2.2**: Slightly weathered, moderately strong, light greenish brown, coarsely layered, medium - fine sandstone, heavily bioturbated
- **Unit 2.3**: Slightly weathered, moderately weak, light greyish brown, finely layered silty mudstone with laminated carboniferous mudstone
- **Unit 2.4**: Slightly weathered, moderately weak, light greyish brown, finely layered, fine sandstone.
- **Unit 2.5:** Slightly weathered, moderately weak- moderately strong, light greyish brown, massive, medium – coarse sandstone.

Basement – Greenland Group Hornfels – Berlins Porphyry

- **Unit 3.1** Slightly weathered – highly weathered, strong, dark greenish grey, massive, Hornfels.
- **Unit 3.2** Slightly weathered, strong, light greyish blue, massive, granite
  - Completely weathered, weak, light yellowish brown, massive, granite

2.2.2 Lithological Description of Geotechnical Units

Kaiata Mudstone (Units 1.1 & 1.2)

Units 2.1 and 2.2 have a maximum drilled thickness of ~85metres in the Cypress North basin, with unit 2.1 dominating and having a weak calcareous content concentrated in the upper extent of the formation. Typically only the bottom 5-6 m incorporates increased sand content (Unit 2.2) due to the interface with the BCM with a gradational contact generally occurring over a 2-3 m interval.

Figure 2.1 Representative Samples* of Unit 1.1 and 1.2

*** All Representative Sample sizes are ~ 40mm X 40mm.**

The basal part of the Kaiata sequence, along with an increased silt and fine sand content, is characterized by the inclusion of fine sand sized muscovite and increase

carbonaceous content. Veins of resolutioned calcite are present within defect fractures. The Kaiata mudstone is sparsely fossiliferous, with a fauna of Echinoderm fragments and Gastropoda. The fossil assemblages indicate a Runangan to Kaiatain age and near-shore deposition (Kennedy 1988).

Brunner Coal Measures (Units 2.1-2.5)

The massive coarse lithologies present in this geotechnical unit are med-coarse grained sandstones (Unit 2.1) which is in a gradational contact with the Kaiata mudstone (Unit 1.2) and as a coarse grained conglomerates resting unconformably on the basal sequence (Unit 2.5). Both these units are coarse sandstones, typically quartz-rich with feldspar, minor pyrite, and sand sized mica grains that mimics the parent rock. Both units show a varying degree of weathering, especially associated with fractures which commonly display extensive iron staining. The quartz grains tend to be the dominant larger grain, and are typically sub angular to angular. Unit 2.1 has minor bioturbation and gradational change into the next unit which has increased bioturbation. Unit 2.5 tends to be lighter in colour, with less frequent inclusions of carbonaceous bands. The depositional environment for these coarser units was most likely a braided stream environment, like the peneplain discussed in Chapter One.

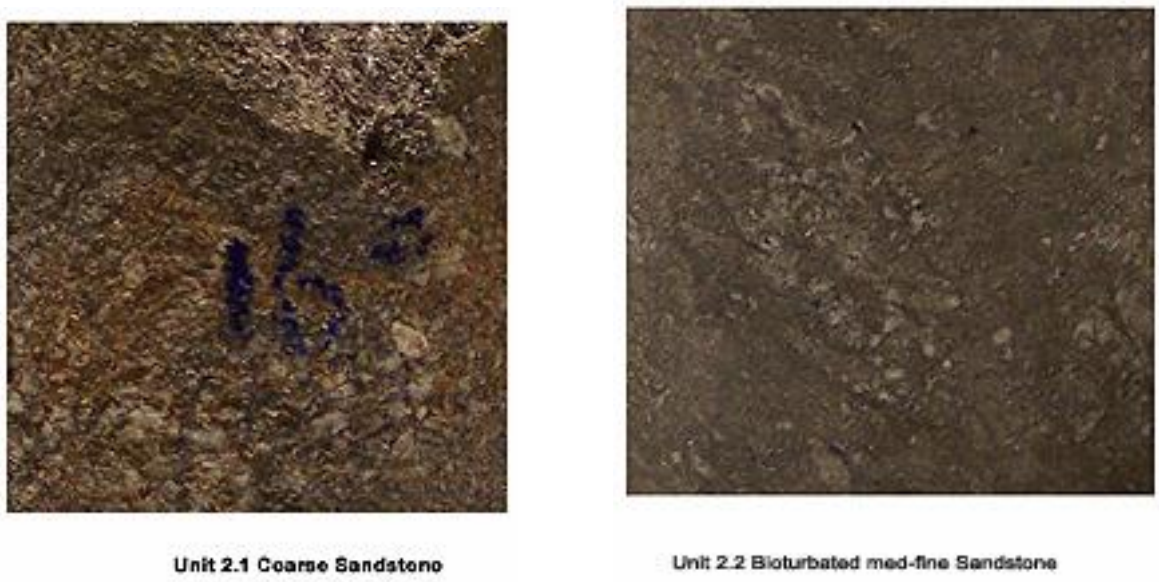

Figure 2.2 Representative Samples* of Unit 2.1 and 2.2

Unit 2.2 represent a fining downwards of the upper unit (2.1), with the same composition dominated by quartz grains. Greater transportation associated with the finer sequence as suggested as the grains tend to be sub-angular. The unit also represents increased bioturbation and carbonaceous banding. The presence of bioturbation indicates less constant reworking and probably marks the transition from a tidal to a shelf environment.

The laminated units are separated on the basis of the grain size, with a finely laminated silty mudstone (Unit 2.3) and finely laminated fine sandstone (Unit 2.4) being recognised. The laminations in the units are pronounced alternating dark/light layers with the dark layers representing increased carbonaceous/mica-rich mudstones, while the lighter layers are generally siltstones/fine sandstone. The units are inter-bedded with the coal seams present in the basin, and make up the majority middle sequence seen in the Brunner Coal measures section with predominant thick bands of medium sandstone. These units represent coastal channel distributaries and inter-distributaries at areas such as the mouths of fluvial systems discharging into the sea.

2.3 Representative Samples* of Unit 2.3 and Unit 2.4

2.4 Representative Sample* of Unit 2.5

Basement (Units 3.1, 3.2, & 3.2b)

The Greenland Group consists of greywacke and argillite, which is usually bedded and closely jointed, with a slaty cleavage. The unit is thermally altered to biotite Hornfels near granitic intrusions which extend the length of the MWFZ, and is generally dark grey, fine to medium grained with foliation 30-50° degrees with frequent veins of quartz, porphyry and rare calcite. The Contact with the Berlins Porphyry (Unit 3.2) is usually distinct and sharp along foliation, and is usually associated with increased quartz content near the contact.

The granitic lithology (Unit 3.2) present along the Mt William Range comprises medium-grained biotite granite and granodiorite. The intrusive nature of the pluton lends to interfingering with the hornfel basement unit (unit 3.1). Close fracturing of the basement rocks near the MWFZ lends itself to extreme weathering (Unit 3.2b), and this propagates along joint and defect sets. The composition is predominantly quartz crystals, with subordinate feldspars, mica, limonite, and mafic minerals.

Unit 3.1 Hornfel

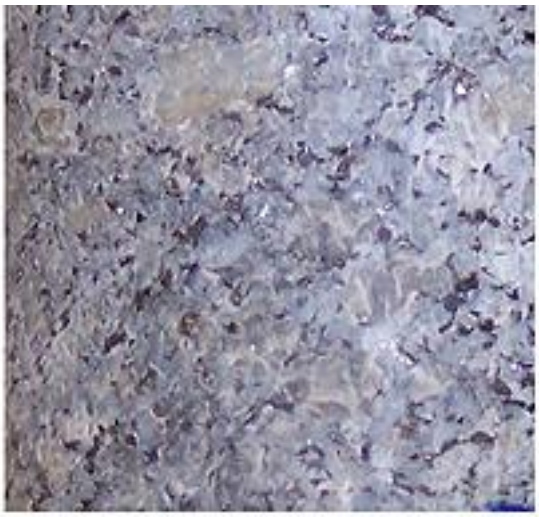

Unit 3.2 Granite

3.2b Weathered Granite

2.5 Representative Samples* of Units 3.1, 3.2 and 3.2b

2.3 Sampling Methodology

Samples were collected by extraction of core samples from 5 exploratory drillholes at Cypress North Block, Upper Waimangaroa Sector, completed between June and September 2003. Samples, where possible, were wrapped and boxed on extraction from the drillhole with the intention of preserving the insitu moisture content. Samples were

then transported, via helicopter, to the store shed at Solid Energy's office in Westport. Then the samples were transported to Christchurch, where they were stored at constant temperature and moisture in the Rock Mechanics Laboratory, University of Canterbury. Ideally, following ISRM standard, samples should be tested within 1 month of extraction from the ground, but due to delays with drilling the majority of the testing commenced after the one month deadline however, all samples were tested under saturated conditions and the moisture content of the examined core samples, closest to extraction time, registed a near saturated moisture content with negligible difference between insitu density and saturated density.

Sample selection was dictated by availability of intact core over the required length, with no visible defects where possible, this was to give the best account of the intact rock parameters and maximum values of intact rock strength. The drilled core was of HQ size and averaged a diameter of 61 mm which equated to a required length of 152.5mm to give a minimum L:D ratio of 2.5:1.0. The ratio was selected to both adhere to ISRM (L:D 2.5-3.0) and other international standards (L:D 2.0-2.5). Samples were then grouped into similar geotechnical units and tested through the laboratory programme in the Rock Mechanics Laboratory.

2.4 Physical Properties

2.4.1 Test Methods and Procedures

The methods used for testing the Physical Properties (and mechanical properties) of the geotechnical units were outlined in previous sections of this chapter. They included Porosity–Density determination and Slake-Durability Index testing, which are both outlined in more detailed in appendix 2. The raw data from both the tests are included, and are also provided in excel format on the CD insert.

2.4.2 Porosity-Density Determination

Porosity, density, and water content are classified as point properties and therefore are not dependent on the effect of interaction with discontinuities (Hudson 1993). These properties relate to the presence of pores, and their interaction, in the rock material. This interaction has a direct effect on the overall strength of the rock, and is a major factor in determining the minimum strength of the rock under saturated conditions as pore pressure can decrease overall friction between grains by limiting the compactability of the sample. The dry density of a sample can usually be directly related to the porosity, with a lower density equating to a greater void content and therefore interaction between the voids. The direct properties determined by the porosity - density test are porosity and dry mass density, and from these other parameters can be derived. Table 2.1 outlines the properties for each of the stratigraphic units. Values were determined using calculations outlined in the ISRM (1981) standard testing procedures (appendix 2).

Table 2.1 Summary of Density-Porosity Parameters.

Unit	Berlins Porphyry Granite Unit 3.2 -3.2b	Greenland Group Hornfels Unit 3.1	Brunner coal measures Bio – Sandstone Units 2.1,2.2,	Kaiata Mudstone Massive Unit Unit 1.1	Mixed Basement interfingering Mixed Unit
Number Tested	8	1	3	6	2
Porosity (n= Vv/V).					
Average percentage	0.8	1.9	7.9	9.9	2.3
Range	0.2-1.3	1.9	7.8-8.0	7.8-12.0	0.5-4.0
Dry Density (Kg/m^3)					
Average Density	2666	2658	2411	2377	2657
Range	2659-2704	2658	2386-2435	2308-2477	2575-2740
Saturated Density (Kg/m^3)					
Average Density	2681	2677	2489	2476	2680
Range	2671-2706	N/A	2466-2513	2408-2.593	2616-27444
Void Ratio	0.01	0.02	0.08	0.10	0.02
Vv (x10^{-5})(m^3)	0.33	0.78	3.20	3.96	0.93

- **Berlins Porphyry**

Results from the unit vary with degree of weathering, unweathered rock samples having very low porosity (n = 0.8%) and a very high dry density (ρ_d = 2666Kg/m^3). The difference between dry and saturated density (12Kg/m^3) indicates that pore volume, and therefore connectivity is minimal, and this is represented by the lowest void ratio (0.01) of the geotechnical units. An increased in weathering sees an increase in porosity (n=3.4) and a loss of overall density (2577Kg/m^3).

- **Greenland Group Hornsfel**

The only representative sample of this stratigraphic unit sees a very low porosity (n = 1.9%) and a very high dry density (ρ_d = 2658Kg/m^3). The Greenland Group metasediment is comparable with the Berlins Porphyry, with a low void ratio (0.02) which indicates that intact rock material has low permeability.

- **Brunner Coal Measures**

The bioturbated sandstone of the Brunner Coal Measures has a medium porosity (n=7.9%) and a high dry density (ρ_d = 2489Kg/m^3). The medium to coarse grain size gives way to a higher void ratio (0.08) which is an indication of greater void volume and pore connectivity (permeability).

- **Kaiata Mudstone**

Out of the stratigraphic units tested the Kaiata Mudstone had both the highest void ratio (0.10) and the highest porosity (n=9.9%). Kaiata mudstone also had the lowest Dry Density (ρ_d = 2377Kg/m^3) but it is still considered having a high density.

- **Mixed Basement**

The mixed units vary in both density and porosity, having the greatest range out of all the units tested. Contrast can be drawn between both the Berlins Porphyry and Greenland Group Hornfels, with the mixed unit displaying a very high density (ρ_d = 2657Kg/m^3) and very low porosity (n = 2.3%) with samples individual porosity ranging from 0.5 through to 4.0. Pore space between samples varies due to changes in compositional components within the mixed units with varying degrees of mixing between the hornfels and the granite intrusive.

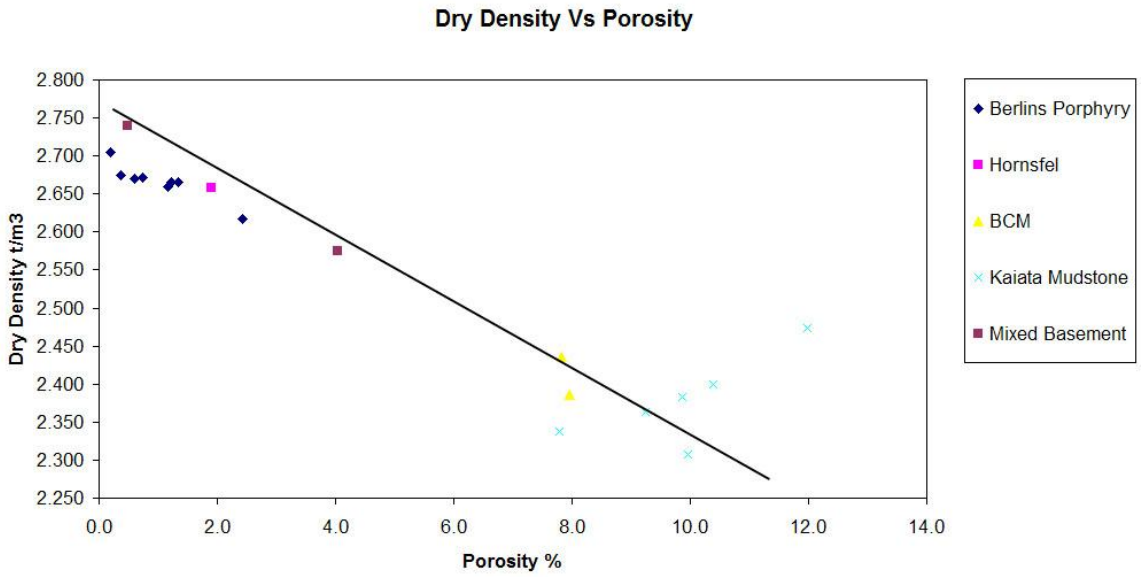

Figure 2.6 Graph of Dry Density Vs Porosity for Stratigraphic layers.

2.4.3 Slake Durability Index (I_d)

The Slake Durability Index test was first designed to test the slaking of clay samples in water. Such tests are very often empirically based and care was required to simulate the engineering environment in which the clay shales occurred (Hudson 1993). Slake Durability Tests are now used in a broader sense to assess the susceptibility of rock (mainly weak rock) under weathering conditions by an accelerated programme meant to simulate long periods of sustained weathering incorporating cycles of wetting and drying.

The ISRM adopted the Slake Durability Index test as a suggested method based on tests for assessing road subgrades.

The Slake Durability Index test was selected primarily to test the weathering effects on the Kaiata Mudstone unit, as its high sulphur content makes the unit susceptible to generating sulphuric acid when exposed to oxygen. The sulphuric acid is the cause of Acid Mine Drainage (AMD), where oxidized sulphur dissolves into water as it infiltrates through the exposed unit, reacting to forming sulphuric acid. The acid is then transported into to the local water tributaries lowering the base Ph level.

The Slake Durability test is normally reserved for weak rocks, from its initial conception for clays, but representative samples were tested from all the stratigraphic units. Each sample consisted of 10 spherical pieces with no visible signs of existing defects. The test was used to help with the characterization of the physical properties of each of the stratigraphic units, with emphasis placed on the Kaiata Mudstone for reasons discussed previously. While the test gives a good indication of the effect of prolonged natural weathering, it doesn't take into account the effect of chemical weathering on the samples especially with the development of acid which would lead to the acceleration of the degradation of the mudstone unit. The end result is an overview into the initial breakdown of the stratigraphic units, and an overall indication of the susceptibility of short-term breakdown in waste and exposed batters.

The Slake Durability Index (I_{d2}) for all the stratigraphic units were classified using Johnson and DeGraffs (1988) modified slake-durability classification (Table 2.3). Samples from each of the stratigraphic units were tested in accordance with ISRM (1981) standards. Sample collection (drillhole allocation) and sample depths are outlined with the data results in excel format (appendix 2).

Table 2.2 Summary of Slake Durability Results.

Unit	Berlins Porphyry Granite Unit 3.2 -3.2b	Greenland Group Hornfels Unit 3.1	Brunner coal measures Bio – Sandstone Units 2.1,2.2,	Kaiata Mudstone Massive Unit Unit 1.1	Kaiata Mudstone Massive Unit (Crushed Zone Sample)	Berlins Porphyry (Weathered) Granite Unit 3.2b
Number Tested	40	40	20	40	20	10
Primary Cycle Percentage Remaining (I_{d1})	99.5	99.8	96.3	96.9	43.4	92.5
Range	99.07-99.82	99.76-99.90	96.21-96.40	95.37-98.76	42.82-43.97	88.06-96.21
Secondary Cycle Percentage Retained (I_{d2})	99.0	99.6	94.0	94.5	32.9	86.0
Range	98.27-99.71	99.57-99.80	92.73-95.22	94.03-97.11	30.16-35.67	78.34-93.66

Table 2.3. Two-cycle Slake-Durability Classification (Johnson & Degraff), (1988)

Slake Durability (I_{d2})	Classification
0-30	Very Low
30-60	Low
60-85	Medium
85-95	Medium High
95-98	High
98-100	Very High

Conclusions from this testing regime are as follows:

- **Berlins Porphyry:** This unit has a classification of very high durability having the second highest I_{d2} value (99.0% retained) with very high retention of the rock samples. Observations from the testing showed that the samples retained most of their rough edges with only minimal breakdown. Mass loss was uniform, and minimal loss was observed during both wetting and drying cycles with a 0.5% loss in mass each cycle.

- **Weathered Berlins Porphyry:** These samples have a classification of medium – medium high durability, having the second lowest I_{d2} value (86.0% retained) with moderate retention of the rock samples. The selection of the samples was based on the moderate degree weathering observed. Observations from the testing showed a rounding of samples during the first and second cycles with a loss of 7.3% and 6.5% respectively. The sample indicates that an increase in the degree of weathering results in increased porosity (3.4%) and decrease in dry density. Two of the test samples separated along existing fractures during the second cycle with minimal alteration in the overall result.

- **Greenland Group Hornfels:** This unit has a classification of very high durability having the highest I_{d2} value (99.6% retained) with the greatest retention of sample mass. As with the Berlins Porphyry sample only minimal rounding was observed along rough edges. Mass loss was also uniform, and minimal loss was observed during both wetting and drying cycles with a 0.2% loss in mass each cycle.

- **Brunner Coal Measures:** These samples have a classification of medium high durability, having the lowest I_{d2} value (94% retained) of the primary stratigraphic units but still retaining a moderately high retention of sample mass. Samples tested were medium to coarse grained with minor bioturbation with a medium porosity (7.8%). Sample loss was observed to be slightly greater in the initial wetting and drying cycle with a percentage lost of 2.7% compared with 2.3% in the second cycle. All samples remained intact during the testing procedure.

- **Kaiata Mudstone:** This unit retained a classification of medium high durability having the third highest I_{d2} value (94.5% retained). The Kaiata Mudstone is commonly observed to breakdown (slake) rapidly when exposed to surface conditions in the field. Indications of previous tests on the Kaiata mudstone tend to back up this result but contradict the field observations. These results lead to the conclusion that secondary chemical weathering (e.g. oxidation) plays a major part in the break down of this unit. Two of the 40 samples split along existing fractures during testing, but having minimal effect on the end result.

- **Crushed Kaiata Mudstone:** This unit has the lowest I_{d2} from within the stratigraphic sequence according to its low Id_2 value (32.9% retained) which classifies it as having low durability. Prevalent from the first wetting drying sequence was the definition of previously indistinguishable micro fractures. The first cycle (I_{d1}) of the test saw the reduction of the sample mass by 56.4%, the highest out of all the tested samples. During the addition of moisture, after the initial drying sequence, the sample tended to disintegrate and subsequently broke down into pebble sized flakes. During the second cycle these flakes tended to break down further as newly defined edges were worn down by the abrasive nature of the experiment. The weakness of this sample has been attributed more to deformational processes then primary physical properties.

2.5 Mechanical Properties

2.5.1. Methods and Procedures

Intact rock strength estimates are used, along with the physical properties, to help with the determination of slope stability. Identifying the mechanical properties associated with each stratigraphic unit, with regards to rock mass characteristics, helps define factors associated with instability for any proposed highwall. Intact rock variables help, along with rock mass properties, to derive a workable Factor of Safety, for any given slope, which ultimately leads to the calculation of the economic viability of any opencast mining program based on cost of stripping overburden per unit of recoverable ore (Hoek & Bray 1977).

The laboratory programme was designed to quantify the intact rock strength of the stratigraphic units using available techniques. Samples were obtained to meet the criteria for sample length and smoothness (laterally), and that had no visible defects. The testing programme combined three separate tests; Brazilian testing, Unconfined Compressive Strength testing, and Triaxial Compression testing. The UCS and Triaxial tests were used to help define a Mohr Coulomb failure envelope for each of the stratigraphic units. The Brazilian test was decided upon to develop a comparative relationship between the force

applied during tensile splitting failure and overall Unconfined Compressive Strength, which also allows the determination of UCS for samples that do not meet the length requirements (>150mm). The tests defined the parameters of friction angle and cohesion, which form part of any Hoek Brown rock mass analyses.

The UCS and Triaxial tests were carried out to specifications by the International Society for Rock Mechanics (ISRM 1981) standard testing procedures while the Brazilian tests followed ISRM (1977). All tests were carried out on HQ sized core samples (61mm) in the Rock Mechanics Laboratory, Department of Geological Sciences, University of Canterbury. UCS and Triaxial tests were carried out using core samples with a length-to-diameter ratio (L:D) as close to 2.5 as possible and lateral axis not deviating by more that 0.25 degrees. The L:D ratio of 2.5 was chosen due to discrepancies in testing procedures with the American Society for Testing and Materials opting for a specimen ratio of 2.0-2.5 (1968) and the ISRM opting for a specimen ratio of 2.5-3.0 (1981). Brazilian testing was carried out on test samples with a length no greater then the sample diameter (L:D ratio < 1). All test were carried out under fully saturated conditions, as insitu moisture content could not be guaranteed in most cases. Samples were tested under fully saturated conditions under recommendation by ISRM (1981) standards as it is commonly accepted that rock samples are at there weakest under these conditions. Testing methods for each of the mechanical tests are outlined in appendix 2 along with all tabulated raw data and failure mechanism.

2.5.2 Unconfined Uniaxial Compression

2.5.2.1 Test Methodology

The methodology of this test is intended to measure the Unconfined Compressive Strength (UCS) of the intact rock samples. The test is mainly intended for strength classification and characterisation of intact rock (σ_c), and the UCS test is by far the most common laboratory test undertaken for rock mechanic studies (Hudson 1993) being the basis for numerous design methods. The intact rock strength is one of the primary measures for predicting rock performance, with the objective set forth by this type of

testing to define the overall compressive strength of the stratigraphic units. These tests can also be used in the assessment of the rippability of the overburden units' e.g. future determination of blasting requirements.

The UCS results are compared with the physical properties, as a rock with high density and low porosity (e.g. siltstone) typically yields higher strength σ_c values due to the greater degree of cementation and denser packing of grains, than a lower density and higher porosity rock (e.g. coarse sandstone) (Lucas 2002).

2.5.2.2 Results and Discussion

Table 2.4 provides a summary of the results obtained during testing, with analysis of individual unit results below. Graphical relationships are then discussed in relation to physical properties presented in previous sections. Data incorporated in table 2.4 was obtained by viable failure mechanisms, these are,

- Cataclastic (C) – internal crushing and collapse.
- Longitudinal Shearing (LS) – fracture along a single shear plane.
- Conjugate Shear Fracturing (CSF)– fracture along conjugate shear planes.

The following table is a summary of the results from the UCS tests carried out.

Table 2.4 Summary of UCS for Geotechnical Units (1.1, 2.2, 3.1, & 3.2).

Unit	Berlins Porphyry Granite Unit 3.2 -3.2b	Greenland Group Hornfels Unit 3.1	Brunner coal measures Bio – Sandstone Units 2.2	Kaiata Mudstone Massive Unit Unit 1.1	Mixed Basement Laminated interfingering Mixed Unit 3.1/3.2
Number Tested	3	1	3	15	3
Compressive Strength (σ_{csat})					
Average Strength (MPa)	78.2	136.1	15.3	9.9	47.0
Range	72.8-84.8	136.1	12.0-19.8	8.3-11.0	18.1-97.1
Saturated Density (Kg/m^3)					
Average Density	2681	2677	2489	2476	2680
Range	2671-2706	N/A	2466-2513	2408-2593	2616-2744

* tested under saturated conditions

Individual results and failure mechanisms for each of the samples are included in the tabulated data in appendix 2, with representative failure models below (figure 2.7 & figure 2.8).

- **Berlins Porphyry:** This unit has the most variable strength (including weathered samples) of all the geotechnical units, with results ranging from only a few MPa for highly weathered samples (outlined in test results appendix 2) which fall apart with little external pressures, to a marble like texture with compressional strengths (84.8MPa). Due to interaction with the MWFZ, and its zone of influence, it is common for samples from a depth of 70 meters to still exhibit a slight degree of weathering. Only a limited amount of defect free samples could be obtained over any particular depth at the required length (>150mm).

- **Greenland Group Hornfels:** This unit exhibited the highest compressive strength of all the stratigraphic units (MPa = 136.1). Representative samples were hard to obtain over the length required for UCS and triaxial due to the disruptive nature of the MWFZ, and as such testing was limited to one sample without the influence of existing defects (failure along existing defects) Weathering effects on the samples collected tended to be limited to within a few mm of the fractures with all but the most exposed samples still retaining the intact rock strength.

- **Brunner Coal Measures:** This unit has the second lowest compressive strength with a value of 15.3MPa. Variations in the results for the three samples are minimal and may be due to compositional variations between the drill holes from which the samples were taken. All samples exhibited the same amount of slight weathering and were obtained from the same lithography.

- **Kaiata Mudstone** This unit has the lowest compressive strength with a value less then 10 MPa. Variations in the strength results had minimal variation with

a low range (2.7MPa). Samples exhibited slight to no weathering effects throughout the Kaiata formation.

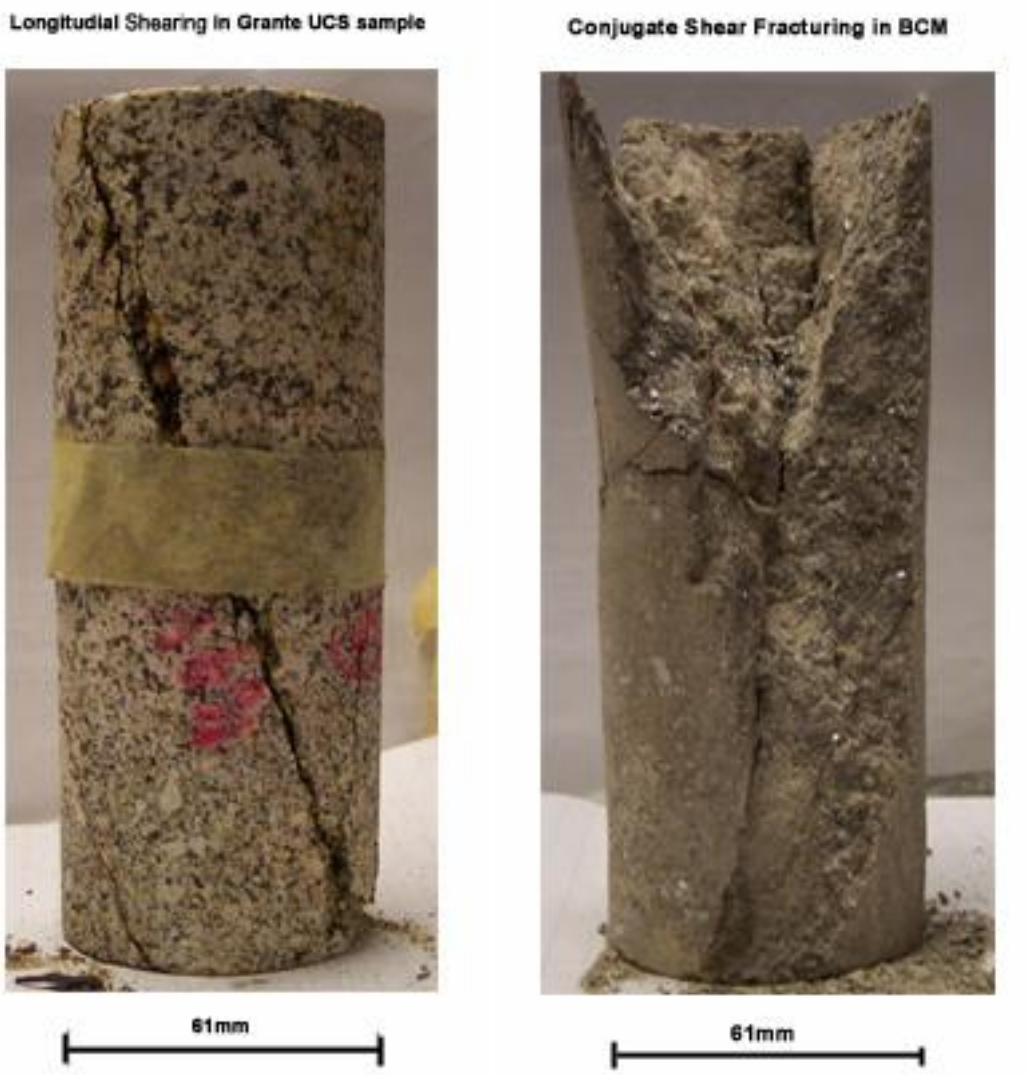

Figure 2.7. Core samples after UCS testing, displaying Longitudinal Shearing (LS) in granite unit 3.2 (left photo), and conjugate shear fracturing (conical failure) in Brunner Coal Measure Unit 2.2 (right photo).

- **Mixed Basement** This unit exhibits the greatest variation in composition which resulted in an inconclusive result with regards to a mean standardised compressive strength for this particular geotechnical unit. As such the minimum result was chosen as the guideline for any statistical analysis to be carried out

with an average compressive strength (47.0MPa). The range within the results gives it a variability that mimics that of the Berlins Porphyry unit.

Figure 2.8. Weathered Berlins UCS core displaying cataclastic failure.

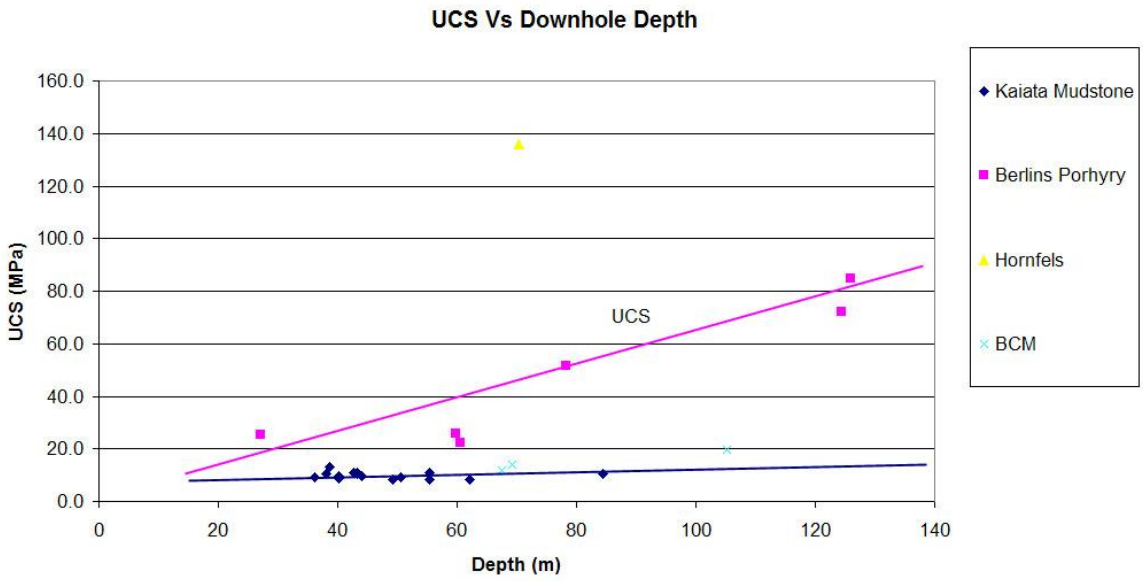

Figure 2.9. Graph of UCS (σ_{csat}) versus Down Hole depth (m). (values include weathered B/P)

Figure 2.9 shows the relationship between the different stratigraphic units with regards to downhole vertical depth (m) and overall saturated compressive strength (σ_{csat}). The lines of best fit associated with the Berlins Porphyry and the Kaiata Mudstone show the projected strength of the samples with regards to depth. The graph highlights the relationship in the Berlins Porphyry which shows that an increase in the depth of the sample (and therefore a decrease in the degree of weathering) results in an increase in overall compressive strength, a trend which is not exhibited in the Kaiata mudstone. The degree of weathering associated with the Berlins Porphyry is also directly related to the depth downhole with initial signs of weathering starting at depths greater then 60 metres. Increased degrees of weathering are responsible for increased porosity and decreased density which contributes to the decrease in compressive strength. In contrast the there seems to be little to no variation in the resulting compressive strength of the Kaiata mudstone with respect to depth which lends to the conclusion that penetrative weathering effects on the unit is limited to shallow depths. The lack of comprehensive data on the other units leads to an inconclusive relationship between depth of sample/weathering effects and overall compressive strength. Studies tend to show that the hornfels group is resistant to weathering effects with only localized staining prevalent in cored samples.

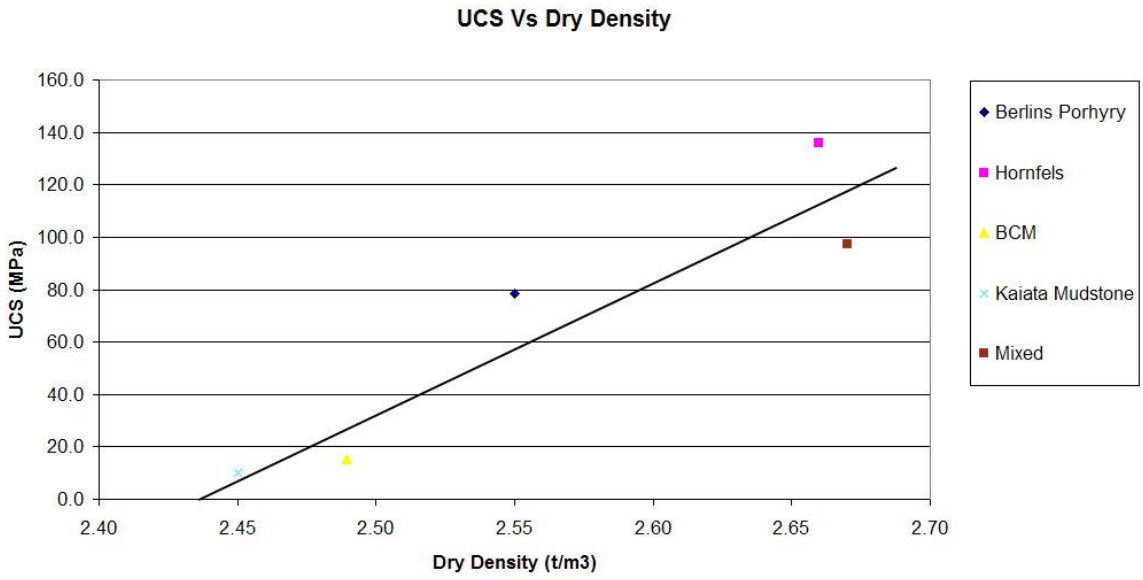

Figure 2.10. Graph of UCS (σ_{csat}) versus Dry Density (ρ_d)..

Figure 2.10 shows the relationship between the different stratigraphic units with regards to Dry Density (ρ_d) and overall compressive strength (σ_{csat}). The trend shows that an increase in dry density is accompanied by an increase in compressive strength with the basement units.

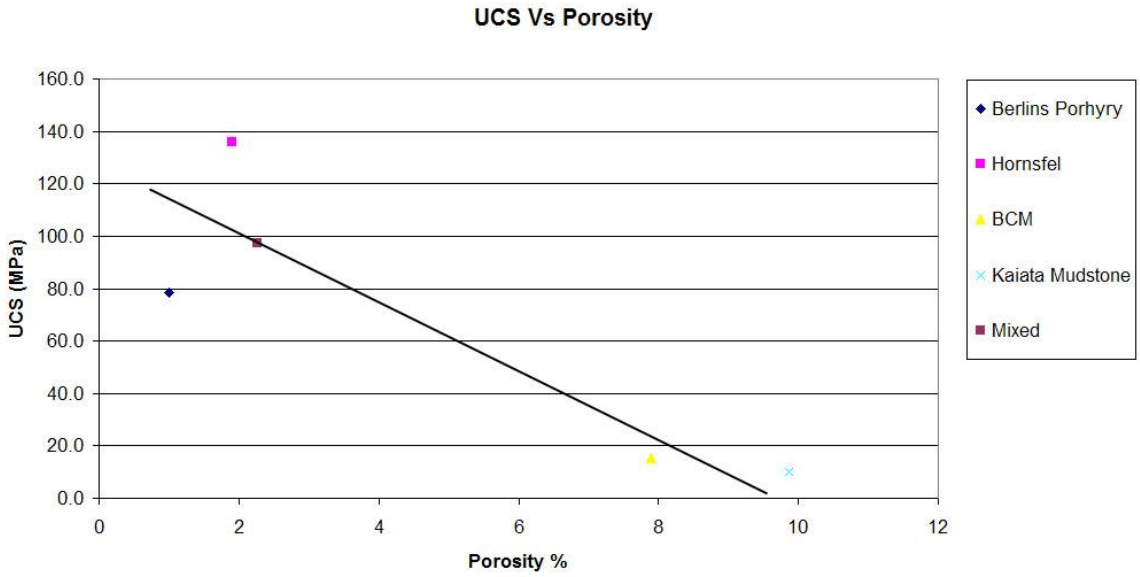

Figure 2.11 Graph of UCS (σ_{csat}) versus Porosity (n).

Figure 2.11 shows the relationship between the different stratigraphic units with regards to porosity (n) and overall uniaxial compressive strength (σ_{csat}). The graph displays a negative trend, with a decrease in porosity accompanied by an increase in the compressive strength. This is an opposite relationship to that observed in figure 2.9 as expected with the porosity and density relationship outlined back in figure 2.6. This graph also highlights the negative effect that porosity has on the effective strength of intact rock samples.

2.5.4 Brazilian Test (tensile splitting)

2.5.3.1 Test Methodology

The Brazilian test is generally useful for all rocks with unconfined strengths greater than about 5 MPa (Hudson 1993). The test can be performed on very short core specimens (less that 25mm) and is therefore very useful when only short core lengths are available. There is generally correlation between UCS and Brazilian tensile strength, and once this correlation is established for a particular rock type it is possible to carry out Brazilian tests to determine UCS for the rock samples. This is beneficial due to the need to have sizable undisturbed core lengths to carry out the UCS testing, and the bias this may introduce into mean results.

Comparisons have been made between Brazilian testing and Direct Uniaxial Tensile testing, with Brazilian testing being the preferred method as the test can be done on very short lengths (25mm) of core which means that the test details are therefore not biased by the need to have quality rock at a particular size (typically 150mm – 300mm). The second reason Brazilian testing is preferred is that during sample preparation with Brazilian samples do not requiring the ends to be ground flat and parallel. Thirdly, the test apparatus for Brazilian testing is relatively simple as outlined in the ISRM (1977) suggested test procedures.

2.5.3.2 Results and discussions

Table 2.5 provides a summary of the test results obtained during testing procedures with analysis of individual unit results below. Graphical relationships are then discussed in relation to physical properties tested in previous sections as well as comparisons and correlation with UCS testing. Failure mechanisms for each of the Brazilian test results are displayed with testing procedures and raw data (appendix 2) with representative samples given below (figure 2.12). The following table summarises the results of the Brazilian tests with complete test results included in appendix 2.

Table 2.5 Summary of Brazilian Test Results with direct comparison to average UCS.

Unit	Berlins Porphyry Granite Unit 3.2 -3.2b	Greenland Group Hornfels Unit 3.1	Brunner coal measures Bio – Sandstone Units 2.1,2.2,	Kaiata Mudstone Massive Unit Unit 1.1	Mixed Basement interfingering Units 3.1/3.2	Berlins Porphyry (Mod Weathered) Granite Unit 3.2b
Number Tested	9	3	2	16	5	3
Brazilian Test (σ_t) Strength (MPa)	6.18	5.08	1.32	1.47	5.51	2.74
Range	5.03-8.40	3.17-6.14	1.21-1.43	1.12-1.87	2.89 -12.39	2.21-3.19
Compressive Strength (σ_{csat})						
Average Strength (MPa)	78.5	136.1	15.27	9.9	47.0	23.85
Range	72.2-84.8	136.1	12.0-19.8	8.3-11.0	18.1-97.1	22.5-25.2

- **Berlins Porphyry:** This unit exhibited the highest average tensile strengths (6.18MPa) of all the stratigraphic units but, as with both USC testing and the physical properties, displays greatest variation in tested samples when incorporating the weakened weathered samples. As seen with the UCS testing samples tensile strength increases marketedly with depth of sample. Moderate degree of weathering sees the tensile strength decrease by over 50% (2.74MPa) which leads to the conclusion that overall unit strength is highly dependant on degree of weathering. This variation in the strength of the Berlins Porphyry with respect to weathering allows better correlation between compressive and tensile strengths (figure 2.15).

- **Greenland Group Hornfels:** This unit displayed the third highest average tensile strength (5.08MPa), with moderate variation in tested samples. Lack of comparative samples to test UCS to Brazilian relationship meant that no further comparison can be made with regards to direct correlation between the two tests.

- **Mixed Basement:** This unit displayed great variability in the average tensile strength (5.51MPa), recording the two highest individual results (12.39MPa and 10.48MPa). The variability of the testing samples means classifying the tensile

strength should be confined to the lowest recorded results (2.63MPa). An increased sample range, with classification of weathering, will help better define the average tensile strength for this unit. Results show, as seen with UCS testing, that variability is proportional to the degree of weathering.

- **Brunner Coal Measures:** This unit displayed the lowest of the recorded tensile strengths (1.32MPa) with a ratio of ~10:1 between compressive and tensile strengths. Limited samples were available for testing in attempts to find a correlation between UCS and Brazilian tests. Representative samples were taken for both tests, but showed inconsistent results and without increase sample base no correlation between the two tests can be determined.

- **Kaiata Mudstone** This unit recorded the second lowest average tensile strength (1.47MPa). The unit showed the greatest consistency with only minor variation seen over the 16 samples (0.6 MPa) and as such a good correlation was achieved over the test range (graphical relationships figure 2.16).

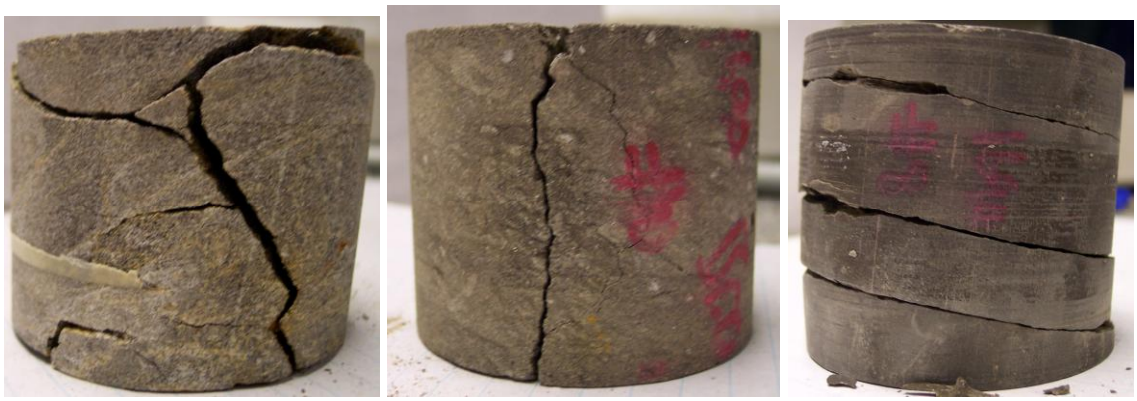

Figure 2.12 Examples of Modes of Failure in Brazilian Test, from left to right; Cataclastic failure (C), Central Splitting(CS), and Bedding Failure (BF). (Representative samples are of average core width (61mm))

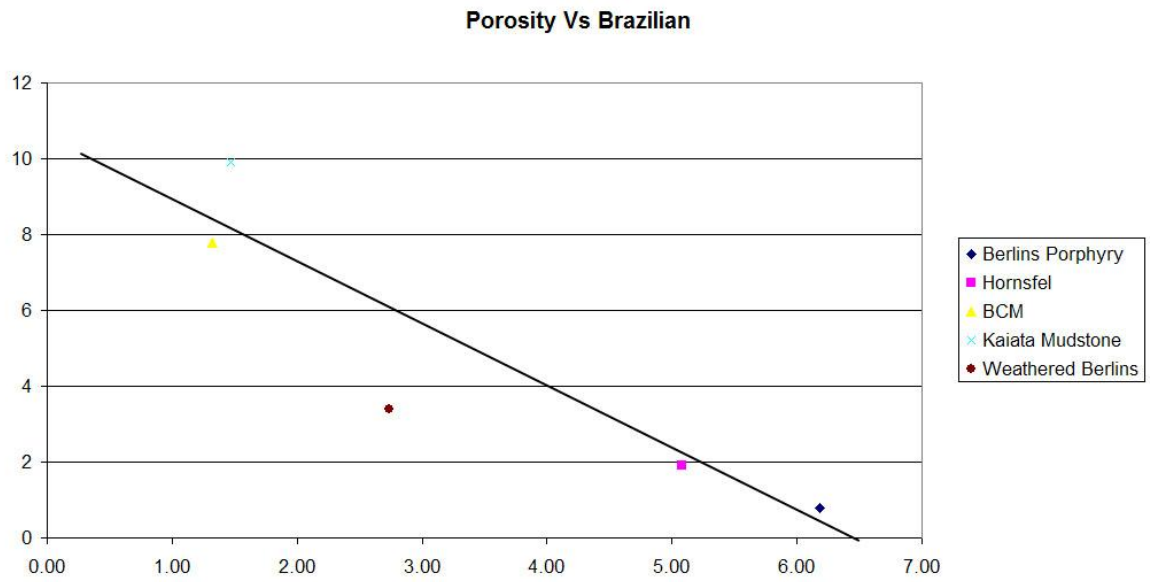

Figure 2.13. Graph of Tensile Strength(σ_t) Vs Porosity (n).

Figure 2.13 shows the relationship between the different stratigraphic units with regards to Porosity (n) and overall tensile strength (σ_t). The graph highlights the negative effect that porosity has on the tensile strength, with samples having a high porosity having a comparatively lower tensile strength. Samples with a low porosity show a significant increase in their respective tensile strengths highlighting the effect of pore spacing on tensile strengths as it does in unconfined compressive strengths.

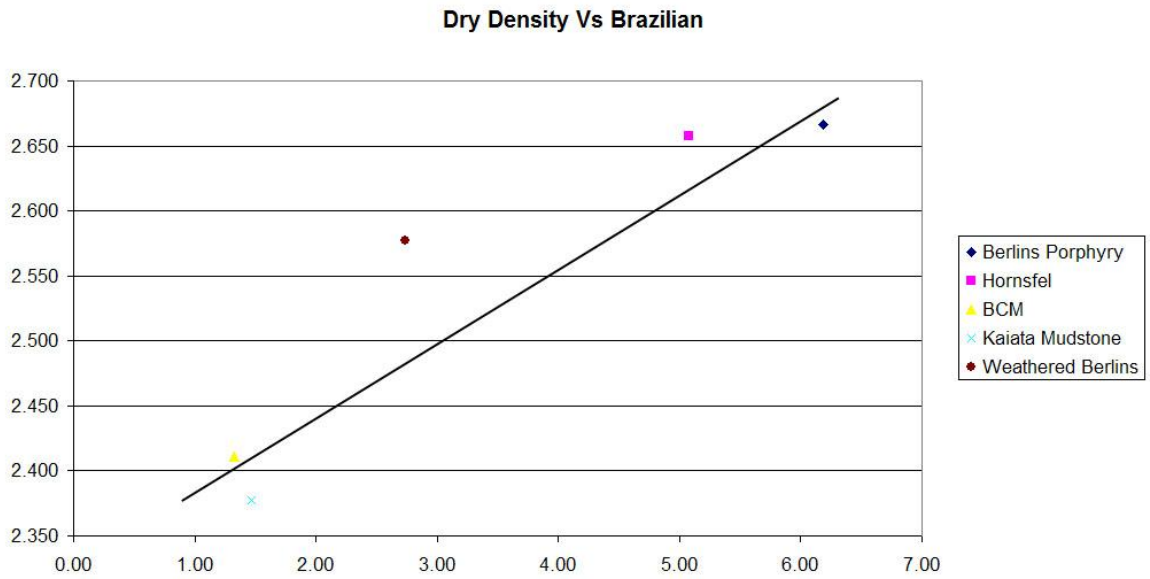

Figure 2.14. Graph of Tensile Strength(σ_t) Vs Dry Density (ρ_d).

Figure 2.14 shows the relationship between the different stratigraphic units with regards to Dry Density (ρ_d) and overall Tensile Strength (σ_t) The graph highlights a positive relationship with higher density units having increased tensile strength. This again confirms the relationship between porosity and density (figure 2.6)

Table 2.6 Correlation between UCS and Brazilian Testing

	Unit	UCS	Tensile	$\sigma_{(c)}$ $\sigma_{(t)}$	Mean Ratio
Weaker Rock Units (MPa <20)	Mudstone	10.3	1.87	5.5	6.9
		13.2	1.41	9.4	
		9	1.27	7.1	
		11	1.65	6.7	
		10.6	1.64	6.5	
		9.6	1.39	6.9	
		8.3	1.29	6.4	
	BCM	12	1.43	8.4	10.0
		14	1.21	11.6	
Harder Rock Units (MPa >20)	Hornfels	136.4	6.03	22.6	22.6
	Mixed	97.1	12.39	7.8	8.4
		25.8	2.86	9.0	
	B/P	51.4	5.4	9.5	10.7
		72.2	5.72	12.6	
		84.8	8.4	10.1	

Figure 2.15 shows the relationship between the stronger stratigraphic units (table 2.6) with regards to unconfined compressive (σ_{Csat}) and tensile (σ_t) strengths. The graph shows a correlation between the two tested strengths with a low tensile strength indicating a relative low in the unconfined compressive strength. The equation for the line of best fit for the Berlins Porphyry ($y=8.13x + 18 \pm 8$) allows for a general correlation of UCS samples derived from Brazilian testing. A greater sample range is necessary to confine the uncertainty associated with this calculation. The mixed basement samples, incorporated in the graphical results, show a continued trend with a shift in the y intercept of the equation

(y= 8.13x +8). A greater number of testable samples need to be acquired to further develop this relationship. The only Greenland Group sample provided a ratio of 22.6:1 between the UCS and Brazilian results with more samples required to better constrain this ratio. As with both the UCS and the Brazilian the effect of porosity and dry density greatly affect the overall trend seen.

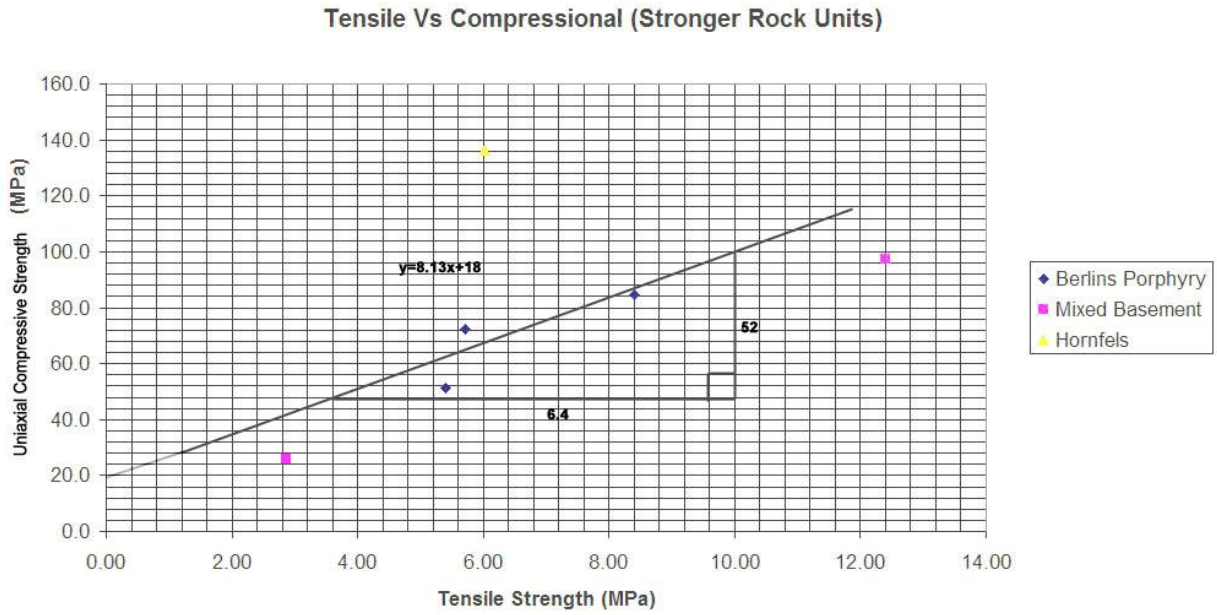

Figure 2.15 Graph of Tensile Strength (σ_t) Vs UCS for the Stronger Rock Units (σ_{Csat}).

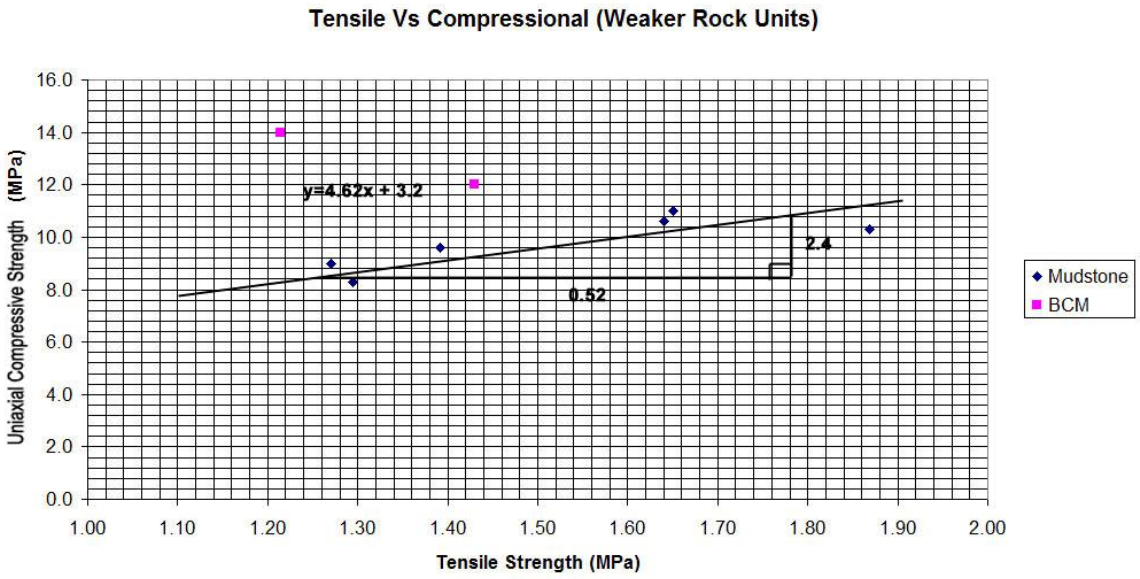

Figure 2.16. Graph of Tensile Strength (σ_t) Vs UCS for the Weaker Rock Units (σ_{Csat}).

Figure 2.16 shows the relationship between the weaker stratigraphic (table 2.6) units with regards to Unconfined Compressive (σ_{Csat}) and Tensile (σ_t) strengths. The graph highlights an overall correlation between the two tested strengths with a decrease tensile strength indicating a relative decrease in the unconfined compressive strength. The equation for the line of best fit ($y=4.62x + 3.2 \pm 0.8$) allows the calculation of UCS samples derived from Brazilian testing of the Kaiata Mudstone. The sample range was sufficient to correlate the tensile strength to that of the unconfined compressive strength, increased testing of sample would be useful to continue to confine the uncertainty associated with this calculation.

2.5.4 Triaxial Compression Test

2.5.4.1 Test Methodology

The Triaxial testing was performed on representative samples from each of the stratigraphic units (except Greenland group due to lack of intact samples) to the specifications outlined by the ISRM (1981) recommended testing procedure for Triaxial Compression. Testing was carried out using a standard triaxial cell on HQ core with a L/D ratio of 2.5. External testing by Strata Testing Services Ltd, NSW, Australia, was also included in these results (tested with L:D ratio of ~2.0). A strength envelope was then obtained by fitting mean curve to the confining pressures and the corresponding compressive strength values using the RocLab programme (Rocscience Inc 2003) and Hoek-Brown Criterion (2002). This determined the equation for the envelope of best fit and the gradient of curve (*m*) and the Y intercept (*b*). Using the parameters *m* and *b*, the internal friction angle (Ø) and a value for the apparent cohesion (*C*) were then calculated. Samples representing each of the stratigraphic units were tested at three different confining pressures which simulated the insitu rock environment. Specimens tested in the laboratory were fully saturated with load applied parallel to core sampling. The methodology and the tabulated raw data are outline in appendix 2.

2.5.4.1. Results and Discussion

Table 2.7 presents the summary of Triaxial results for each of the stratigraphic units after the data was processed using the RocLab programme (Rocscience 2003). Rocklab calculated a best fit Mohr-Coulomb failure envelope and in turn retained values for both Cohesion (C) and friction angle. The results show that the stratigraphic units which had stronger overall unconfined compressive strength displayed a higher degree of cohesion and a higher angle of friction. The Berlins Porphyry unit retained the highest degree of cohesion (C=6.38MPa) with the Bioturbated Sandstone (BCM) exhibiting the lowest (C= 2.11MPa). The Kaiata Mudstone unit displayed the lowest friction angle (Ø= 18.6º) with the mixed basement unit displaying the highest (Ø=44.5º). All results included in the triaxial tests failed either by longitudinal shearing or by Cataclastic failure (figures 2.7 and 2.8) with longitudinal shearing more prevalent. Cohesion was derived using the equation:

$$C = b\,\frac{1-\sin\emptyset}{2\cos\emptyset}$$

Table 2.7 Summary of Friction Angle (Ø) and Apparent Cohesion (*C*)

Unit	Berlins Porphyry Granite Unit 3.2 -3.2b	Brunner coal Measures Bio – Sandstone Units 2.1,2.2	Brunner Coal Measures Med fine Sand Units 2.5	Kaiata Mudstone Massive Unit Unit 1.1	Mixed Basement interfingering Units 3.1/3.2
Cohesion (C)(MPa)	6.4	2.1	4.0	3.0	2.9
Friction Angle (Ø)	40.6	33.2	31.4	18.6	44.5
Intact Compressive Strength (b intercept) (σ_{ci})	27.7	7.8	14.4	8.4	14.2

Mohr stress diagrams generated using the RocLab programme, following Hoek-Brown classification, are represented below in figures 2.17-2.21.

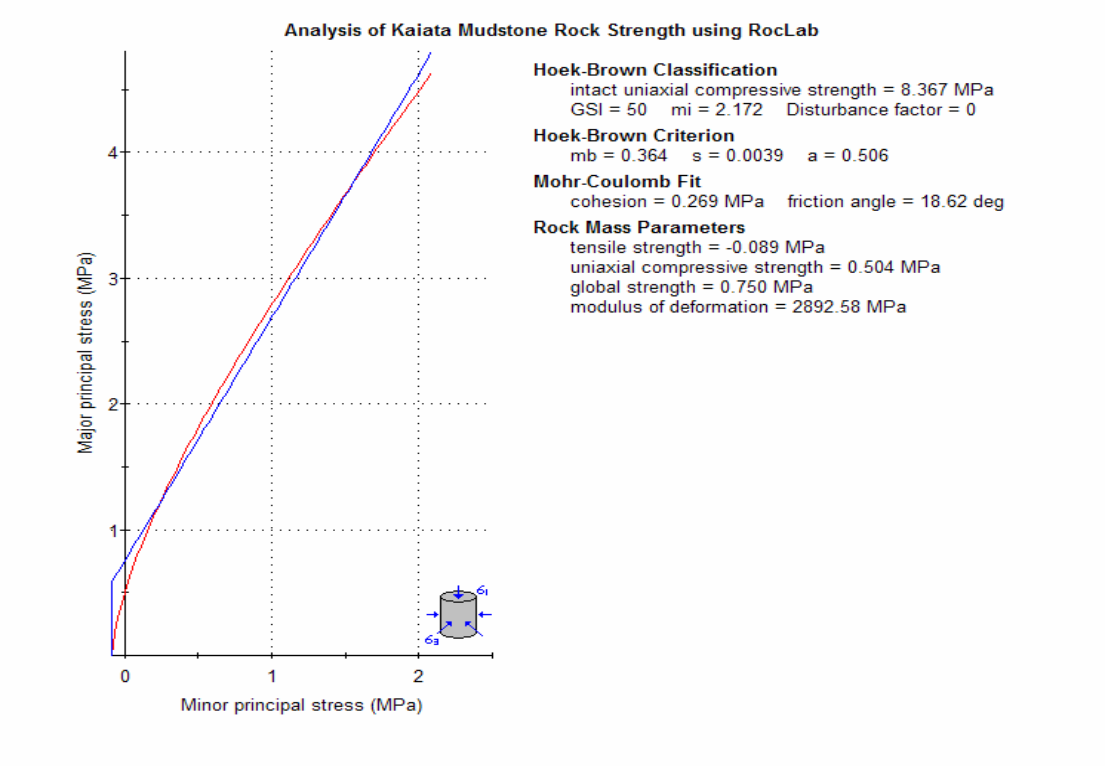

Figure 2.17. Mohr stress diagram of σ_1 Vs σ_3 for Kaiata Mudstone (using Roclab programme).

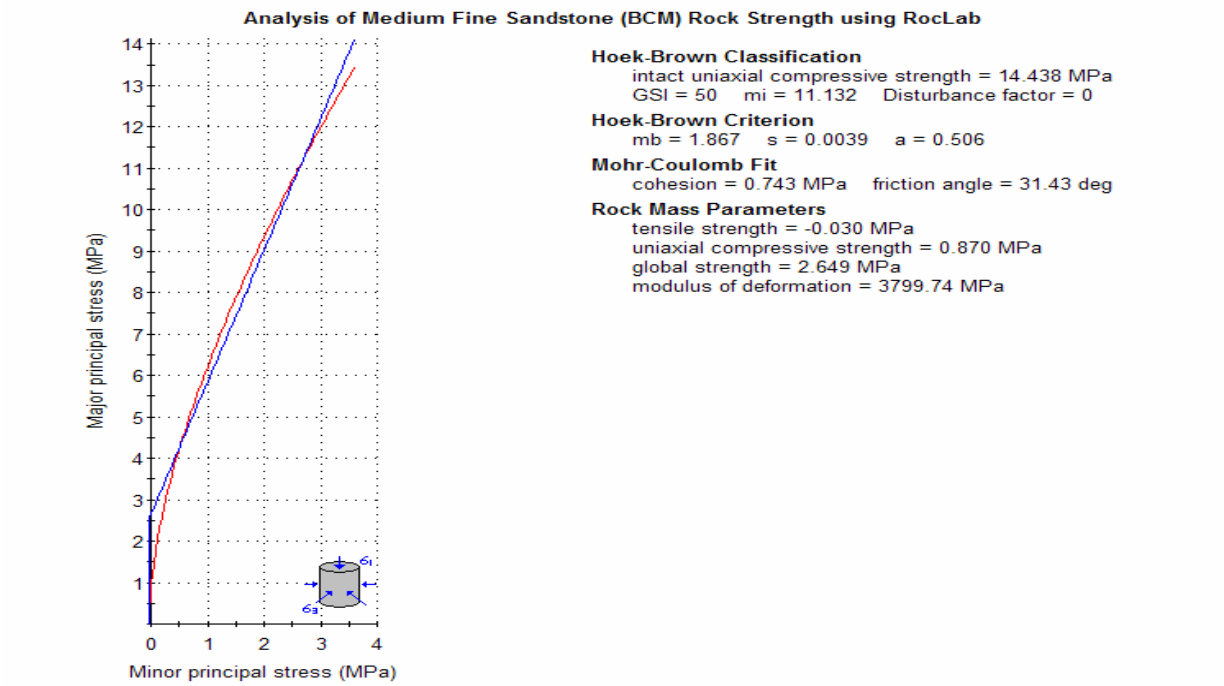

Figure 2.18. Mohr stress diagram of σ_1 Vs σ_3 for Medium Fine Sandstone (BCM) (using Roclab programme).

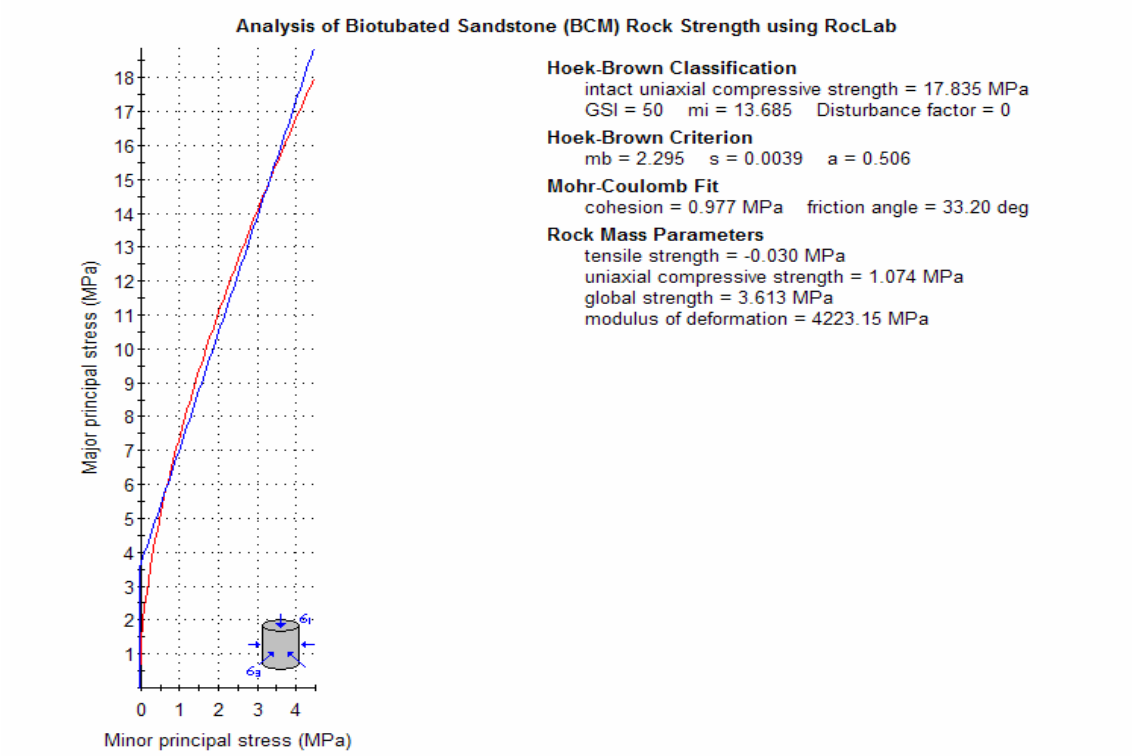

Figure 2.19. Mohr stress diagram of σ_1 Vs σ_3 for Bioturbated Sandstone (BCM) (using Roclab programme).

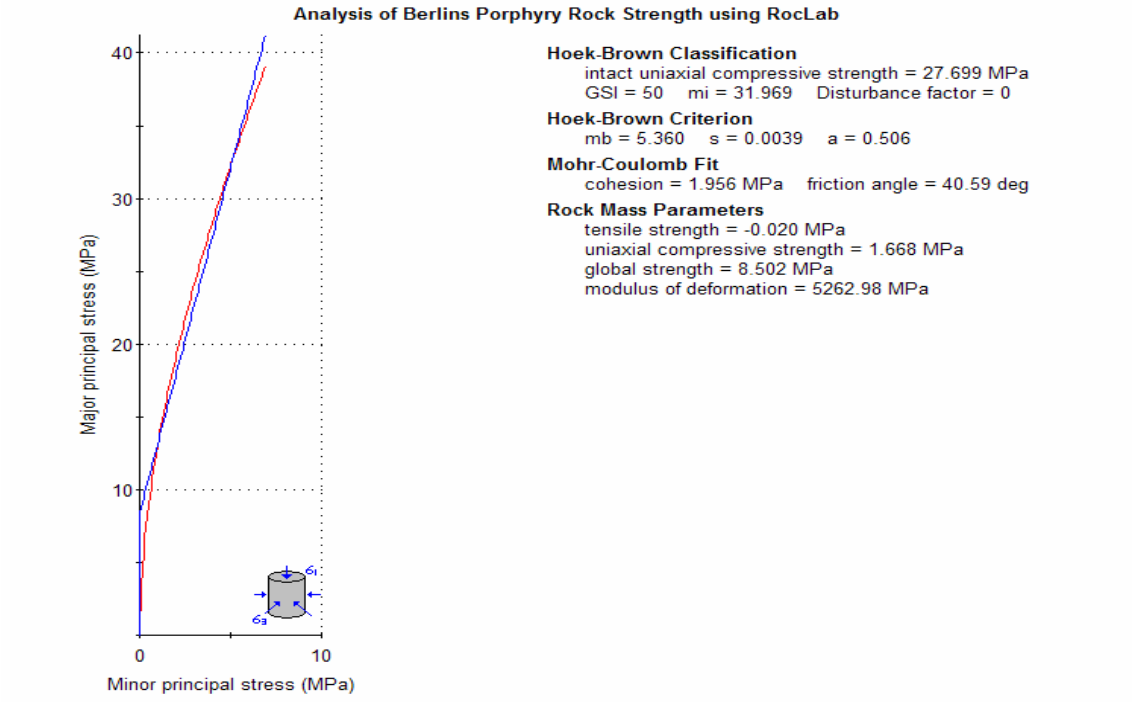

Figure 2.20. Mohr stress diagram of σ_1 Vs σ_3 for Berlins Porphyry (using Roclab programme).

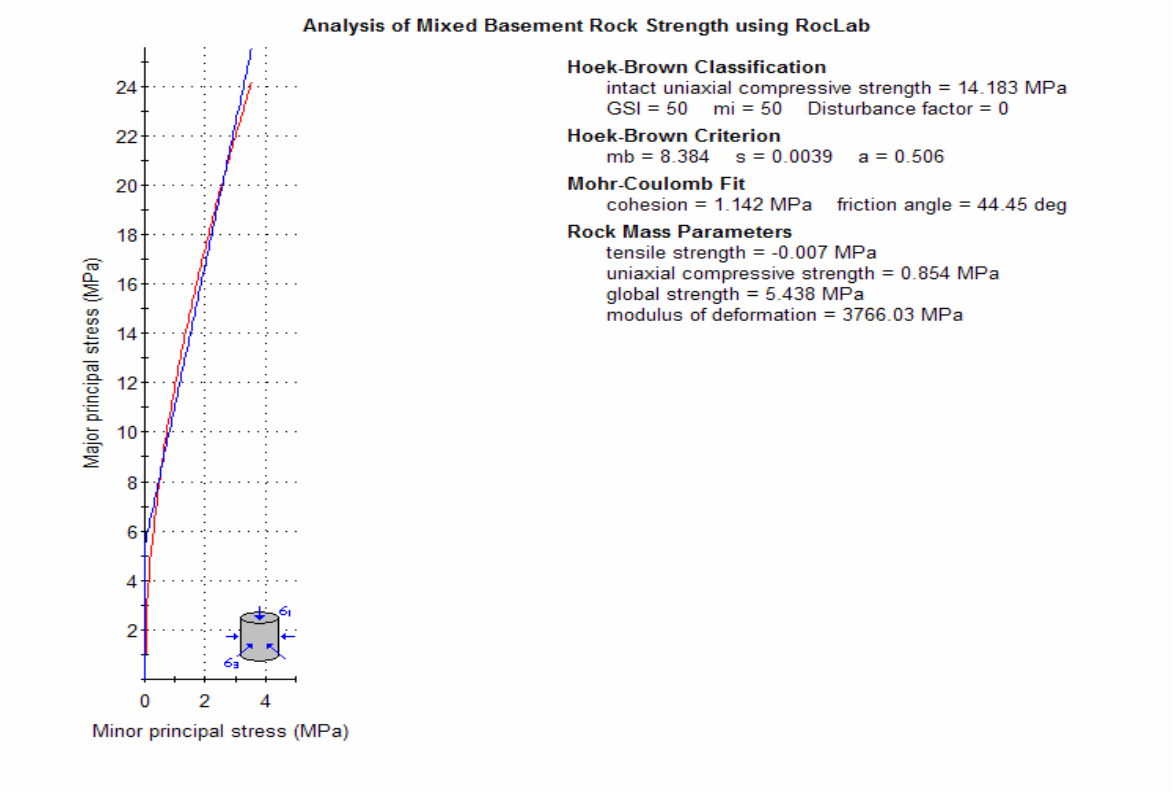

Figure 2.21. Mohr stress diagram of σ_1 vs σ_3 for Mixed Basement (using Roclab programme).

*The Mohr Coulomb Fit Outlines in blue for all figures

Correlation can be derived from the Hoek-Brown Criterion (Ø & σ_{ci}) with relation to the physical and mechanical properties of each of the stratigraphic units. A relationship between stratigraphic units with high internal friction angle and increased grain size can be seen from the results. A greater value for cohesion also is observed with an increased grain size which is directly controlled by the roughness of the grain interaction.

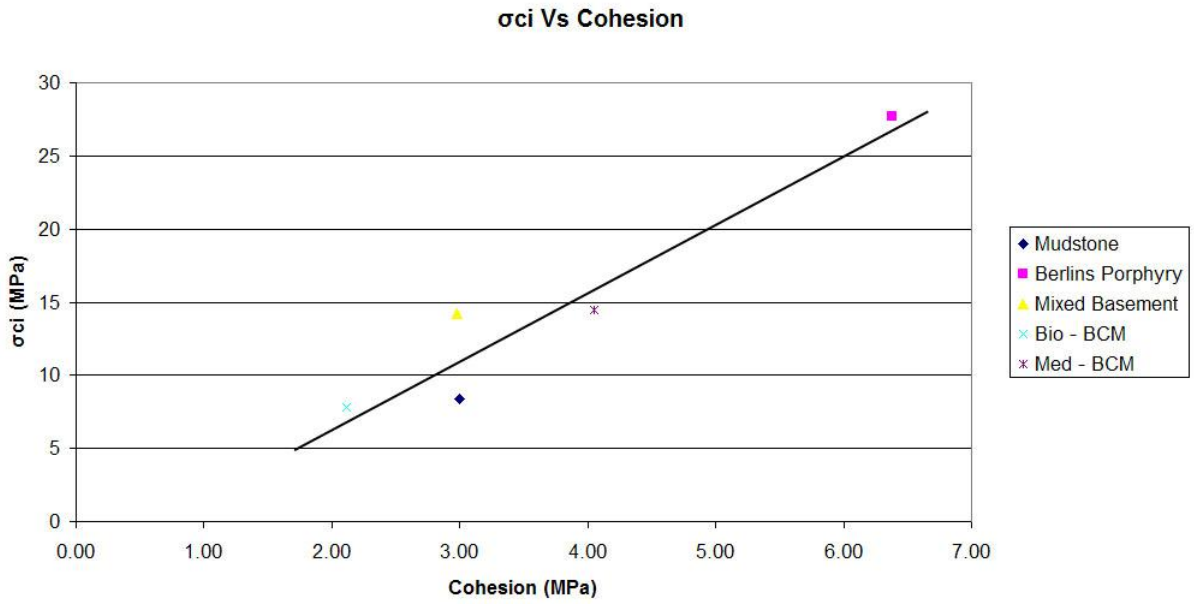

Figure 2.22. Graph of σ_{ci} vs Cohesion (*C*)

Figure 2.22 displays a moderately strong correlation between intact compressive strength (σ_{ci}) and apparent cohesion (*C*). The tends to indicate that there is a general indication between the intact compressive strength and cohesion in a samples, but other controlling factors are involved and need to be taken into consideration. The intact uniaxial compressive strength relates to the initial intact rock mass strength as determined by the tangent to the line of best fit of the Mohr circle. Other initial factors which would need to be taken into account are the porosity (higher porosity, lower cohesion), foliation (inherit weakness along foliations), and Bedding (weakness in the direction of bedding due to orientation of grains and added strength against the grain). Secondary influences which could influence cohesion could be degree of weathering (breakdown in physical bonds) and prolonged strain in direction of failure (weakening of physical bonds). Figure 2.23 also outlines this relationship with the intact compressive strength displaying the same moderate trend.

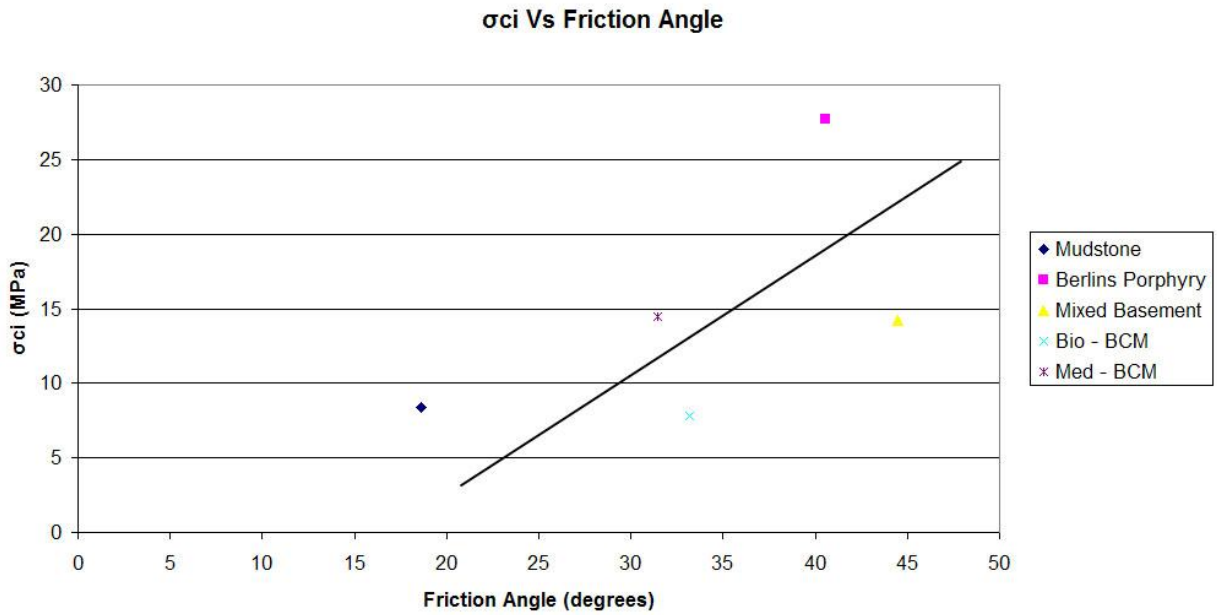

Figure 2.23 Graph of σ_{ci} Vs friction Angle (Ø).

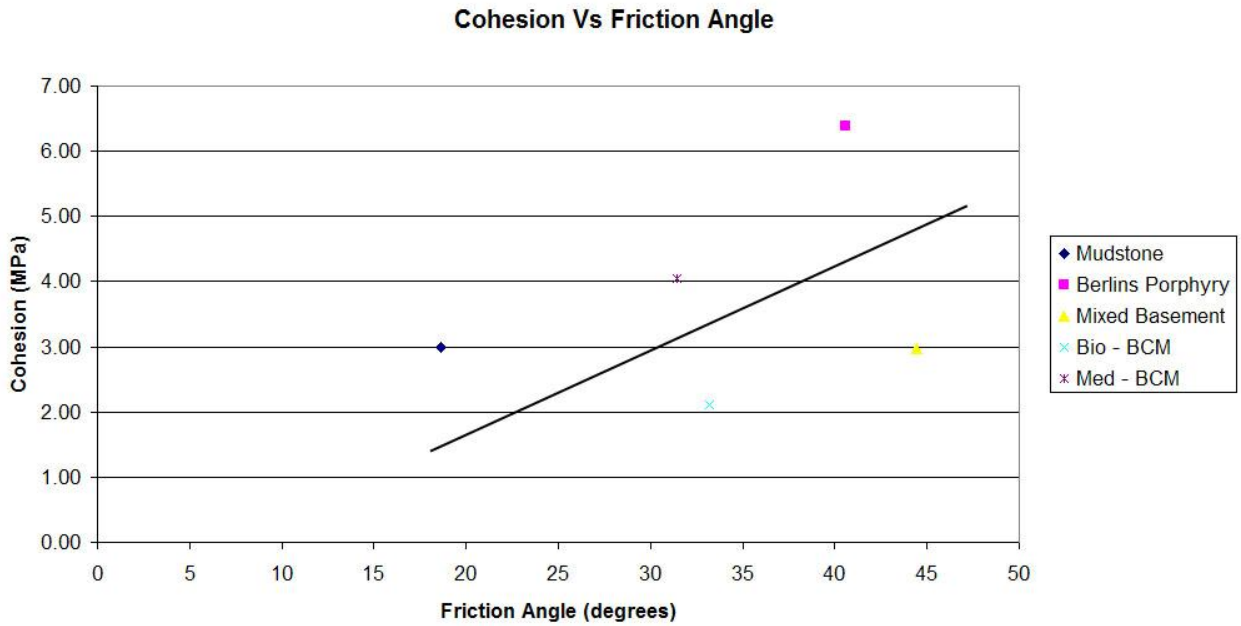

Figure 2.24 Graph of Friction Angle (Ø) Vs Cohesion (C)

Figure 2.24 shows a direct relationship between the friction angle and cohesion, with a weak correlation between the two parameters which mimics that of figure 2.23. The graph shows the positive trend within the geotechnical units with an increased friction angles showing a relatively high cohesion value. The mixed basement, and the bioturbated

BCM units show a variation from the trend having higher friction angles but still retaining low cohesion values. One interpretation of this is that these units have weaker inter-granular bonds.

2.6 Summary of Physical and Mechanical Testing

Table 2.8 provides a summary of the rock material classification for both the physical and mechanical properties. The physical properties outlined are porosity, density and slake durability index. Porosity determination showed a large variation between the geotechnical units tested with the Berlins Porphyry having the lowest porosity (n=0.8%) and the Kaiata mudstone having the highest (n=9.9%). Density showed a reverse correlation with the Kaiata mudstone exhibiting the lowest mean densities (2377Kg/m^3) and the Berlins Porphyry showing the highest (2666Kg/m^3). Slake durability index testing showed a high durability for all units tested with Berlins Porphyry showing the highest retained mass (99% retained).

The Mechanical properties showed the highest compressive strength (UCS) belonging to the Greenland Group formation (136.1MPa) and the lowest exhibited by the Kaiata formation (9.9 MPa). Tensile Splitting tests showed a moderate variation between the units with the Berlins Porphyry having the highest (6.4 MPa) and the BCM with the lowest (1.3 MPa). Triaxial testing of the samples showed that the Berlins Porphyry had the highest intact compressive strength (27.7 MPa) and cohesion (6.6 MPa), and the mixed basement unit with the highest friction angle (44.5º). The BCM had both the lowest intact compressive strength (7.8 MPa) and cohesion (2.1 MPa), with the Kaiata Mudstone having the lowest friction angle (18.6º)

Table 2.8. Summary table of average physical and mechanical properties

	Berlins Porphyry	Greenland Group Hornfels	Brunner Coal Measures Bioturbated sandstone	Kaiata Mudstone	Mixed Basement
Porosity (n)(%)	0.8	1.9	7.9	9.9	2.3
Dry Density (Kg/m3)	2666	2658	2411	2377	2657
Saturated Density(Kg/m3)	2681	2677	2489	2476	2680
Slake-Durability (I_{d2}) (%)	99.0	99.6	94.0	94.5	N/A
UCS (MPa)	78.2	136.1	15.27	9.9	47.0
Tensile Strength (MPa)	6.2	5.1	1.3	1.5	5.5
σ_{ci} (MPa)	27.7	N/A	7.8	8.4	14.2
Cohesion (c') (MPa)	6.4	N/A	2.1	3.0	3.0
Friction Angle (Ø)	40.6	N/A	33.2	18.6	44.5

During testing there was limited delineation of the geotechnical units, initially outlined using the drillhole logs, as limited samples meant that differentiation between the units could not always be achieved. Limitations were observed within all the stratigraphic units for varying reasons.

The majority of the Kaiata mudstone (units 1.1 and 1.2) is comprised of the massive silty mudstone (unit 1.1) which made up ~90% of the recovered samples within this layer and meant that there were limited samples associated with the sandy lithology (unit 1.2). Testing was carried out on both units with variation in the results obtained indistinguishable between the two geotechnical units and therefore treated as having homogeneity.

Limited samples within BCM due to low recovered core saw the viability in testing only the bioturbated massive med – coarse units (2.1 and 2.2), further testing will need to be carried out to establish the rock material classification of the other lithographies.

The basement lithographical units (3.1 & 3.2) exhibited high degrees of brittle deformation which resulted in poor recovery of suitable samples for testing. The Greenland

Group lithology (unit 3.1) showed a higher degree of fracturing in the recovered core and as such saw only minor testing done on the Greenland Group lithology. Results show a greater delineation between weathered samples and strength loss then with compositional changes, with depth to surface directly proportional to lost of strength.

While the testing carried out during this laboratory programme provided a good general guide to the physical and mechanical properties associated with some of the stratigraphic units (Units 1.1 and 3.2), further testing will be required to quantify these relationships. Limited samples in both the Brunner Coal Measures and the Greenland Group Hornfels meant the rock material classification of these units was incomprehensive. Interaction with the fault zone and the intrusive nature of the Berlins Porphyry has seen major brittle deformation within the Greenland Group lithologies which has made collection of quality samples difficult.

The graphical analysis of the tested units has derived many correlations between the testing procedures such as the strong correlation between the physical properties, porosity and dry density, and the mechanical properties associated with tensile splitting and unconfined compressive strength. This showed that high density low porosity units, such as the Berlins Porphyry, exhibit increased overall strength. Triaxial testing highlighted a relationship between friction angle and cohesion and therefore a relationship between the physical grain size and tested units. Units that exhibited a high friction angle and high cohesion displayed greater intact rock strength generally due to a composition of coarse well cemented grains.

CHAPTER 3

Rock Mass Properties

3.1 Introduction

A rock mass can be defined as the in-situ rock which has been rendered discontinuous by systems of structural features such as joints, faults and bedding planes (Hoek and Bray 1981). This Chapter discusses the rock mass properties that were described when conducting 30-50m detailed scanline surveys of traversed bed rock exposed by surface runoff along the Mt William Range. The selected rock mass defect properties recorded were based on the discontinuity data survey sheets Geological Society Engineering Group Working Party (Anon, 1977)(appendix 3 – CD insert). A total of 12 scanlines were performed along the range crest (figure 3.2) in areas of exposed basement rock, Cypress North Block.

During the feasibility and design stages of the Cypress North Block project the identification of overburden rock mass characteristics is necessary to be able to predict mechanical behaviour which may result in the destabilization of any proposed highwall. To this end the objectives of these scanlines were to find similar mechanical properties of defects along the length of the highwall. The rock mass properties recorded were; defect type, dip and dip direction, persistence (where possible), aperture, nature of infilling, defect roughness, and amplitude and waviness (again where applicable). This information is then used to identify which parameters have a greater effect on the rock mass strength by kinematic analysis (chapter 4). The location of the scanlines traverses are presented on the Engineering Geology Structural Map (Map Pocket), and are situated immediately to the east of the MWFZ. Only the physical properties of defects, including defect orientation, are described here.

3.2 Defect or Discontinuity Type

There were many defect types identified by the scanline surveys along the MWFZ, with the dominant type of defect found in the basement rock, both Berlins Porphyry and Greenland Group Metasediments, to be joint fracturing which made up 88% of all rock defects. Other defects were dominated by minor faults (shear zones) at 10%, with fault and contact zones making up the last 2%. Figure 3.1 display the total distribution of the defects across the field area.

The Joint defects are defined as a rock fracture along which there has been no visible displacement. Observational studies and measurements reveal that fractures often occur in planar, sub - parallel groups or sets; such joints are said to be systematic (Priest 1993). The study of these systematic joints has led to the conclusion that they often display spatial and orientational relationships with folds and faults formed during the same period of tectonic activity (Price 1966). Joints are distinguished from other defects by their system sets of strong delineation and regularity, with new or random fractures having generally curved clean surfaces. These systematic (joint) sets generally appear in groups with the same strike and similar dip, and are generally regularly spaced. The next most common group encountered along the ridge was shear planes which are smaller forms of faults showing reduced persistence. The basement rock mass is so intensely deformed and fractured that small discrete fault planes are not distinguishable and therefore the term ‘shear plane’ is used to define these defect planes with the term ‘fault’, being reserved for defects with recognizable signs of displacement. The third most common defect type is zones of mass disruption which resulted from the intrusive nature of the Berlins Porphyry. These zones exhibit totally random fracture orientations over extended distances (>600mm) of alternating basement lithologies.

The scanline surveys incorporated both the Berlins Porphyry and the Greenland Group Metasediments. These basement lithologies are interfingered blocks Greenland Group metasediments bounded by intrusive Berlins Porphyry, with large sections of each type which alternate down the majority of the scanlines. Defect occurrence varies over the two lithotypes, with the Greenland Group unit displaying a greater degree of fracturing in

most cases. Contact zones are frequent and propagate as zones of highly fractured rock which accelerates the rate of weathering particularly of the granite unit which breaks down into clays.

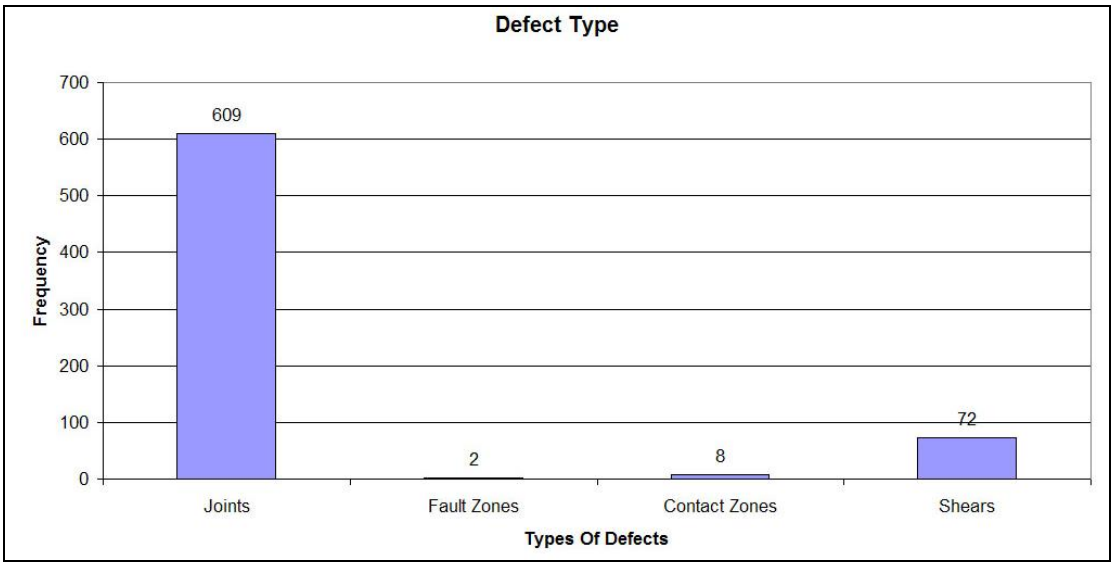

Figure 3.1. Graph delineating frequencies of defect types.

3.3 Corrections to Scanline Surveys

It is important to note at this stage that there corrections made to the collected data ranges for each of the scanlines. The Terzaghi correction was applied to the data sets to develop a true representation of defect frequency observed at each of the scanline surveys. The Terzaghi weighting function accounts for the sampling bias introduced by orientation data collection along traverses during the scanline survey. When orientation measurements are made, a bias is introduced in favour of those features which are perpendicular to the direction of surveying. Terzaghi's correction allows for this bias and corrects for it using a weighting function for each defect based on the orientation of the scanline with respect to the defects and their frequency. Terzaghi's correction was applied to each of the scanline data sets using the auto correction function available on the Rocscience Dips programme (version 5.1) and the methodology is outlined in appendix (3).

3.4 Defect Orientation

Defect attitudes measured within the basement lithologies were related in space along individual datum lines. The datum lines were assigned marker pegs which were then surveyed, by surveyors contracted to Solid Energy New Zealand Ltd, at a later date to identify their locations within the Cypress North basin itself. This was done to preserve the accuracy of the data obtained during the traverses. The major defects measured were dominantly sub-vertical joints in both basement lithologies.

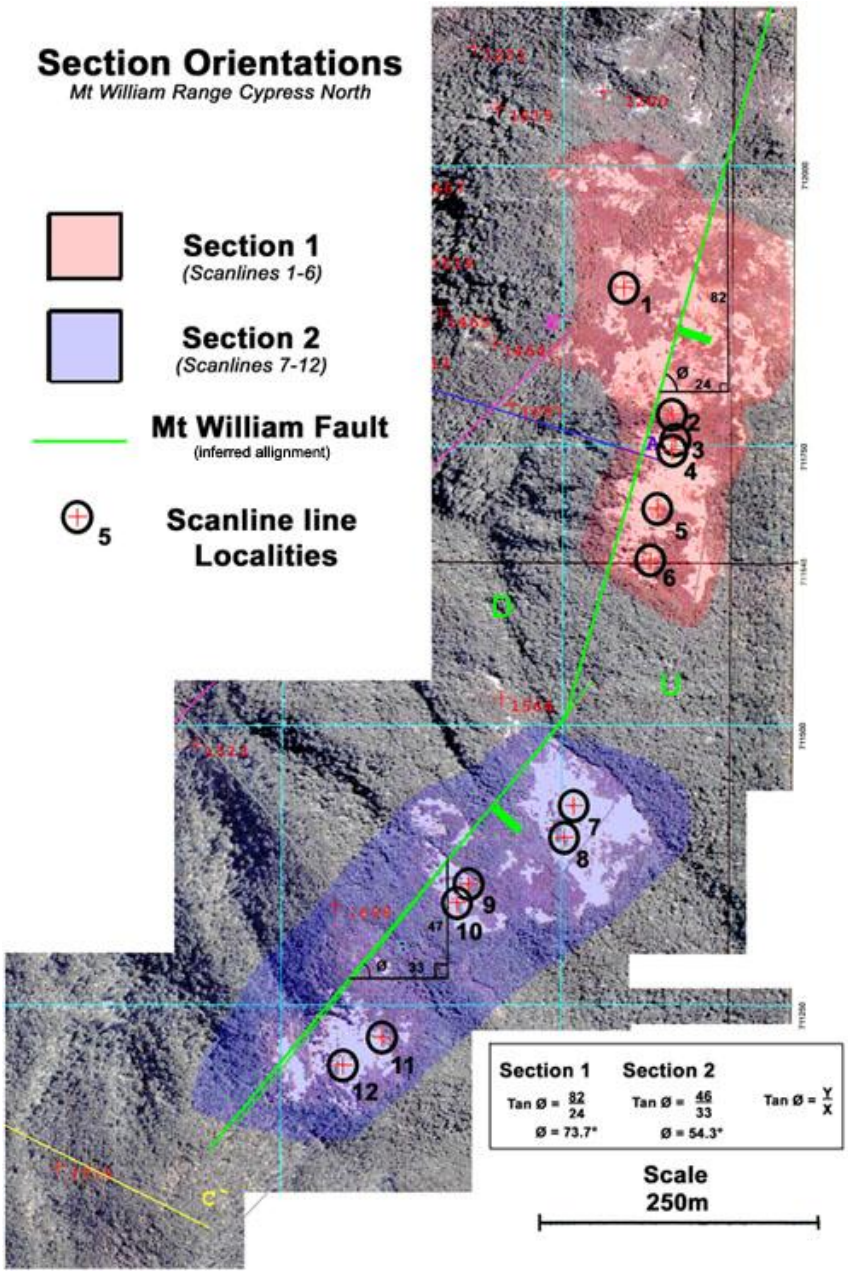

Figure 3.2 Assigned Section in relation to Relative Projected Orientation of Mt William Fault

The defect attitudes measured for each of the 12 scanline were then projected using the DIPS Rocscience program (Version 5.050) utilizing lower hemisphere stereographic projections. These individual stereographic projections were then used to identify the major joint sets associated with each. A correlation was then derived incorporating the major defect attitudes with respect to location along the ridge crest to try and identify an overall trend. Orientation of the scanline datums are outlined in table 3.1.

Table 3.1 Summary of the Scanline datum orientations (scanlines 1-12)

Scanline	Dip/Dip Direction
1a	7/011
1b	022/12
2	12/299
3	23/302
4	23/302
5	5/016
6	12/247
7a	24/027
7b	0/96
8a	10/329
8b	14/315
9a	12/320
9b	14/005
9c	15/302
10	16/342
11a	9/282
11b	9/299
12	19/344

3.4.1 Major Fault Structures

There are two major influential faults along the length of the Cypress North Basin that will cause major disruption to the highwall. The first of which, the Mt William Fault, trends in a NE-SW trend and will have the greatest effect in the highwall design. This reverse fault gouge zone thickness varies along the length of the basin with drill holes registering sheared zones of between 2.3 and 5.8 metres. The dip angle of the fault also varies over the distance with its steepest point at the southern end as the fault rotates. The variation in dip along strike does not appear to conform to any pattern, either because fault surface actually has an irregular form or because exposures and drillcore observations are

not reliable or representative of the fault. Interpreted dip values estimate the fault dips ~60° eastward along the length of the Cypress North basin (L&M 1986). Available data indicates uplift increases to the south-west; from about 100-120m in the Cypress North Block to 300m in Cypress South Block, to 350-500m+ in Kelly Block.

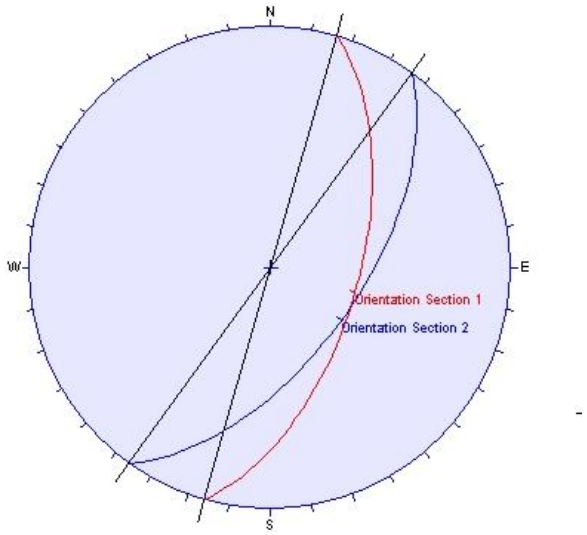

Figure 3.3 Stereographic Projection of the Mt William Fault Adjacent to Defect Sections

The second of the faults, the McCay fault, has a normal component that mimics the overall trend of the Mt William Fault, striking parallel for the majority of the basin (cross section - figure 1.6 map pocket). The McCay fault splits from the Mt William Fault near the southern extent of the basin (map 1 – map pocket). Interpretation of the McCay fault is believed to be either compensation for the observed rotation in the fault orientation, or that the McCay fault was the original displacement of the normal component of the Mt William fault and its present position is actually a spur fault which propagated to the surface. Dips associated with McCay are also predicted to be ~60º which mimic that of the Mt William fault with gouge zones associated with the fault under a metre.

3.4.2 Shearing Defects

Shear defects isolated in the scanline traverses (figure 3.4), for each of the sections, display a random placement throughout the stereographic projection. This plot incorporates representative samples from each of the joint sets identified in the next section (set number). The representation of shears is proportional to the observed spread of the

joint poles plotted in figures 3.5 and 3.7 with a high concentrated observed with orientations similar to the dominant joint set orientations (parallel to MWFZ), with defects exhibiting sub vertical dips (90 ± 15º). The highest concentration of shears was found in the same orientations as joint sets two and three (~80%), as outlined in the area contour plot (figure 3.4).

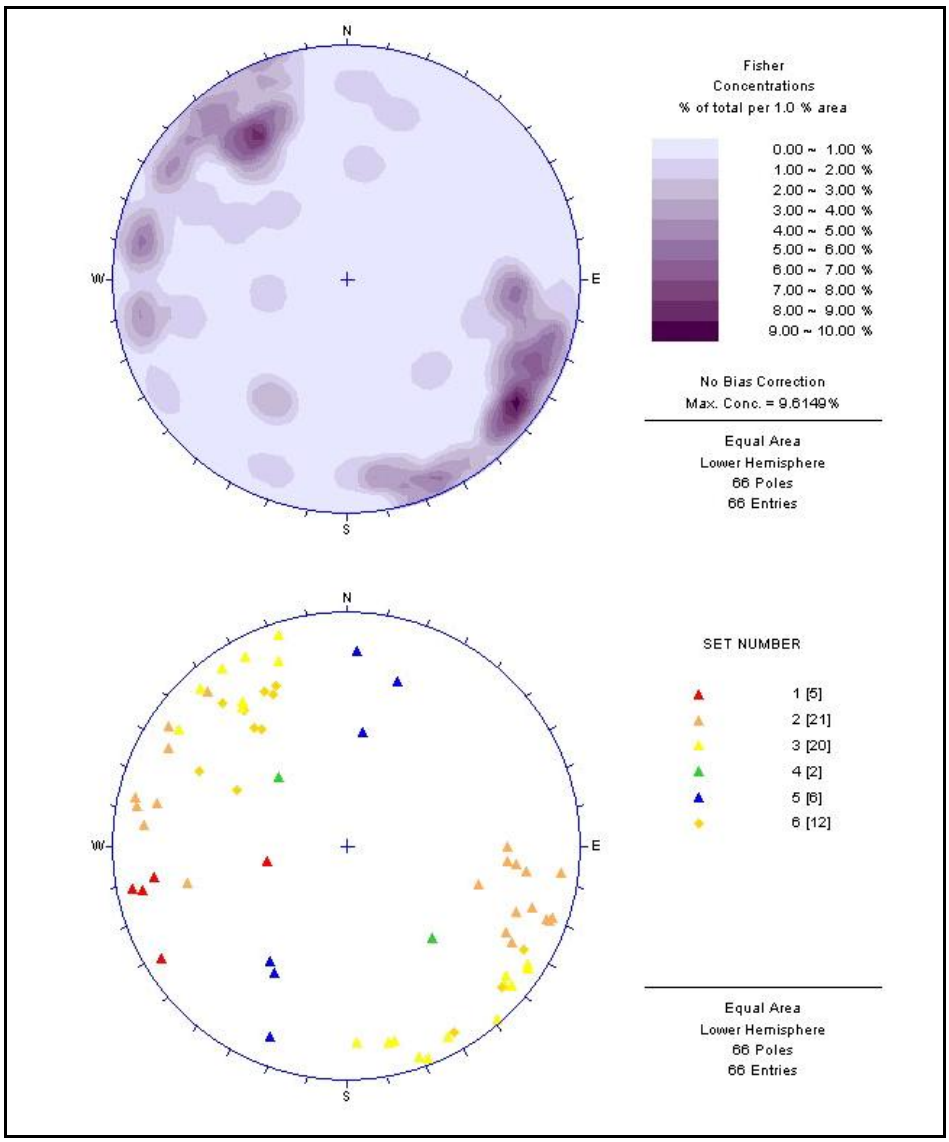

Figure 3.4 Area Contours and Scatter Plot for Stereographic Projection of Correlated Shear Defects with Defect Sets (Outlined by Set Numbers).

The random spread of the shear poles suggests that movement along all these shears was more than likely initiated to accommodate lateral and vertical displacement in the Mt William Fault. Infill thickness seldom exceeds 5mm, but with isolated shear

showing as much as 80mm in thickness. Infill material usually comprises highly weathered basement which has broken down into silty/sandy clay, with fine sand, calcite and muscovite also present with iron staining common. Persistence of the shear defects, along with the joint sets, is hard to ascertain due to the nature of the testing environment with some defects in excess of 8 metres but with most visible lengths not much greater then 1m.

3.4.3 Crushed Contact Zones

Frequent crushed zones are incorporated in the interfingering of the two basement lithologies as discussed earlier, and are generally the result of the injection of magma into Greenland Group Greywacke. These zones of weakness exhibit no coherent defect orientation with widths of .3-.4m to 3m+ observed along scanlines. The unpredictability of these defects makes them the most prominent in terms of safety with regards to failures within the highwall. The highly fractured rock would react like a stiff gravel with regards to its rock mass characteristics under dry conditions. Under wet conditions the weathered basement would weaken due to the expansion of the clay component as it swells due to absorption of moisture.

3.4.4 Bedding Defects

Bedding is included as a defect in many surveys as a mode of failure or plane of weakness in rock mass analysis. The prevalent bedding throughout the basement Greenland Group lithology is moderately metamorphosed, and does not provide a mode of weakness in the sandstone unit. The Kaiata Mudstone unit which will be incorporated into the final highwall design, to varying degrees dependant on economic constraints, does exhibit bedding orientation weakness, as shown by tensile strength testing. The prediction of this bedding and any effect it may have on the final stability of the highwall depends on its final orientation due to upturn of bedding orientations due to association with the MWFZ (figure 1.6). The Kaiata mudstone bedding initially dips gently east at 8-12° degrees into the Mt William Range, but undergoes upturn as it approaches the reverse fault structure. Any change in the bedding will more than likely be offset by the disruptive nature of the Fault zone with the zone of influence increasing the fracturing observed within the unit.

3.4.5 Joint Defects Mt William Fault Zone

3.4.5.1 Joint Sets

Joints sets, as defined previously, make up the predominant defect observed along the top of the Mt William Range, comprising close to 90% of recorded defects. Joints observed both in the Northern and Southern Sections (map 2) are dominated by sub vertical defect sets which strike NNE and SSW parallel to the fault orientation. Initial observation separated the defects into 6 joint sets (JS), but on further investigation this was reduced to 5 sets with JS6 being of parallel orientation to JS3 and JS4, and effectively a transition between the two joint sets of intermediate dip. The observed separation of the joints for each section (figures 3.5 and 3.7) is as follows;

- JS1 strikes effectively sub parallel to all scanlines except Scanlines 1 and 7 (table 3.1). The under sampling of this group and slight variations from scanline to scanline make definition of a mean dip and dip direction difficult due to the scattering of the recorded data. The JS1 defects have a mean pole at 76°/041º in Section 1 and 78°/025° in Section 2.

- JS2 is the second dominant joint set defect observed in both section 1 and section 2 (figures 3.5 and 3.7). The orientation of the joint set is effectively perpendicular within 10°-20° to the scanline orientations in all but Scanlines 1 and 7 where it trends at approximately 45°. Mean poles for JS2 are 89°/261° for Section 1 and 70°/245° for Section 2.

- JS3 is a sub-vertical joint set which is the dominant defect observed in both sections (figures 3.5 and 3.7). The orientations of the joint sets are effectively perpendicular to all but scanlines 1 and 7, where the joint set is under sampled (figure 3.10). Mean poles for JS3 are 79°/118° for Section 1 and 84°/285° for Section 2.

- JS4 has the lowest recorded dip of all the joint sets which are observed as a sub set to JS3 and effectively represents that sets low dip transition. Due to

the horizontal nature of the scanline surveys JS4 is under sampled in all scanline surveys and absent from traverses 1 and 7 (figure 3.10). Mean poles for JS4 are 47°/106° for Section 1 and 43°/106° for Section 2 which are effectively the same and may be the result of under sampling.

- JS5, as with JS1, has an orientation that is sub-parallel to most of the scanline orientations and is therefore under-sampled in most survey traverses which strike east-west (figure 3.9). Mean poles for JS5 are 85°/174° for section 1 and 79°/161° for section 2.

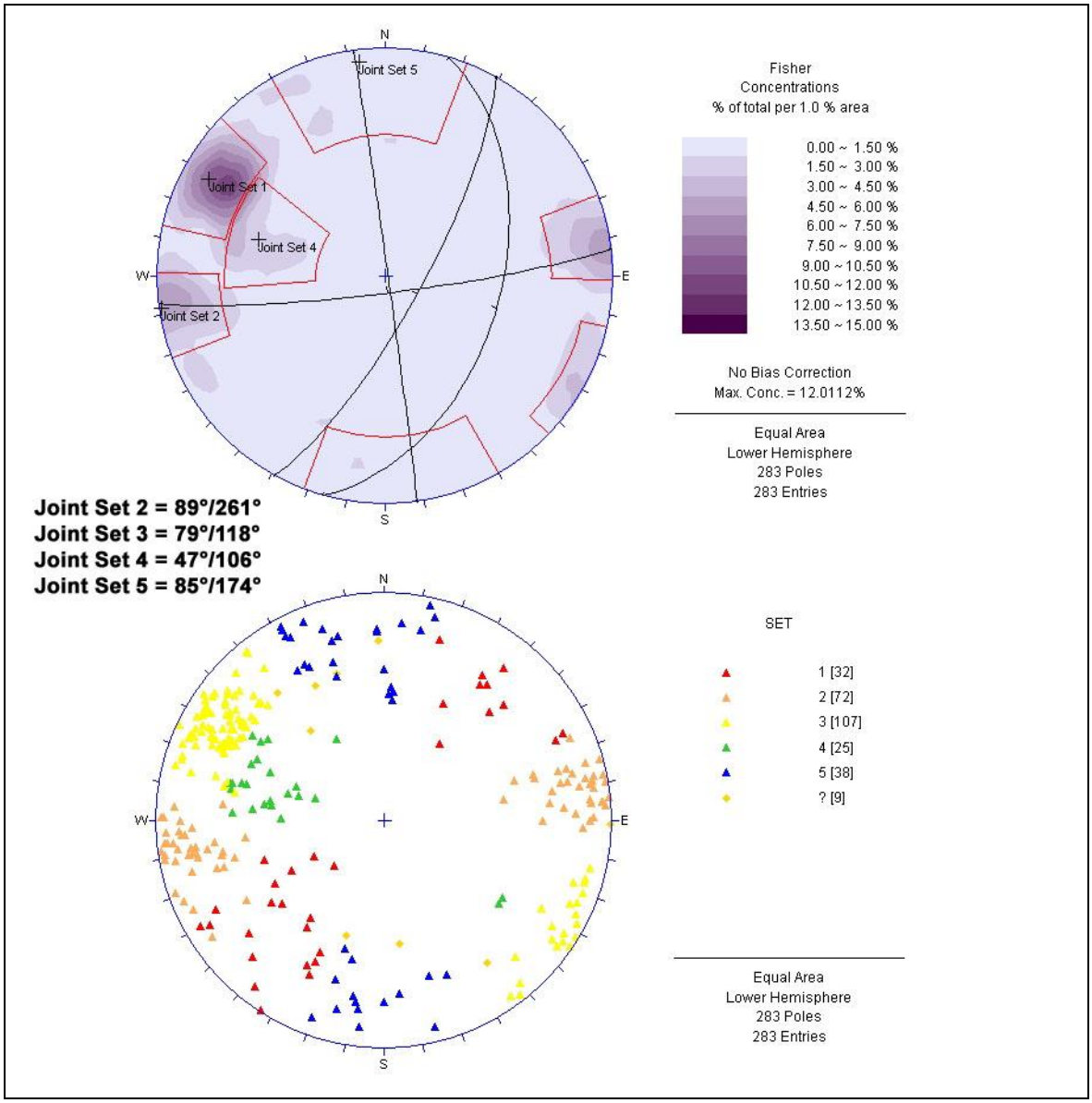

Figure 3.5 Stereographic projection of all points observed in Section 1 with division of poles into joint sets (set 1-6) and mean orientation.

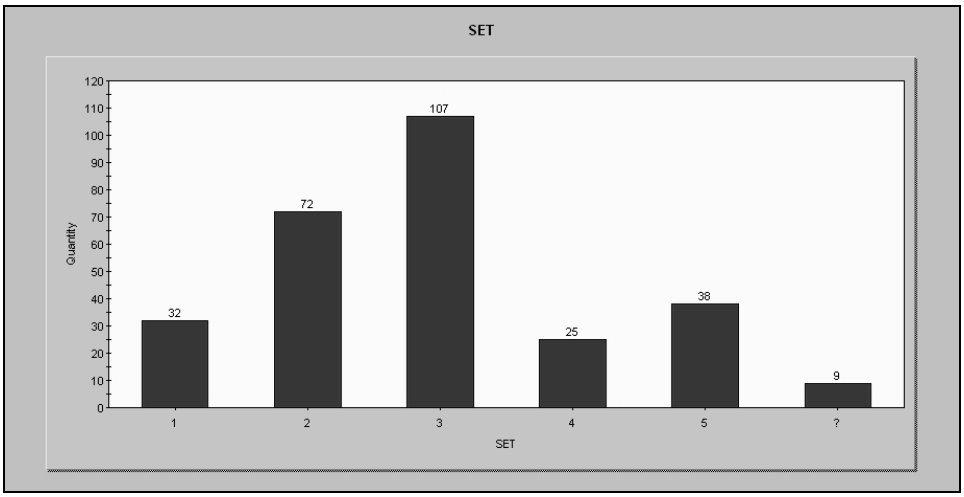

Figure 3.6 Graphical Representation of Joint Set Frequency in Section 1

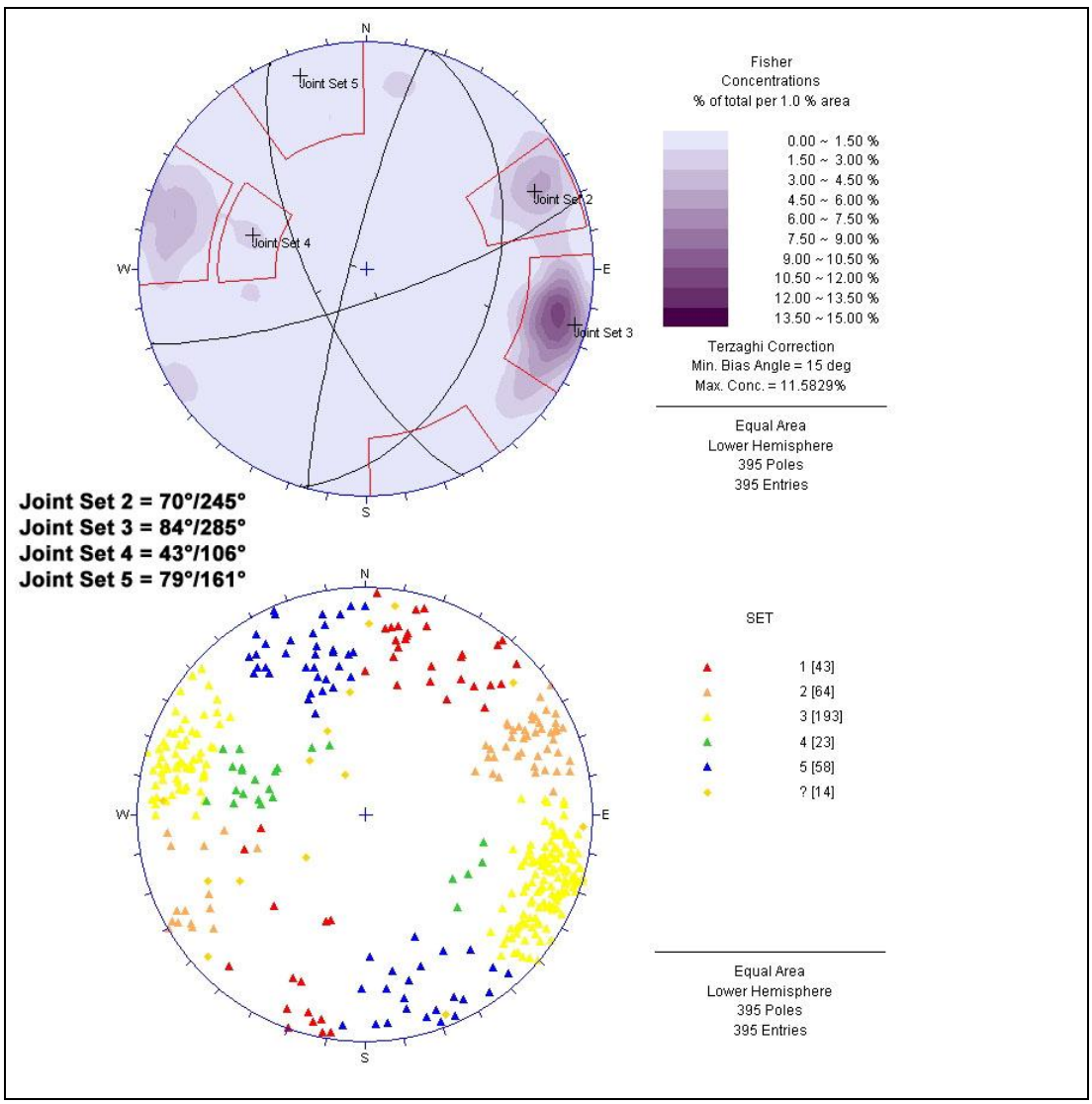

Figure 3.7 Stereographic projection of all points observed in Section 2 with division of poles into joint sets (set 1-6) and mean orientations.

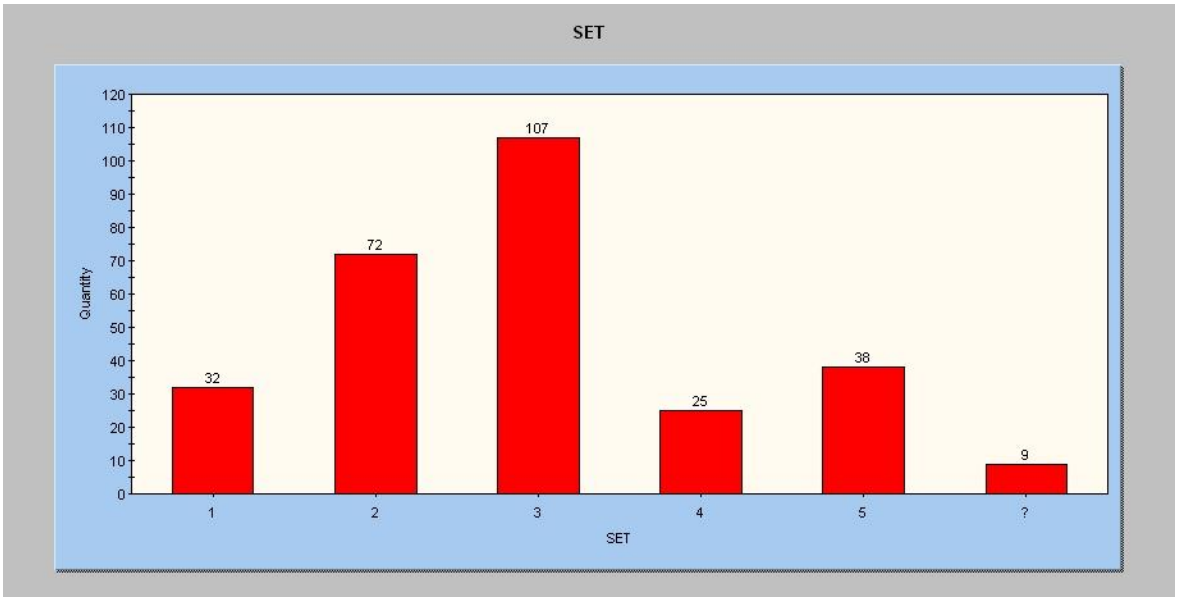

Figure 3.8 Graphical Representation of Joint Set Frequency in Section 2

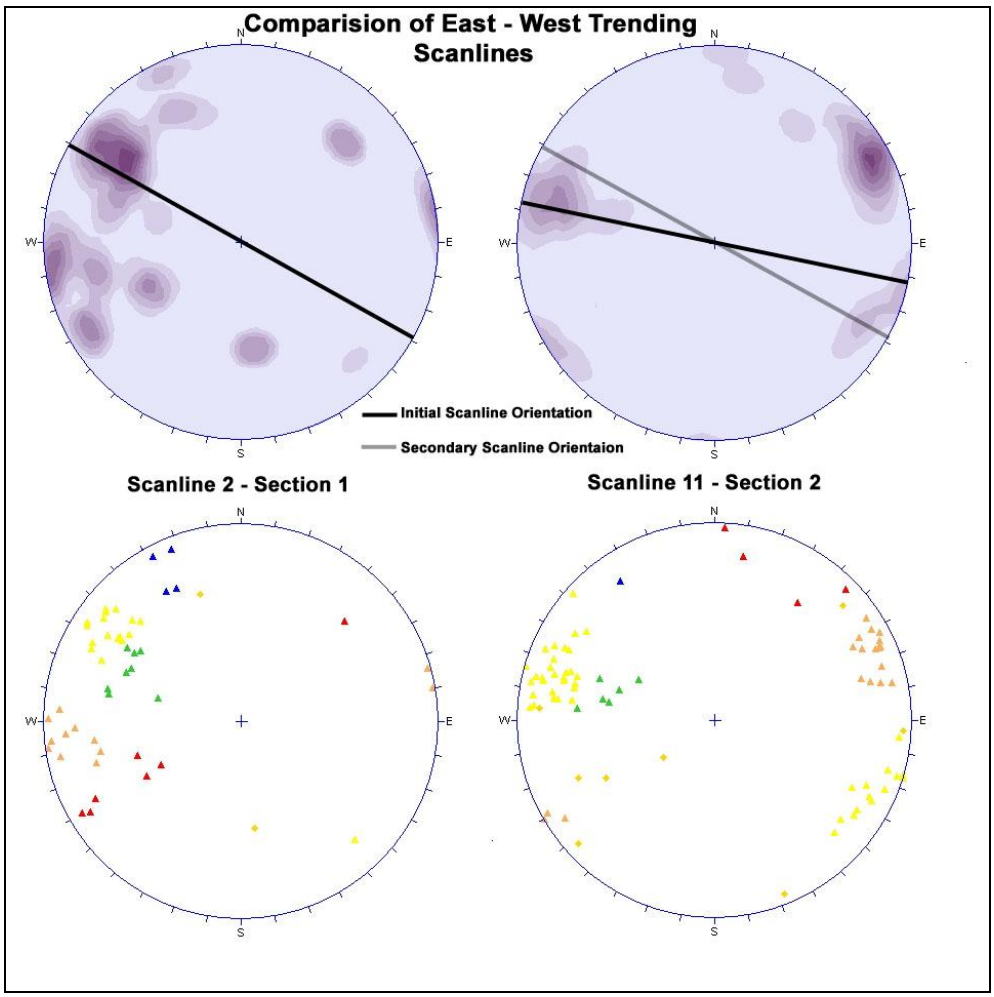

Figure 3.9 Stereographic Comparisons between Scanlines Orientated in a East-West Trend taken from Section 1 and Section 2

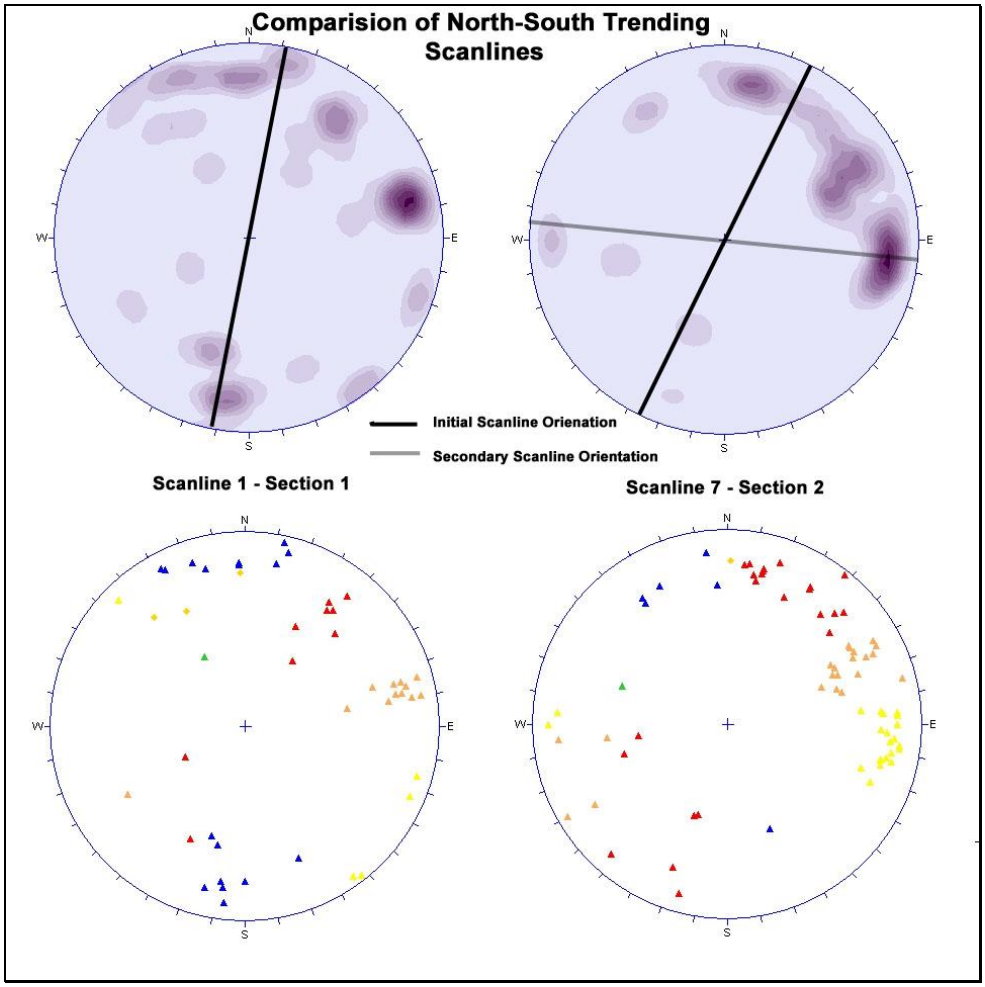

Figure 3.10 Stereographic Comparisons between Scanlines Orientated in a North-South Trend taken from Sections 1 and Section 2

Figures 3.9 and 3.10 were chosen to represent the differences in sampled data due to a change in Scanline orientation and the bias that is then created. Figure 3.9 represents the majority of the traverse orientations with 10 out of the 12 scanlines running east to west with an example derived from both of the assigned sections. Figure 3.10 shows the remaining two scanline traverses (scanlines 1 & 7) and the degree of bias introduced by the orientation of the scanlines when then compared to figure 3.9. As well as showing the sampling bias due to orientation, figures 3.9 and 3.10 show a comparison between scanlines recorded in both sections and the rotational effect which can be seen within the mean joint set orientations. This rotation of the mean joint set orientations coincides with the projected rotation in the strike of the Mt William fault (figure 3.2), with an observed rotation of 13°-16° to the north between the mean dip directions in Sections 1 & 2 (figures 3.5 & 3.7). The inferred rotation within the Mt William Fault sees a shift from the initial

orientation of 016° adjacent to Section 1 to an orientation striking 036° adjacent to Section 2 (rotation of 20°). On initial observations there seems to be a correlation between the fault and defect orientation.

A graphical summary of each of the scanline survey traverse (1-12) in the form of area contour plots of pole densities is presented on the Geotechnical Map (Map 2 – Map Pocket) and in appendix 3 (Scanline data).

3.4.5.2 Joint Origins

The observations in Section 3.4.5.1 suggest that the major joint sets coincide with the formation and continued activity of the Mt William Fault Zone. Therefore it is important to identify the mechanism involved in the formation of the defect sets.

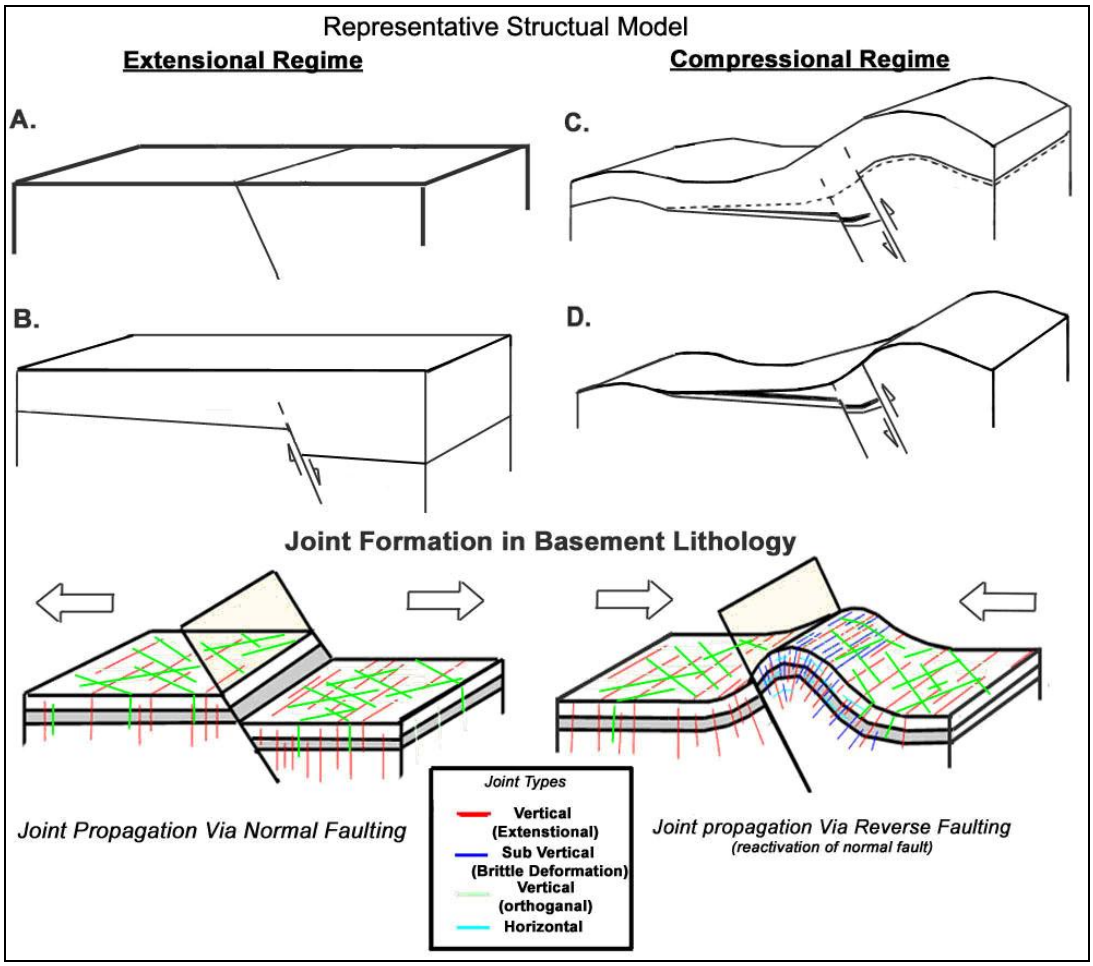

Figure 3.11 Diagram Showing Postulated Joint Formation

Through the incorporation of typical stress diagrams for fault related processes (Lacazette, 2000) and discussion with Mrs J.K. Campbell, University of Canterbury, a flow diagram showing associated jointing has been developed to identify their origins (figure 3.10). This shows the idealized transition of the Mt William Range though periods of extension (A and B) and then compression (C and D) with the associated joint formation expressed for each phase (extension and compression). 'A' (figure 3.11) shows the initial representative block. 'B' shows the propagation of normal faulting within the basin and sedimentation. 'C' shows the transition into a compressional regime, with either the reverse of normal faulting within the basin, or the formation of spur faults. 'D' shows the final form of the basin with erosional effects removing sedimentary layers from the ridge.

Joints are found in all competent rocks within about 1 km of the earth's surface, at all orientations, and at sizes ranging from a few millimetres to several hundred metres. Joints are many thousands of times more frequent than faults with many geologists (Price 1966, Cundall 1987, Priest 1993) believing that studying joints and their origins can provide valuable clues to the tectonic processes in near-surface rocks. Using the concept of systematic joint formation (that the joints formed during the same period of tectonic activity) the tectonic geological history of the Cypress North basin the construction of the tensional environment that led to the formation of the joints associated with the Mt William Fault can be developed ('joint formation in basement lithologies', figure 3.11).

The structural deformation of the basement lithologies (figure 3.11) outlines the formation of the joint sets associated with the Mt William Fault. JS2 and JS3 signify two phases of sub vertical jointing, the first via extensional partings (seen in red) and the second by the brittle deformation due to uplift (seen in blue). This translates into the dominant 'primary' defect set observed along the Mt William Ridge. The joint sets JS1 and JS5 are due to the formation of oblique joints (seen in green) in response to the vertical component in an extensional environment and form the 'secondary' defect sets. JS4 results from the formation of the horizontal defect component associated with the deformational processes, and are also seen as 'secondary' to the sub vertical joints.

3.4.5.3 Persistence of Jointing

By definition the persistence is the length of the defect trace observed along its exposure. The method of scanline surveying (along exposed gullies), and the impractical nature of exposing every joint, due to overburden, meant that persistence measurements were limited to visual surface expression. Because of this defects seldom were measured greater then 2m with the majority of surface expression restricted to exposed creek bed. The largest persistence was observed at greater then 8m in the Greenland Group rocks parallel to the exposed creek bed. The majority of the larger persistences observed often occurred sub-parallel (~20^{o}) with the orientation of the scanline traverses, and therefore crossings of the scanline were infrequent and under-sampled. It was also observed of the larger defects (persistence >4m) were mainly restricted to the 'primary' defect sets, as outlined above, with 'secondary' defects being truncated by the 'primary' defects. Persistence was measured using a standard tape measure with a length of 30m, allowing persistences measured to the nearest metre to be easily categorized.

From field estimates the majority of defects had an overall persistence less then 4m, with an average of around 2m observed often truncated by other defects. These observed persistences can be used to give an indication to the degree of rock material that would be released due to failures which would propagate along discontinuities. Indications are that failures along these minor defects would be localized events involving small scale rock material volumes (i.e. < 100m^3).

3.4.5.4 Aperture and Infilling of Joints.

The Aperture and Infilling of the joints relates to the separation of the joint faces and the type of material present in that defect. Combining aperture and infilling allows for both the strict definition of aperture which is "the perpendicular distance separating the adjacent rock surfaces of an open discontinuity, in which the intervening space is either air or water filled" (ISRM, 1978), and the defects apertures with infill material. This allowed for the use of the definition outlined in the scanline guidelines by Anon (1977) where the aperture is the distance between surfaces of an open or filled discontinuity.

The definition of the infill material is defined as the material that separates the adjacent rock wall of a discontinuity (ISRM, 1978). The infill material usually comprises a weaker unit, predominantly crushed sediments or altered parent rock. The strength, aperture and the consistency of the infill material has a direct effect on the shear strength of rock mass defect, often by lowering the friction coefficient. The fill material observed amongst the basement lithologies is either altered Berlins Porphyry which breaks down into silty clay, or fine-grained micaceous sandy sediment usually derived from the Greenland Group metasediments. These types of infill materials tend to lower the degree of "roughness" associated with the defects and therefore reduce the shear strength of the defects by lowering the observed friction angles. Other types of infill observed were iron-staining, which indicated a degree of weathering on the joint surface, and calcite deposits on the surface of jointed rock faces. Both of these deposits represented a decrease in the strength associated with the intact rock mass.

The aperture between the surfaces of the infilled defects is a major controlling factor in determining the influence of the infill material. If the aperture of the defect, and infill material, is sufficiently close that during movement it allows the joint surfaces to interlock, the strength of the joint will revert back to the shear strength associated with the surface on surface contact. But if the aperture is wide enough as to negate the surface on surface contact, then the shear strength associated with that joint reverts back to the usually soil properties of the infill material.

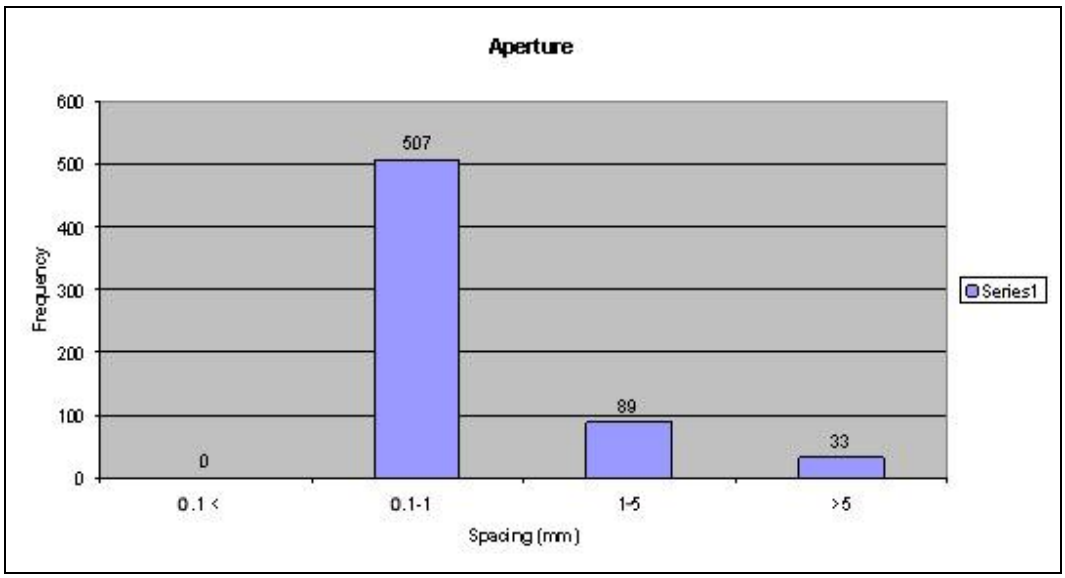

Figure 3.12 Frequency of Joint Aperture.

The discontinuity apertures along the Mt William Range show considerable variation ranging from a classification of wide (>200mm) associated with crush zones, to tight (.1-1mm). Joint aperture observed along the proposed highwall shows a range from tight to moderately narrow (20-40mm), with the predominant aperture being typically tight (>70%) and iron stained (figure 3.12). Crush Zone apertures show a range of results ranging from Wide, to 'Moderately Wide' (60-200mm) and usually infilled with highly fractured weathered basement rock.

3.4.5.5 Defect Spacing

In its most general sense, defect spacing is the distance between one discontinuity and another. Frequency is the number of defects per unit distance, and is the reciprocal of spacing (i.e. the mean of these intersection distances). This statistical distribution of discontinuity spacings is generally recorded as a mean value and is expressed as a mean percentage. Determination of this mean percentage of discontinuities is labelled the Rock Quality Designation (RQD) and is used in both in scanline traverses and boreholes. RQD was initially proposed by Deere (1964) as a measure of the quality of borehole core, is defined as the percentage of length of a given length of core (of length of borehole) that consists of sound, intact pieces that are 0.1m (threshold value) or longer. Since RQD is relatively easy to calculate, and provides an unambiguous numerical value, it has become widely accepted as a measure of discontinuity spacing. For scanline data, the RQD is estimated by the number of joint spacing obtained for the length of the traverse. The RQD is then derived from this average joint spacing based on the following equation by Priest and Hudson (1976):

$$RQD = 100e^{-.1\lambda} + (.1\lambda + 1)$$

RQD values were retrieved from the borehole geotechnical logs (DHs 1694, 1697, 1698, 1715, & 1717) and were selected above scanline data as a more accurate means of deriving a direct measure of rock quality. RQD values for each of the drillholes were then compared and the data analyzed by plotting histograms of the sampled values. Mean RQD values for each lithologies downhole and overall RQD value are outlined in table 3.3.

Table 3.2 Definition of Rock Quality using RQD, Deere (1966)

RQD	Rock Quality
0-25%	Very Poor
25-50%	Poor
50-75%	Fair
75-90%	Good
90-100%	Excellent

Table 3.3 Summary of RQD Frequency (Derived from Drillhole Data).

Numerical Frequency					
RQD Freq	1694	1697	1698	1715	1717
0-20 %	17	63	66	82	56
21-40 %	14	11	18	7	12
41-60 %	10	1	12	6	20
61-80 %	8	1	2	1	10
81-100 %	4	1	1	0	17
Total	53	77	99	96	115
Percentage Frequency					
0-20 %	32.1	81.8	66.7	85.4	48.7
21-40 %	26.4	14.3	18.2	7.3	10.4
41-60 %	18.9	1.3	12.1	6.3	17.4
61-80 %	15.1	1.3	2.0	1.0	8.7
81-100 %	7.5	1.3	1.0	0.0	14.8
Total	100.0	100.0	100.0	100.0	100.0

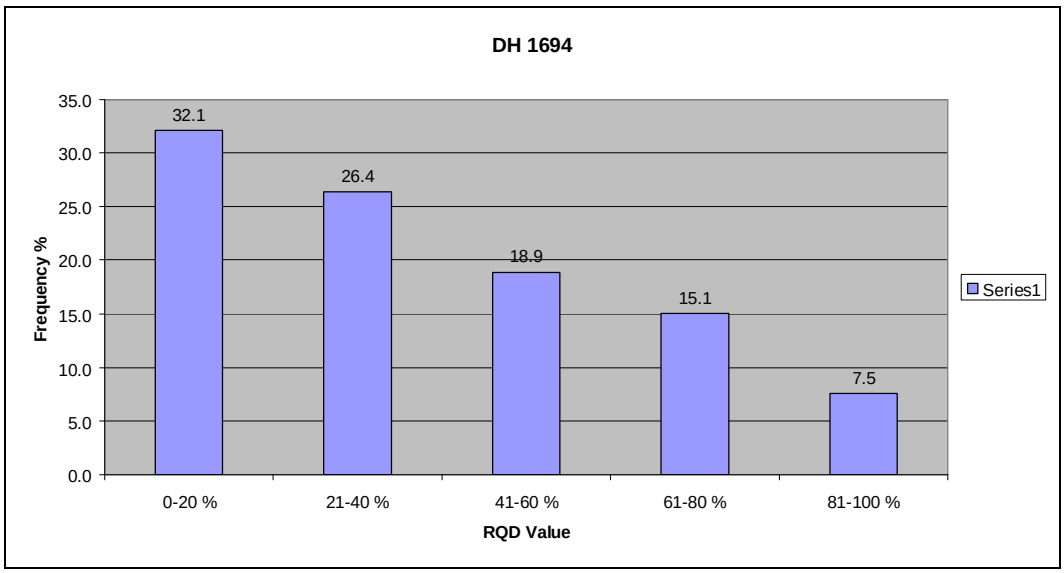

Figure 3.13 Frequency of RQD values for DH 1694

Drillhole 1694 is situated below the Mt William Fault line near the base of the Mt William Range adjacent to DH 1697 (Map 1 & 2 – map pocket). 1694 is comprised of the Tertiary stratigraphic units the Brunner Coal Measures and the Kaiata Mudstone. The RQD value for the length of the drillhole is 38.2%, which gives it a classification of poor rock quality (25<50%). The breakdown of the RQD values shows a value of 51.0% for the BCM (fair rock quality), 39.3% for the Kaiata Mudstone (poor rock quality), and 11.8% for the coal seam. Figure 3.13 shows the frequency of overall RQD values for drillhole 1694.

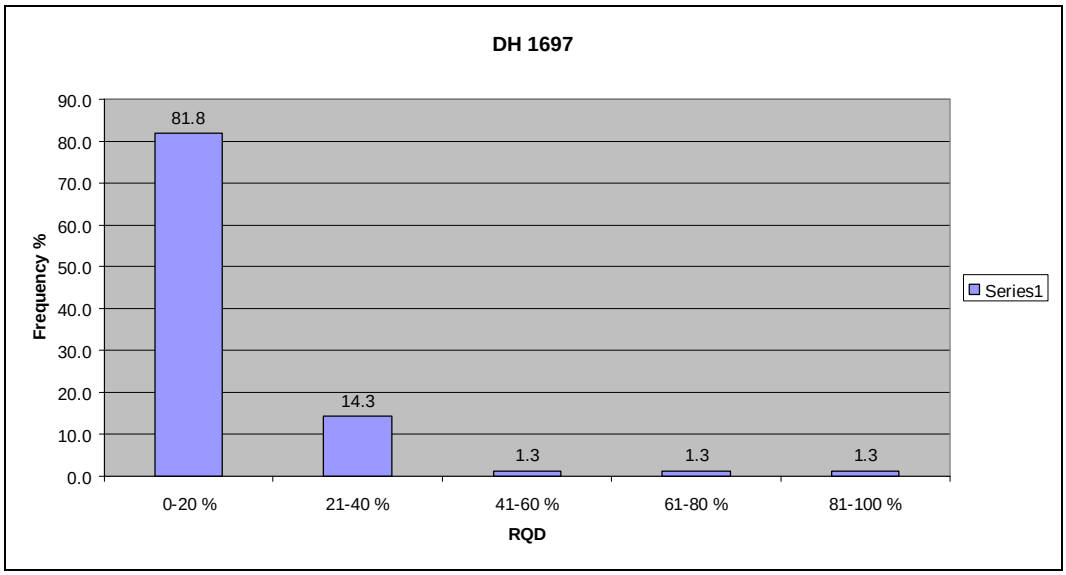

Figure 3.14 Frequency of RQD values for DH 1697

Drillhole 1697 is situated at the northern extent of the basin adjacent to Section 1, and has good correlation with scanlines 2-4 (geotechnical map – map pocket). 1697 is situated in basement lithologies with an overall RQD of just 9.2% which, according to Deere (table 3.2), gives it a classification of very poor rock quality (<25%). Figure 3.14 provides a breakdown of the RQD values over the length of the drillhole, with the majority of RQD values per metre below 20%. Separate RQD values of the basement lithologies see an increase in fracturing in the Greenland Group unit (+5.1%).

Drillhole 1698 is situated in the middle of the basin adjacent to Section 2 and is located between scanlines 10 and 11 (geotechnical map – map pocket). 1698 is situated in the same basement lithologies as 1697, with an overall RQD of 17.5%. This also gives it a

classification of very poor rock quality (<25%). Figure 3.15 provides a breakdown of the RQD values over the length of the drillhole with the majority of RQD values per metre still below 20% but is slightly less fractures (20% drop within 0-20% range) when compared to the same values observed in figure 3.14. Separation of the RQD values into lithologies again sees an increase in fracturing in the Greenland Group (+9.3%).

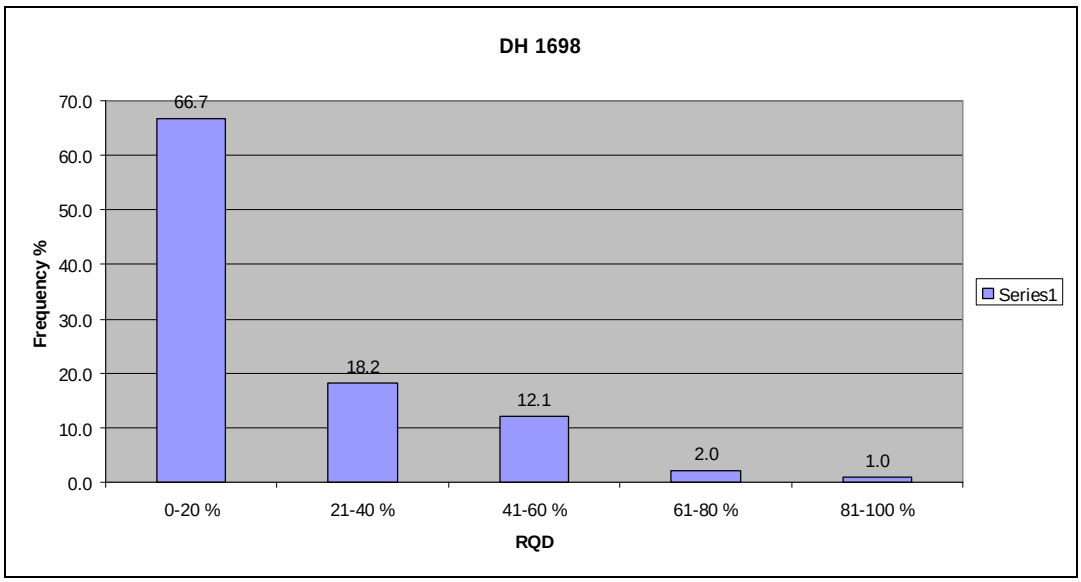

Figure 3.15 Frequency of RQD values for DH 1698

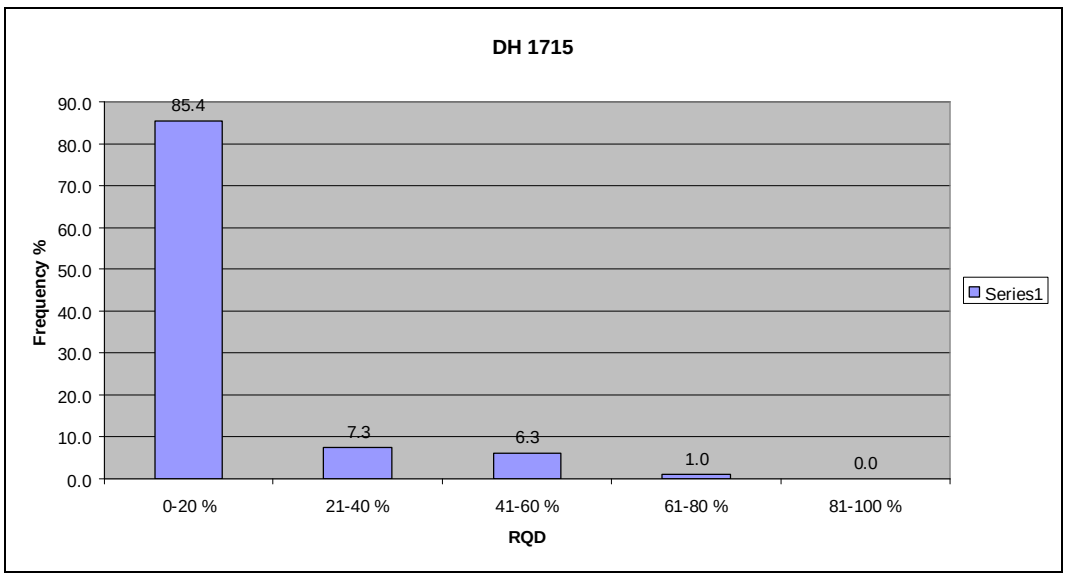

Figure 3.16 Frequency of RQD values for DH 1715

Drillhole 1715 is situated at the southern extent of the basin and is situated in the same basement lithologies as 1697 and 1698 with an overall RQD of 8.3%. This is the

poorest quality rock seen in this suite of drillholes and gives it a classification of very poor rock quality (<25%). Figure 3.16 provides a breakdown in of the RQD values over the length of the drillhole, with over 85% of RQD values per metre below 20%. Separation of the RQD values into lithologies again sees an increase in fragmentation in the Greenland Group Hornfels (+3.3%).

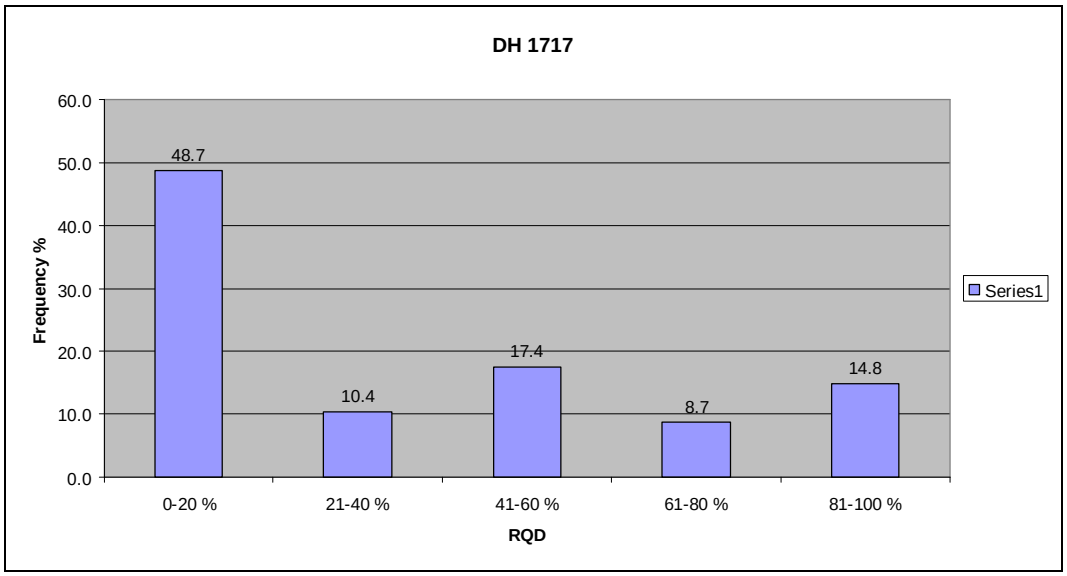

Figure 3.17 Frequency of RQD values for DH 1717

Drillhole 1717 is situated just above the Mt William Fault line, situated midway down the slope the Mt William Range adjacent to DH 1715. 1717, like 1694, is comprised of Tertiary stratigraphic units the Brunner Coal Measures and the Kaiata Mudstone. The RQD value for the length of the drillhole averages 33.5% which gives it a classification of poor rock quality (25<50%). The breakdown of the RQD values shows a value of 68.9% for the BCM (fair rock quality), 31.8% for the Kaiata Mudstone (poor rock quality), and just 0.9% for the coal seam. Figure 3.17 shows the distribution in the frequency of the rock quality over the length of the drillhole.

3.4.5.6 Weathering and Durability Factors

The effects, rate, and influence of weathering in surface exposures are often orders of magnitude higher than those encountered at depth, but the actual processes involved in the weathering of all of the components contained in a rock mass are often extremely

difficult to determine. Exposure to atmospheric conditions results in a decrease in the condition of both the rock material and discontinuity properties. The weathering of a rock mass within the engineering life span of a structure will have a detrimental effect on the strength of both the rock material and the discontinuities (Campbell 2000). Hence the susceptibility of weathering (primary and secondary) is an important factor for long term stability of any proposed highwall design. The influence of weathering will normally be greatest for rock masses exposed to atmospheric conditions at the earth's surface, and thus susceptibility to short-term weathering will play a significant role in slope stability. Pre-existing weathering present within the geotechnical units (e.g. in Berlins Porphyry) also has a significant implications to highwall stability.

The basement lithologies show a variation in the degree of weathering with exposed Berlins Porphyry along the length of the ridge crest showing a high (grade iv) to complete (grade v) degree of weathering (based on Bell and Pettinga's (1983) classification system (appendix 1 - CD insert), whereas the Greenland Group Hornfels shows generally a slight (grade II) to moderate (grade III) degree of weathering. The degree of weathering has a direct effect on the shear strengths associated with the defects, as well as the overall strength of the rock mass (chapter 2). Observations of the lithologies down drillholes shows slight (grade II) degree of weathering experienced up to 60 metres extending to depth via joint fracture. Rate of weathering in the basement lithologies in relatively slow, with moderate to high degree (grades III-IV) of weather confined to the upper 30 metres in the Berlins Porphyry.

The degree of weathering has extensive implications with regards to highwall stability as weathering lowers the intact rock strength (chapter 2) and therefore the friction angle of the defects. These weak zones / planes can act as potential failure surfaces if unfavourably orientated with respect to the highwall.

Figure 3.18 Sampled Greenland Group Exhibiting Iron Staining on Joint Surface

3.4.5.7 Joint Roughness

The roughness parameter quantifies the variation observed on defect surfaces by visual reference and classification. Degree of roughness was carried out using Barton and Choubey's (1977) ten standard roughness profiles (Figure 3.18) which were then categorized into degrees of roughness and applied to the discontinuities observed in the field. The roughness of the defect surfaces can greatly influence the overall shear strength of the individual discontinuity as it is directly related, along with degree of weathering, to the friction angle. Infill and aperture of the defect surfaces also is a controlling factor and can increase of decrease the friction coefficient depending on the situation as outlined previously.

The assessment of defect surface roughness of the discontinuities along the scanlines was based on standard roughness profile (figure 3.19). Delineation was made between the roughness of discontinuities in the field by comparing defect surfaces within a

broader classification system then the one proposed by Barton and Choubey but still based on JRC values. The broader classification system developed consisted of Slickensided (JRC 0-2), Smooth (2-4), Semi Rough (JRC 4-8), Rough (JRC 8-14), and Very rough (JRC 14 –20). Roughness was determined by visual comparison and by the feel of the defect with the hand.

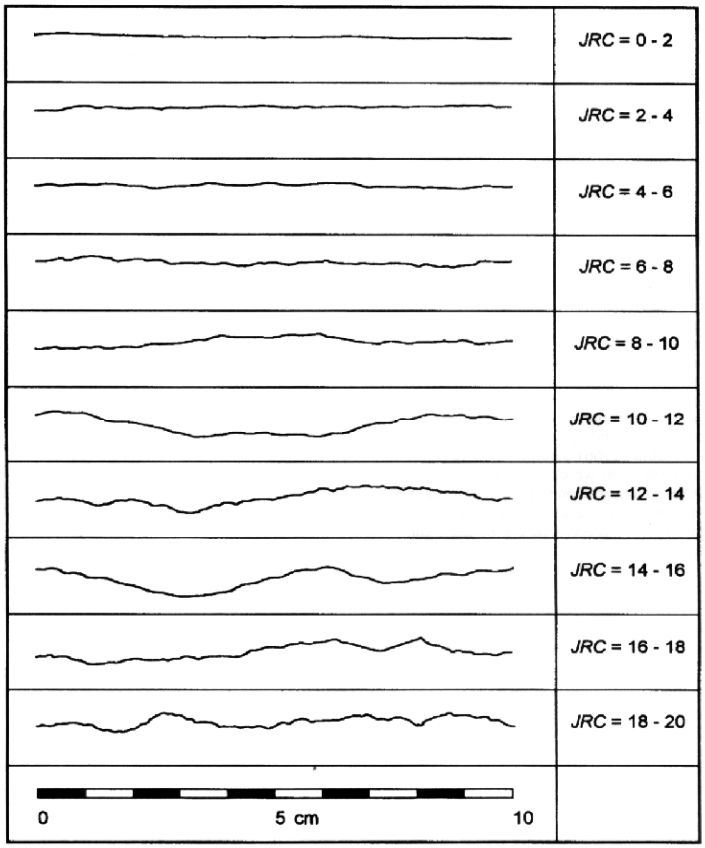

Figure 3.19 Joint Roughness Coefficient (*JRC*) Table, Barton and Choubey (1977).

Surface roughness varies considerably in the defects observed in the basement lithologies along the Mt William Range, with joint roughness profiles ranging from Slickensided (JRC 0-2) to Very rough (JRC 14 –20). The frequency histogram of joint roughness (Figure 3.20) shows a JRC value of 4-8 (semi rough) as the dominant joint surface making up over 60%. The next highest frequency is observed at a JRC of 8-14 (rough) with 23%, and 12% of the joint surfaces have a JRC less than 4. The moderate JRC values associated with most of the joints reflects a moderate shear component (friction angle, Ø = 35º) but the sub vertical nature of the predominant joint sets means that they

will provide little resistance if joint planes were to go into shear by daylighting in the pit slope face.

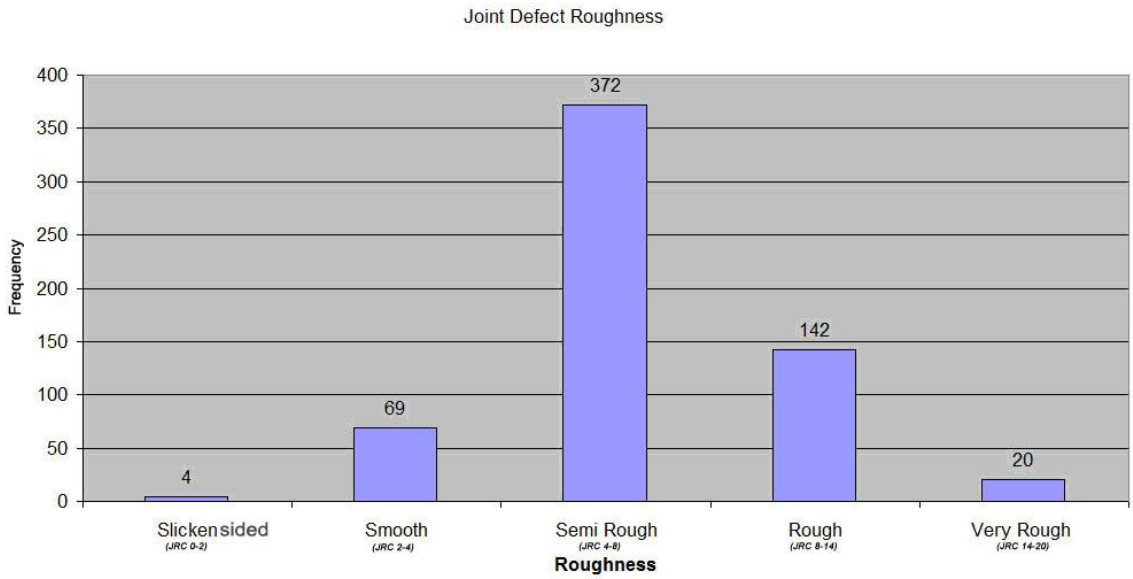

Figure 3.20 Graph of Joint surface roughness on Total Scanline Traverses.

Shear Defects display a range of surface roughness profiles and are typically slickensided (JRC 0-2), smooth (JRC 2-4), semi rough (JRC 4-8), or rough (JRC 8-14). Figure 3.20 shows that 68% of defect shears had JRC values lower then 4 with no value higher then 14 JRC, and therefore provide little shear strength due to a low associated friction angles.

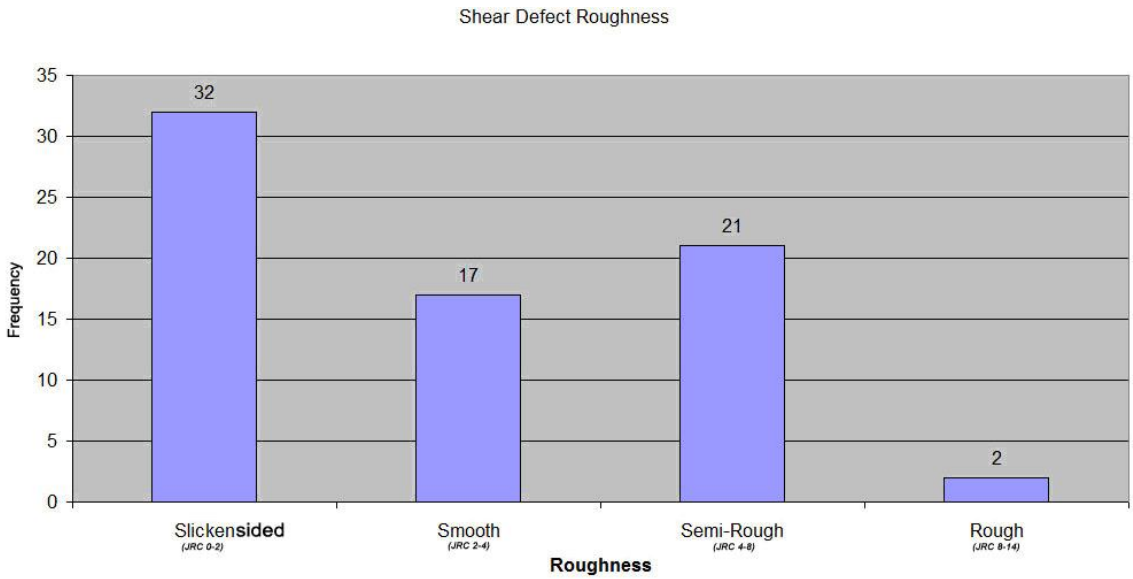

Figure 3.21 Graph of Shear Surface Roughness for Total Scanline traverses.

3.5 Hydrological Conditions

The Cypress North Block experiences high precipitation throughout the year with rainfall exceeding 6 m in the basin. As such through most of the year the rock mass will remain saturated with the water table only a few metres below the surface at most. Permeability is also increased throughout the basement lithologies due to the highly fractured nature of the rock mass as shown by the low RQD values (figures 3.14-3.16).

Signs of seepage (weathering effects) associated with fracture interaction are prevalent along the Mt William Range, with some artesian pressures observed in drillholes above the MWFZ. Surface conditions along the range tend to remain moist or damp for the majority of the year with minimal periods of drying out. Based on observations in the field during periods of precipitation, laboratory testing, and drillhole analysis, water in flow will be a significant feature in assessing slope stability at Cypress North Block. The high degree of saturation (and precipitation) exhibited within the stratigraphic units will require extensive drainage of the pit slope face to counter destabilizing effect due to the decrease in strength of the infill materials.

3.6 Synthesis

The greatest challenge to the stability of any proposed highwall will remain the need to incorporate the influence of the Mt William Fault Zone both with respect to the direct influence of the gouge zone, and secondary effects such as joint and shear defects associated with zone of influence. The presence of sheared defects and the highly disturbed fractured nature of the rock mass lead to the conclusion that initial intact rock strength will be of secondary consideration if the rock mass properties. Failure will more than likely propagate along existing defects as the intact rock strength of the basement lithologies greatly exceed any compressional forces (Max σ_c=~5MPa) which would arise due to overburden thickness. Other areas of concern are the crushed contact rock defects, which exhibit no coherent orientation and display variation of infill characteristics between crushed rock and broken-down highly weathered material in the form of silty/sandy clay. These zones represent a significant weakness in the basement lithologies.

Joint Set Orientations:

Section 1

Joint orientations observed in this section are predominantly sub vertical in nature with 4 sets exhibiting mean dips greater then 70°. JS3 is the prominent set with an orientation parallel to the Mt William Fault and a mean dip / dip direction of 79/118°. The second most dominant set is also effectively parallel to the Mt William Fault with an offset of less that 30° with a mean dip/dip direction of 89°/261°. Secondary sets are comprised of the oblique joint sets JS1 76°/041° and JS5 85°/174°. Joint set JS4 exhibits the lowest concentration of pole densities with a relatively low dip component with a mean orientation of 47°/106°. Sub horizontal sampling of joint orientations (e.g. JS4) is subject to bias introduced by the relatively low dip of the scanline surveys which means that defects exhibiting a low dip are under sampled.

Section 2

Joint orientations observed along Section 2 are, as in Section 1, dominated by sub-vertical joint sets with dominant orientations observed perpendicular to scanline surveys. JS3 again was the dominant set with an orientation of 84°/285°. The second most common defect set was JS2 with a mean dip/dip direction of 70°/245°. Secondary sets were again comprised of the oblique joint sets JS1 and JS5 with orientations 78°/025° and 79°/161° respectively. JS4 again is under sampled along this section with only a representative sample observed at a mean orientation of 43°/106°.

Comparisons can be made between the two sections with both of them showing the 5 major joint sets observed between scanline orientations. Variation between the Mean joint set orientations observed which may signify a point of rotation along the Mt William Fault, with a rotation of 13-16° towards the north observed in the sub vertical sets using stereographic projection. The fault itself is estimated to have a rotation of approximately 20° towards the north which suggests a correlation between the fault rotation and the rotation observed within the sub vertical defect sets. No rotation is observed in JS4 the

reason for this maybe the under sampling of the defect set as points do plot outside the mean orientation with minimal pole density.

Persistence of Jointing

Surface expression of persistence in the joint defects is minimal and therefore prediction based on visible persistence is required to predict the overall trend. Based on this limited surface expression, observations in the highly fractured basement lithologies show an average defect persistence of approximately 4 metres with a maximum observed persistence of over 8 metres in the Greenland Group Hornfels. Dominant persistence is orientated along primary defect sets JS2 and JS3 which are both sub vertical, with other joint sets being truncated by these joint sets. Interpretation of persistence will be used in the kinematic analysis to predict failure volumes.

Aperture and Infilling of Joints

The aperture between the surfaces of the infilled defects is a major controlling factor in determining the influence of the infill material. Apertures associated with the scanline surveys were predominantly narrow (0.1<1 mm), and usually iron stained. The apertures are generally close enough that during movement it will allows the joint surfaces to interlock, and therefore the strength of the joint reverts back to the shear strength associated with the surface on surface contact.

Spacing of Joints

RQD values for basement lithologies in both Sections 1 and 2 provided values which equated to very poor rock quality (RQD < 25%), with DH1697 adjacent to section one having a mean RQD of just 9.2% and DH 1698 adjacent to section two with an RQD of 17.5%. Breakdown of the frequency of RQD values down scope showed that more than 80% of all recorded RQD values for both drillholes was lower then 20%.

Table 3.4 Summary of RQD values

Hole #	Rock Type	Ave RQD	Total RQD
1694	Kaiata Mudstone	39.3	
	Brunner Coal Measures	51.0	38.2
	Coal	11.8	
1697	Berlins Porphyry	12.4	9.2
	Greenland Group	7.3	
1698	Berlins Porphyry	23.5	17.5
	Greenland Group	14.2	
1715	Berlins Porphyry	9.9	8.3
	Greenland Group	6.6	
1717	Kaiata Mudstone	31.8	33.5
	Brunner Coal Measures	68.9	
	Coal	0.9	

Interpretation of the separate lithologies in the basement stratigraphic units showed a proportionally lower degree of fracturing in the Berlins Porphyry when compared to the Greenland Group Hornsfel. Comparisons that were made between the Tertiary sedimentary units showed a marked increase in RQD values with the Kaiata Mudstone averaging ~36% (poor rock quality) and the Brunner Coal Measures with an RQD value of ~60% (fair rock quality).

Weathering and durability factors

The effects, rate, and influence of weathering in surface outcrops are often orders of magnitude higher than those encountered at depth, with exposure to atmospheric conditions resulting in a decrease in the condition of both the rock material and discontinuity properties. The basement lithologies show a variation in the degree of weathering, with exposed Berlins Porphyry along the length of the ridge crest showing a high to complete degree of weathering whereas the Greenland Group Hornfels shows generally a moderate degree of weathering. The degree of weathering has a direct effect on the shear strengths associated with the defects with drillholes exhibiting weathering effects to depths greater than 60m which has a significant effect on the overall strength of the rock mass (chapter 2).

Roughness

JRC values associated with the joint surfaces were predominantly semi rough with 60% of the joint surfaces recording a JRC of between 4-8. The next highest frequency is observed at a JRC of 8-14 (rough) with 23%. Only 12% of the joint surfaces showed a JRC less than 4. The moderate JRC values associated with most of the joints reflects a moderate shear component (friction angle, Ø = 35º) but the sub-vertical nature of the joint sets means that they will provide little resistance if joint planes were to day light in the pit slope face. Shear defects predominantly show JRC values lower than 4 (~68% of defects), with no value higher then 14 JRC (rough), and therefore provide little shear strength due to a low associated friction angles.

Hydrological Conditions

Signs of seepage associated with fractures are prevalent along the Mt William Range with some artesian pressures are observed in drillholes above the MWFZ. Surface conditions along the range tend to remain moist or damp for the majority of the year. Based on observations in the field during periods of precipitation, laboratory testing, and drillhole analysis water flow out of the rock mass will be a significant feature in assessing slope stability at Cypress North Block.

CHAPTER 4

HIGHWALL STABLITY ANALYSIS OF KINEMATIC FAILURES AND MINING IMPLICATIONS

4.1 Introduction

This chapter involves the systematic analysis of the data in the previous two chapters by using the parameters defined there to help establish the feasibility of kinematic failures in the basement rock mass. Accurate interpretation of possible instability mechanisms, and their relationship to defect orientation, is necessary in determining the safest highwall orientation. Factors such as the physical and mechanical properties of materials (chapter two), and the geological structure and groundwater flow (chapter three) are required for the development of an effective geotechnical model. This investigation has been focused on the analysis and characterisation of geological structure and lithological variation within the geotechnical lithologies. Interpretation of the Brunner Coal Measures and the Kaiata mudstone is limited and therefore the scope of the present chapter will be focused within the basement units.

The interpretation of the previous chapters, with regards to the basement lithologies found at the Cypress North Block, identified the rock mass as being heterogenous and anisotropic in nature due to the interfingering of the differing rock types, the presence of defects, and intact rock strength variations due to weathering effects. It was also identified that the rock mass interaction classified the feasible failure mechanisms as those shown by a discontinuum (Hudson 1997), where failure mechanisms were dictated directly by the presence of pre-existing discontinuities due to the relatively high intact rock strength and linear nature of the defects. The representative joint formation (figure 4.1) and basic failure mechanism associated with a discontinuum (figure 4.2) are associated with brittle deformation. In characterisation of the rock mass geological boundaries the intrinsic rock mass are defined by lithological contacts, major discontinuities (such as faults), or common defect orientations.

In the geotechnical evaluation of the Mt William Fault Zone the rock mass was separated into structural domains defined by mean discontinuity/defect characteristics. Summation of the structural domains was first defined by theoretical interpretation along the range but was revised by statistical distribution of the defect sets (chapter three) and kinematic analysis with regards to planar, wedge, and toppling failures. These modes of failure typically occur in a jointed rock mass, and can influence decisions made regarding the design of the highwall, and the overburden stripping sequence. As well as the kinematic analysis of each of the structural domains, individual analysis on each scanline was carried out to determine both a general classification with regards to failure by section and also a localized interpretation. Selected orientational models were developed to give a best case – worst case scenarios for these failures modes. The kinematic failure is only made possible by defect orientations daylighting in the highwall under certain criteria, therefore models were examined to determine the orientation that provides optimum highwall stability in the basement lithotypes.

4.2 Kinematic Analysis of Rock Mass Properties

The linear nature and strong rock characteristics associated with the basement lithologies indicates that the basic failure mechanism will be that of a discontinuum. A discontinuum is dictated more directly by a presence of specific pre-existing discontinuities then due to the weaknesses in the strength of the intact rock (figure 4.1).

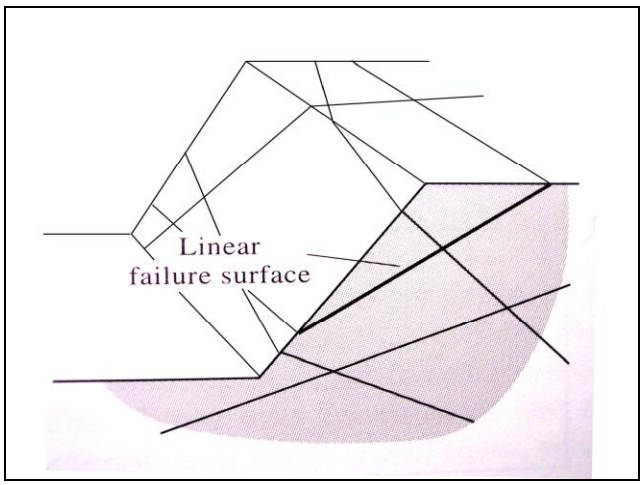

Figure 4.1 Illustration of Slope Instability Behaving as a Discontinuum, Modified from Hudson (1997).

Once the intrinsic properties of the rock slope are established relevant stability analysis can be carried out on the rock mass to determine the feasibility of kinematic failure associated with the discontinuities that daylight in the excavated surface. Kinematic analysis is carried out by the use of stereographical projection of the defects criteria outlined for each of the failure modes listed (figure 4.2);

- *Planar Failures* result from a single discontinuity surface dipping out of the slope face (figure 4.2a).
- *Wedge Failures* result from two or more two intersecting discontinuities whose line of intersection daylights and is inclined out of the slope face (figure 4.2b).
- *Toppling Failures* results in slabs or columns of rock defined by discontinuities that dip steeply into the slope face (figure 4.2c).

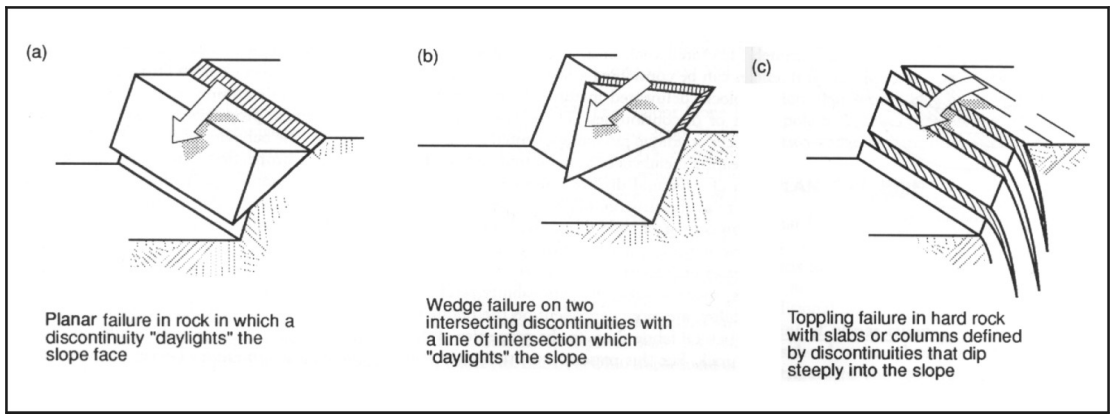

Figure 4.2 Potential rock slope failure modes. (Diagrams modified from Hoek and Bray, 1981)

4.3. Stereographic Analysis of Scanline Data

4.3.1 Analytical Methodology

The *DIPS Rocscience* program (version 5.1) was utilised for the various kinematic checks of the 12 individual scanline traverses. This was carried out by tabulation of the defect data sets into corresponding sections for analytical interpretation. This programme used a lower hemispherical projection of the poled dip orientations in a visual extrapolation of the statistical data. The data was inserted directly into the DIPS program from the transcription of field data into Microsoft Excel format (appendix 3, scanline information – CD insert). Pole plots were then developed for each of the scanline data, sets and contour plots of pole densities generated.

The rule of thumb is that clusters of data concentrations greater than 6% of the total per 1.0% area are deemed very significant when assessing mean joint sets, as dominant joint sets will have clusters of poles in this category as they have poles that will plot in a similar region of the stereo-net. Those concentrations between 4 and 6% represent a marginally significant cluster, with anything under 4% regarded with suspicion unless using a lot of data points (DIPS, Rocscience Manual, 2000). This allows for the identification of and grouping of significant clusters associated with each of the scanline surveys. This grouping, via set windows using *DIPS*, allows for the mean pole/plane to be displayed for each data set concentration.

After the joint sets were established for each scanline the kinematic checks for planar, wedge, and toppling failure were then performed and analysed as defined below. Contour plots used to establish all the joints sets, and the three kinematic checks performed (toppling, wedge, & planar failure) on all scanline traverses, are presented as appendix 4 (CD insert). All highwall, joint set, and faults are described using a dip/dip direction format in a lower hemispheric projection. Kinematic analyses were performed with a proposed highwall orientated in the same direction as the Mt William Fault Zone (Map 2)

dipping back in towards the basin. The reasoning behind this is to incorporate the influence of the fault zone in any batter design and minimize its overall effect on stability.

The scanline survey traverses were analysed separately to determine both lateral variation in surveyed data as well as to identify orientation bias. An interpretation of variation between the sections (1&2) was also derived to establish any structural domains associated with the defect sets in regards to their orientation and failure mechanism with respect to Mt William Fault. Comparisons were then made in terms of types of failures, scanline orientation, and discontinuity types.

4.3.2 Planar Failures

A planar failure is comparatively rare in rock slopes because it is only occasionally that all geometrical conditions required to produce such a failure occur in an actual slope (Hoek 1977). Planar failures consist of a relatively simple two-dimensional failure in which movement occurs by sliding along a single discontinuity, usually bounded by 'release surfaces' at the lateral extremities. These release surfaces are not considered to contribute to the stability of the potential failure mass. In the interpretation of a planar failure it is usual to consider a slice of unit thickness taken at right angles to the slope face. This means that the area of the sliding surface can be represented by the length of the visible surface on a cross sectional area and the volume defined by its lateral extent (figure 4.3).

In order that sliding should occur on a ***single plane***, the following geometrical conditions must be satisfied (Hoek 1977).

- The plane on which sliding occurs must strike parallel or nearly parallel (within approximately ± 20°).
- The failure plane must 'daylight' in the slope face. This means that is dip must be smaller than the dip of the slope face. i.e. $\psi_f > \psi_p$.

- The dip of the failure plane must be greater than the angle of friction of this plane. i.e. $\psi_p > Ø$.
- Release surfaces which provide negligible resistance to sliding much be present in the rock mass to define the lateral boundaries of the slide. Alternatively, failure can occur on a failure plane passing through the convex apex of a slope.

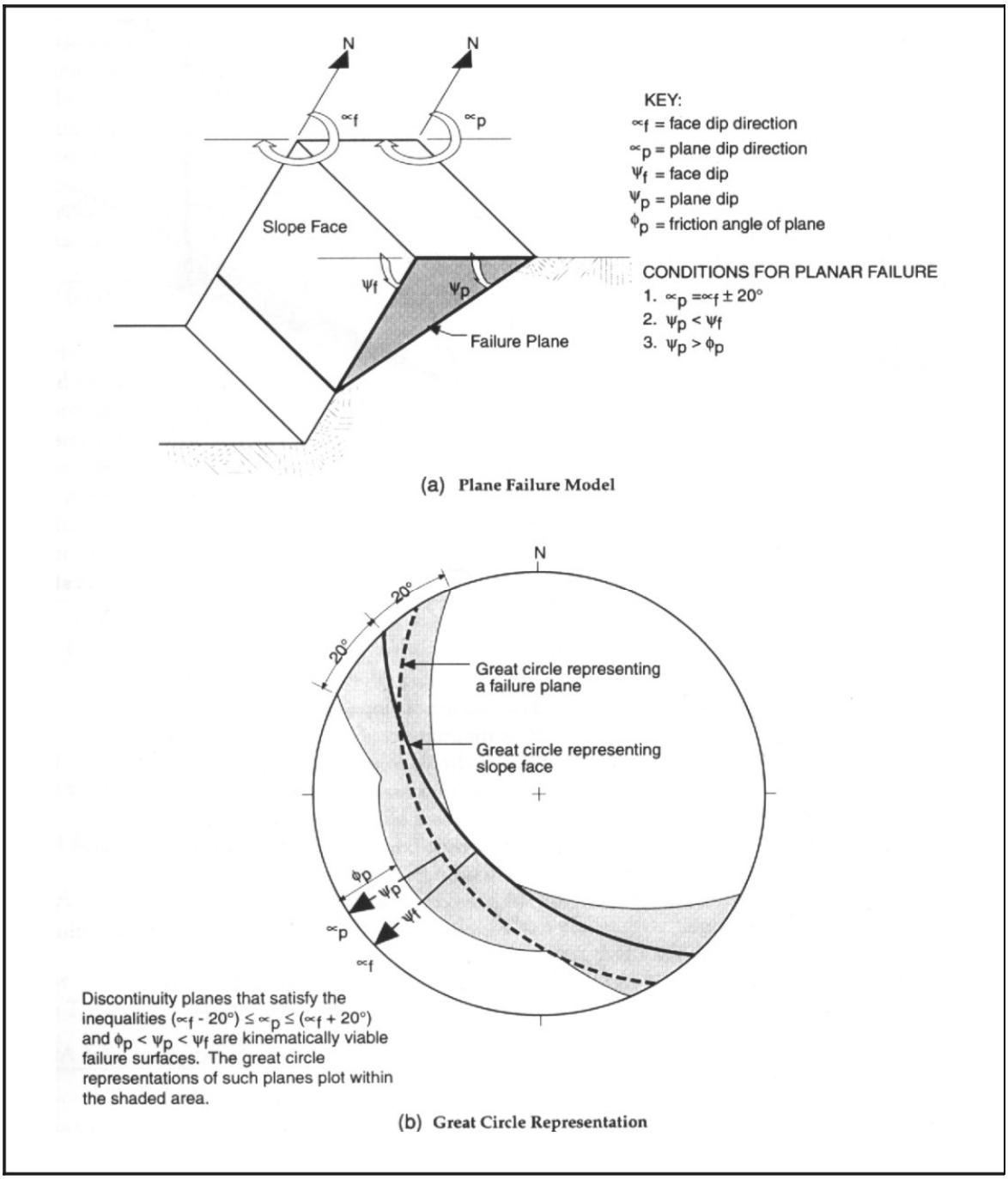

Figure 4.3. Kinematic analysis for planar failure (Norrish & Wyllie, 1996).

4.3.3 Wedge Failure Kinematic Analysis

The previous section was concerned with slope failure resulting from sliding on a single planar surface dipping into the excavation and striking parallel or nearly parallel to the slope face. Wedge failure is concerned with the failure of slopes in which structural features, upon which sliding can occur, strike across the slope crest and where sliding takes place along the line of intersection of the two discontinuities. These rock wedges are exposed by excavations that daylight the line of intersection forming the axis of sliding, initiating movement of the rock mass either along both planes simultaneously or along the steeper of the two planes into the direction of maximum dip. The size of the initial wedge failure depends on the relative persistence of the defect along which is it formed, but after initial failure occurred can incorporate similarly orientated rock blocks giving way to the formation of 'families' of wedge failures.

As with the case of planar failure for wedge failure to occur set conditions are required, defined by $\psi_{fi} > \psi_i > Ø$, where ψ_{fi} is the inclination of the slope face, ψ_i is the dip of the line of intersection, and Ø is the friction angle of the defect surfaces. These conditions are outlined below:

- The trend of the line of intersection must be within 20^0 either side of the dip direction of the slope face.
- The plunge of the line of intersection must be less that the dip of the slope face, i.e. the line of intersection is said to daylight on the slope face. ($\psi_{fi} < \psi_i$)
- The plunge of the line of intersection must be greater than the angle of friction on the surface. i.e. $\psi_i < Ø$

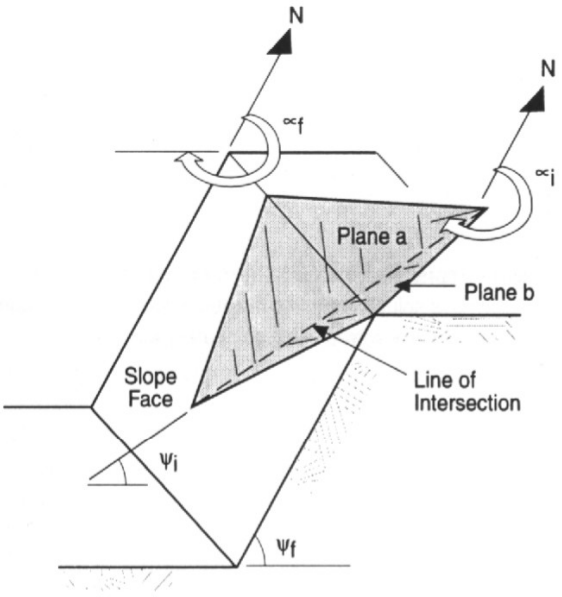

KEY:
$\propto_f$ = dip direction of face
$\propto_a$ = dip direction of plane a
$\propto_b$ = dip direction of plane b
ψ_f = dip of face
ψ_a = dip of plane a
ψ_b = dip of plane b
ϕ = friction angle
ψ_i = plunge of intersection
$\propto_i$ = azimuth of intersection

CONDITIONS FOR WEDGE FAILURE
1. $\propto_i = \propto_f \pm$ (to daylight slope face)
2. $\psi_i < \psi_f$
3. $\phi < \psi_i$

MARKLAND'S TEST
If $\propto_a$ or $\propto_b$ is between $\propto_i$ and $\propto_f$ then sliding will occur on the steeper of planes a and b in the direction of maximum dip; otherwise sliding occurs along line of intersection.

(a) **Wedge Failure Model**

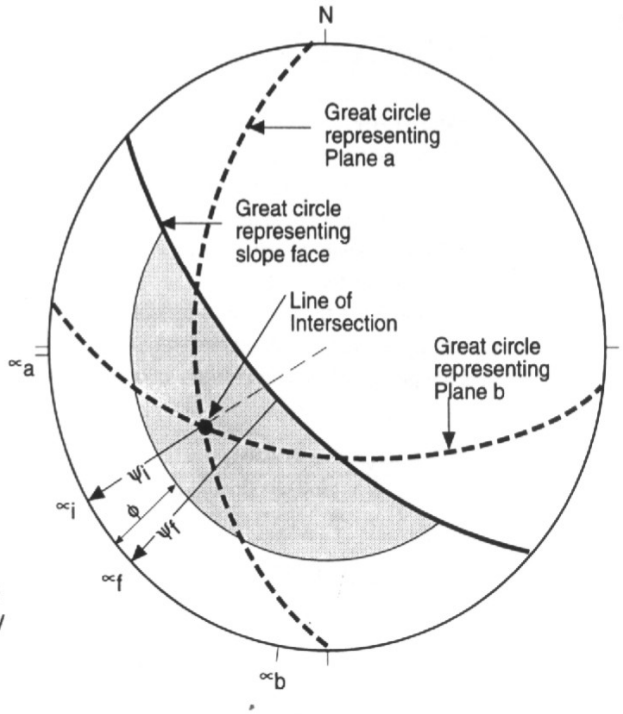

Combinations of discontinuity planes with a line of intersection that "daylights" the slope face, $\propto_i = \propto_f \pm$, and that satisfy the inequality $\phi < \psi_i < \psi_f$ represent kinematically viable wedge failures. The lines of intersection of such planes plot within the shaded area.

(b) **Great Circle Representation**

Figure 4.4. Kinematic analysis for wedge failures (Norrish & Wyllie, 1996).

4.3.4 Toppling Failure Kinematic Analysis

The previous two failure modes incorporated sliding of a rock mass along an existing failure surface(s). Toppling failures involves rotation of columns of rock about some fixed base, and commonly occur in rock masses that are subdivided into a series of slabs or columns formed by sets of fractures that strike approximately parallel to the slope face and dip steeply into the face. In order for toppling to occur, the centre of gravity of the slab must fall outside the dimension of the base, and toppling failures are therefore characterised by significant horizontal movements at the crest and very little movement at the toe. Goodman and Bray (1967) describe a number of different types of primary toppling failures which may be encountered in the field. The first of these is Flexural Toppling, and in occurs in hard rock slopes with well developed steeply dipping discontinuities which break in flexure as they bend forward (figure 4.5a). The second type is Block Toppling, which occurs when columns of hard rock are divided by widely spaced orthogonal joints (figure 4.5b). The third type is Block-Flexure Toppling which is a combination of the both Flexural and Block failures (figure 4.5c).

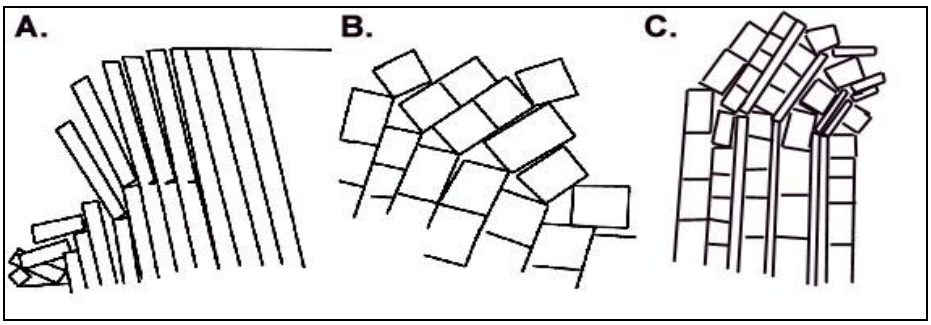

Figure 4.5 illustration of toppling failures, Flexural, Block, and Block-Flexure respectively (Hoek 1977)

The conditions for Toppling to occur are:

- The strike of the slab must be approximately parallel to the slope face. Differences in these orientations of between 15 and 30º have been quoted by various workers, and a conservative value of 30º been used in the analysis performed on the stereonets.
- The dip of the discontinuities must be into the slope face.

- Goodman (1980) states that in order for interlayer slip to occur, the normal to the toppling plane must have a plunge less than the inclination of the slope face minus the friction angle of the surface.
- The lateral extent of the potential failure mass must be defined by either lateral release surfaces that do not contribute to the stability of the mass or by the presence of a convex slope shape that is intersected by the planar discontinuity.

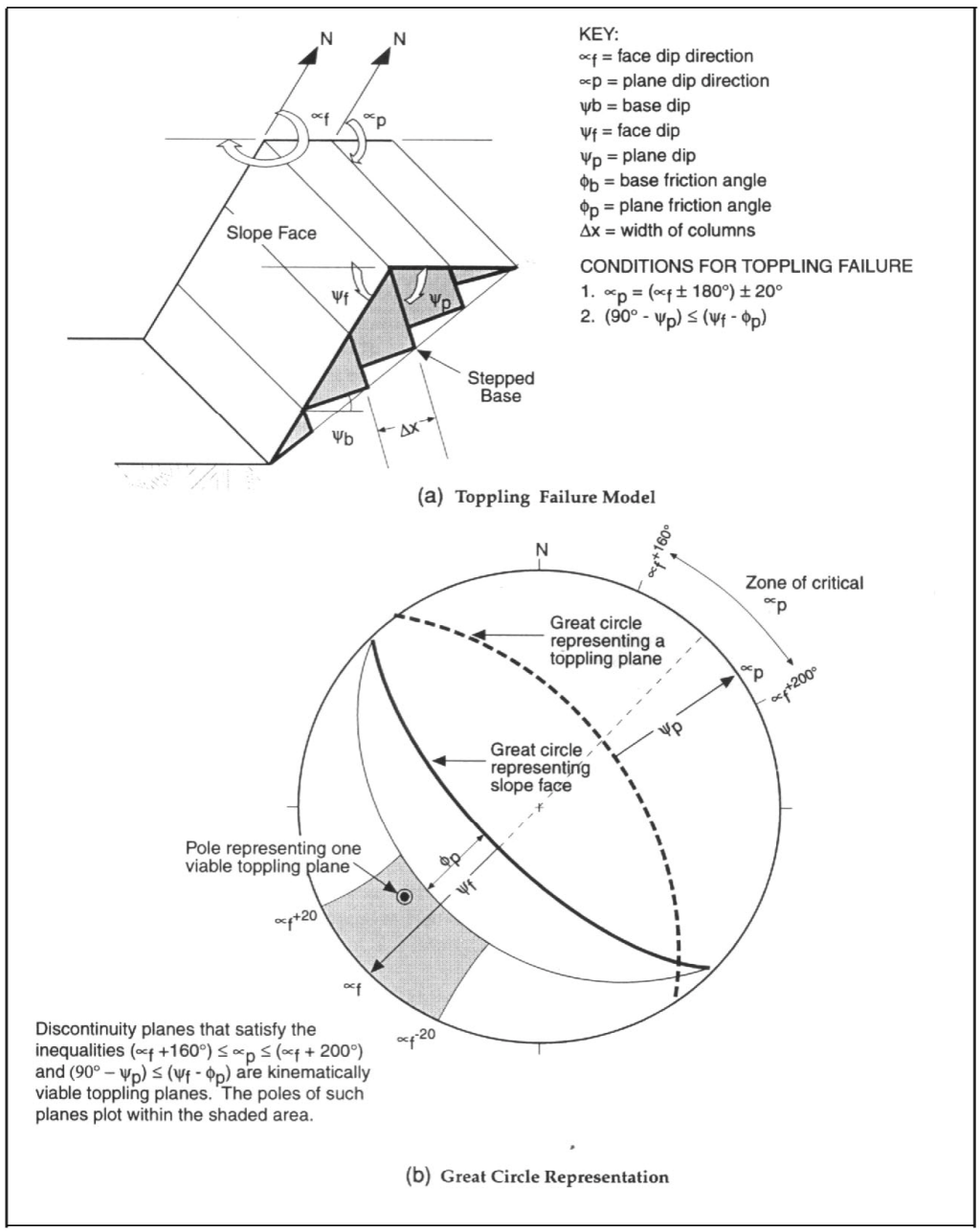

Figure 4.6 Kinematic analyses for toppling failure (Norrish & Wyllie, 1996).

4.4. Results of Kinematically Possible Slope Failure Analysis

4.4.1 Planar Failure

The first of the kinematic failures assessed from the scanline defect data was planar failure, which occurs on the basis that any pole that is kinematically free to slide and is frictionally unstable poses a plausible plane of failure. Unlike with the proceeding Kinematic analysis planar failure is interpreted on a defect by defect analysis (as it only requires one defect plane for failure) with added mean pole density relating more to probability of failure and the potential size of that failure.

A planar sliding analysis uses variability cones, a friction cone, and daylight envelope to test for combined frictional and kinematic possibility of planar sliding. Interpretation using the intersection of the daylight envelope and the pole friction cone generates a crescent shaped zone which encloses the region of planar sliding (figure 4.7). This crescent-shaped area represents the variability cone which defines the statistical probability of failure (95%). Any poles within this region represent planes which can slide. The daylight envelope allows for kinematic determination (i.e. a rock slab must have somewhere to slide into free space), with defects having poles within this area exposed to daylight within the slope face. The pole friction cone represents an area of the rock mass in which frictional forces along the joint faces are greater than opposing kinematic forces causing failure. The Pole friction cone was defined using joint survey joint roughness data with joint surfaces interpreted to have a friction angle of 35º based on joint roughness (chapter 3).

Section 1

Section 1 is a grouping of the first 6 scanlines (Map 2), which were found to have similar joint set orientations, at the northern end of the Cypress North Basin along the Mt William Range. Planar analysis of the data collected following the guidelines set out above in the methodology was interpreted with regards to this type of failure.

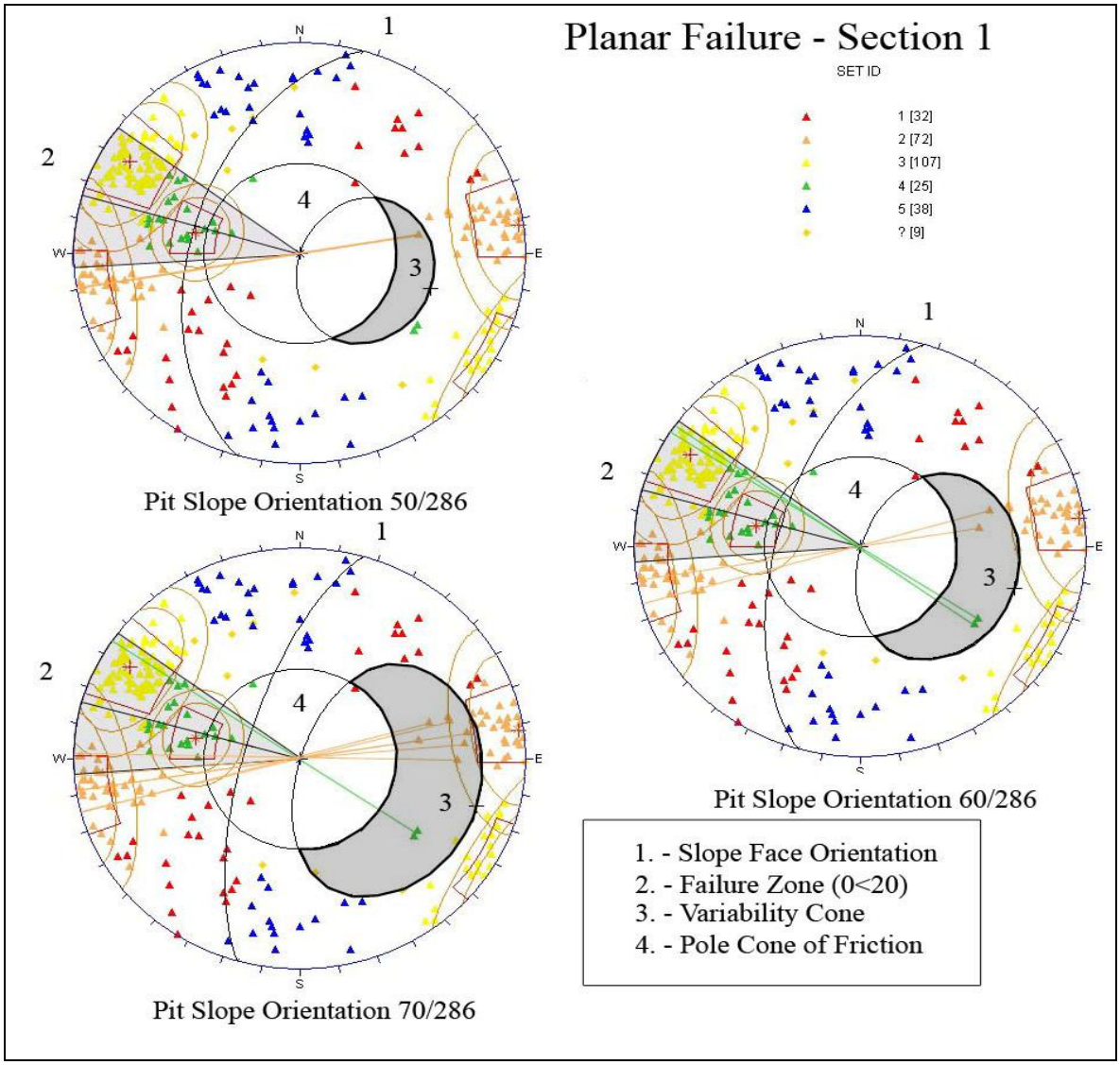

Figure 4.7 Planar Failure Associated with Section 1 – Scanlines 1-6 Inclusive. Pit Slope Orientation of 286º is Based on the Orientation of the Mt William Fault Adjacent to Section 1.

After applying kinematic checks to each of the individual scanlines they showed a low level risk of planar failure along most traverses, with only sporadic poles plotting inside the variability cone. The only scanline to not show a representative poling inside the variability cone was scanline 2. The grouping of the first 6 scanlines increases the sample density, as shown in figure 4.7 which displays three different pit slope dips. Using an orientation similar to the orientation of the Mt William Fault as a reference other slope orientations can be quickly interpreted. The greatest risk of planar failure, shown in 4.7, is

associated with JS 2 and JS 4 with both sets having representative samples which both are kinematically viable and are orientated within 20 degrees of the pit slope orientation.

The risk of planar failures along this section of the Mt William Range is minimal even, when factoring in the bias associated with low angle dips which are countered by a pole friction cone of 35º. The orientation of both JS 2 and JS 4 is on the outer limits of 20º failure limit (which defines the kinematic failure limit) and therefore incorporate greater degrees of influence from release surfaces. As would be expected an increase in the steepness of the pit slope also sees an increase in the kinematic viability of planar failure with the inclusion of the low level dips associated with JS 2. The greatest risk through planar failure would be if the pit slope was orientated in a North – South trend which would see the failure propagating along joint sets JS 1 and JS 2.

Section 2

Section 2 is a grouping of scanlines 7-12 situated at the middle to southern end of the Cypress North Basin along the Mt William Range. Planar analysis of the data collected following the guidelines set out above in the methodology was interpreted with regards to this type of failure. A collaboration using the 6 scanlines to increase the sample density is outlined in figure 4.8.

After applying kinematic checks to each of the individual scanlines most showed a similar low level risk of planar failure as in Section 1. Scanline 8 showed the highest kinematic viability of planar failure. Scanlines 9, 10, 11, and 12 show no poles plotting within the variability cone with a pit slope less than 60º. The greatest risk of planar failure is associated with JS 4, with the set having a strong representative sample which is both kinematically viable and is orientated within 20 degrees of the pit slope orientation.

The risk of planar failures along this section of the Mt William Range shows a risk of kinematic failure within the JS 4 joint set. The orientation of JS 4 projects very close to the orientation of the hypothesized proposed highwall, and therefore exhibits a lesser degree of influence from release surfaces (secondary joint sets JS 1 and JS 5) and the

greatest chance of planar failures. Incorporation of other joint sets is limited even at a pit slope of 70º. As would be expected an increase in the pit slope does see an increase in the kinematic viability of planar failure with the inclusion of the low level dips associated with JS 3. Possible planar failure would have to be bounded by release surfaces (JS 1 and JS 5) on the outer extent of the failure plane.

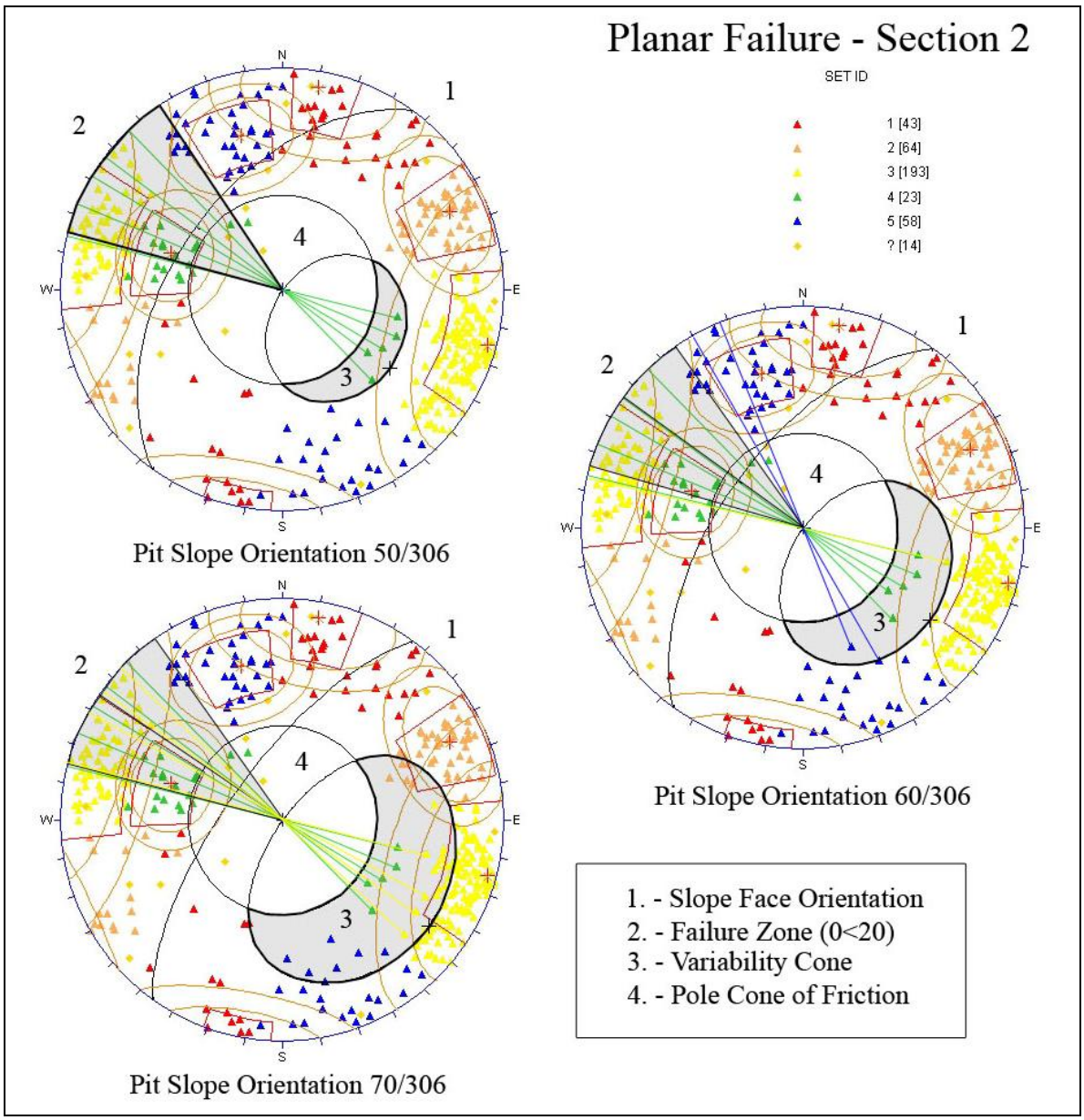

Figure 4.8 Stereographic Projection of Planar Failure Associated with Section 2 – Scanlines 7-12 Inclusive. Pit Slope Orientation of 306º is Based on the Orientation of the Mt William Fault Adjacent to Section 2.

4.4.2 Wedge Failure

The second of the kinematic failures analyzed was the wedge failure, which incorporates the use of the mean pole orientations determined from pole cluster densities as outlined previously. Wedge sliding may occur if the mean joint set orientation intersections fall within the zone defined by the plane friction cone and the pit slope. The plane friction cone is defined as the inverse of the pole friction cone, as this time the analysis is not dealing with poles but an actual sliding surface or line, so the friction angle is take from the equator.

Section 1

Kinematic checks for wedge failures were carried out on the scanline data and the viability of such failures assessed. Analysis was carried out on each individual traverse with regards to local mean defect pole/plane densities. As well as these individual analyses a grouping of the first 6 scanlines (as seen with the planar failures) was used to interpret the major defect sets seen along Section 1. The defect sets are dominated by joint sets JS 2 and JS 3, which make up 63% of the joint sets and have the highest cluster densities.

The individual analysis of mean plane intersections for each of the 6 scanline surveys showed no kinematic wedge failures. Most intersections analysed between joint sets plotted within the plane friction cone but outside the window of viability for failure to propagate. Although all mean joint set combinations plotted outside this window, it did show two mean combinations which were close enough that under the right conditions between the two joint sets failure could be possible. Slight variations of the mean joint sets saw the kinematic viability of wedge failure combinations of the primary joint set JS 2 with secondary joint sets JS 1 and JS 5, as highlighted by wedge analyse on scanlines 2 and 6.

Although outlined as kinematically possible the right conditions (as outlined in the methodology) for these two joint sets to fail reduce the risk considerably. If the right conditions for wedge failure do occur the size of the failure, due to the highly fractured

nature and the low persistence, would be minimal. An increase in the highwall steepness only slightly increases the possibility of wedge failure.

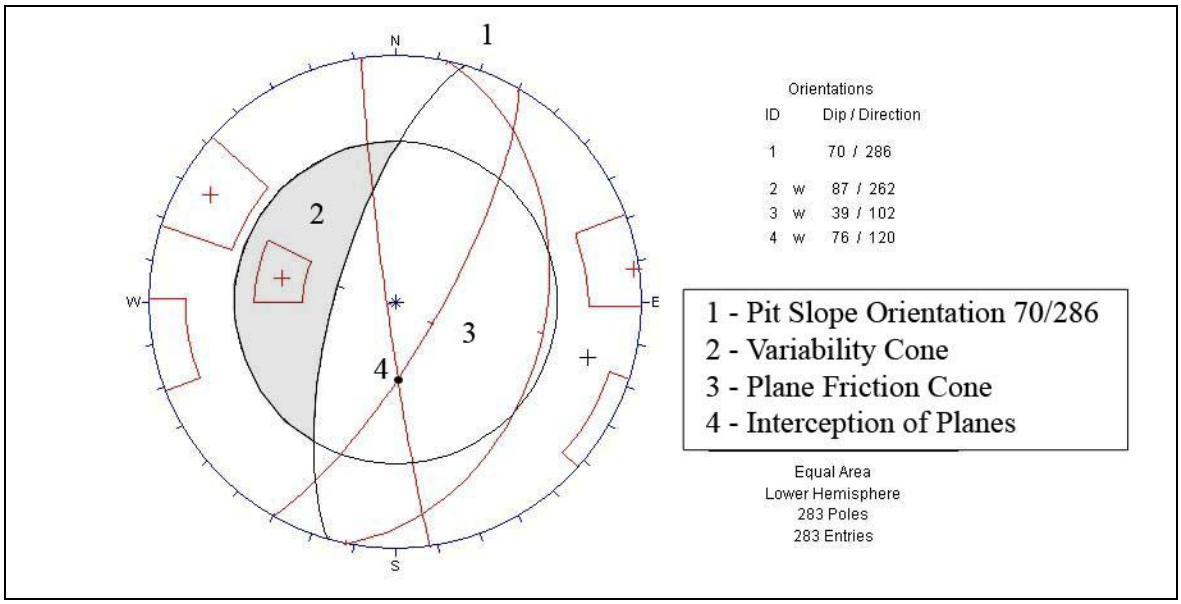

Figure 4.9 Stereo Projection of Wedge Failure Associated with Section 1 – Scanlines 1-6 inclusive

The grouping of the of the first 6 scanlines (figure 4.9) sees only two of the five joint sets outlined in the previous chapter with densities strong enough to considered significant. The incorporation of JS 4 is to cover any bias introduced via the horizontal orientation of the scanline traverses. Figure 4.9 highlights a low risk due to wedge failure within this particular highwall orientation with a face slope of 70º. This projection of wedge failure, along with the analyses of individual scanlines, shows that the greatest risk for this type of failure would occur if the pit face was sloping to the south – southeast.

Section 2

The individual kinematic checks of the scanlines (7-12) in Section 2 again, as with Section 1, showed no possible wedge failures. The majority of the joint set interactions occurred within the plane friction cone but outside the viability window. Highlighted by the individual scanlines was that the combinations of lower cluster densities carried the possibility of wedge failures, in particular the orientation of JS 3 observed in scanline 8. Projection of the orientation of the mean plane of joint set JS 3 into the other scanlines shows a dramatic increase in the possibility of wedge failures along this section. Therefore

if the poles observed within the scanline 8 are a true representation of an under-sampled joint set, wedge failure would be possible though the combination with JS 2 in all scanline surveys and in combination with JS 5 in the majority of the scan lines.

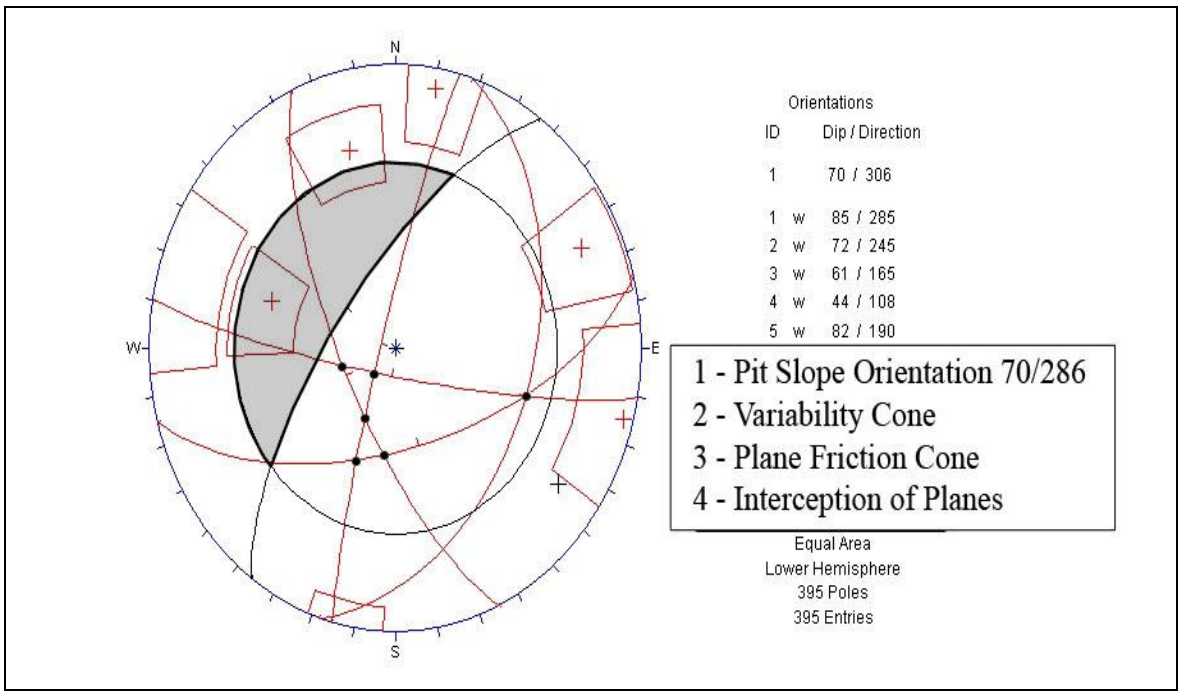

Figure 4.10 Stereo Projection of Wedge Failure Associated with Section 2 – Scanlines 7-12 inclusive

The grouping of Scanlines 7-12 (figure 4.10) again sees that only two of the five joint sets have densities strong enough to be considered significant (pole contour density >6%). The incorporation of the other joint sets was included as marginally significant densities (pole contour density between1.5 and 3%). Figure 4.10 highlights a low risk due to wedge failure within this particular highwall orientation with a dip of 70 degrees. This projection of wedge failure, along with the analyses of individual scanlines, shows that the greatest risk for this type of failure would occur if the pit slope face was orientated to the south – southwest (~210-220^{o}).

4.4.3 Toppling Failure

The last of the basic checks to be carried out on the scanline data was that of kinematic failure via toppling. Goodman (1980) states that for failure to occur, the defect set normal to the pit slope face must be inclined less steeply than a line inclined at an angle equivalent to the friction angle above the slope known as the slip limit. The slip limit makes up the upper limit of the failure zone which is known as the viability cone, and is defined laterally by a limit of 30 degrees parallel to a cut slope which was revised from an earlier 15 degree limit which was found to be too small. This viability cone is said to represent a statistical probability of 95%.

Section 1

The kinematic checks for toppling failure carried out on each individual scanline traverses found in Section 1 (scanlines 1-6) showed some degree of toppling failure within each of the surveys. The only traverse with low percentages for toppling failure was the first scanline transect, which was orientated parallel to the dominant defect sets and therefore under-sampled those sets. There are varying degrees of toppling viability depending on the defect cluster densities of the primary defect sets JS 2 and JS 3, which represent the viable modes of failure in the highwall at this orientation (286º). Visual estimates of the defects sets range between 40-80% of the set plotting within the viability window for scanlines 2-6 which are normal to the fault trace.

The grouping of the first 6 sets (figure 4.10) shows a high probability of toppling failure in the highwall, as a high percentage of defect poles plot inside the viability cone. The type of toppling is predicted to be block toppling due to the highly fractured nature of the rock mass. Rotation of the proposed highwall orientation would see a reduction in the risk of toppling failure with the present orientation presenting the greatest risk of this type of failure (figure 4.11). Any viable orientation (with respect to overburden constraints) of the slope face into the Mt William Range would also see some degree of toppling failure associated with the pit slope with a rotation up to 30º in either direction also displaying a high probability of failure. An increased steepness of the pit slope would see a dramatic

increase in the probability with this kind of failure. Increased pit slope angle (50-70º) sees the increase of pole densities JS 2 and JS 3 plotting within the viability cone.

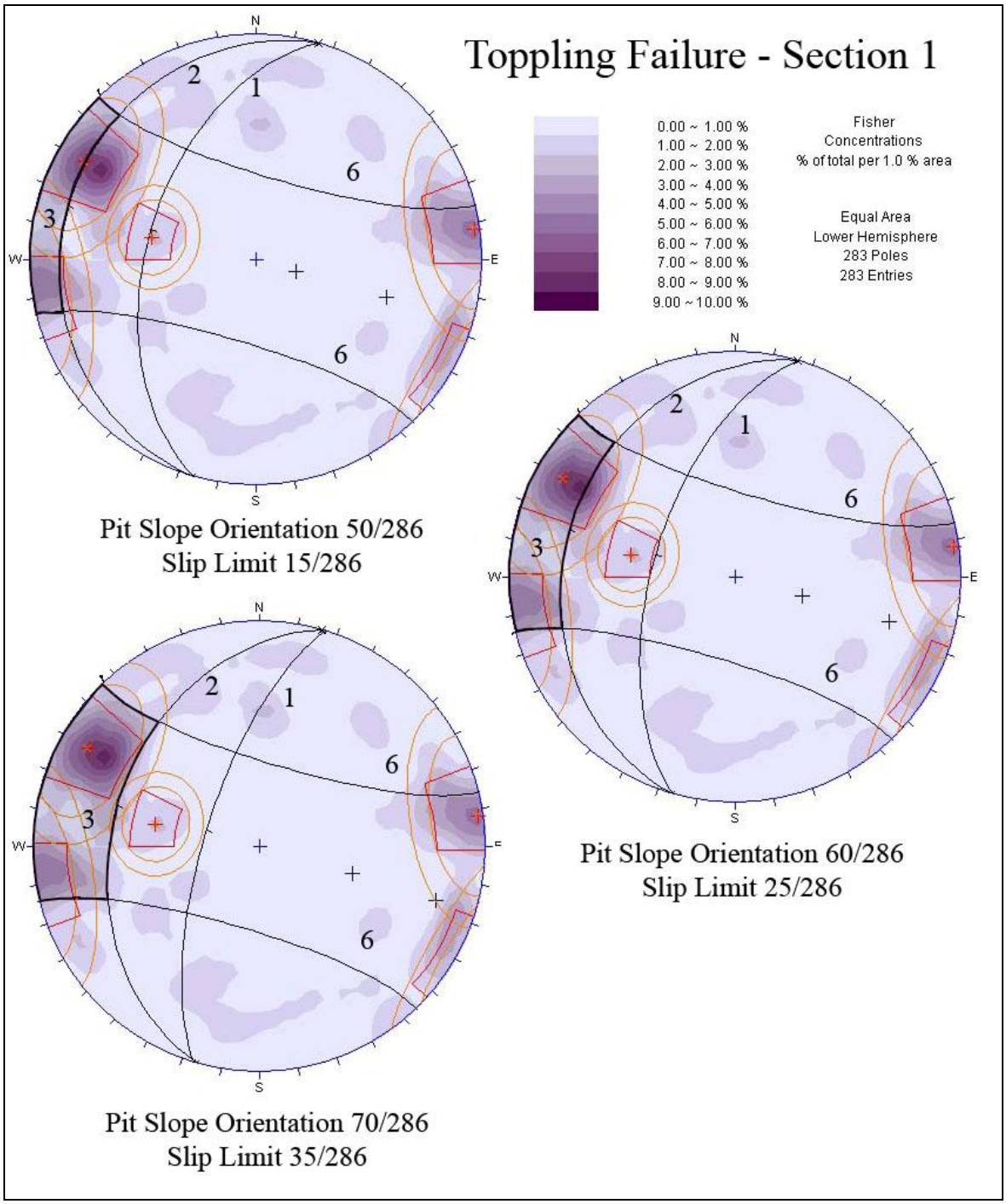

Figure 4.11 Stereographic Projection of Toppling Failure for Section 1, Scanlines 1-6.

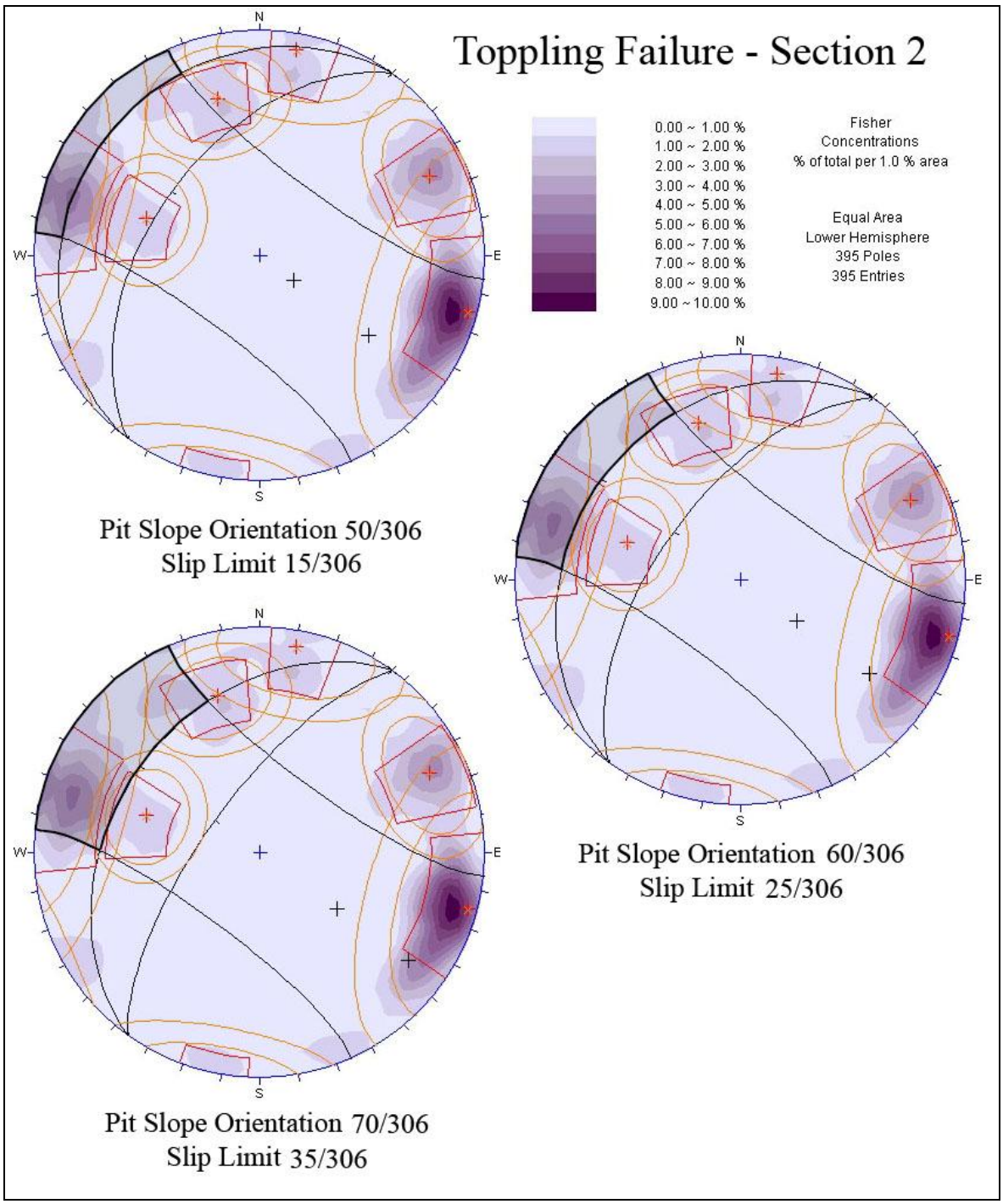

Figure 4.12 Stereographic Projection of Toppling Failure for Section 2, Scanlines 7-12.

Section 2

The kinematic checks for toppling failure carried out on the second set of scanline traverses found in Section 2 (scanlines 7-12) also showed some degree of toppling failure within each of the surveys. The majority of the scanlines displayed low viability with regard to this type of failure, and the orientation of the major defect set associated with toppling, in Section 1, now tending to dip back into the slope. Scanlines 10 and 11 (normal to the fault) show the highest probability of toppling failure, with approximately 40-50% of the pole densities residing within the viability cone. Scanline 7 (orientated parallel to the fault) shows all but no pole density within the viability cone, but carries bias due to the orientation of the scanline. The primary defect set associated with toppling failure in Section 2 is JS 3, which represents the only viable mode of failure in the highwall at this orientation.

The grouping of Scanlines 7-12, shown above in figure 4.12, shows a moderate probably of failure due to toppling in the JS 3 defect set. As predicted with Section 1 the mode of failure is more then likely to be block toppling due to the highly fractured nature of the rock mass. Rotation of the proposed highwall orientation (up to 30º in either direction) would see less of a reduction in the risk from toppling failure with respect to the present orientation. As would be predicted a higher overall pit slope sees an increase in the probability of this kind of failure, but with less influence than the effect of slope steepness in Section 1. The increase of the overall dip angle from 50-70º sees only a mild increase in the proportion of JS 3 present inside the viability cone.

4.5 Discussion of Highwall Stability

The overall stability of any proposed highwall along the Mt William Range at Cypress North Block will be determined after examination of the kinematic failure potential and individual locality characteristics. Highwall orientations for the proposed opencast pit are limited and confined by the existing orientation of the range. To this end minimizing the influence of the basic failure mechanism will be dependent on the orientation of the batters, with the orientation determining whether defects will daylight in the highwall face or create toppling failure on steeply dipping joints. The approach in determining the stability of the slope should therefore be to examine the potential for instability mechanisms, and to gradually refine the design and analysis. The initial approach was to establish the possibility of instability by the method of basic kinematic analysis.

Kinematic feasibility checks are but the first in a series of design and analysis tools. Kinematic checks do not provide a numerical measure of the degree of safety of the slope, but whether or not instability is feasible in the first instance. In combining the kinematic analysis of the proposed highwall in relation to the Mt William Fault, a series of maximum slope orientations can be assessed and determined.

4.5.1 Mining Implications of Joint Sets - Section 1

Individual joint sets examined tend to be stable with regards to the kinematic mechanisms of wedge and planar failure, with toppling failures being the most viable of the failure mechanisms. High risk of toppling failures are present on all transects which are orientated perpendicular to the proposed highwall, with mean poles for JS 2 and JS 3 frequently plotting within the viability window. The mining implications due to the instability of this kind of failure would see a transgression of the upper extent of the highwall design back into the range to negate the highly weathered extent of the upper 20m. The reduction in the degree of weathering would see an increase of strength along the joint defects due to an increase in the overall shear strength and interlocking of rock

blocks. This would see toppling failures probably limited to the top 20m of the proposed highwall design and allow for steeper batter design which will increase the overall steepness of the pit slope.

The size of potential failures outlined above tends to be relatively small scale ($10m^3$ – $100m^3$) due to the rock mass properties outlined in the previous chapter. Rock mass properties such as aperture, persistence, joint roughness, and defect frequency (RQD) all seem to favour small block sizes ($<1m^3$). The block size depends on these rocks mass properties and relates directly to the size of potential failures. In terms of excavation and support, it is helpful to have an estimate both of the mean block size and the block size distribution. Due to the highly fractured nature of the rock mass of both Sections, rock mass size and distribution can be said to be homogenous with failures due to block toppling failure acting more like stiff gravel with a 'crumbling' effect with minor debris displacement.

4.5.2 Mining Implication of Joint Sets – Section 2

Individual joint sets examined within this section tend to show stability with regard to wedge failures, but a greater degree in potential planar failures (as outlined for Scanline 8). Kinematic failures due to toppling showing a decrease with high risk toppling failures only present on Scanlines 10 and 11. As seen with Section 1 the greatest potential for toppling failure resides in JS 3 where poles frequently plot within the viability window. The mining implications due to toppling instability are outlined for Section 1, and also apply to Section 2. The potential of planar failure is increased within this orientation of the highwall, with an alignment seen within joint set JS 4. The risk of this type of failure is still minimal because of the need for lateral release surfaces (JS 1 and JS 5). If the pole density seen in Scanline 8 is a true representative sample of defects along the length of the section, implications are that this would also increase the risk of wedge failures.

The size of potential failures outlined above tends to be relatively small scale ($10m^3$ – $100m^3$) again due to the relatively small block size ($<1m^3$). Wedge and planar failures

have the potential to be of a greater scale then the toppling failures with potential from the initial failure to propagate and causes instability in the adjacent rock mass.

4.5.3 Mining Implications of the Faults

The major fault zones associated with the Mt William Range, the Mt William Fault and the McCay Fault, dip back into the range front and do not pose an immediate threat to the stability of the highwall, with the suggestion that any surface expression of the faults exhumed could be incorporated into the batter design and effectively locking their influence within a bench. The faults pose an extensive release surface which could see degradation in the strength of individual batters and cause an increased frequency of toppling failure in sub vertical joint sets JS 2 and JS 3.

Two further zones of fault influence have been outlined on Map 2 (Map Pocket). The first of these zones is located between the two sections representing a plane of discontinuity. This particular defect is situated perpendicular to the fault trace which minimizes its influence with respect to planar failure along the feature. It is theorised that the fault has a dip inclination mimicking that seen in the joint set JS 5, and that it extends across the width of the Range and into the basin behind. The fault face therefore poses a plausible major release surface for both toppling and wedge kinematic failures to propagate along. The second defect zone is theorized to be a southern extensional expression of the Mt William Fault trace as it separates to the north into the McCay fault. The trace orientation seems to mimic that observed within the joint set JS 3, with an up throw to the west. The fault represents a high risk section of the rock mass with respect to kinematic failures via toppling, the influence of the fault has also seen an increased in the fracturing of the surrounding rock mass as can be seen in the RQD values for DH 1715.

Failures associated with the fault defect planes could potentially be the largest failures within the highwall design due to the relatively small persistence observed within the surface expression of the other minor defects. Failure sizes are hard to determine as there is no reference point in which to base calculations. Conclusions derived from analysis of the fault orientations poses that the greatest potential for kinematic failure still remains

toppling failures with the presence of release planes in the form of fault shear zones. The risk of complete failure to the highwall is minimal with small scale toppling failures more likely.

4.6. Establishment of Structural Domains.

The establishment of structural domains in the Mt William Range at Cypress North Block Basin is based on an engineering geological evaluation of the structural discontinuities or defects present. A structural domain is defined as a mapped area that is lithologically and structurally homogeneous. In a general sense one could surmise that the entire range exhibits enough uniformity along the length of the crest for it to be characterised as one domain. The uniformity of structure has implications on the proposed highwall design and stripping procedures within the domain. Major joint sets are present in both sections and are theoretically controlled by the interface with the Mt William Fault. It was proposed that there was enough of a variation in the orientation of these major joint sets to warrant the division of the two sections identified. The range was therefore divided into two structural domains, the division of which is defined by defects sets that share a common orientation, principally joints and shears. Divisions also can be derived from the interpretation of the kinematically viable failure of the defects present. The special orientation of scanline surveys and structural domains are outlined on Map 2 (Map Pocket).

4.7 Synthesis and Conclusions

This chapter incorporated the analysis of the previous two chapters in the definition of potential kinematic failures with regards to highwall orientations. In doing so the kinematic analysis was also used to further the interpretation and division of the structural domains initially outlined in chapter three. The initial approach was to establish the possibility of instability by the method of basic kinematic analysis as summarised in table 4.1.

Table 4.1. Summary Table of Potential Kinematic Failures for Pit Slope of for Each Scanline Traverse.

	Type Of Kinematic Failure					
Scanline No.	Planar Failure	Sets	Wedge Failure	Sets	Toppling Failure	Sets
	(Max Slope Plane)		(Max Slope Plane)		(Max Slope Plane)	
Section 1 – 286º	√	JS3	X	-	√	
1	X (83)	-	X (90)	-	X	-
2	X (90)	-	X (76)	JS 1&2	√	**JS2&3**
3	√ (56)	JS3	X (90)	-	√	**JS2&3**
4	X (62)	-	X (90)	-	√	**JS2&3**
5	X (63)	-	X (90)	-	√	**JS2&3**
6	√ (55)	JS3	X (66)	JS 2&5	√	JS2&3
Section 2 – 306º	√	**JS3**	X	-	√	JS3
7	X (62)	-	X (77)	JS 1&2	√	JS3
8	√ **(37)**	**JS3**	X (82)	JS 1&5	√	JS3
9	X (68)	-	X (83)	JS 2&3	√	JS3
10	X (62)	-	X (90)	-	√	**JS3**
11	X (71)	-	X (89)	JS 1&2	√	**JS3**
12	X (75)	-	X (80)	JS 1&3	√	JS3

*** Underlined symbols represent a moderate to high risk of failure.**

**** Bracketed values represent slope angles at which kinematic failure is possible**

Once the potential kinematic instability was established, development of the structural domains was carried out and sections 1 and 2 were defined with regards to structural deformation. Interpretation on both individual scanlines and groupings of the scanlines into the respective structural domains was used in the interpretation.

Section 1 can be classified as a highly disturbed area of basement lithology comprised of 5 major defect sets having surface expression. The dominant joint set being sub-vertical, with a mean orientation of 79º/118º, which poses a high level risk of kinematic failure through toppling with 50-80% of the defect orientations plotting within the viability cone for a 60º pit slope. Other kinematic risks, wedge and planar failure, were interpreted to have low probability of failure.

Section 2 can also be classified as a highly disturbed area of basement lithology comprised of 5 major defect sets exhibiting surface expression. The dominant discontinuity is a sub-vertical joint set, with a mean orientation of 84º/285º which poses a moderate risk of kinematic failure through toppling with between 20-40% of joint set JS 3 plotting within

the viability cone. An increase in the overall steepness of the pit slope generates a higher level of the defect poles plotting within the viability cone. Other kinematic risks, wedge and planar failures, were interpreted to have a low probability of failure. Scanline 8 shows the possible inclusion of a joint set (JS 4) that warrants greatest cause for caution as interactions between other joint sets could see a marketed increase in risk of both wedge and planar failures if the joint set represents an under-sampled defect.

In carrying out kinematic analysis on the defect sets it was necessary to place an arbitrary reference plane to interpret the data. It was deemed appropriate to assign this plane the same orientation as the Mt William Fault strike, as it allow for the incorporation of this major defect in the final design of the highwall, and any proposed highwall will in most part be dictated by the orientation of the MWFZ. Deviations from the proposed highwall orientations investigated are limited to rotations within 20-30º of the overall trend of the range itself. The rotation of the highwall design will increase the removal of overburden and limit the recoverable coal. The selected orientation saw a favourable stability even when including the moderate to high risk of toppling failure as rotation would see an increased in the other types of failure mechanisms due to alignment of the joints sets with the pit slope face. The joint sets associated with the range are statistically dominated by two sets of defects designated JS 2 and JS 3, and these account for over 60% of all data points collected and pose the immediate risk to toppling failure.

Toppling Failure

A rotation of 30º in the slope face to the north would see only a slight reduction in the risk associated with toppling failures. The rotation would see a reduction in the degree of toppling failures for Section 1 by the removal of JS 2 as a potential means for failure. There would also be a reduction in Section 2 with a reduced influence from JS 3, but a renewed risk from JS 5 and the incorporation of JS2 as a possible release surface causing increased risk. A rotation of 30º to the south (giving it a westward facing dip) would also give a relative reduction in the risk of toppling failures for both sections. In Section 1 it would see a transfer in kinematic viability from JS 3, the dominant set along the ridge, to

JS2, with a reduced frequency of possible release surfaces. In Section 2 the rotation would see a considerable drop in the frequency of defects plotting in the viability window.

Planar Failure

The effects of rotation of the highwall orientation (<30º) on planar failures sees that a rotation to the north would see an alignment of the lower dipped defect set JS 4 in Section 1 and with it an increased risk from this type of failure. In the case of Section 2 a rotation would see the reduction of risk associated with JS 4 but an increased risk from the variable dipping JS 5 defect set. The effect of rotation in the opposite direction would see in both sections an increased alignment of the primary defect set JS 2 at pit slope orientations greater then 55 degrees.

Wedge Failure

The effect of slope orientation on kinematic wedge failures shows that a rotation of the slope face 30º to the north would see an increased risk of wedge failure from the interaction of joint sets JS 2 - JS 5 which would result in high angled low volume wedge failures out of the pit slope surface (~10m^3). The effect of rotation to the south sees an increase risk of wedge failures from the interaction between JS 1 - JS 5 and JS 2 – JS 5 in Section 2 and JS 1 – JS 5 in section 1. Scanline 8 shows the possible inclusion of a joint set which warrants further investigation via trenching of the basement lithologies, with the possibility of significantly increased risk of wedge failure. The scanline orientations were orientated in a way which would under-sample a representative group plotting in this area of the stereographic projections.

Taking into account the interpretation of the data obtained during the kinematic analysis of the scanline traverses, a highwall orientation running parallel with the range (and the fault zone), although having higher risk of instability with respect to toppling failure, provides the most favourable orientation. Reduction in the risk from toppling failure can be addressed in the batter design by increasing bench width and reducing batter height, with a reduction of the overall slope angle for the upper quadrant of weathered

material (Top 15-20m). The nature of the weathered material and the weakness associated within the basement lithologies will require addressing during excavation regardless of the risk from toppling failure. The risks associated with other kinematic failures were assessed to have a low risk in with the pit slope face in this orientation.

The size of potential failures tends to be relatively small scale (10-100m^3) due to the rock mass properties such as aperture, persistence, joint roughness, and defect frequency (RQD) all seem to be in favour of small block sizes. In terms of excavation and support, it is helpful to have an estimate both of the mean block size and the block size distribution. Due to the highly fractured nature of the rock mass of both sections rock mass size and distribution are said to be homogenous, with failures due to block toppling failure acting more like stiff gravel with a 'crumbling' effect with minor debris displacement.

CHAPTER 5

Summary & Conclusions

5.1 Thesis Outline

The primary objective of this study was to perform a detailed engineering geological investigation of the proposed Cypress North Block Opencast Highwall in the Upper Waimangaroa Sector, Buller Coalfield. The study was initiated by Solid Energy New Zealand Ltd with the idea of developing an understanding for the rock characteristics in Cypress North basin and the Mt William Range. A feasibility study has been carried out by them within the basin assessing viability of the economic return on the coal resource based on overburden thickness to recoverable seam thickness ratios. As part of this feasibility analysis the geotechnical interpretation of the proposed highwall is essential. To this end detailed information on both intact rock properties and rock mass characteristics of the stratigraphic units needed to be obtained.

An investigation was therefore undertaken to provide information on the rock properties of the Kaiata Mudstone, Brunner Coal Measures, and basement lithologies that make up the proposed highwall in the Mt William Range. The investigation defined the intact rock strength characteristics by means of a laboratory programme designed to interpret the physical and mechanical properties of the mapped stratigraphic units. The intact rock characteristics for the basement units were then identified using relative borehole data and scanline traverse surveys carried out on the Mt William Range. This methodology was adopted to interpret the distribution and interaction of identifiable defects such as faults, joints, shears, and crush zones along the proposed highwall. This information was then used to provide a kinematic analysis for each of the scanline surveys, with emphasis on the basement lithologies that will comprise the majority of the final highwall design.

5.2 Rock Material Testing

The Tertiary units (Kaiata Mudstone and Brunner Coal Measures) along with the basement lithologies of Berlins Porphyry and Greenland Group comprise the overburden that will be encountered in Cypress North basin. The Tertiary units are comprised of the Kaiata Mudstone, which is a massive mudstone unit, and the Brunner Coal Measures which are an alternating sedimentary sequence of massive sandstones, laminated sandstones, siltstones, mudstones, and coal (with only the massive med-coarse and med-fine sandstone units tested). The basement is comprised of Greenland Group, which is slightly metamorphosed greywacke, and the Berlins Porphyry which is an intrusive body of granite/granodiorite of the Karamea Suite. These units were subdivided into their respective geotechnical units based on field descriptions and analysis of drill core records.

Physical and mechanical intact rock material parameters were determined for these geotechnical units where sample numbers permitted, using a laboratory programme that involved determination of Porosity-Density, Slake-Durability Index, Unconfined Uniaxial Strength, Brazilian Tensile Strength and Triaxial compressive Strength tests. A summary table of the rock material results is provided in table 5.1.

Table 5.1 Summary Table of Mean Physical and Mechanical Properties.

	Berlins Porphyry	Greenland Group Hornfels	Brunner Coal Measures	Kaiata Mudstone	Mixed Basement
Porosity (n) (%)	0.8	1.9	7.9	9.9	2.3
Dry Density (Kg/m^3)	2666	2658	2411	2377	2657
Saturated Density(Kg/m^3)	2681	2677	2489	2476	2680
Slake-Durability (I_{d2}) (%)	99.0	99.6	94.0	94.5	N/A
UCS (MPa)	78.2	136.1	15.3	9.9	47.0
Tensile Strength (MPa)	6.18	5.08	1.32	1.47	5.51
σ_{ci} (MPa)	27.7	N/A	7.8	8.4	14.2
Cohesion (c') (MPa)	6.4	N/A	2.11	3.0	2.9
Friction Angle (Ø) °	40.6	N/A	33.2	18.6	44.5

The geotechnical units with highest dry densities (2657-2666Kg/m^3) typically have the lowest porosities (n=0.8-2.3%) due to smaller void ratios (e=0.01-0.02) and less void connectivity. Slake-durability index results (I_{d2}=94.0-99.0% retained) showed that all geotechnical units exhibited high durability, with the exception of Kaiata Mudstone core from drillhole 1717 in which very low results were retained (I_{d2}=32.92%).

Representative samples of the geotechnical units that underwent Slake-Durability Index testing were observed to either remain intact (massive coarse to fine lithologies), or to split along existing fractures/bedding. The splitting of the slake-durability samples occurred in only a few cases and was observed to create little decrease in the sample size, and therefore little variation in the recorded results.

UCS results were obtained saturated for the basement lithologies and have a mean range of between 78.2-136.1MPa. UCS results for the Tertiary lithologies are much lower, with mean results that range between 9.9-15.3MPa, due to lower densities, increased pore interaction, and weaker inter-granular bonds.

Brazilian testing results for the saturated basement lithologies have a mean range of between 5.1-6.2MPa, and are also the highest values obtained. The results for the Tertiary lithologies had a mean range of between 1.3-1.5MPa, which is a direct correlation to the UCS test results. Graphical relationships were defined between the UCS and the Brazilian results for both the Berlins Porphyry ($y=8.13x + 18 \pm 8$) and Kaiata Mudstone ($y=4.62x + 3.2 \pm 0.8$**)** units, and as a result UCS values can be estimated from smaller core samples that are required by the Brazilian testing.

Triaxial testing of the saturated Berlins Porphyry unit showed that this lithology typically had the highest friction angle, with a mean result of 40.6º and highest cohesion with a mean cohesion value of 6.4MPa. The Tertiary lithologies yielded lower friction angles, with the Kaiata mudstone recording the lowest mean value 18.6º, and the BCM 33.2º. These units also had the lowest cohesion values ranging from 2.1-3.0 MPa, reflecting their finer grain size and low degree of cementing.

While the testing carried out during this laboratory programme provided a good general guide to the physical and mechanical properties associated with some of the stratigraphic units (Units 1.1 and 3.1), further testing will be required to quantify these relationships. The data spread (scatter) observed within the results varied between the units, with both Berlins Porphyry and Kaiata Mudstone returned good graphical correlations and low scatter of data points. The results within Brunner Coal Measures and the Greenland Group generally showed poor correlation due to limited sample base. The limited samples in both these units meant the classification of these units was unsatisfactory.

5.3 Rock Mass Properties

Scanline survey traverses were conducted along the extent of the proposed highwall situated in the Mt William Range adjacent to the Cypress North Block. These scanlines were conducted along shallow gully features to characterise the basement rock mass on the ridge crest in the approximate position of the proposed highwall. The rock mass properties recorded were; defect type, dip and dip direction, persistence, aperture, nature of infilling, and defect roughness.

5.3.1 Defect Orientations

The predominant defects detailed along the extent of the scanline surveys were joint fractures, which made up 88% of all discontinuities found. The second largest discontinuity was found to be shear defects (minor fault like structures ~10%), but displayed no apparent concentration towards any orientation and therefore were calculated into the joint defect sets as a percentage distribution. Joint sets present within the Cypress North Block have slight variations over the length of the Range, with the greatest deviation of concentrations exhibiting a slight rotation (~13-16º) in the mean pole populations between Section 1 and Section 2. The mean pole concentrations were derived from stereo-projected contour plots of each of the scanlines using *DIPS* (Rocscience 2002). The scanlines were then separated into two Sections using this rotation, with Section 1

occupying the northern area encompassing scanlines 1-6, and Section 2 occupying the southern area which includes scanlines 7-12.

Section 1

Joint orientations observed in this section are predominantly sub vertical in nature, with 4 sets exhibiting mean dips greater then 70°. JS3 is the prominent set with an orientation parallel to the Mt William Fault and a mean dip / dip direction of 79°/118°. The second most dominant set JS2 also trends effectively parallel to the Mt William Fault with an offset of less than 30°(from parallel) with a mean dip/dip direction of 89°/261°. Secondary sets are comprised of oblique joint sets formed due to extensional processes (JS1 76°/041° and JS5 85°/174°). Joint set JS4 exhibits the lowest concentration of pole densities with a relatively low dip component with a mean orientation of 47°/106°. Sub horizontal sampling of defect orientations (e.g. JS4) is subject to bias introduced by the relatively low plunge angle (<20º) associated with the scanline surveys which means that defects exhibiting a low dip are under sampled.

Section 2

Joint orientations observed along Section 2 are, as in Section 1, dominated by sub-vertical joint sets with orientated perpendicular to the scanline surveys. JS3 again was the dominant set, with an orientation of 84°/285°. The second most common defect set was JS2 with a mean dip/dip direction of 70°/245°. Secondary sets were again comprised of the oblique joint sets JS1 and JS5, with orientations 78°/025° and 79°/161° respectively. JS4 again is under-sampled along this section with a representative sample observed at a mean orientation of 43°/106°.

5.3.2 Bedding

Bedding is included as a defect in many surveys as a mode of failure or plane of weakness in rock mass analysis. The prevalent bedding throughout the basement

Greenland Group lithology is moderately metamorphosed and does not provide a mode of weakness in the sandstone unit. The Kaiata Mudstone unit, which will be incorporated into the final highwall design, does exhibit bedding orientation weakness as shown by tensile strength testing. The prediction of this bedding and any effect it may have on the final stability of the highwall depends on its final orientation due to upturn of the bedding orientations associated with the MWFZ. Bedding in the Kaiata mudstones initially dips gently east at 8-12° (regional trend for the Upper Waimangaroa Sector) into the Mt William Range, but undergoes upturn as it approaches the reverse Mt William Fault Structure.

5.3.3 Defect Persistence

The method of the scanline surveying (along exposed gullies) and the impractical nature of exposing every joint, due to overburden, meant that persistence measurements were limited to visual surface expression. Defects were seldom measured greater than 2m, with the majority of surface expression restricted to the exposed creek bed. From field estimates the majority of defects had an overall persistence less then 4m, with an average of around 2m observed with defects often truncated by other defects.

5.3.4 Defect Apertures

The discontinuity apertures along the Mt William Range show considerable variation ranging from a classification of ‘wide’ (>200mm) associated with crush zones, to ‘tight’ (0.1-1mm). Joint apertures observed along the proposed highwall show a range from tight to moderately narrow (20-40mm), with the predominant aperture being typically ‘tight’ (>70%). Crush Zone apertures show a range of results ranging from ‘Wide’ (>200mm), to ‘Moderately Wide’ (60-200mm).

5.3.5 Joint Spacing (RQD)

Defect joint spacing was derived from adjacent drillhole data interpreted from RQD values. This method was adopted in order to develop a more accurate understanding of the

rock mass behaviour. Drillhole 1697 is situated at the northern extent of the basin adjacent to Section 1, and has good correlation with scanlines 2-4. 1697 is situated in basement lithologies with an overall RQD of just 9.2%, which gives it a classification of very poor rock quality (<25%). Separation of the rock types into lithologies sees an increase in fracturing in the Greenland Group Hornfels by 5.1%.

Table 5.2 Summary of RQD Frequency (Derived from Drillhole Data).

Numerical Frequency					
RQD Freq.	1694	1697	1698	1715	1717
0-20 %	17	63	66	82	56
21-40 %	14	11	18	7	12
41-60 %	10	1	12	6	20
61-80 %	8	1	2	1	10
81-100 %	4	1	1	0	17
Total	53	77	99	96	115
Percentage Frequency					
0-20 %	32.1	81.8	66.7	85.4	48.7
21-40 %	26.4	14.3	18.2	7.3	10.4
41-60 %	18.9	1.3	12.1	6.3	17.4
61-80 %	15.1	1.3	2.0	1.0	8.7
81-100 %	7.5	1.3	1.0	0.0	14.8
Total	100.0	100.0	100.0	100.0	100.0

Drillhole 1698 is situated in the middle of the basin adjacent to Section 2, and is located between scanlines 10 and 11 with an overall RQD of 17.5%. This also gives it a classification of very poor rock quality (<25%). Separation of the rock types into lithologies again sees an increase in fragmentation in the Greenland Group Hornfels (9.3%). Separation and comparison of the RQD values for drillholes 1697 and 1698 are provided above (Table 5.2).

5.3.6 Weathering and Durability Factors

The basement lithologies show a variation in the degree of weathering, with exposed Berlins Porphyry along the length of the ridge crest showing a high to complete degree of weathering whereas the Greenland Group Hornfels shows generally a moderate degree of weathering. The degree of weathering has a direct effect on the shear strength

associated with the defects, as well as the overall strength of the rock mass (chapter 2). Observations of the lithologies down drillholes show a degree of weathering experienced up to 60m along defect fractures. The degree of weathering varies greatest within the Berlins Porphyry unit with moderate to high degree of weather exhibited to 30m depth from the surface.

5.3.7 Joint Roughness

Surface roughness varies considerably in the defects observed in the basement lithologies along the Mt William Range, with joint roughness profiles ranging from Slickensided (JRC 0-2) to Very rough (JRC 14–20). Interpretation of overall joint roughness shows a JRC value of 4-8 (semi rough) as the dominant joint surface making up over 60% of those examined. The next highest frequency is observed at a JRC of 8-14 (rough) with 23%, and only 12% of the joint surfaces showed a JRC less than 4.

5.4 Analysis of Kinematic Failures

Kinematic analysis of the scan line defect data was used to further the interpretation and division of the structural domains that had been initially outlined using rock mass properties. The initial approach was to establish the possibility of instability by the method of basic kinematic analysis, as shown in tables 5.3.

Table 5.3. Summary Table of Kinematically Feasible Failures for pit slope of 60º for each scanline traverse.

	Type Of Kinematic Failure					
Scanline No.	Planar Failure (Max Slope Plane)	Sets	Wedge Failure (Max Slope Plane)	Sets	Toppling Failure (Max Slope Plane)	Sets
Section 1 - 60/286	√	JS3	X	-	√	_
1	X (83)	-	X (90)	-	X	-
2	X (90)	-	X (76)	JS 1&2	√	**JS2&3**
3	√ (56)	JS3	X (90)	-	√	**JS2&3**
4	X (62)	-	X (90)	-	√	**JS2&3**
5	X (63)	-	X (90)	-	√	**JS2&3**
6	√ (55)	JS3	X (66)	JS 2&5	√	JS2&3
Section 2 - 60/306	√	**JS3**	X	-	√	JS3
7	X (62)	-	X (77)	JS 1&2	√	JS3
8	√ **(37)**	**JS3**	X (82)	JS 1&5	√	JS3
9	X (68)	-	X (83)	JS 2&3	√	JS3
10	X (62)	-	X (90)	-	√	**JS3**
11	X (71)	-	X (89)	JS 1&2	√	**JS3**
12	X (75)	-	X (80)	JS 1&3	√	JS3

*** Underlined symbols represent a moderate to high risk of failure.**

**** Bracketed values represent angles at which kinematic failure is possible**

In order to establish the theoretical relationship between slope height and slope angle, the following assumptions have been made;

a. Because the geological mapping revealed dominant through-going structures (Mt William Fault – McCay Fault) which could control the stability of the slopes in question, it was assumed that the orientation of the highwall would be used to incorporate the orientation of these defects to minimise their overall influence.
b. It was also assumed that therefore any failure, if it were to occur, would be concentrated on the intersection of defect sets which daylight in the proposed fault orientation.
c. From the shear strength data (joint roughness) a conservative friction angle Ø = 35° was chosen as the starting point for this analysis.
d. Finally that the orientation of the final highwall design incorporated defect orientations observed in the development of this analysis, and that they are uniform over the extent of the highwall (i.e. defects orientated at the base of the highwall are essentially orientated in the same manner as those surveyed).

Section 1 is classified as a highly disturbed area of basement lithology comprised of 5 major defect sets having surface expression. The dominant joint set is a sub-vertical joint set population with a mean orientation of 79º/118º which poses a high risk of kinematic failure through toppling as 50-80% of the defect orientations plot within the viability cone for a 60º pit slope. Other kinematic risks, wedge and planar failure, were interpreted as having low risk of failure.

Section 2 is also classified as a highly disturbed area of basement lithology comprised of 5 major defect sets from surface data. The dominant joint set is again sub-vertical joint set population with a mean orientation of 84º/285º which poses a moderate risk of kinematic failure through toppling with between 20-40% of joint set JS 3 plotting within the viability window. An increase in the overall steepness of the slope generates a higher level of the defect orientations poling within the viability cone of the pit slope. Other kinematic risks, wedge and planar failure, were interpreted to have low risk, with the greatest cause for caution with regards to wedge and planar failures identified in Scanline 8 associated with JS4.

The strike of the Mt William Fault was used as an arbitrary highwall orientation for each section to carry out kinematic interpretations, and in doing so this also allows for the incorporation of the fault in the final design of the highwall. The final highwall design will in most part be constrained by the orientation of the Mt William Range, as deviations from this will result in excess overburden removal. Orientations investigated for plausible highwalls were therefore limited to rotations within 30 degrees of the overall strike of the range itself.

The selected orientation incorporates a high risk to stability from toppling failures, but is interpreted as the most favourable orientation for any highwall design. Rotations of the selected orientation would result in an increased risk in the other failure modes due to alignment of the joints sets which would see the defect sets daylighting into the pit slope face. The joint sets associated with the range are statistically dominated by two sets of

defects designated JS 2 and JS 3, accounting for over 60% of all data points collected and posing an immediate risk of toppling failure.

The size of potential failures tends to be relatively small scale (<100m^3) due to the rock mass properties such as aperture, persistence, joint roughness, and defect frequency (RQD), all seem to indicate of small block sizes. In terms of excavation and support, it is helpful to have an estimate both of the mean block size and the block size distribution. Due to the highly fractured nature of the rock mass of both sections, rock mass size and distribution are said to be homogenous with failures due to block toppling failure acting more like stiff gravel with a 'crumbling' effect and minor debris displacement.

5.5 Further Research

Further research for the proposed Cypress North Block Opencast Coalmine should focus on ascertaining the lateral and vertical variation of both joint set orientations (JS4) and persistence of defects associated with the structural domains, and the extent of these defects in the other stratigraphic units (Tertiary). The Cypress North Block rock mass is complex and further mapping should be undertaken as the highwall is progressively stripped. This ongoing monitoring of defects in the highwall is important in recording changes in the defect data, and in ascertaining new possible failure modes. All highwall instability should be carefully investigated and documented so that detailed records of failures can be referenced to improve future design techniques associated with the progressive development of the Upper Waimangaroa Sector.

This work should be combined with basin analysis to interpret the history of both the basement and sedimentary stratigraphic units within the basin, and in doing so, develop the relationship of the influence of fault interaction with regards to depositional environment and propagation of defects within each unit. This is deemed important in interpreting the coal seam genesis, and seam split models, as well as interpreting possible defect orientations with spatial relationship to the Mt William Fault.

Since there is no comparative slope within the Buller Coalfield, and no failure has taken place within the basement slopes, deciding upon the factor of safety of the proposed slopes posed a difficult problem. Geological mapping and laboratory testing of intact rock characteristics and the rock mass properties in the basement lithologies has provided a useful guide to the possible failure modes, but the range is too wide to permit the factor of safety to be determined with a reasonable degree of confidence.

The geotechnical interpretation could be further developed and improved by applying Bieniawski's (1989) rock mass rating (RMR) system to each structural domain and major fault zones associated with the Mt William and McCay Faults. This system relies on expanding the initial data outlined in this thesis, such as intact rock strength characteristics (UCS, Brazilian), and rock mass properties (RQD, condition of discontinuities, orientation of discontinuities), along with the use of measured groundwater conditions from installed piezometers.

Groundwater, increased defect analysis (by mode of trenching), and further intact rock characterisation of the under sampled stratigraphic units (e.g. hornfels) would be required to successfully apply the RMR system to the overburden strata at Cypress North Block. In combination with data obtained from rock material characterisation, such as porosity and density, the application of this classification system to the rock mass at Cypress North Block may also prove most beneficial to blasting design practices.

All potential failure blocks are assumed (via geotechnical assessment) to fail along discontinuity surfaces, and therefore the determination of shear strength parameters for the discontinuity surfaces and weak zone materials (crush zones) as opposed to intact rock, is considered more relevant. Therefore the development of a 3-D model displaying change joint orientation with spatial relationship to the fault zone is beneficial to highwall design.

REFERENCES

Adams, C.J.D., Harper, C.T., and Laird, M.G, (1975): *K-Ar Ages of Low-Grade Meta-sediments of the Greenland and Waiuta Groups in Westland and Buller, New Zealand*. New Zealand Journal of Geology and Geophysics, Vol.18: 39-48.

Anonymous, (1977): *The Description of Rock Masses for Engineering Purposes*. Report by the Geological Society Group Working Party. Quarterly Journal of Engineering Geology, Vol.10: 355-388.

Barry, J. and Caffyn, P. (1988): *Buller Coalfield: The geology of the Sullivan Mine Area.* New Zealand Coal Resources Survey, New Zealand.

Barton, N., and Chouby, V., (1977): *The Shear Strength of Joints in Theory and Practice.* Rock Mechanics, Vol.10, Nos. 1-2, pp 9-38.

Bell, D.H, Pettinga, J.R. (1983): *Rock Material Description System*, University of Canterbury, Christchurch, New Zealand.

Bradshaw, J.D (1989): *Cretaceous Geotectonic Patterns in the New Zealand Region Tectonics*, Volume 8 Pages 803-820.

Cook, G.K., (2001): *Rock Mass Structure and Intact Rock Strength of New Zealand Greywackes.* Unpublished M.Sc. Thesis . University of Canterbury, Christchurch, New Zealand.

Coote, T.P. (1991): *Engineering Geological Investigation of the Brunner Coal Measures Overburden for Opencast Mining*. Unpublished M.Sc. Thesis. University of Canterbury, Christchurch, New Zealand.

Cundall, P.A. (1987): *Distinct Element Models of Rock and Soil Structure.* Analytical and Computational Methods in Engineering Rock Mechanics, E.T. Brown (Ed), George Allen & Unwin, London.

Deere, D. U. (1964): *Technical Description of Rock Cores for Engineering Purposes,* Rock Mechanics and Engineering Geology, Vol 1, No. 1, pp 17-22.

Duncan, N (1969): *Engineering Geology and Rock Mechanics,* Volume 1, Leonard Hill : London

Flores, R.R and Sykes, R. (1996): *Depositional Controls on Coal Distribution and Quality in the Eocene Brunner Coal Measures, Buller Coalfield, South Island, New Zealand.* International Journal of Coal Geology 29, p291-336

Goodman, R.E. and Taylor, R.L., (1967): *Methods of Analysis of Rock Slopes and Abutments*: Review of Recent Developments. in Failure and Breakage of Rocks(i) Edited by C.Fairhurst. Pg 303-320

Hoek, E., Bray, J.W. (1977): *Rock Slope Engineering*, Revised second edition. The Institution of Mining and Metallurgy, London.

Hudson, J.A (editor) (1993): *Comprehensive Rock Engineering, Principles, Practice & Projects.* Volume 2 & 3. Pergamon Press. Oxford, New York, Seoul, Tokyo

Hudson, J.A., Harrison J.P. (1997): *Engineering Rock Mechanics - and Introduction to the Principles*. Pergamon Press. Oxford, New York, Singapore , Tokyo

ISRM, (1978): *Commission on Standardization of Laboratory and Field Tests.(*a). Suggested Methods for the Quantitative Description of Discontinuities in Rock Masses. Intnl. Jl. Rock Mech. Min. Sci. & Geomch. Abstr. Vol.15: 319-368.

ISRM, (1978): *Commission on Standardization of Laboratory and Field Tests.*(b). Suggested Methods for Determining the Strength of Rock Materials in Triaxial Compression. Intnl. Jl. Rock Mech. Min. Sci. & Geomch. Abstr. Vol.15: 47-51.

ISRM, (1979): *Commission on Standardization of Laboratory and Field Tests.* Suggested Methods for Determining the Uniaxial Compressive Strength and Deformability of Rock Materials. Intnl. Jl. Rock Mech. Min. Sci. & Geomch. Abstr. Vol.16(No.2): 135-140.

ISRM, (1981): *Rock Characterization, Testing and Monitoring.* International Society for Rock Mechanics Suggested Methods, ET Brown (editor), Pergamon Press, Oxford, 211pp.

Kennedy, J.F., (1988): *Engineering Geological Characterization of the Brunner Coal Measures, Cedar Creek area, Buller Coalfield*. Unpublished M.Sc. Thesis, University of Canterbury, Christchurch, New Zealand.

Laird, M.G., (1968): *The Paparoa Tectonic Zone.* New Zealand Journal of Geology and Geophysics, Volume 11, No. 2; pg 435-454

Laird, M.G., (1972): *Sedimentology of the Greenland Group in the Paparoa Range, West Coast, New Zealand*. New Zealand Journal of Geology and Geophysics, Vol.15: 372-393.

Laird, M.G., (1981): *The Late Mesozoic Fragmentation of the New Zealand Segment of Gondwana*. In: Gondwana Five; selected papers and abstracts of papers presented at the Fifth international Gondwana symposium. pp. 311-318

Muir, R.J., Weaver, S.D., Bradshaw, J.D., Eby, G.N., Evans, J.A., and Ireland, T.R., (1996): *Geochemistry of the Karamea Batholith, New Zealand and comparisons with the Lachlan Fold Belt granites of SE Australia*. Lithos. Vol.39: 1-20.

Lacazette. A., (2000): *Natural Fracture Nomenclature*, L.B. Thompson (editor) Atlas of Borehole Images, AAPG Data-pages Discovery Series 4, American Association of Petroleum Geologists, Tulsa.

Nathan, S.; Anderson, H.J.; Cook, R.A.; Herzer, R.H.; Hoskin, R.H.; Raine, J.I. and Smale, D. (1986). *Cretaceous and Cenozoic Sedimentary Basins of the West Coast Region, South Island, New Zealand.* New Zealand Geological Survey Basin Studies, Department of Scientific and Industrial Research, Wellington, New Zealand. pp 90

Norget, C.L., Boreham, C.J., Kamp, P.J.J., Newman, J., (1997): *Relationships between hydrocarbon generation, coal type and rank for middle Eocene coals, Buller Coalfield, New Zealand*. Journal of Petroleum Geology, 20; 4, pp 427-458

Norrish, N.I., Wyllie, D.C., (1996): *Rock Slope Stability Analysis*. In: A. Turner, and RL Schuster (Editor), Landslides Investigation and Mitigation, Special Report 247. Transportation Research Board, National Research Council, pp. 673.

Price, N.J. (1966): *Fault and Joint Development in Brittle and Semi-Brittle Rock*, Pergamon, Oxford.

Priest, S.D., J.A. Hudson (1976). *Estimation of discontinuity spacing and trace length using scan line surveys*. Int. J. Rock Mech. Min. Sci and Geomech., Vol. 18, pp. 183-197.

Priest, S.D. (1993): *Discontinuity Analysis for Rock Engineering*, University of South Australia, Melbourne Australia

RockData, 1992. Version 2.36, Copyright Rocscience Inc., Toronto, Canada.

Rocscience, (1989-2000): *Dips, Plotting, Analysis and Presentation of Structural Data using Spherical Projection Techniques*. Rocscience Inc., Toronto.

Suggate, R.P., (1990): *New Zealand Coals: Their Geological Setting and its Influence on their Properties*. Department of Scientific and Industrial Research 134.

Suggate, R.P. Boudou, J.P., (1993): *Coal Rank and Type Variation in Rock-Eval Assessment of New Zealand coals*. Journal of Petroleum Geology, 16;1 pp. 73-88.

Titheridge, D.G., (1992): *The Depositional Setting of the Brunner Coal Measures, Buller Coalfield*. Resource informational report 13, Ministry of Commerce, New Zealand.

Titheridge, D.G., (1993): *The Influence of Half-Graben Syn-Depositional Tilting on Thickness Variation and Seam Splitting in the Brunner Coal Measures, New Zealand*. Sedimentary geology, 87; pg 195-213.

Vutukuri, V.S, Lama R.D, Saluja S.S, (1974): *Mechanical Properties of Rocks*, Volume 1, Series on Rock and Soil Mechanics

APPENDIX 1

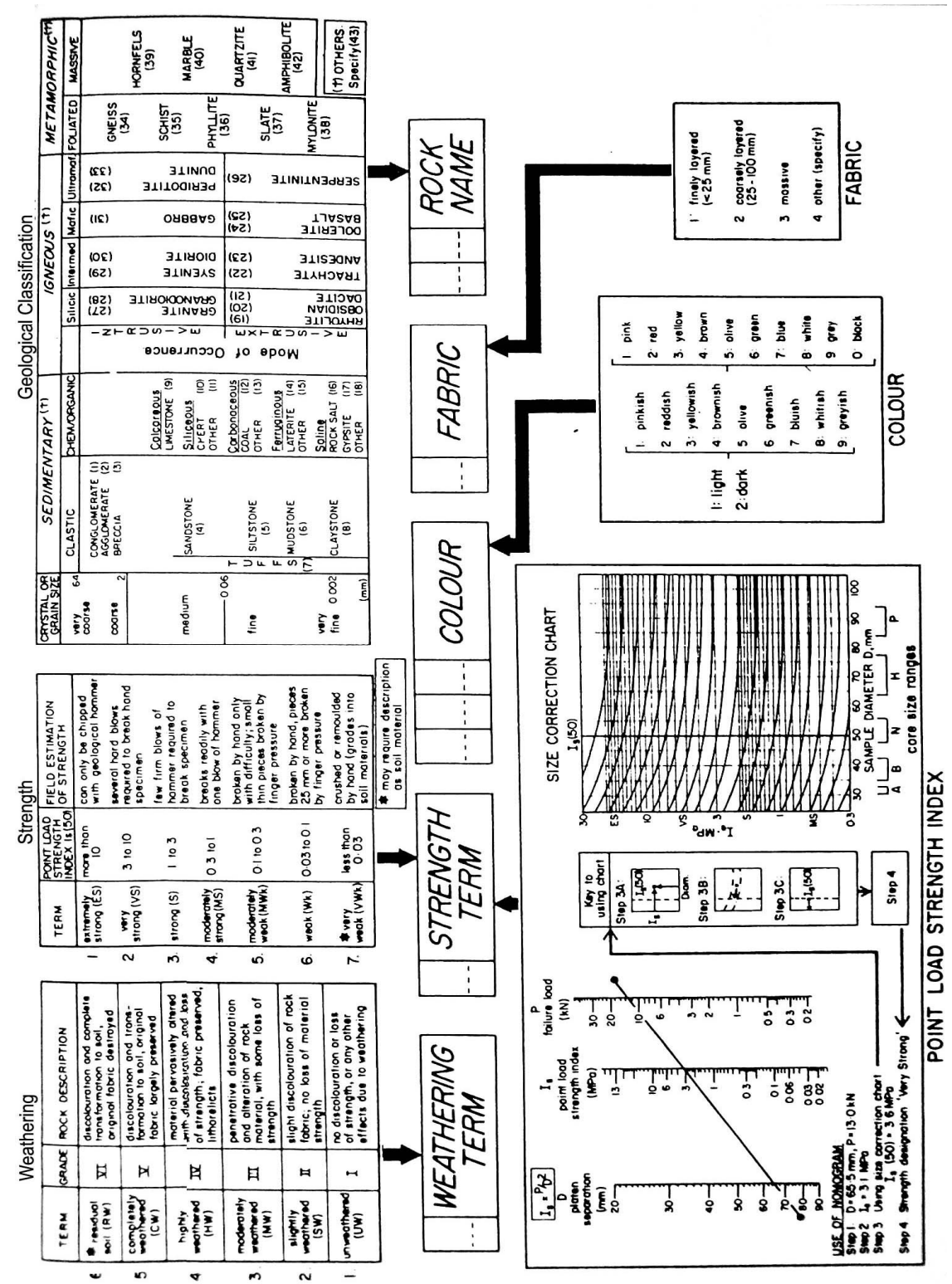

Bell and Pettinga's Rock Classification System (1983).

APPENDIX 2

Rock mass Properties

Physical Properties Tests

A2.1 - Porosity and Density Determination

A2.2 - Slake Durability Index

Mechanical Properties

A2.3 – Uniaxial Compressive Strength (UCS)

A2.4 – Brazilian (Tensile Splitting) Testing

A2.5 – Triaxial Testing

A2.1 Porosity and Density Determination

A2.1.1 Procedures

Porosity and density specimens were prepared and tested according to methods suggested by ISRM as documented by Brown (1981).

All rock cores were supplied by Solid Energy New Zealand Ltd.

A2.1.2 Data Manipulation

The calculations used in the data manipulation follow those suggested within the IRSM guidelines (1981). Properties measured and calculated were;

D	=	Specimen Diameter (mm)
L	=	Specimen Length (mm)
A	=	Area (mm^2)
V	=	Volume (m^3)
IM	=	Initial Mass (g)
SM	=	Saturated Mass (g)
DM	=	Dry Mass (g)
*P*D	=	Dry Density (t/m^3)
*P*S	=	Saturated Density (t/m^3)
Vv	=	((*P*S/ *P*D) x V) x 100 (%)
n	=	Vv/V

A.2.1.3 Results

Drillhole #	Depth of sample	Rock Type	Ave D (mm)	L (mm)	A (mm2)	Volume (m3)	Moisture %	IM	SM	DM	PD	PS	n
1697	74.95-75.10	Berlyns Porphyr	60.8	140.77	2905.2	0.00040897	0.9	1049.1	1054.0	1040.1	2.543	2.577	3.4
1698	44.70-44.98	Berlyns Porphyr	60.7	142.35	2897.6	0.00041247	0.3	1102.5	1105.1	1099.6	2.666	2.679	1.3
1698	41.73-42.02	Berlyns Porphyr	60.8	141.56	2902.4	0.00041086	0.5	1080.1	1085.2	1075.2	2.617	2.641	2.4
1698	78.8-79.2	Berlyns Porphyr	60.7	140.5	2890.0	0.00040604	0.4	1086.2	1087.1	1082.1	2.665	2.677	1.2
1698	78.8-79.2	Berlyns Porphyr	60.7	141.81	2895.7	0.00041064	0.4	1095.8	1096.7	1091.9	2.659	2.671	1.2
1698	80.43-80.70	Berlyns Porphyr	60.7	141.59	2890.0	0.00040919	0.2	1094.6	1095.0	1092.5	2.670	2.676	0.6
1698	110.7-111.0	Berlyns Porphyr	60.6	141.78	2885.2	0.00040907	0.1	1107.0	1107.1	1106.3	2.704	2.706	0.2
1715	117.60-117.87	Berlyns Porphyr	60.6	141.05	2883.3	0.00040669	0.1	1088.5	1089.0	1087.5	2.674	2.678	0.4
1715	121.55-121.84	Berlyns Porphyr	60.6	140.85	2884.3	0.00040625	0.2	1088.2	1088.5	1085.5	2.672	2.679	0.7
1697	59.05-59.32	Biotite Sandstor	60.6	141.64	2884.3	0.00040853	0.6	1092.1	1093.7	1085.9	2.658	2.677	1.9
1694	68.48-68.76	Biotubated Sand	60.5	140.45	2874.8	0.00040376	2.9	1011.4	1014.8	983.2	2.435	2.513	7.8
1694	71.4-71.68	Biotubated Sand	60.5	141.54	2876.7	0.00040716	3.2	1002.4	1003.9	971.5	2.386	2.466	8.0
1697	59.49-59.77	Mixed	60.6	140.8	2885.2	0.00040624	1.3	1060.2	1062.6	1046.2	2.575	2.616	4.0
1697	84.07-84.40	Mixed	60.8	141.14	2900.5	0.00040937	0.1	1123.1	1123.5	1121.5	2.740	2.744	0.5
1694	32.62-32.83	Mudstone	60.4	141.2	2865.3	0.00040457	4.1	972.3	974.1	933.8	2.308	2.408	10.0
1694	56.17-56.36	Mudstone	60.5	141.65	2874.8	0.00040721	4.7	1054.4	1055.9	1007.1	2.473	2.593	12.0
1717	60.1-60.35	Mudstone	60.7	141.3	2890.0	0.00040835	3.3	986.2	986.1	954.3	2.337	2.415	7.8
1717	86.72-86.96	Mudstone	60.6	140.2	2884.3	0.00040437	4.0	1002.1	1003.4	963.5	2.383	2.481	9.9
1717	32.65-33.0	Mudstone	60.5	139.5	2870.0	0.00040037	4.2	1001.8	1002.6	961.0	2.400	2.504	10.4
1717	35.10-35.30	Mudstone	60.6	132	2885.2	0.00038085	3.8	934.0	935.2	900.0	2.363	2.456	9.2

Average Saturated Density Kaiata Mudstone	2.476	t/m3
Average Saturated Density Berlins Porphyry =	2.665	t/m3
Average Saturated Density Bio Sandstone =	2.489	t/m3
Average Saturated Density Hornfels =	2.677	t/m3
Average Saturated Density Mixed Granite/Ho	2.680	t/m3

A2.2 - Slake Durability Index

The Slake Durability Index Test in this research follows the suggested methods set forth by ISRM as documented by Brown (1981).

A2.2.1 Procedures

A representative sample is selected comprising ten rock lumps, each with a mass of 40-60g, to give a total sample mass of 450-550g. Samples are oven dried from 2 to 6 hr (usually over night) at a temperature of 105ºC. Samples are put through a series of two wet drying cycles of 10mins duration, dried, and weighed.

A2.2.2 Data Manipulation

The slake-durability test index (2^{nd} cycle) is calculated as a percentage ratio of final to initial dry sample masses as follows.

$$Id_2 = \frac{C - D}{A - D} \times 100\ \%$$

Where A = Initial Mass of oven dried sample and drum (g)

B = Mass of drum plus retained portion of the sample (1^{st} cycle) (g)

C = Mass of drum plus retained portion of the sample (2^{nd}cycle) (g)

D = Mass of drum (g)

A2.2.3 Results

Slake Durability Test	A	B	C	D	A-D	B-D	C-D	Id1	Id2
Berlins Porphory (1715) Unweathered	2904.6	2903.4	2902.7	2254.4	650.2	649	648.3	99.82%	99.71%
Berlins Porphory (1697) Unweathered	3116.6	3113.2	3110.8	2254.3	862.3	858.9	856.5	99.61%	99.33%
Berlins Porphory (1715) Weathered	2852.0	2780.6	2722.5	2254.1	597.9	526.5	468.4	88.06%	78.34%
Sandstone - Banded (1715)	2922.6	2921.0	2919.7	2254.1	668.5	666.9	665.6	99.76%	99.57%
Mudstone (1694)	3069.8	3043.6	3020.2	2254	815.8	789.6	766.2	96.79%	93.92%
Sandstone - Banded (1698)	3069.4	3068.6	3067.8	2253.9	815.5	814.7	813.9	99.90%	99.80%
Berlins Porphory (1715) Slight weathering	2784.4	2780.3	2776.3	2182.9	601.5	597.4	593.4	99.32%	98.65%
Berlins Porphory (1697) Weathered	2892.2	2885.6	2879.9	2182.8	709.4	702.8	697.1	99.07%	98.27%
Berlins Porphory (1715) Mod Weathered	2781.7	2762.6	2743.1	2172.4	609.3	590.2	570.7	96.87%	93.66%
Mudstone (1694)	2981.3	2971.3	2957.9	2172.4	808.9	798.9	785.5	98.76%	97.11%
Sandstone - Banded (1698)	2914.2	2913.3	2912.3	2172.3	741.9	741	740	99.88%	99.74%
Sandstone - Banded (1715)	2763.6	2762.2	2761.2	2172.2	591.4	590	589	99.76%	99.59%
Mudstone (1717)	3043.1	2561.0	2442.2	2182.7	860.4	378.3	259.5	43.97%	30.16%
Mudstone (1717)	3021.4	2541.3	2481.3	2181.8	839.6	359.5	299.5	42.82%	35.67%

A2.3 – Uniaxial Compressive Strength (UCS)

All the samples specimens were prepared and tested according to ISRM suggested methods as documented by Brown (1981).

A2.3.1 Procedure

Where possible, the specimens were cut to a length : diameter ratio of 2.5 :1 using the rock mechanics laboratory, Department of Civil Engineering, University of Canterbury. Core lengths to be tested were trimmed to the desirable length, and then had the ends ground flat and parallel. All specimens were tested under saturated conditions as suggested by Brown (1981) when in situ moisture content could not be constrained.

All testing was carried out in Civil Engineering's rock mechanics laboratory utilising a Controls 50-C36H2 loading frame.

The specimens were loaded at an average rate of 0.5 to 1 MPa per minute (20KPa) so that failure occurred within 5 to 15 minutes.

A2.3.2 Calculations

The Uniaxial Compressive Strength of the specimen was calculated by dividing the maximum load carried by the specimen during the test, by the original cross sectional area, Brown (1981).

A2.3.3 Results

Drillhole #	Sample #	Depth of sample (m)	D1 (mm)	D2 (mm)	D3 (mm)	Ave D (mm)	L (mm)	L:D	A (mm2)	F KN	MPa	Rock Type	Weathering	TOF
1694	3	38.06-38.28	60.76	60.78	60.79	60.78	150.0	2.47	2901	29.8	10.3	Mudstone		LS
1694	4	38.66-38.97	60.61	60.74	60.73	60.69	154.0	2.54	2893	38.2	13.2	Mudstone		LS
1694	5	39.00-39.40	60.77	60.75	60.77	60.76	153.0	2.52	2900	29.3	10.1	Mudstone		C
1694	8	52.67-53.00	60.71	60.74	60.75	60.73	152.0	2.50	2897	46.8	16.1	Mudstone		EF
1694	10	67.54-67.80	59.73	59.84	59.87	59.81	155.0	2.59	2810	33.7	12.0	BCM		LS
1694	13	69.23-69.49	60.18	60.09	60.11	60.13	153.0	2.54	2839	39.7	14.0	BCM		CSF
1697	5	59.49-59.77	60.56	60.63	60.55	60.58	157.0	2.59	2882	27.9	9.7	Berlyns Porphyry	Moderately	EF
1697	6	65.90-66.30	60.74	60.64	60.65	60.68	150.0	2.47	2892	52.3	18.1	Mixed	Moderately	LS
1697	13	90.20-90.51	60.73	60.72	60.77	60.74	153.0	2.52	2898	52.3	12.5	Berlyns Porphyry		EF
1697	21	27.20-27.93	60.27	60.44	60.39	60.37	158.0	2.62	2862	72.0	25.2	Berlyns Porphyry		LS/EF
1697	23	89.72-90.20	60.79	60.74	60.75	60.76	157.0	2.58	2900	74.8	25.8	Mixed		LS
1698	1	36.82-37.20	60.38	60.20	60.29	60.29	154.0	2.55	2855	4.8	~	Berlyns Porphyry	Highly	C
1698	5	60.66-61.04	60.68	60.68	60.64	60.67	157.0	2.59	2891	65.7	22.5	Berlyns Porphyry	Moderately	LS
1698	6	52.48-52.80	60.70	60.65	60.67	60.67	157.0	2.59	2891	9.0	~	Berlyns Porphyry	Highly	LS
1698	7	70.46-70.84	60.76	60.78	60.77	60.77	148.0	2.44	2900	394.7	136.1	GG Sandstone		C
1698	10	78.20-78.58	60.46	60.51	60.47	60.48	154.0	2.55	2873	147.5	51.4	Berlyns Porphyry		LS
1698	12	80.70-81.03	60.40	60.39	60.42	60.40	155.0	2.57	2866	128.6	44.9	GG Sandstone		EF
1698	14	93.25-93.50	60.48	60.50	60.48	60.49	150.0	2.48	2873	206.3	71.8	GG Sandstone		EF
1698	15	110.30-110.66	60.44	60.46	60.45	60.45	150.0	2.48	2870	278.7	97.1	Mixed		LS
1698		59.80-60.06				60.70	156.6	2.58	2894		25.6	Berlyns Porphyry		
1715	3	50.53-50.75	60.75	60.79	60.76	60.77	149.0	2.45	2900	9.4	~	Berlyns Porphyry	Highly	C
1715	5	90.05-90.42	60.28	60.32	60.29	60.30	157.0	2.60	2855	77.6	27.2	Berlyns Porphyry	Moderately	EF
1715	10	123.69-13-23.91	60.39	60.41	60.42	60.41	156.0	2.58	2866	124.0	43.3	Berlyns Porphyry		LS
1715	11	124.43-124-67	60.48	60.47	60.57	60.51	156.0	2.58	2875	207.5	72.2	Berlyns Porphyry		LS
1715	12	125.87-16-26.10	60.47	60.44	60.43	60.45	155.0	2.56	2870	243.4	84.8	Berlyns Porphyry		LS
1717	4	49.85-50.30	60.17	60.12	60.26	60.18	158.0	2.63	2845	21.0	7.4	Mudstone		EF
1717	5	49.30-49.68	60.42	60.37	60.37	60.39	154.0	2.55	2864	23.8	8.3	Mudstone		LS
1717	7	42.60-42.90	60.80	60.72	60.79	60.77	158.0	2.60	2900	32.0	11.0	Mudstone		LS
1717	8	50.55-50.85	60.30	60.29	60.19	60.26	154.0	2.56	2852	26.1	9.2	Mudstone		LS
1717	9	44.00-44.35	60.54	60.52	60.44	60.50	149.0	2.46	2875	27.6	9.6	Mudstone		LS
1717	10	36.07-36.31	60.89	60.94	60.92	60.92	154.0	2.53	2914	26.3	9.0	Mudstone		LS
1717	1A	43.20-43.78	60.52	60.47	60.44	60.48	152.0	2.51	2873	32.4	11.0	Mudstone		LS
1717	1B	43.20-43.79	60.51	60.42	60.37	60.43	154.0	2.55	2868	29.5	10.3	Mudstone		C
1717	2A	55.30-55.80	60.12	60.22	60.31	60.22	152.0	2.52	2848	25.4	8.5	Mudstone		LS
1717	2B	55.30-55.81	60.40	60.40	60.38	60.39	149.0	2.47	2865	31.3	10.9	Mudstone		LS
1717	3A	40.10-40.50	60.75	60.62	60.48	60.62	154.0	2.54	2886	25.4	8.8	Mudstone		C
1717	3B	40.10-40.51	60.65	60.67	60.67	60.66	155.0	2.56	2890	27.1	9.4	Mudstone		C
1717		62.21-62.56				60.40	153.0	2.53	2865		8.3	Mudstone		
1717		84.41-84.65				60.40	153.8	2.55	2865		10.4	Mudstone		
1717		105.28-105.55				60.80	154.3	2.54	2903		19.8	BCM		

Controls 50-C36H2

Height Variation 153mm +/- 5 mm

Load Applied parrallel to core sampling

Machine Controls 50-C36H2

Test Conditions

Tested under saturated conditions

Width Varation 60.42mm +/- .5 mm

Average Density Kaiata Muds	2.45	t/m3	
Average Density Berlins Porp	2.55	t/m3	
Average Density Bio Sandsto	2.64	t/m3	
Average Density Hornfels =	2.66	t/m3	
Average Density Mixed Grani	2.67	t/m3	

UCS and Triaxial Failure modes
LS = Longitudial Splitting
CSF = Conjugate Shear Fracturing
EF = Existing Fracture
C = Cataclastic

Strata Testing Services

TOF = Type of Failure

Failed Samples

A2.4 – Brazilian (Tensile Splitting) Testing

All the samples specimens were prepared and tested according to ISRM suggested methods (1977).

A2.4.1 Procedure

Where possible, the specimens were cut to a length : diameter ratio of less than 1 using the rock mechanics laboratory, Department of Civil Engineering, University of Canterbury. Core lengths to be tested were trimmed to the desirable length, and then had the ends ground flat and parallel. Specimens were then wrapped around its periphery with one layer of masking tape and mounted squarely on the apparatus. All specimens were tested under saturated conditions as suggested by Brown (1981) when in situ moisture content could not be constrained.

All testing was carried out in Civil Engineering's rock mechanics laboratory utilising a Controls 50-C36H2 loading frame.

The specimens were loaded at an average rate of 200 N per seconds so that failure occurred within 15-30 seconds.

A2.4.2 Calculations

Tensile strength of the specimen

$\sigma_t = 0.636\ P/Dt$ (MPa)

P = Load at failure (N)
D = Diameter of test specimen (mm)]
t = thickness of test specimen

A2.4.3 Results

Drillhole #	Sample #	Depth of Sample	D	L	L/D	A	F	MPa	% of D	Rock Type	Weatherin	TOF
		(m)	(mm)	(mm)		(mm2)	(KN)					
1694	10	67.54-67.80	60.20	52.46	0.87	2846.3	7.1	1.43	87.14%	BCM		CF
1694	13	69.23-69.49	60.14	51.36	0.85	2840.6	5.9	1.21	85.40%	BCM		CF
1697	13	90.20-90.51	60.83	51.98	0.85	2906.2	11.1	2.23	85.45%	Berlyns Porphory	minor	CF
1697	19	73.40-73.58	60.52	49.64	0.82	2876.7	6.4	1.35	82.02%	Berlyns Porphory		EF
1697	22A	89.22-89.46	60.69	43.75	0.72	2892.8	12.3	2.95	72.09%	Berlyns Porphory	minor	CF
1697	22B	89.22-89.46	60.67	44.78	0.74	2890.9	12.8	3.00	73.81%	Berlyns Porphory	minor	CF
1697	23A	89.72-90.20	60.55	49.56	0.82	2879.5	13.5	2.86	81.85%	Berlyns Porphory	minor	CF
1697	23B	89.72-90.20	60.55	50.76	0.84	2879.5	10.7	2.21	83.83%	Berlyns Porphory	minor	CF
1698	1	36.82-37.20	60.66	47.16	0.78	2890.0	2.0	0.44	77.74%	Berlyns Porphory	Very	C / EF
1698	2	40.38-40.46	60.72	48.59	0.80	2895.7	14.8	3.19	80.02%	Berlyns Porphory	Moderate	CF
1698	3	41.73-42.02	60.87	48.81	0.80	2910.0	8.4	1.80	80.19%	Berlyns Porphory		EF
1698	5	60.66-61.04	60.80	49.00	0.81	2903.3	5.6	1.20	80.59%	Berlyns Porphory	Moderate	EF
1698	12A	80.70-81.03	60.49	47.45	0.78	2873.8	28.4	6.29	78.44%	Berlyns Porphory		CF
1698	12B	80.70-81.03	60.47	46.85	0.77	2871.9	22.4	5.03	77.48%	Berlyns Porphory		CF
1698	12C	80.70-81.03	60.55	47.04	0.78	2879.5	24.2	5.40	77.69%	Berlyns Porphory		CF
1698	12D	80.70-81.03	60.48	48.02	0.79	2872.9	23.2	5.08	79.40%	Berlyns Porphory		CF
1715	11	124.43-124.67	60.56	44.83	0.74	2880.5	24.4	5.72	74.03%	Berlyns Porphory		C
1715	12	125.87-136.10	60.50	45.04	0.74	2874.8	36.0	8.40	74.45%	Berlyns Porphory		CF
1715	1A	40.05-40.50	60.35	48.20	0.80	2860.5	5.1	1.12	79.87%	Berlyns Porphory	Very	CF
1715	1B	40.05-40.50	60.43	48.12	0.80	2868.1	5.2	1.14	79.63%	Berlyns Porphory	Very	CF
1715	8A	120.50-120.72	60.43	43.35	0.72	2868.1	26.6	6.46	71.74%	Berlyns Porphory		CF
1715	8B	120.50-120.72	60.60	43.24	0.71	2884.3	27.6	6.70	71.35%	Berlyns Porphory		CF
1715	8C	120.50-120.72	60.59	43.45	0.72	2883.3	27.2	6.57	71.71%	Berlyns Porphory		CF
1697	5	59.49-59.77	60.49	52.67	0.87	2873.8	15.9	3.18	87.07%	Mixed		Contact Failure
1698	15	110.30-110.66	60.59	49.64	0.82	2883.3	58.6	12.39	81.93%	Mixed		CF
1694	4	38.66-38.97	60.58	52.81	0.87	2882.4	9.4	1.87	87.17%	Mudstone		CF / SBF
1694	5	39.00-39.40	60.74	51.31	0.84	2897.6	6.9	1.41	84.47%	Mudstone		BF
1694	8	52.67-53.00	60.67	56.40	0.93	2890.9	5.2	0.97	92.96%	Mudstone		BF
1694	7A	50.05-50.22	60.41	52.19	0.86	2866.2	3.8	0.77	86.39%	Mudstone		BF
1694	7B	50.05-50.22	60.34	52.84	0.88	2859.6	4.2	0.84	87.57%	Mudstone		BF
1717	9	44.00-44.35	60.49	49.09	0.81	2873.8	6.5	1.39	81.15%	Mudstone		CF
1717	1A	43.20-43.78	60.59	48.02	0.79	2883.3	8.3	1.81	79.25%	Mudstone		CF
1717	1B	43.20-43.78	60.57	46.08	0.76	2881.4	6.6	1.50	76.08%	Mudstone		CF
1717	1C	43.20-43.78	60.56	49.61	0.82	2880.5	7.8	1.65	81.92%	Mudstone		CF
1717	1D	43.20-43.78	60.58	50.27	0.83	2882.4	7.8	1.63	82.98%	Mudstone		CF
1717	4A	49.85-50.30	60.00	49.94	0.83	2827.4	6.1	1.29	83.23%	Mudstone		CF
1717	4B	49.85-50.30	60.05	50.69	0.84	2832.1	6.4	1.34	84.41%	Mudstone		CF
1717	4C	49.85-50.30	60.16	51.05	0.85	2842.5	5.1	1.06	84.86%	Mudstone		EF
1717	4D	49.85-50.30	60.04	48.18	0.80	2831.2	5.1	1.12	80.25%	Mudstone		C
1717	6A	37.38-37.41	60.69	49.34	0.81	2892.8	5.5	1.17	81.30%	Mudstone		C
1717	6B	37.38-37.41	60.65	46.75	0.77	2889.0	6.1	1.37	77.08%	Mudstone		C / BF
1717	7A	42.60-42.90	60.77	50.11	0.82	2900.5	8.1	1.69	82.46%	Mudstone		CF
1717	7B	42.60-42.90	60.76	49.98	0.82	2899.5	6.4	1.34	82.26%	Mudstone		C
1717	7C	42.60-42.90	60.77	51.44	0.85	2900.5	8.1	1.65	84.65%	Mudstone		CF
1717	8A	50.55-50.85	60.29	49.10	0.81	2854.8	6.1	1.31	81.44%	Mudstone		EF
1717	8B	50.55-50.85	60.34	46.70	0.77	2859.6	5.6	1.26	77.39%	Mudstone		C
1697	2	56.77-56.97	60.58	49.32	0.81	2882.4	14.9	3.17	81.41%	Sandstone		C
1698	17A	104.70-104.90	60.59	47.86	0.79	2883.3	47.8	10.48	78.99%	Mixed		CF
1698	17B	104.70-104.90	60.56	51.52	0.85	2880.5	34.7	7.07	85.07%	Mixed		EF
1698	7	70.46-70.84	60.75	46.74	0.77	2898.6	11.5	2.58	76.94%	Sandstone		EF
1715	6A	99.90-100.45	60.49	45.04	0.74	2873.8	26.3	6.14	74.46%	Sandstone		CF
1715	6B	99.90-100.45	60.54	45.81	0.76	2878.6	16.4	3.76	75.67%	Sandstone		EF
1715	6C	99.90-100.45	60.37	43.81	0.73	2862.4	24.6	5.92	72.57%	Sandstone		CF

Load Applied perpendicular to core sampling
Load Rate .5N/mm^2
Machine Controls 50-C36H2
Test Conditions
Tested under saturated conditions

Failed Samples

TOF = Type of Failure

Brazilian Failure modes
CS = Central Spliting in core
EF = Existing Fracture
BF = Bedding Failure
C = Cataclastic
SBF = Secondary Bedding Failure outside sample area

Average Tensile Strength Kaiata Mudstone	1.56 +/- 0.27
Average Tensile Strength BCM	1.32 +/- 0.11
Average Tensile Strength Mixed	11.44 +/- 0.94
Average Tensile Strength Weathered Granite	2.35 +/- 0.74
Average Tensile Strength Granite	6.24 +/- 1.21
Average Tensile Strength Hornsfel	6.03 +/- 0.11

A2.5 – Triaxial Testing

All the samples specimens were prepared and tested according to ISRM suggested methods as documented by Brown (1981).

A2.5.1 Procedure

Where possible, the specimens were cut to a length : diameter ratio of less than 1 using the rock mechanics laboratory, Department of Civil Engineering, University of Canterbury. Core lengths to be tested were trimmed to the desirable length, and then had the ends ground flat and parallel. Specimens were then wrapped around its periphery with one layer of masking tape and mounted squarely on the apparatus. All specimens were tested under saturated conditions as suggested by Brown (1981) when in situ moisture content could not be constrained.

All testing was carried out in Civil Engineering's rock mechanics laboratory utilising a Controls 50-C36H2 loading frame.

The specimens were loaded at an average rate of 0.5 to 1 MPa per minute (20KPa) so that failure occurred within 5 to 15 minutes. The maximum axial load and corresponding confining pressure recorded.

A2.5.2 Calculations

Friction Angle Determination:

$$\emptyset = \arcsin \frac{m-1}{m+1}$$

m = gradient of failure envelope (tangent of the inclination)

Cohesion Determination:

$$C = b \frac{1-\sin \emptyset}{2\cos \emptyset}$$

b = interception of gradient (Y intercept)

A2.5.3 Results

Drillhole #	Depth of sample (m)	Rock Type	Ave D (mm)	L (mm)	L:D	A (mm2)	F (KN)	MPa	Sig3 (MPa)	Weathering	TOF	Density (t/m3)	Moisture %
1694	32.62-32.83	Mudstone	60.4	141.2	2.34	2865.3							0.9
1694	56.17-56.36	Mudstone	60.5	141.65	2.34	2874.8							0.3
1694	68.48-68.76	Biotubated Sandst	60.5	140.45	2.32	2874.8	68.1	23.6	1.7	high	C		0.5
1694	71.4-71.68	Biotubated Sandst	60.5	141.54	2.34	2876.7	89.3	31.3	1.7		LS		0.4
1697	59.05-59.32	Biotite Sandstone	60.6	141.64	2.34	2884.3	117.7	40.8	1.5		LS		0.4
1697	59.49-59.77	Mixed	60.6	140.8	2.32	2885.2	101.4	35.2	1.5	Moderately	LS/EF		0.2
1697	74.95-75.10	Berlyns Porphyry	60.8	140.77	2.31	2905.2	140.0	48.2	2.2		EF		0.1
1697	84.07-84.40	Mixed	60.8	141.14	2.32	2900.5	275.0	94.8	2.0		LS		0.1
1698	44.70-44.98	Berlyns Porphyry	60.7	142.35	2.34	2897.6	99.4	34.3	1.4	Slightly	LS/EF		0.2
1698	41.73-42.02	Berlyns Porphyry	60.8	141.56	2.33	2902.4	165.5	57.0	2.0	Moderately	LS		0.6
1698	78.8-79.2	Berlyns Porphyry	60.7	140.5	2.32	2890.0	239.5	82.9	1.0		LS		2.9
1698	78.8-79.2	Berlyns Porphyry	60.7	141.81	2.34	2895.7	283.0	98.0	2.0		LS		3.2
1698	80.43-80.70	Berlyns Porphyry	60.7	141.59	2.33	2890.0	337.2	116.7	2.0				1.3
1698	110.7-111.0	Berlyns Porphyry	60.6	141.78	2.34	2885.2	371.5	128.8	1.5		EF		0.1
1715	117.60-117.87	Berlyns Porphyry	60.6	141.05	2.33	2883.3	422.4	146.5	3.0				4.1
1715	121.55-121.84	Berlyns Porphyry	60.6	140.85	2.32	2884.3	282.0	97.8	3.0				4.7
1717	60.1-60.35	Mudstone	60.7	141.3	2.33	2890.0							3.3
1717	86.72-86.96	Mudstone	60.6	140.2	2.31	2884.3							4.0
1717	32.65-33.0	Mudstone	60.5	139.5	2.31	2870.0							4.2
1717	35.10-35.30	Mudstone	60.6	132	2.18	2885.2							3.8
1694	32.83-33.14	Mudstone	60.8	122.7	2.02	2903.3	26.5	9.13	2.0		LS	2.510	4.4
1694	32.83-33.14	Mudstone	60.8	122.7	2.02	2903.3	39.1	13.47	4.0		LS	2.510	4.4
1694	32.83-33.14	Mudstone	60.8	122.7	2.02	2903.3	49.6	17.08	6.0		LS	2.510	4.4
1694	39.60-39.86	Mudstone	60.8	120.8	1.99	2903.3	33.9	11.68	2.0		LS	2.515	4.4
1694	39.60-39.86	Mudstone	60.8	120.8	1.99	2903.3	50.1	17.26	4.0		LS	2.515	4.4
1694	39.60-39.86	Mudstone	60.8	120.8	1.99	2903.3	56.1	19.32	6.0		LS	2.515	4.4
1694	54.57-54.90	Mudstone	60.8	121.6	2.00	2903.3	35.9	12.37	2.0		LS	2.526	3.7
1694	54.57-54.90	Mudstone	60.8	121.6	2.00	2903.3	55.9	19.25	4.0		LS	2.526	3.7
1694	54.57-54.90	Mudstone	60.8	121.6	2.00	2903.3	63.7	21.77	6.0		LS	2.526	3.7
1694	67.80-68.12	Biotubated Sandst	58.0	128.8	2.22	2642.1	75.0	28.39	2.0		LS	2.487	4.0
1694	67.80-68.12	Biotubated Sandst	58.0	128.8	2.22	2642.1	100.9	38.19	4.0		LS	2.487	4.0
1694	67.80-68.12	Biotubated Sandst	58.0	128.8	2.22	2642.1	122.8	46.48	6.0		LS	2.487	4.0
1698	42.82-43.06	Berlyns Porphyry	60.7	119.3	1.97	2893.8	168.9	58.37	2.0		LS	2.662	1.0
1698	42.82-43.06	Berlyns Porphyry	60.7	119.3	1.97	2893.8	223.5	77.23	4.0		LS	2.662	1.0
1698	42.82-43.06	Berlyns Porphyry	60.7	119.3	1.97	2893.8	265.4	91.71	6.0		LS	2.662	1.0
1698	60.06-60.52	Berlyns Porphyry	60.8	124.6	2.05	2903.3	134.4	46.3	2.0		CSF	2.645	1.1
1698	60.06-60.52	Berlyns Porphyry	60.8	124.6	2.05	2903.3	180.8	62.3	4.0		CSF	2.645	1.1
1698	60.06-60.52	Berlyns Porphyry	60.8	124.6	2.05	2903.3	220.9	76.1	6.0		CSF	2.645	1.1
1717	61.20-61.50	Mudstone	60.3	121.7	2.02	2855.8	22.9	8.0	1.0		LS	2.514	5.4
1717	61.20-61.50	Mudstone	60.3	121.7	2.02	2855.8	37.7	13.2	3.0		LS	2.514	5.4
1717	61.20-61.50	Mudstone	60.3	121.7	2.02	2855.8	46.2	16.2	5.0		LS	2.514	5.4
1717	90.53-90.81	Mudstone	60.4	125.2	2.07	2865.3	24.0	8.4	1.0		LS	2.525	4.0
1717	90.53-90.81	Mudstone	60.4	125.2	2.07	2865.3	59.4	20.7	3.0		LS	2.525	4.0
1717	90.53-90.81	Mudstone	60.4	125.2	2.07	2865.3	65.6	22.8	5.0		LS	2.525	4.0
1717	96.38-96.61	f.m.Sandstone	60.5	123.6	2.04	2874.8	60.2	20.9	1.0		LS	2.481	3.3
1717	96.38-96.61	f.m.Sandstone	60.5	123.6	2.04	2874.8	84.5	29.4	3.0		LS	2.481	3.3
1717	96.38-96.61	f.m.Sandstone	60.5	123.6	2.04	2874.8	105.0	36.5	5.0		LS	2.481	3.3

Height Variation 141.1+/-1.6
Load Applied parrallel to core sampling
Machine Controls 50-C36H2
Test Conditions
Tested under saturated conditions
Width Varation 60.42mm +/- .5 mm

TOF = Type of Failure
UCS and Triaxial Failure modes
LS = Longitudial Splitting
CSF = Conjugate Shear Fracturing
EF = Existing Fracture
C = Cataclastic

APPENDIX III

A3.1 Scanline survey data points, Location of reference point for each scanline survey traverse.

LISCAD Report: Point Report
Monday, 8 September 2003 16:58

Point ID	East	North	Elevation	Description
3)	326055.31	711198.76	810.320	T12
4)	326088.34	711223.97	809.050	T11
5)	326154.64	711340.93	802.240	T10
6)	326167.97	711356.55	800.590	T9
7)	326251.70	711389.48	799.060	T8
8)	326257.39	711427.63	795.990	T7
9)	326328.65	711652.79	788.620	T6
10)	326330.79	711687.17	789.740	T5
11)	326344.95	711744.07	788.430	T4
12)	326347.38	711752.65	787.740	T3
13)	326343.58	711779.48	784.940	T2
14)	326303.66	711891.20	777.450	T1
15)	326018.44	711709.46	711.460	DH 1694
16)	325804.32	711905.15	699.780	DH 1695
17)	325721.77	711729.11	702.870	DH 1696
18)	325720.00	711731.02	702.720	DH 1696R
19)	326199.40	711787.02	767.120	DH 1697
20)	326053.61	711337.94	799.110	DH 1698
21)	325585.80	711556.90	698.350	DH 1699
22)	325814.92	711106.19	815.800	DH 1715
23)	325446.12	711416.54	699.760	DH 1716
24)	325662.89	711236.50	752.780	DH 1717
25)	325354.51	711343.28	698.530	DH 1718

* Distance Units in Metres

Distance (m) Along Datum	Defect type	Dip Direction	Corrected D/D	Correlated D/D	Dip	set #	Hardness vh	h	mh	m	s	vs	Persistence (m)	Aperture (cm)	Roughness vr	r	sr	sm	sl	Spacing (mm) < .1	.1-1	1-5*	>5	Infill (mm) Thickness	Discription	Fracture Spacing (mm)	Notes
#1 Section 1 length = 12m 011/7																											
40	shr	271	293	277	81	3			x		x		>5						x				x	20-40	gritty clay		Associated Jointing 300 mm each side
129	j	195	217	201	64	1			x							x					x						
143	j	202	224	208	56	1			x							x					x						
112	j	156	178	162	68	?			x							x					x						
113	j	192	214	198	66	1			x							x					x						
217	j	185	207	191	48	1			x							x					x						
237	j	193	215	199	62	1			x							x					x						
303	j	232	254	238	68	2			x				>2			x					x						
471	j	236	258	242	71	2			x				>2			x					x						
389	j	352	14	358	74	5			x							x					x				20~150	Highly Fractured down datum
366	j	170	192	176	86	5			x							x					x						
431	j	172	194	178	81	5			x							x					x						
472	j	169	191	175	74	5			x							x					x						
470-710	Crsh Zn, Contact B/p																										
882	shr	113	135	119	81	3			x				>1						x			x					
819	j	156	178	162	73	5			x				>1			x											
774	j	194	216	200	34	1			x							x					x						
786	j	238	260	244	44	2			x							x					x				60		
902	j	140	162	146	77	5			x							x					x						
851	j	4	26	10	54	1			x							x					x						
971	shr	38	60	44	59	2			x									x				x					Banded weak GG
1157	j	130	152	136	81	5			x							x					x						
1142	j	131	153	137	79	5			x							x					x						
#1 Section 2 Length 11m 022/12																											
1252	j	316	338	322	62	5			x				>1			x					x						
1367	j	346	8	352	72	5			x							x					x						
1371	shr	300	322	306	86	3			x		x								x			x		1~5	grey clay		
1384	shr	238	260	244	81	2			x		x						x					x		1~5	Iron stains		
1403	shr	144	166	150	72	5			x		x						x					x		1~5	Burn margin		
1410	contact																										
1462	shr	351	13	357	52	5			x		x								x			x		1~5	grey clay		Crush zone of GG boarded on either side by
1471	shr	355	17	1	49	5			x		x								x			x		1~5	grey clay		" "
1526	j	238	260	244	64	2			x										x			x		1~5	Burn margins/calcite		
1538	j	236	258	242	68	2			x							x					x			#2			
1489	j	131	153	137	56	?			x				>2			x					x						
1811	j	238	260	244	76	2			x				>1				x				x						
1833	j	234	256	240	74	2			x				>1				x				x						
1838	j	232	254	238	81	2			x				>1				x				x						
1770	j	345	7	351	80	5			x				>1				x				x						
1762	j	347	9	353	69	5			x							x					x						
1892	j	232	254	238	72	2			x				>1				x				x						
1806	shr	302	324	308	84	3			x		x								x			x					
2028	shr	231	253	237	58	2			x		x								x			x					
2048	shr	41	63	47	28	1			x		x		>5					x					x	30-50	Clay		Contact between B/p and GG
2091	j	128	150	134	34	4			x				>3			x					x						
2122	j	156	178	162	72	5			x				>2			x					x						
2286	j	338	0	342	68	5			x							x					x						
2254	shr	264	286	270	81	3			x		x							x				x					
2300	j	196	218	202	74	1			x							x					x						
2293	j	118	140	124	62	?			x							x					x						

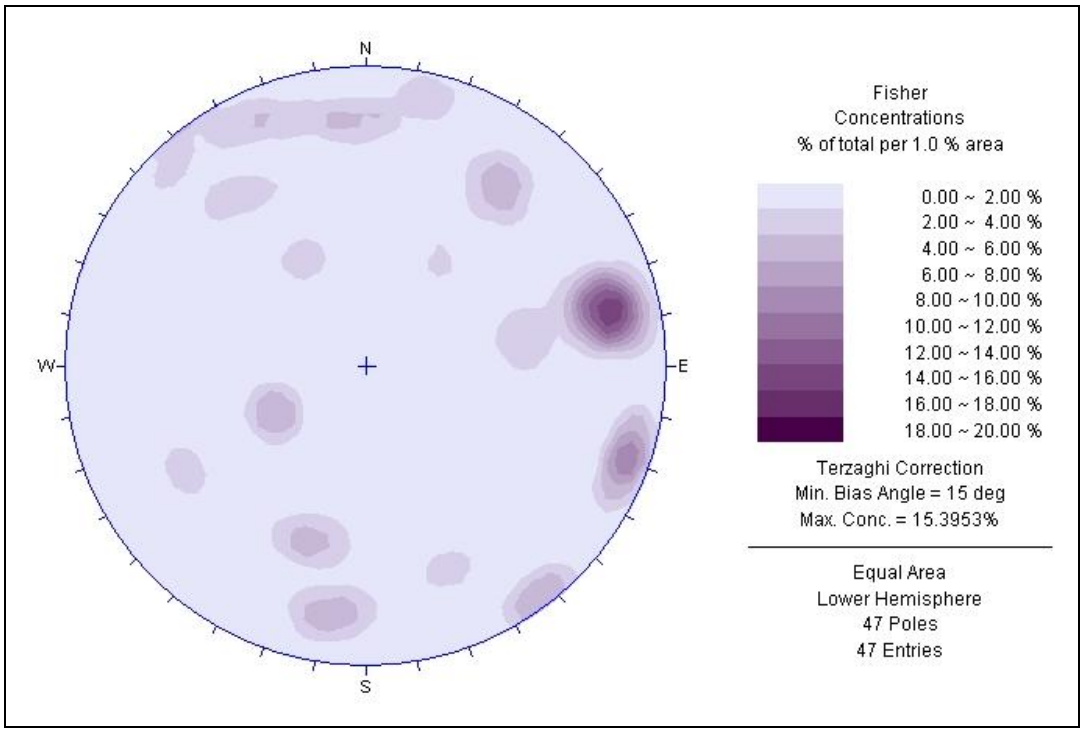

Scanline 1 Contour Plot – Pole Density Distribution

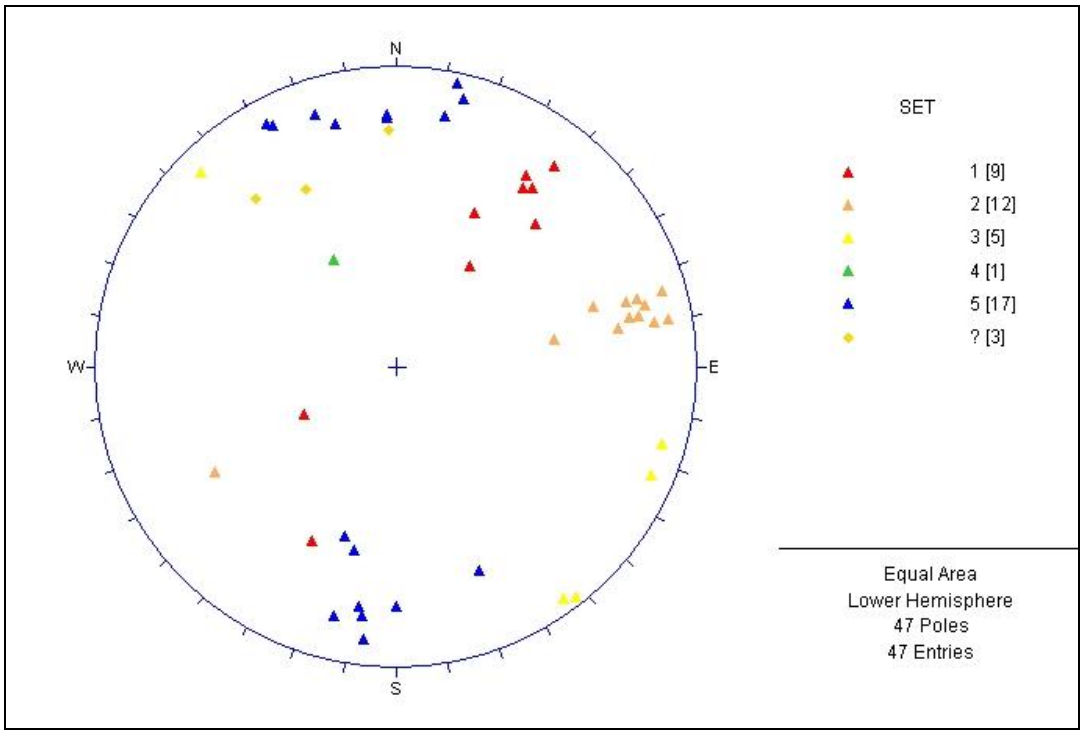

Scanline 1 Scatter Plot – Joint Sets

Distance	Defect	Dip	Corrected	Correlated	Dip	Set #	Hardness						Persis	Aperture	Roughness					Spacing				Infill Thick~		Fracture	Notes
Along Datum (c	type	Direction	D/D	D/D			vh	h	mh	m	s	vs	tence (m)	(cm)	vr	r	sr	sm	sl	< .1	.1-1	1-5*	>5	ness (mm)	Discription	Spacing (mm)	
#2	Bearing 299 / 12												< 1 unless otherwise indicated								x						
124	j	94	116	100	52	4		x									x				x						
132	j	91	113	97	53	4		x									x				x						
176	j	69	91	75	87	2		x									x				x						
233	j	50	72	56	46	1			x									x			x						
261	j	72	94	78	81	2			x									x			x						
235	j	140	162	146	57	?			x								x				x						
406	shr	40	62	46	72	1			x										x				x	20mm	C/M		C/M consists of greenland group
462	shr	38	60	44	82	1					x								x				x	6-7mm	Grey Clay		Soft Mauable Clay
478	shr	37	59	43	78	1					x								x				x	6-7mm	Grey Clay		
581	j	102	124	108	64	3			x								x				x						
622	shr	331	353	337	45	?				x						x	x				x						
656	j	92	114	98	66	3				x							x				x						GreenLand Group Inclusion
838	j	100	122	106	81	3		x									x				x						
846	j	105	127	111	76	3		x									x				x						
861	j	106	128	112	61	3		x									x				x						
872	j	101	123	107	82	3		x									x				x						
896	j	110	132	116	74	3		x									x				x						
901	j	108	130	114	78	3		x									x				x						
1023	j	232	254	238	88	2		x									x				x						
971	j	238	260	244	88	2		x									x				x						
1050~1120	B/P Intrusive highly fractured GG either side																										
1146	j	57	79	63	82	2		x									x				x					40mm	x 14 joints up to 1280 increased fracturing
1220	j	60	82	66	88	2		x									x				x					40mm	towards 1280
1262	j	62	84	68	86	2		x									x				x					40mm	
1154	j	136	158	142	83	5		x									x				x						
1183	j	130	152	136	84	5		x									x				x						
1300~1420	Crush Zone																x										
1433	j	66	88	72	73	2		x									x				x						
1462	j	64	86	70	78	2		x									x				x						
1502	j	103	125	109	64	3		x									x				x						
1562	j	107	129	113	77	3		x									x				x						
1621	j	94	116	100	73	3		x									x				x						
1658	j	96	118	102	74	3		x									x				x						
1662	j	101	123	107	69	3		x					>1				x				x						
1653	j	82	104	88	59	4		x									x				x						
1672	j	80	102	86	58	4		x									x				x						
1791	j	128	150	134	65	5			x				>1				x				x						
1770	j	132	154	138	64	5			x								x				x						
1789	j	56	78	62	62	2				x								x			x						
1861	j	101	123	107	58	4				x							x				x						
1871	j	52	74	58	65	2				x							x				x						
1860	j	40	62	46	38	1			x	x							x				x						
1172	j	294	316	300	72	3			x							x					x						

Change in Datum @ 20m to 246 / 16																														
2011	j	61	83	67	64	2			x										x						x	5-10mm	Crush Material			
2040~2300	Crush Zone contact with B/P																													
2410	Contact with GG																													
2480	j	84	106	90	36	4				x								x											
2612	Sheared Contact with B/P																										20-40mm	X 10 sets		
2616	shr	102	124	108	62	3				x								x					x	4-10mm	Calcite/Course sand				
2641	shr	111	133	117	64	3				x							x					x			"				
2652	shr	113	135	119	61	3				x								x				x				"				
2681	shr	103	125	109	52	4				x							x					x				"				
2721	shr	101	123	107	54	4				x							x					x				"				
2798	j	38	60	44	46	1				x								x			x									
2850~2880	B/P Intrusive highly fractured GG either side																													
2798	j	204	226	210	62	1				x								x			x									

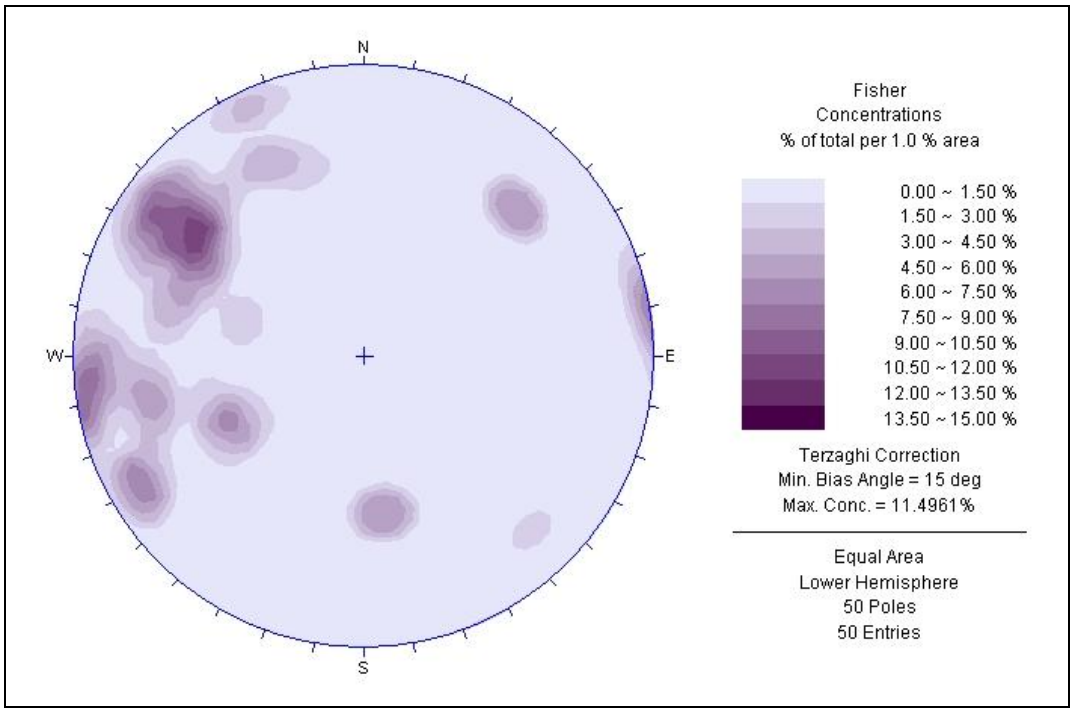

Scanline 2 Contour Plot – Pole Density Distribution

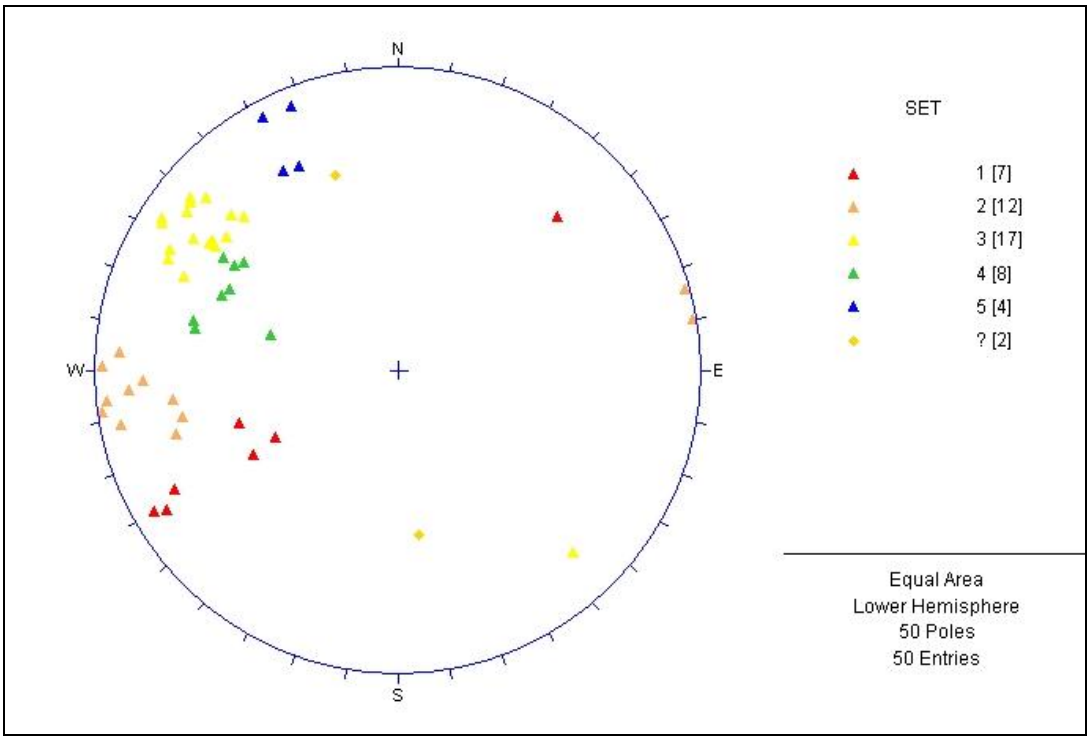

Scanline 2 Scatter Plot Joint Sets

Distance along	Defect	Dip	Corrected	Correlated	Dip	Set #	Hardness						Persis	Aperture	Roughness					Spacing (mm)				Infill Thick~		Fracture	Notes
Datum (cm)	type	Direction	D/D	D/D			vh	h	mh	m	s	vs	tence (m)	(mm)	vr	r	sr	sm	sl	< .1	.1-1	1-5*	>5	ness (mm)	Discription	Spacing (mm)	
# 3 Length = 25	280/23												<1 unless otherwise stated														
-10	j	239	261	245	82	2			x								x				x					200	
0	j	243	265	249	85	2		x								x					x						
139	j	98	120	104	62	3		x									x				x						
165	j	237	259	243	82	2		x									x				x						
283	j	246	268	252	73	2		x								x	x				x						
350	j	99	121	105	61	3		x								x							x	5mm	med/fine sand		
430	j	91	113	97	65	3		x					>1				x				x						
434	j	91	113	97	65	3		x					>1				x				x						
419	j	130	152	136	86	5		x					>1		x						x						
478	j	222	244	228	76	1		x					>3	80			x				x						
490	shr	103	125	109	65	3				x							x				x					100	
590	shr	102	124	108	63	3				x							x				x						
675	j	280	302	286	82	3		x					>2				x					x				100	B/P Intrusive along strike
720	j	322	344	328	60	5		x					1>		x						x						
690	j	284	306	290	83	3		x					2>					x			x						
856	j	333	355	339	65	5			x				1>		x							x					
860	j	59	81	65	67	2			x				1>			x					x						
915	j	58	80	64	74	2			x				1>			x					x						
943	j	105	127	111	76	3			x								x				x					50	5 x 930 - 970
950	j	131	153	137	66	5			x									x			x					600	
1003	j	99	121	105	82	3			x								x				x						990-1040 x 6
1100~1270	Obscured																										
1310	j	79	101	85	56	3		x					>2				x				x						
1640	j	80	102	86	61	3			x								x				x						
1720	j	112	134	118	64	3		x								x	x				x						
1732	j	284	306	290	52	4		x									x				x						
1380	j	89	111	95	34	4		x								x					x						
1632	j	52	74	58	62	2			x				>1				x				x					>100	
1810	j	282	304	288	88	3			x									x			x						
1722	j	54	76	60	57	2			x								x				x						
1783	j	83	105	89	65	3			x						x						x						
1902	j	112	134	118	68	3		x									x				x						
1823	j	57	79	63	61	2		x										x			x						
1920	j	82	104	88	60	3		x					>1			x					x						
1932	j	83	105	89	52	4		x					>1			x					x						
1958	j	58	80	64	72	2		x					>1				x				x						
1992	j	65	87	71	79	2		x					>1					x			x						
2069	shr	60	82	66	80	2				x			>1						x				x	30mm	Sandy Clay		
2116	j	93	115	99	66	3		x					>1				x	x			x					400	offset by shr
2209	j	140	162	146	62	5		x									x				x						cut off by B/p
2174	j	58	80	64	76	2		x					>1			x						x					cut off by B/p
2290~2400																											Sheared soft zone
2290	j	60	82	66	74	2			x				>1				x				x						
2260	j	96	118	102	76	3				x			>1			x					x						
2400	j	93	115	99	68	3			x								x				x					100	x4 2400-2456
2490	j	57	79	63	72	2			x				>2			x					x					200	

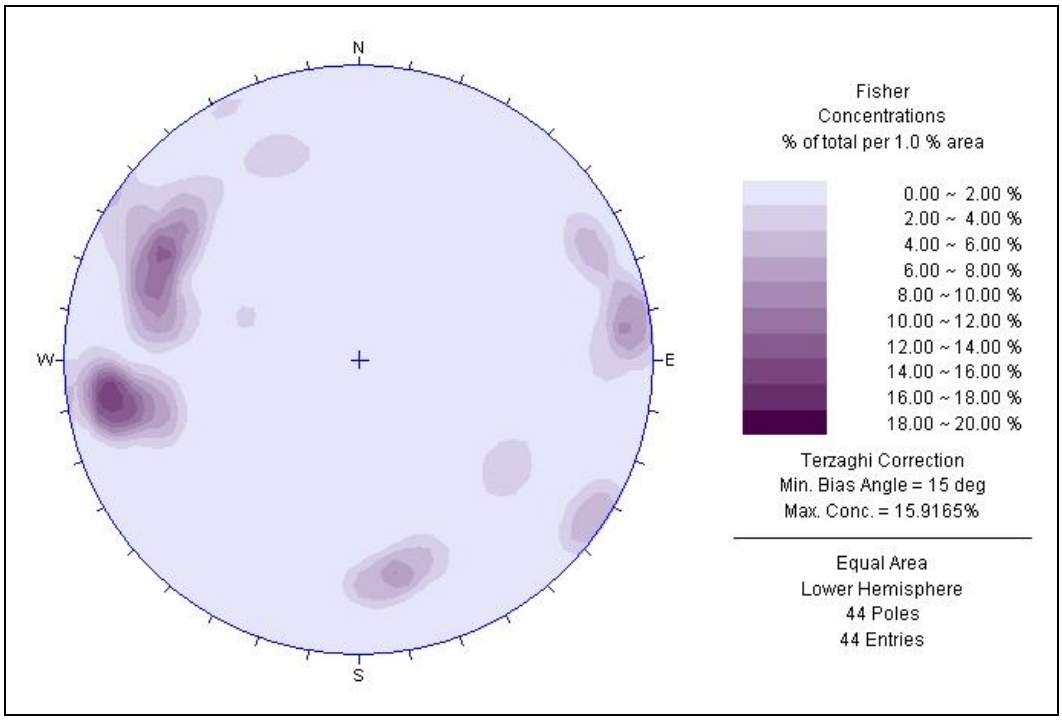

Scanline 3 Contour Plot – Pole Density Distribution

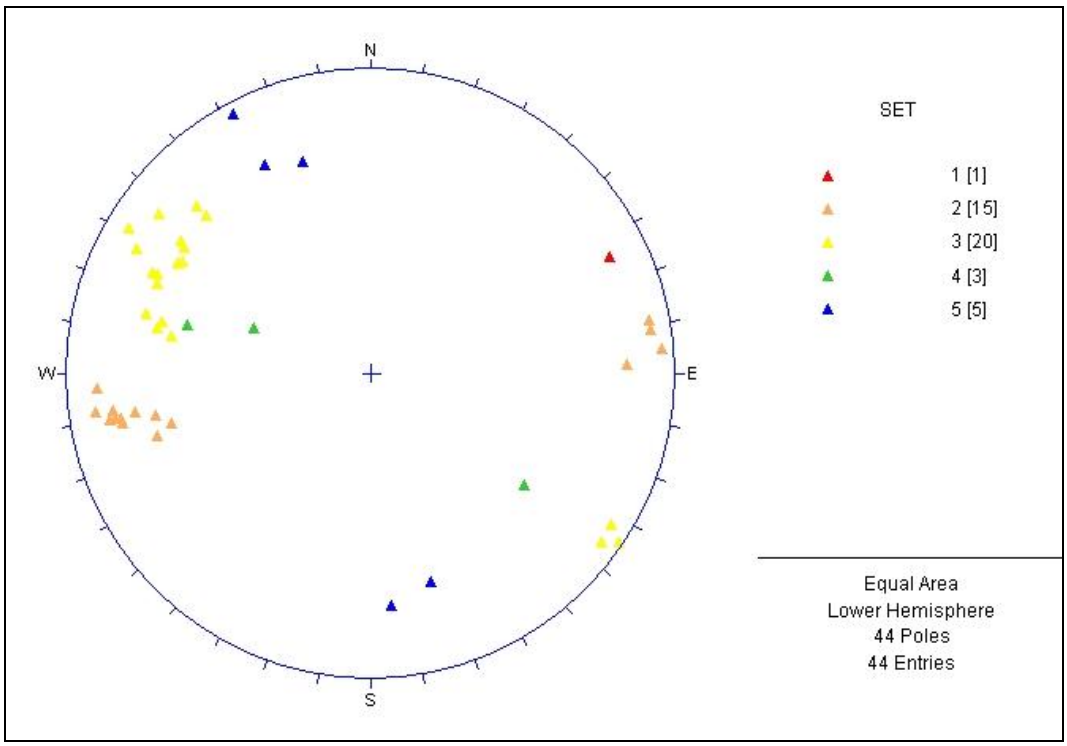

Scanline 3 Scatter Plot – Joint Sets

Distance along	Defect	Dip	Corrected	Correlated	Dip	Set #							Persis	Aperture	Roughness					Spacing (mm)				Infill Thick~		Fracture	Notes
Datum (cm)	type	Direction	D/D	D/D			vh	h	mh	m	s	vs	tence (m)	(mm)	vr	r	sr	sm	sl	< .1	.1-1	1-5*	>5	ness (mm)	Discription	Spacing (mm)	
#4													<1 unless otherwise stated														
30	j	243	265	249	80	2		x					>1				x					x					
50	j	61	83	67	51	2		x					>1			x					x						
120	j	65	87	71	85	2			x								x					x					
450	j	94	116	100	64	3				x			>1				x				x					100-500	
470	j	93	115	99	68	3				x							x				x					"	
493	j	94	116	100	72	3				x			>1				x				x					"	
502	j	94	116	100	71	3				x			>1				x				x					"	
520	j	98	120	104	70	3			x				>2				x				x					"	
531	j	96	118	102	64	3			x				>2				x				x					"	
548	j	94	116	100	65	3			x				>2				x				x					"	
512	j	59	81	65	87	2			x								x				x						
579	j	103	125	109	71	3			x				>4				x				x						
620	j	95	117	101	62	3			x									x			x						
530	j	49	71	55	86	2			x								x				x						
669	j	106	128	112	63	3			x				>3				x				x						
712	j	102	124	108	72	3			x								x				x						
723	j	105	127	111	70	3			x								x				x						
731	j	99	121	105	66	3			x								x				x						
765	j	108	130	114	74	3			x								x				x						
770	j	96	118	102	64	3			x								x				x						
784	j	92	114	98	71	3			x								x				x						
809	j	96	118	102	66	3			x								x				x						
841	j	99	121	105	67	3			x								x				x						
782	j	62	84	68	85	2			x				>3				x				x					200	
842	j	249	271	255	89	?			x								x				x					300	
995	j	162	184	168	47	5				x			>4								x					400	
924	j	103	125	109	67	3				x							x				x						
893	j	86	108	92	26	4			x							x					x					2000	
610	j	84	106	90	32	4			x							x					x						
1109	j	160	182	166	46	5				x							x				x						
1079	j	162	184	168	44	5				x							x				x						
1030	Crush Zone																										
1042	j	161	183	167	49	5				x							x				x						
1123	j	89	111	95	34	4				x								x			x						
1068	j	102	124	108	71	3			x								x				x						
1203	j	104	126	110	75	3				x							x					x					
1374	j	142	164	148	71	5			x							x					x						
1154	shr	62	84	68	82	2					x							x					x			<70	
1233	j	99	121	105	81	3			x								x				x					<100	
1294	j	97	119	103	83	3		x									x				x					<200	
1270	j	103	125	109	86	3			x								x					x					
1415	j	58	80	64	87	2		x									x					x					

1480	sheared	104	126	110	82	3							>1																		
1511	j	140	162	146	56	5		x								x						x	25mm	B/P intrusive		Cemented joints					
1590	shr	76	98	82	44	4				x								x				x	10mm	qtz course							
1531	shr	119	141	125	42	?					x							x				x	10mm	clay							
1672	j	96	118	102	74	3		x								x				x											
1723	j	94	116	100	67	3		x								x				x											
1906	j	223	245	229	72	1		x							x					x											
1867	j	82	104	88	58	4			x									x				x	<10mm	Qtz/calcite							
1905	j	83	105	89	54	4			x									x				x	<10mm	Qtz/calcite							
1960	j	94	116	100	73	3		x								x				x											
1952	j	73	95	79	48	4		x						x						x											
2018	j	242	264	248	62	2		x								x				x					200						
2040	j	100	122	106	78	3		x								x				x					<100						
2162	j	243	265	249	86	2		x							x					x											

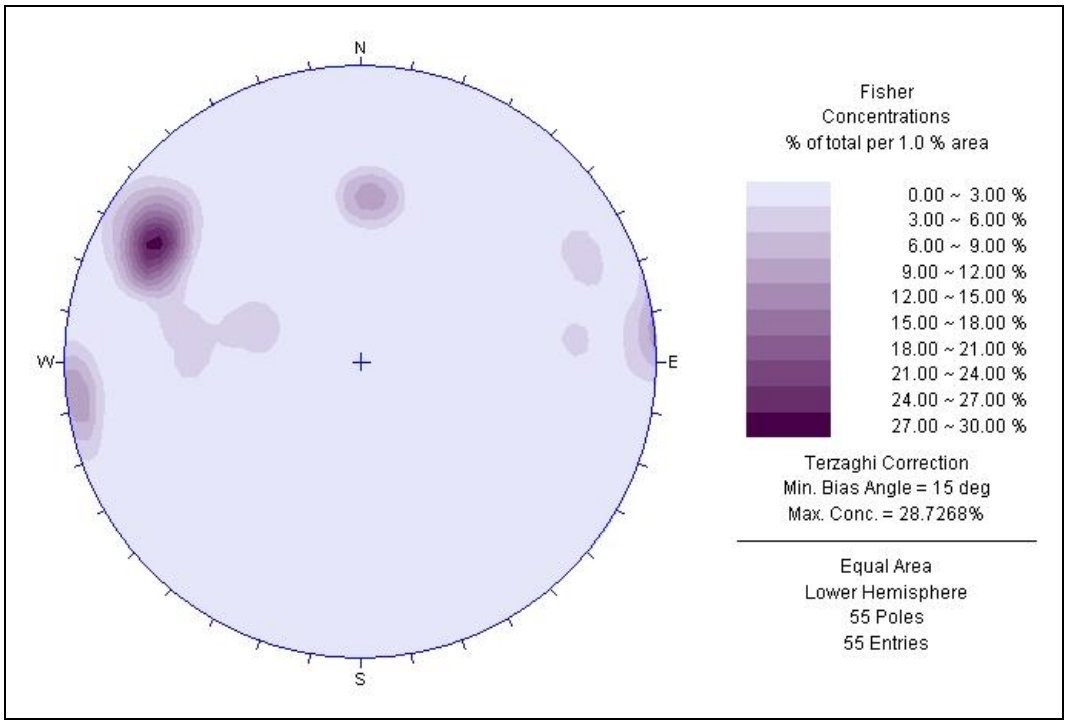

Scanline 4 Contour Plot – Pole Density Distribution

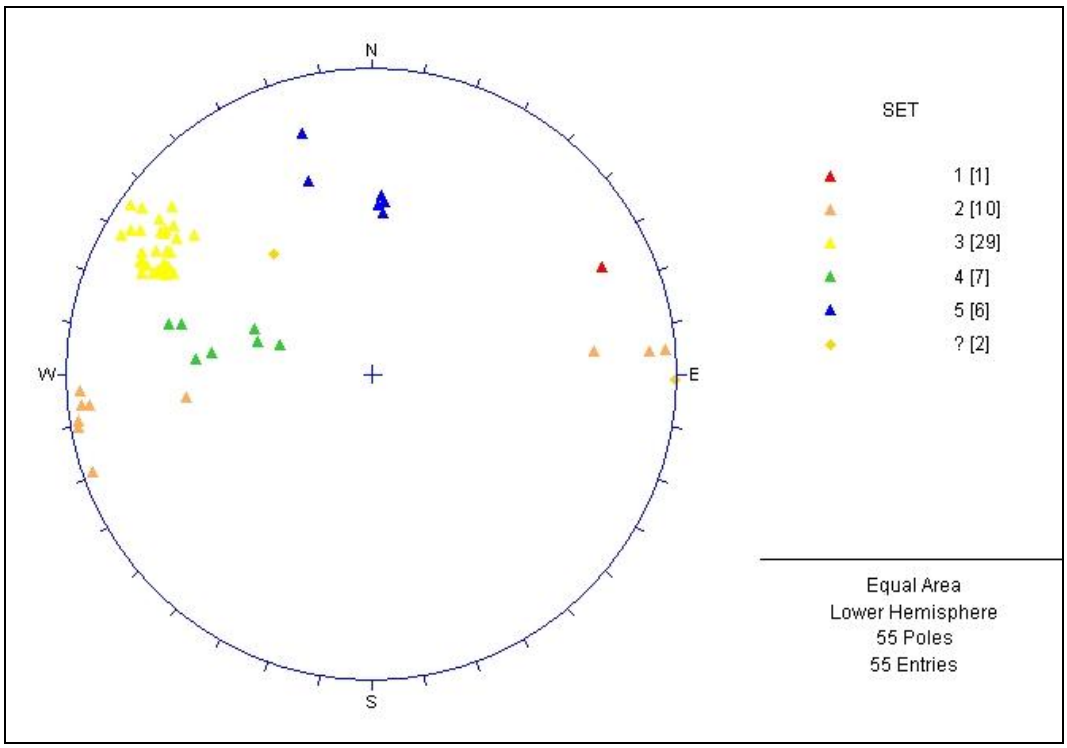

Scanline 4 Scatter Plot – Joint Sets

Distance along	Defect	Dip	Corrected	Correlated	Dip	Set #	Hardness						Persis	Aperture	Roughness					Spacing (mm)				Infill Thick~		Fracture	Notes
Datum (cm)	type	Direction	D/D	D/D			vh	h	mh	m	s	vs	tence (m)	(mm)	vr	r	sr	sm	sl	< .1	.1-1	1-5*	>5	ness (mm)	Discription	Spacing (mm)	
#5 Length 31m 278/16													<1 unless otherwise stated														
410	j	175	197	181	72	1				x			>8	250mm		x							x	>60mm	Muscovite/calcite		
124	shr	94	116	100	81	3				x								x			x					50-200	minor offset of GG inclusions
128	shr	119	141	125	84	3				x								x			x						
172	shr	266	288	272	76	3				x								x			x						
211	shr	261	283	267	82	3				x								x			x						
233	j	272	294	278	78	3				x							x				x						
253	j	274	296	280	83	3				x							x					x					
306	j	102	124	108	72	3				x							x				x						
350	Contact with GG																										
450	Contact with B/P																										
351	j	91	113	97	45	4			x								x				x						
513	j	276	298	282	85	3				x							x				x						
526	j	105	127	111	82	3				x							x				x						
541	j	279	301	285	88	3				x								x			x						
611	j	96	118	102	79	3				x							x				x						
616	j	102	124	108	84	3				x							x				x						
556	j	68	90	74	78	2				x							x				x						
712	j	120	142	126	74	3				x								x			x						
764	j	119	141	125	85	3				x								x			x						
643	j	4	26	10	64	1				x							x				x						
821	j	298	320	304	82	3				x							x					x					
682	j	22	44	28	72	1				x							x				x						
831	j	92	114	98	81	3				x							x				x						
796	j	92	114	98	68	3				x								x				x			calcite		
781	j	32	54	38	51	1						x					x				x						
762	j	29	51	35	48	1				x								x			x						
1010	j	248	270	254	79	2			x								x				x						
1158	shr	60	82	66	72	2					x								x				x	>7mm	clay		
1176	shr	53	75	59	76	2					x								x				x	>6mm	clay		
1410~1600	Crushed Sequence, major shear, highly fractured, indistinguishable joint orientation in crushed rock																										
1602	j	265	287	271	81	3				x							x				x						
1680	j	38	60	44	82	1				x						x					x						
1654	j	64	86	70	76	2				x						x					x						
1677	j	248	270	254	59	2				x						x					x						
1710	j	86	108	92	82	3				x						x					x						
1721	j	282	304	288	84	3				x						x					x						
1755	j	69	91	75	86	2				x						x					x						
1760~2170	Crushed zone																										
2171	j	277	299	283	68	3			x								x				x						
2182	j	268	290	274	82	3		x									x				x						
2236	j	98	120	104	81	3		x								x					x						
2251	j	89	111	95	84	3		x								x					x						
2157	j	250	272	256	76	2		x							x						x						

2302	j	11	33	17	89	1		x				x			x									
2269	j	85	107	91	82	3		x				x			x									
2322	shr	16	38	22	81	1			x				x			x			calcite					
2352	j	242	264	248	80	2		x				x												
2345	Contact with B/P																							
2331	shr	74	96	80	60	2			x					x			x	>5	Sandy clay					
2382	shr	82	104	88	76	3			x					x			x		Sandy clay					
2494	shr	232	254	238	58	2			x					x			x		Sandy clay					
2552	j	324	346	330	82	5	x					x			x									
2683	j	92	114	98	82	3		x				x			x									
2686	j	92	114	98	80	3		x					x		x									
2670	j	90	112	96	78	3		x				x			x									
2638	j	94	116	100	78	3		x				x			x									

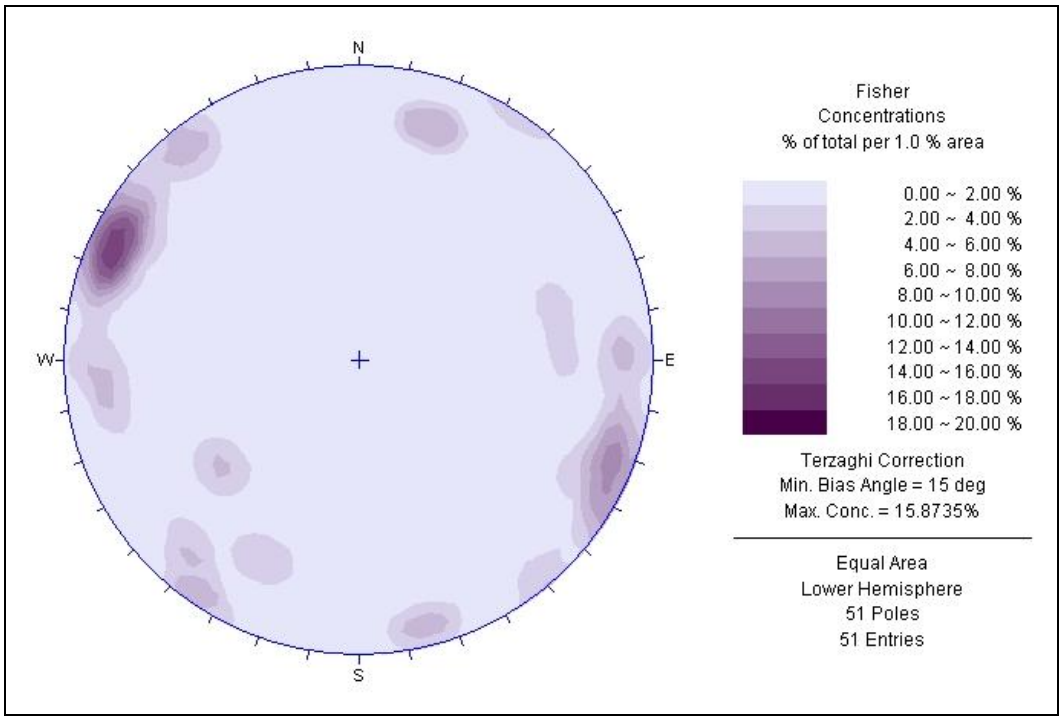

Scanline 5 Contour Plot – Pole Density Distribution

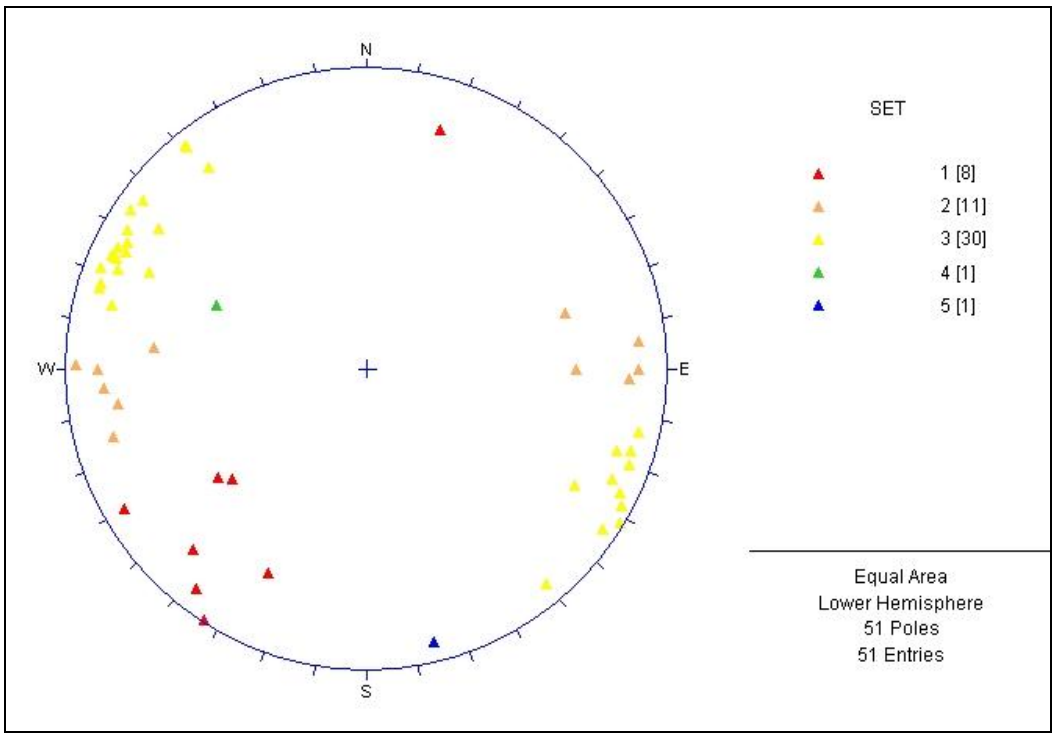

Scanline 5 Scatter Plot – Joint Sets

Distance along	Defect	Dip	Corrected	Correlate(	Dip	Set #	Hardness					Persis	Aperture	Roughness					Spacing (mm)				Infill Thick~		Fracture	Notes
Datum (cm)	type	Direction	D/D	D/D			h	mh	m	s	vs	tence (m)	(mm)	vr	r	sr	sm	sl	< .1	.1-1	1-5*	>5	ness (mm)	Discription	Spacing (mm)	
#6 length= 16m 247/10 (up to 9m) 13 (up to 16)												<1 unless otherwise stated														
44	j	46	68	52	84	2			x							x				x						<60	
32	j	34	56	40	80	2			x							x				x							
84	j	43	65	49	81	2			x							x				x							
55	j	280	302	286	76	3			x			>2			x					x							
98	j	236	258	242	83	2			x							x				x							
179	j	356	18	2	44	?			x							x				x							
214	j	244	266	250	68	2	x									x				x							
293	j	264	286	270	81	3	x									x				x							
302	j	231	253	237	50	2	x					>1				x					x						
359	j	4	26	10	58	1	x					>1				x					x						
310	j	71	93	77	56	4			x							x				x							
461	j	76	98	82	41	4			x							x				x							
473	j	78	100	84	42	4			x							x				x							
451	j	69	91	75	37	4			x							x				x							
519	j	348	10	354	67	5			x							x					x						
553	j	244	266	250	87	2	x									x				x							
581	j	6	28	12	61	1	x									x				x							
638	contact	343	5	349	76	5			x								x				x						
692	j	358	20	4	81	5			x								x			x							
829	j	236	258	242	79	2			x								x			x							
892	j	242	264	248	89	2	x					>1					x			x							
927	j	236	258	242	88	2	x					>1					x				x						
959	j	247	269	253	81	2	x					>1					x				x						
1027	j	83	105	89	84	3	x					>1				x					x						
1023	j	158	180	164	56	5	x										x			x							
1090	j	281	303	287	52	4	x										x			x							
1090	j	302	324	308	66	?		x									x			x							
1171	j	91	113	97	82	3	x									x				x							
1122	Contact with B/P								x																		
1143	Contact	14	36	20	48	1		x								x					x						
1199	j	15	37	21	44	1		x								x				x							
1204	j	283	305	289	79	3	x								x					x							
1255	j	26	48	32	24	1	x									x				x							
1362	j	93	115	99	89	3	x							x						x					60mm		
1366	j	28	50	34	66	1	x								x					x							
1580	j	224	246	230	78	2	x								x					x							
1476	j	355	17	1	62	5	x									x				x							

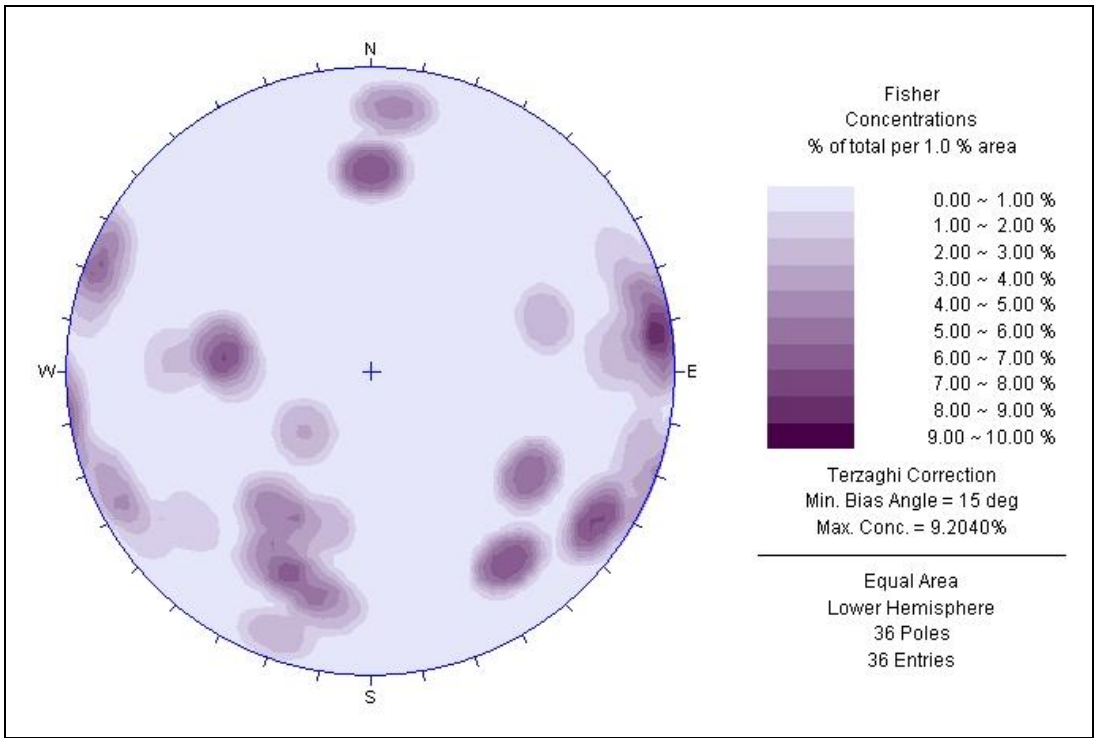

Scanline 6 Contour Plot – Pole Density Distribution

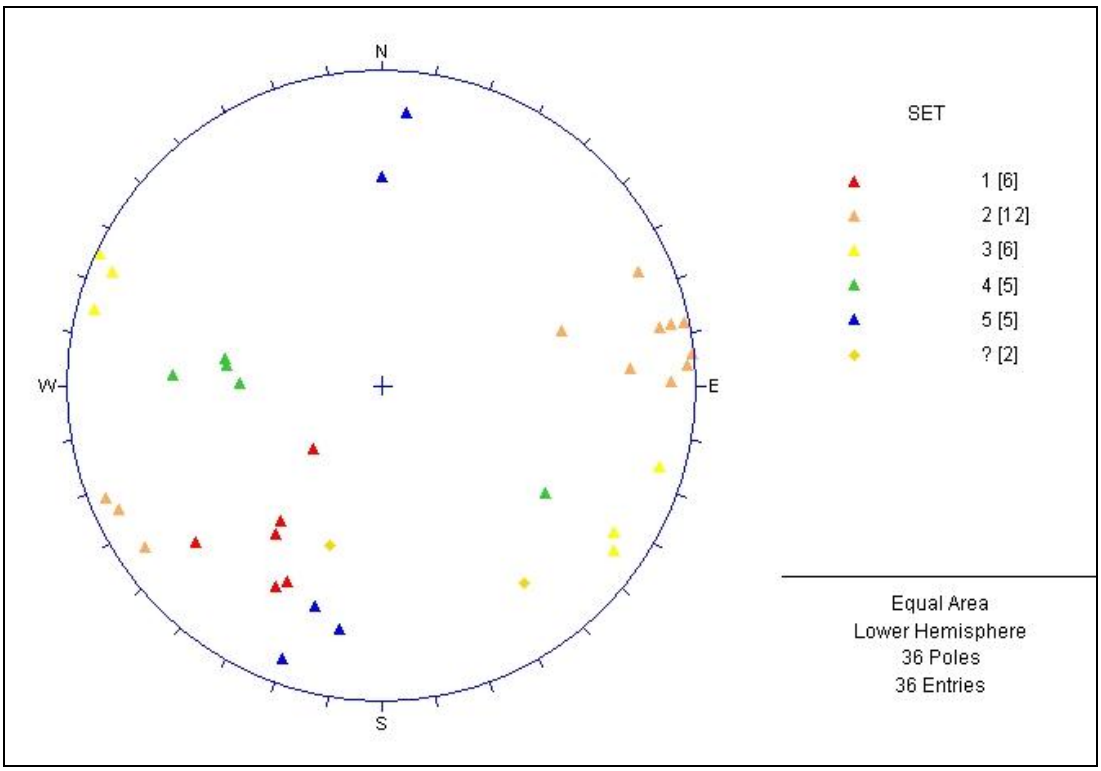

Scanline 6 Scatter Plot – Joint Sets

Distance along	Defect	Dip	Corrected	Correlated	Dip	Set #	Hardness						Persis	Aperture	Roughness					Spacing (mm)				Infill Thick~		Fracture	Notes
Datum (cm)	type	Direction	D/D	D/D			vh	h	mh	m	s	vs	tence (m)	(mm)	vr	r	sr	sm	sl	< .1	.1-1	1-5*	>5	ness (mm)	Discription	Spacing (mm)	
#7 Length Section 1 length 34m 027/24													<1 unless otherwise stated														
28	j	222	244	278	72	2		x								x					x					300	
68	j	176	198	232	76	1		x					>1			x					x					<200	
82	j	171	193	227	70	1		x					>1			x					x					<200	
94	j	159	181	215	73	?		x					>1			x					x					<200	
133	j	52	74	108	46	1		x					>1			x					x						
115	j	61	83	117	38	1		x					>1			x					x					400	
164	j	169	191	225	64	1		x					>1			x					x					<200	
172	j	171	193	227	71	1		x					>1			x					x					<200	
183	j	171	193	227	68	1			x				>1			x					x					<200	
195	j	168	190	224	67	1			x				>1			x					x					400	
221	j	62	84	118	52	2			x				>1			x					x						
253~297	Crush Zone																										
332	j	174	186	220	71	1			x				>1				x				x						
347~361	Crush Zone																										
416	shr	63	85	119	76	2			x									x				x					
424	j	151	173	207	78	?			x				>1				x				x			32mm	C/sand	<200	
449	j	166	188	222	72	?			x				>1				x				x						
459	j	204	226	260	72	1			x				>1						x		x						
452	j	88	110	144	48	4			x				>1				x				x					100	
460	shr	68	90	124	81				x				>2				x					x		4mm	soft clay	70	
484	j	354	16	50	79	1			x								x				x						
491	j	198	220	254	63	1		x									x				x						
503	j	206	228	262	60	1		x									x				x						
569	j	218	240	274	75	2		x									x				x					50	
584	shr	233	255	289	82	2			x				>2				x					x					
651	j	218	240	274	64	2		x									x				x						
663	j	222	244	278	68	2		x									x				x						
682	j	216	238	272	63	2		x									x				x					<100	
712	j	244	266	300	69	2		x					>4			x					x					<100	
743	j	251	273	307	71	2		x					>4			x					x					<100	harder greenland group. Same set slightly
792	j	250	272	306	68	2		x					>2			x					x					<100	different orientation and steeper dip
810	j	245	267	301	76	2		x					>3			x					x					<100	(fracture propagation)
859	j	248	270	304	76	2		x					>1			x					x					<100	
908	j	124	146	180	67	5			x								x				x					<100	
915	j	20	42	76	78	1			x								x				x					400	
915	j	72	94	128	76	6			x								x				x					<100	
973	j	196	218	252	87	1			x								x				x					400	
989	j	189	211	245	71	1				x							x					x				200	
1007	j	202	224	258	68	1			x								x				x					200	
1061	j	242	264	298	58	2			x							x					x						
1065	j	132	154	188	68	5			x								x				x						
1078	shr	230	252	286	49	2			x								x						x	30	clay/bp		
1148	j	261	283	317	75	3		x					>2				x					x					
1192	j	263	285	319	70	3		x					>2				x					x					
1195	j	220	242	276	75	2		x					>4				x					x					

1204	j	261	283	317	69	3	x					>2			x						x				
1329	j	227	249	283	61	2	x									x				x					Softer GG
1450	j	258	280	314	74	3		x				>1			x					x					hardened GG
1371	j	260	282	316	72	3		x							x					x					
1508	j	254	276	310	73	3	x					>3				x				x					
1484	j	220	242	276	52	2	x									x				x					softer GG
1472	j	223	245	279	50	2		x								x				x					softer GG
1532	j	226	248	282	43	2		x				>2				x				x					softer GG
1704	shr	255	277	311	78	3		x				>8						x				x		60	sandy clay	smaller sized rock fragments
1730	shr	220	242	276	62	2		x										x				x		30	soft rock	
1781	j	154	176	210	61	?	x					>2				x				x					massive rock fragment
1961	j	253	275	309	75	2	x									x				x					
2112	j	38	60	94	84	2	x									x				x					
2152	j	124	146	180	64	5		x								x				x					contact with B/P
2161	j	189	211	245	70	1		x									x			x					
2170	t/c	358	20	54	41	1			x								x			x					8x contact related fractures
2252	j	356	18	52	40	1			x								x			x					
2778	j	215	237	271	63			x				>5					x			x					
2668	shr	256	278	312	78	6		x				>4						x		x				calcite	Curves downward running parallel with datum
2675	shr	244	266	300	76	6		x				>4						x		x					
2898	j	37	59	93	68	2		x								x				x				sand/calcite	White sandy infill
2937	j	182	204	238	61	1		x								x				x					
2973	j	316	338	372	48	5		x									x			x					
3160	shr							x										x		x					
3360	j	359	21	55	67	1		x									x			x					
3400	Section 2 Length= 7m 096/00																								
3520	j	232	254	288	51	2	x					>1				x				x					
3714	j	261	283	317	70	6	x					>1				x				x					
3971	j	224	246	280	52	2	x					>1				x				x					
3980	j	270	292	326	68	6	x					>1				x				x					
3984	j	243	265	299	68	6	x					>1				x				x					
3952	j	266	288	322	61	6	x					>1				x				x					
4050	j	218	240	274	51	2	x					>1				x				x					

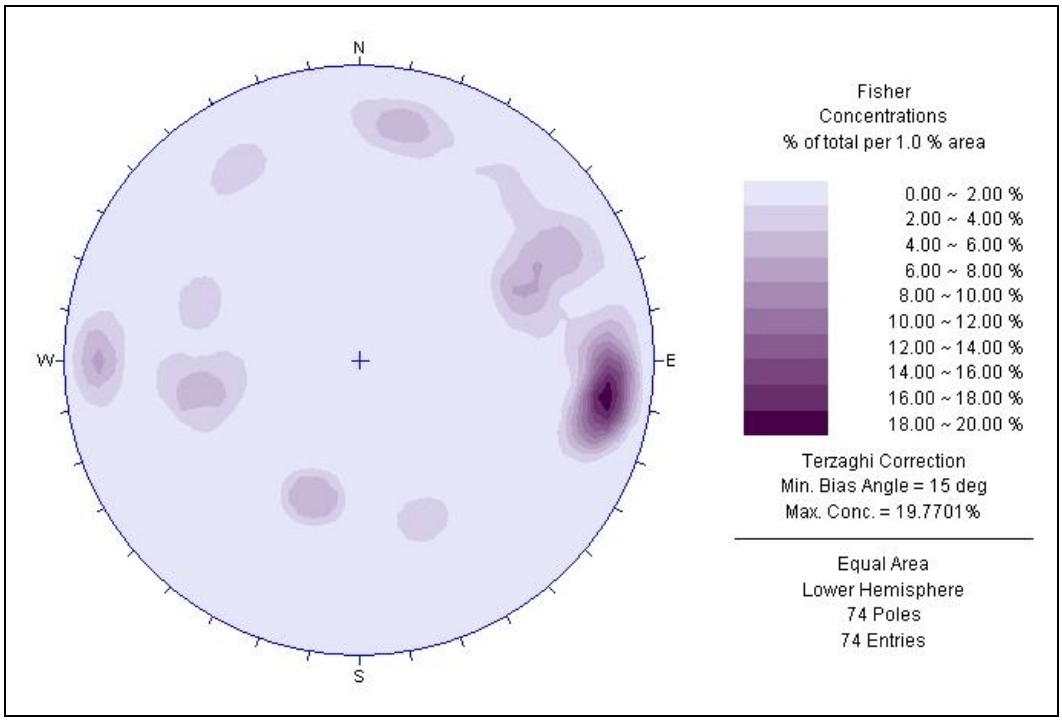

Scanline 7 Contour Plot – Pole Density Distribution

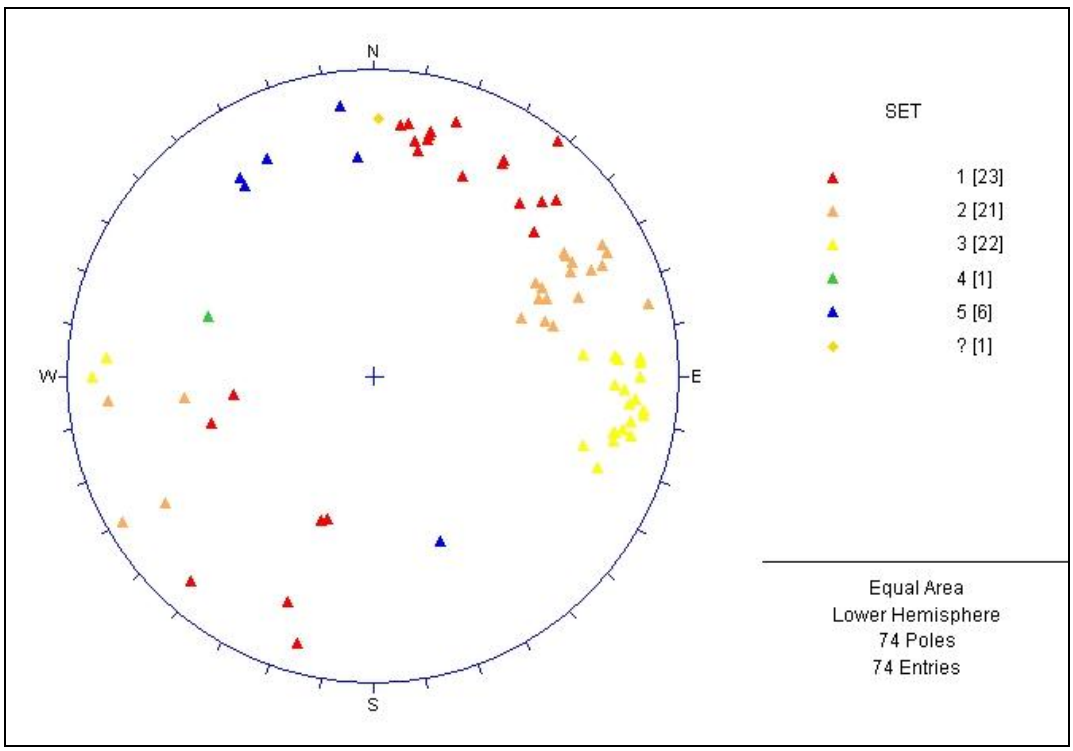

Scanline 7 Scatter Plot – Joint Sets

Distance along	Defect	Dip	Corrected		Dip	Set #	Hardness						Persis	Aperture	Roughness					Spacing (mm)				Infill		Fracture	Notes
Datum (cm)	type	Direction	D/D				vh	h	mh	m	s	vs	tence (m)	(mm)	vr	r	sr	sm	sl	< .1	.1-1	1-5*	>5	thicknes	Discription	Spacing (mm)	
#8 Section 1 length 14 307/10													<1 unless otherwise stated														
112	j	293	315	349	48	4			x							x					x						
166	shr	261	283	317	44	4			x								x					x		10mm	Clay		Stained iron clay. Silty.
255	j	264	286	320	62	6		x					>3			x						x		2mm	staining	600	
256	j	344	6	40	82	?		x					>2			x						x		3mm	staining		
284	j	132	154	188	16	?		x								x					x						
289	j	107	129	163	87	3		x					>1			x					x						
317	j	336	358	392	52	5		x					>1		x						x					200	
344	j	331	353	387	66	5		x					>1		x						x						
377	j	332	354	388	81	5		x					>1		x						x						
400	j	318	340	374	80	5		x					>1				x				x						
402	j	282	304	338	62	6		x								x					x					300	
476	shr	326	348	382	76	5		x					>1				x						x	20mm	Weathered rock		Pinches together
497	j	289	311	345	85	3		x					>1				x					x					
820	j	23	45	79	47	1			x				>4			x					x						
719	j	280	302	336	71	3			x				>1				x				x						
594	j	288	310	344	73	3		x					>2			x					x						
543	j	290	312	346	79	3		x					>1		x						x						
618	j	278	300	334	43	4		x					>2				x				x						
658	j	270	292	326	46	4		x									x				x						
810	j	134	156	190	33	?			x				>2				x				x						
804	j	108	130	164	78	3			x				>2				x				x						
796	shr	83	105	139	70	6			x				>1						x			x		2mm	Sandy clay		
847	shr	100	122	156	64	6			x										x			x		2mm	Sandy clay		
929	j	282	304	338	88	3		x					>2				x				x						
948	j	290	312	346	82	3		x					>2				x				x						
1002	shr	141	163	197	63	5			x										x				x	80mm	Clay/crush		Weathered and crushed rock
1033	j	294	316	350	75	3			x								x				x						
1070	j	285	307	341	72	3		x									x				x						
1141	j	146	168	202	74	5			x				>2			x					x						
1158	j	158	180	214	81	5			x				>2			x					x						injected B/P into joints
1198	j	152	174	208	60	5			x								x				x						
1211	j	148	170	204	56	5			x								x				x					100	
1216	j	284	306	340	39	4			x						x						x					100	
1318	j	271	293	327	81	3			x								x				x					100	X4
1335	j	280	302	336	83	3			x								x				x						
1320	shr	132	154	188	41	5				x									x			x		2mm	sandy clay		

#8 Section 2 Length 19 m 293/14																								
1436	j	291	313	347	64	6		x							x			x						
1454	j	96	118	152	78	3			x						x					x	80mm	M/fine sand		Inclusion of GG bake finges 1 cm
1419	j	127	149	183	82	5			x					x				x						
1472	j	83	105	139	36	4		x								x		x						
1302	shr	172	194	228	49	?					x					x			x		4mm	clay/calcite		
1476	j	132	154	188	47	5		x								x			x		2mm	Calcite		
1487	j	142	164	198	52	5		x								x			x		2mm	Calcite		
1510	j	184	206	240	55	?			x						x			x						Softer section which may be the reason
1522	j	152	174	208	51	?			x			>1			x			x						for the altered orientation.
1556	j	158	180	214	53	?			x			>1			x			x						
1560	j	168	190	224	60	?			x			>1			x			x						
1692	j	139	161	195	58	5		x								x		x						Crushed zone and slight change of dip
1709	j	147	169	203	63	5		x								x		x						orientation due to influence with B/P contact
1936	j	272	294	328	72	3		x								x		x						
1962	j	258	280	314	63	6		x								x		x						
2030	j	256	278	312	71	3		x								x		x						
2583	shr	222	244	278	66	2				x		>6				x		x						Outcrop of GG, contact with B/p along
2142	j	274	296	330	83	3	x									x		x						strike.
2215	j	263	285	319	68	6	x									x		x					400	
2300	j	264	286	320	69	3	x									x		x						
2374	j	256	278	312	81	3	x									x		x						
2390	j	266	288	322	84	3	x									x		x						
2560	Crushed Zone																							
2636	j	241	263	297	72	?			x			>1			x				x		4			Baked zone 2560 -2730
2708	j	274	296	330	79	3		x							x									
2730	Contact with B/P instrusive																							Wedge shaped instrusive V hard B/P Qtz
2920	Contact with GG																							Rich
3021	j	134	156	190	88	5		x				>2				x		x						
3042	j	253	275	309	72	3	x					>2			x			x						
3222	j	262	284	318	86	3	x											x					<50mm	

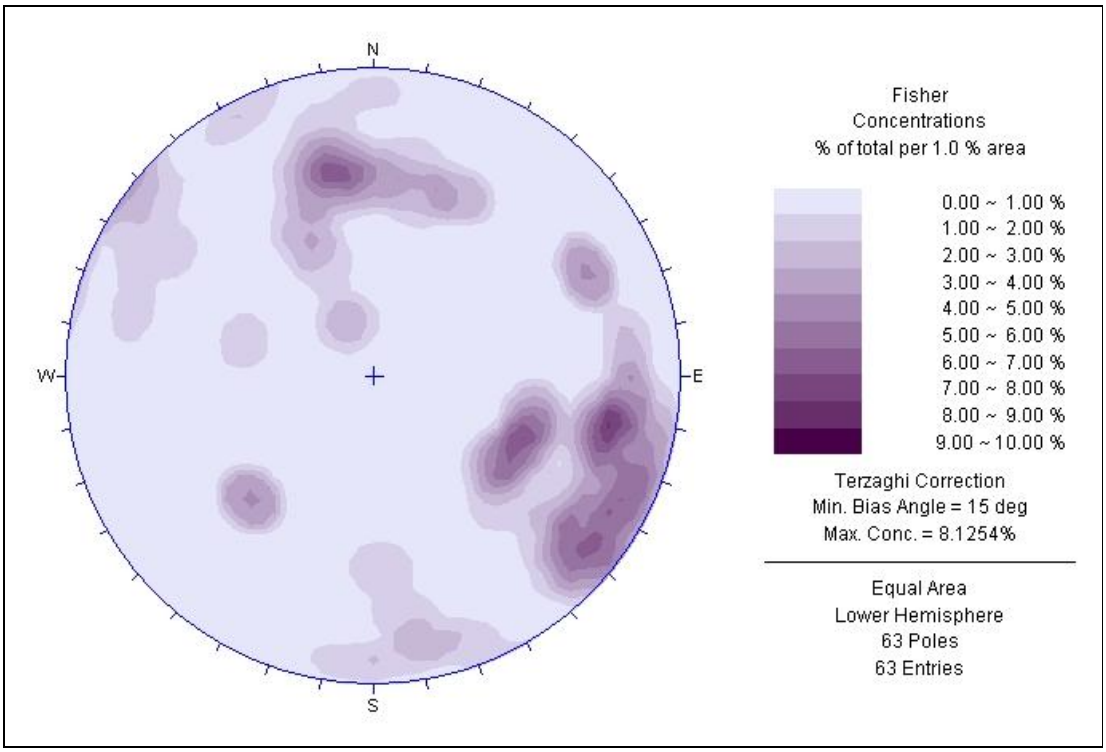

Scanline 8 Contour Plot – Pole Density Distribution

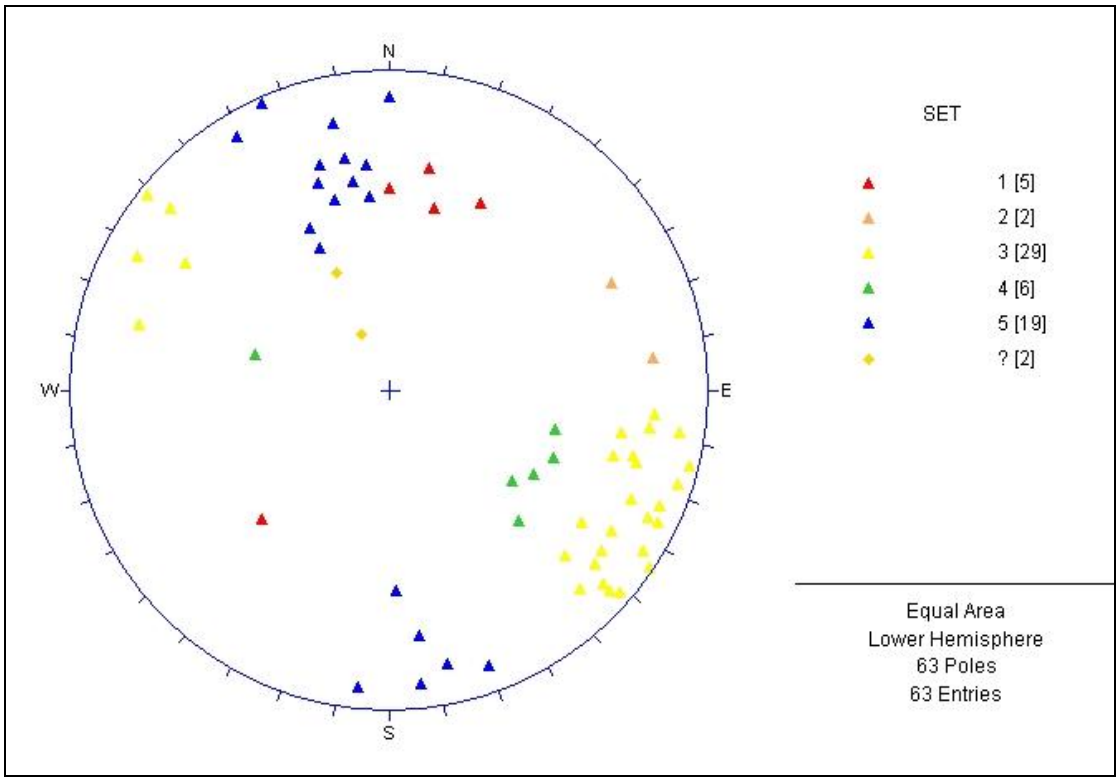

Scanline 8 Scatter Plot – Joint Sets

Distance along	Defect	Dip	Corrected		Dip	Set #						Persis	Aperture	Roughness					Spacing (mm)				Infill Thick~		Fracture	Notes
Datum (cm)	type	Direction	D/D				h	mh	m	s	vs	tence (m)	(mm)	vr	r	sr	sm	sl	< .1	.1-1	1-5*	>5	ness (mm)	Discription	Spacing (mm)	
#9 Section 1298/12												<1 unless otherwise stated														
25	j	310	332	7	81	5		x									x			x						
36	j	312	334	9	78	5		x									x			x						
57	j	318	340	15	86	5		x								x	x			x						
127	j	258	280	315	73	6		x				>1				x				x						
149	j	262	284	319	68	6		x				>2				x				x						
178	j	258	280	315	69	6		x								x				x						
222	j	264	286	321	65	6		x				>1				x					x					
303	j	266	288	323	87	3		x				>1				x				x						
392	j	260	282	317	81	3		x								x				x						
431	j	272	294	329	81	3		x								x				x						
466	j	266	288	323	78	3		x								x				x						
514	j	268	290	325	88	3		x								x				x						
538	j	280	302	337	78	3		x								x				x						
602	shr	275	297	332	81	3		x										x				x	6mm	Silty Clay		
743	j	146	168	203	79	?		x				< .5			x					x						
756	j	303	325	360	84	5		x				< .5			x					x						
830	j	68	90	125	63	2	x								x					x						
895	j	135	157	192	72	5	x								x					x						
918	shr	79	101	136	34	4	x									x					x					
931	j	89	111	146	66	6		x				>2				x										
939	j	92	114	149	63	6		x								x										
960	j	196	218	253	84	1		x									x									
1014	j	92	114	149	62	6	x										x									
1076	j	286	308	343	78	3	x									x										
1194	j	263	285	320	72	3		x				3					x									
#9 Section 2 343/14																										
1436	j	36	58	93	79	2		x								x										
1416	j	41	63	98	82	2		x								x									<100	
1510	j	298	320	355	76	?		x				>2					x								<100	
1600	j	31	53	88	72	2		x									x								<100	
1681	j	226	248	283	63	2		x				>3				x									<100	
1612	j	300	322	357	64	?		x								x									<100	
1880	j	222	244	279	75	2		x				>7				x									300-400	
1868	j	112	134	169	28	?		x								x									<100	
1940	B/P Intrusive						x										x									

#9 Section 3 280/15																<100	
2072	j	228	250	285	74	2		x					x				
2114	j	229	251	286	69	2		x	>7			x				300-400	
2156	j	279	301	336	76	3		x			x						
2259	j	142	164	199	72	?		x									
2352	j	218	240	275	67	2		x	>2	5cm		x					
2312	j	102	124	159	87	3		x					x				
2472	j	226	248	283	78	2		x	>2					x			
2449	j	73	95	130	60	6		x					x				
2324	j	130	152	187	68	5		x	>1				x			100-200	2250-2380 x 7
2451	j	258	280	315	84	3	x							x			
2644	j	224	246	281	84	2	x		>1				x				
2693	j	40	62	97	78	2	x		>1				x				
2560	j	82	104	139	62	6	x						x			400	
2534	j	73	95	130	48	4	x						x				
2474	j	77	99	134	68	6	x						x				
2794	j	260	282	317	82	3	x						x				
2802	j	41	63	98	66	2	x						x				
2832	j	286	308	343	73	3		x				x					
2844	j	269	291	326	84	3		x				x					
2854	j	260	282	317	83	3	x						x				
2871	j	264	286	321	85	3	x						x				
2918	j	254	276	311	75	3	x		>1				x				
2913	j	134	156	191	49	5	x		>1				x				
2950-2970	B/P Intrusive						x					x					
2990	j	284	306	341	84	3		x					x				
2994	j	288	310	345	89	3		x	>1				x				
2984	j	74	96	131	38	4		x	>1				x				
2920	j	76	98	133	39	4		x	>1				x				
3079	j	261	283	318	74	3	x						x				
3186	j	260	282	317	81	3	x		>2				x				
3154	j	259	281	316	76	3		x	>1				x				
3270	j	142	164	199	66	5		x				x					
3209	j	271	293	328	78	3		x					x				

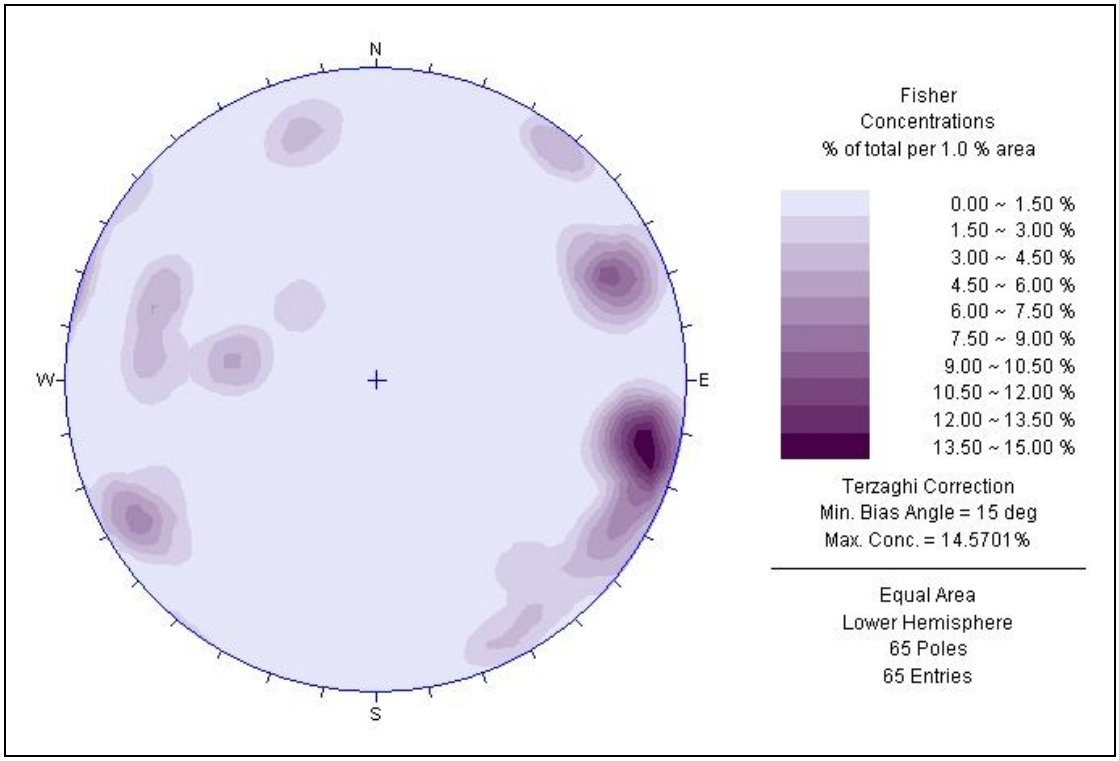

Scanline 9 Contour Plot – Pole Density Distribution

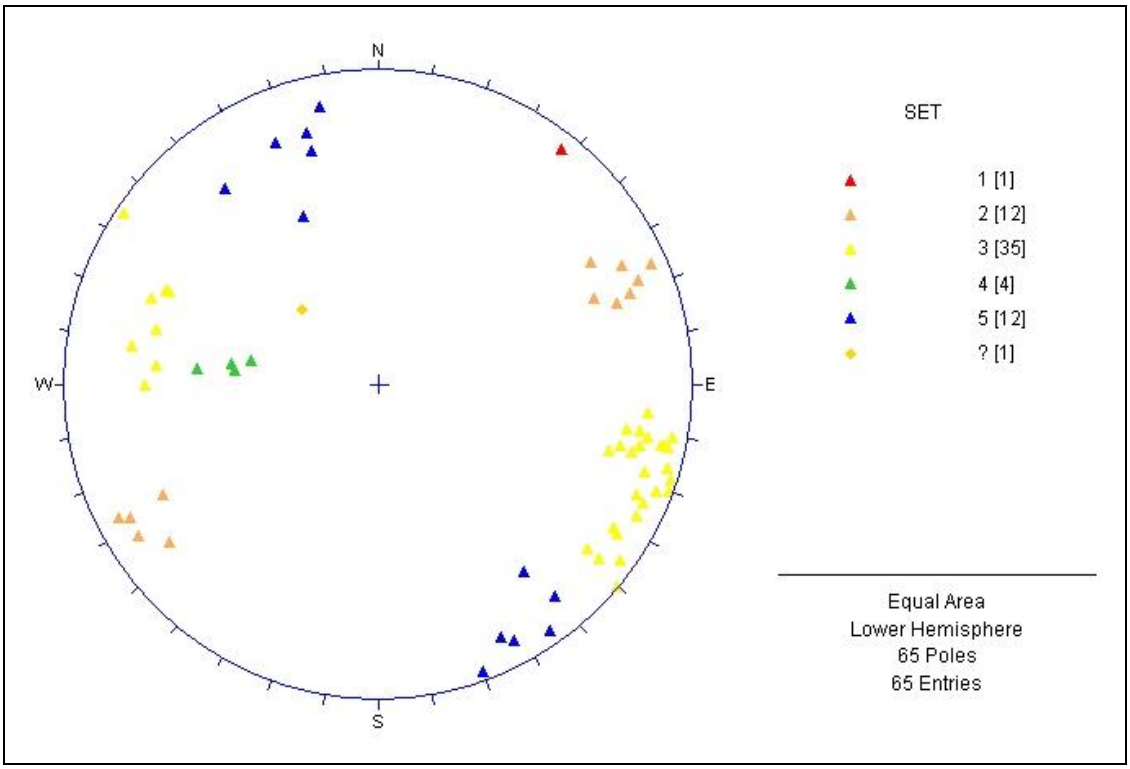

Scanline 9 Scatter Plot – Joint Sets

Distance along	Defect	Dip	Corrected	Correlated	Dip	Set #							Persis	Aperture	Roughness					Spacing (mm)				Infill Thick~		Fracture	Notes
Datum (cm)	type	Direction	D/D	D/D			vh	h	mh	m	s	vs	tence (m)	(mm)	vr	r	sr	sm	sl	< .1	.1-1	1-5*	>5	ness (mm)	Discription	Spacing (mm)	
# 10 Length = 24m 342/16													<1 unless otherwise stated														
30	j	271	293	328	80	3			x				>1				x						x				
89	j	104	126	161	62	6			x								x						x				
102	shr	234	256	291	66	2			x				>4			x							x				iron staining on shear edges
278	shr	262	284	319	87	3			x				>1				x						x				
218	j	122	144	179	69	5			x							x						x					
239	j	151	173	208	45	?		x									x				x						
248	j	84	106	141	82	3		x					>1				x					x					
332	j	86	108	143	84	3			x								x				x						
400	j	74	96	131	74	3			x								x				x						
442	j	128	150	185	76	5			x						x						x						
431	j	122	144	179	75	5			x							x					x						
436	j	79	101	136	73	6			x							x					x						
521	j	89	111	146	74	6			x				>2				x				x						
602	j	193	215	250	52	1			x								x				x						
555	j	213	235	270	89	2			x				>1						x			x					
628	j	59	81	116	75	2			x										x			x					
753	j	339	1	36	65	5			x								x				x						
721	j	328	350	25	59	5			x								x				x						
712	j	89	111	146	48	4			x								x				x						Inclusions of B/p change in composition of G
860	j	289	311	346	71	3			x								x				x						
773	j	82	104	139	74	6			x								x				x						
829	j	134	156	191	86	5			x								x				x						
891	j	166	188	223	82	?			x								x				x						
870	j	291	313	348	78	3			x								x				x						
902	j	269	291	326	76	3			x								x				x						
1046	Contact with B/P																										
1143	j	326	348	23	71	5			x								x				x						
1292	j	83	105	140	74	6			x								x				x						
1187	j	284	306	341	72	3			x								x				x						
1331	j	266	288	323	81	3				x			>2				x				x						
1449	j	265	287	322	84	3				x			>2				x				x						
1486	j	263	285	320	81	3				x			>2				x				x						
1452	j	51	73	108	41	2			x							x					x						
1559	j	255	277	312	78	3				x			>2			x					x						
1476	j	144	166	201	48	5				x							x				x						
1664	j	335	357	392	81	5			x								x				x						
1651	j	314	336	371	86	5				x								x			x						
1898	j	91	113	148	74	6				x								x			x						
1984	j	88	110	145	83	6				x								x			x						
2132	j	263	285	320	78	3			x								x				x						
2160	j	263	285	320	81	3			x								x				x						
2152	j	217	239	274	74	2			x								x				x						
2259	j	267	289	324	82	3			x								x				x						
2248	j	139	161	196	48	5			x								x				x						
2268	j	96	118	153	52	4			x								x				x						
2291	j	350	12	47	81	1			x								x					x					
2404	j	84	106	141	72	6			x								x					x					
2359	j	2	24	59	67	1			x								x					x					
2374	j	139	161	196	54	5			x								x				x						
2319	j	147	169	204	62	5			x								x				x						

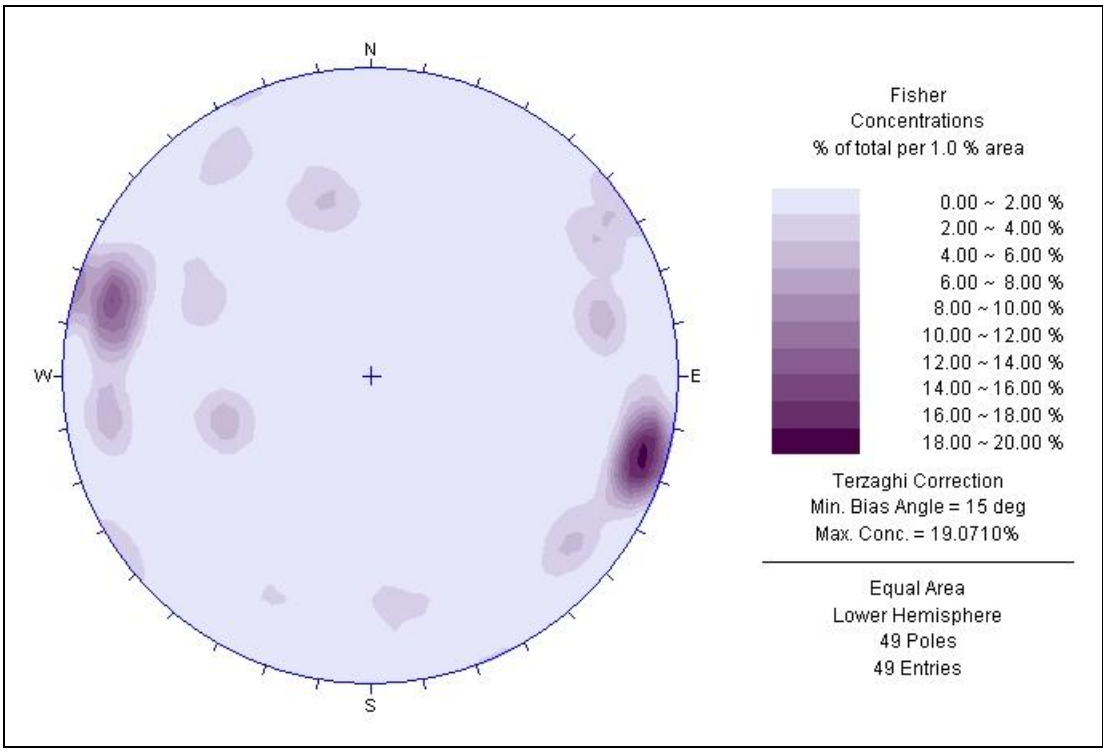

Scanline 10 Contour Plot – Pole Density Distribution

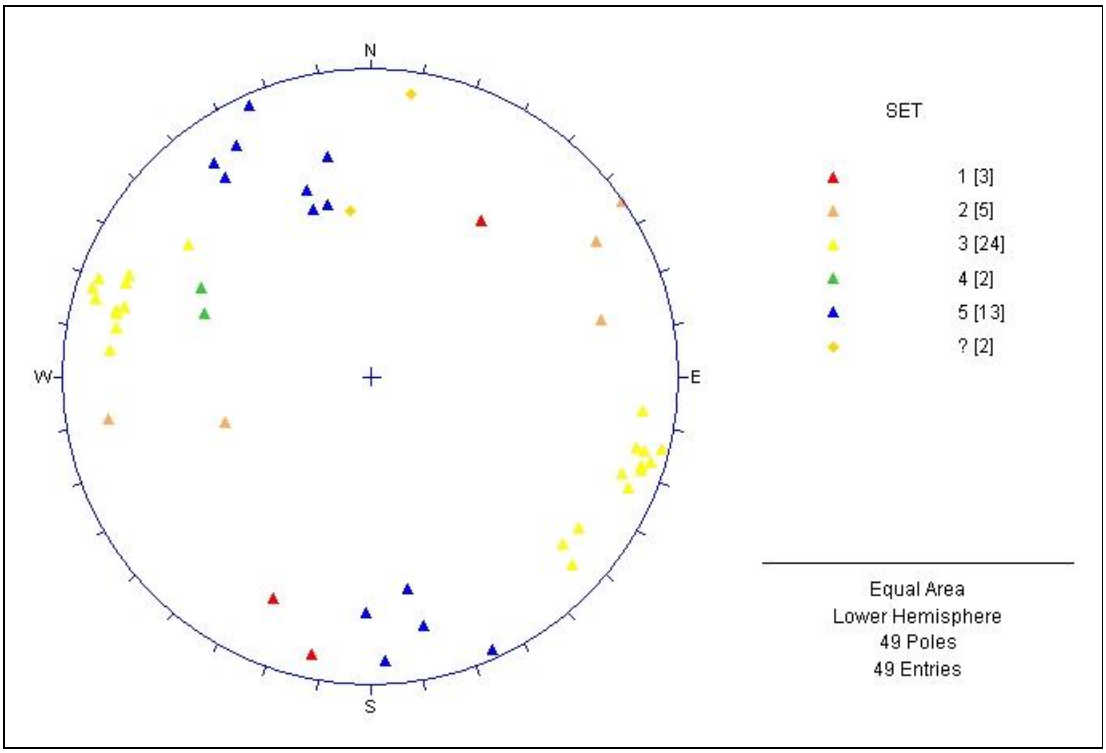

Scanline 10 Scatter Plot – Joint Sets

Distance along	Defect	Dip	Corrected		Dip	Set #	Hardness					Persis	Aperture	Roughness				Spacing (mm)				Infill Thick~		Fracture	Notes
Datum (cm)	type	Direction	D/D				vh	h	mh	m	s	vs	tence (m)	(mm)	vr	r	sr	sm	sl	< .1	.1-1	1-5*	>5	ness (mm)	Discription	Spacing (mm)	
#11 Section 1 length = 23 282/8-10													<1 unless otherwise stated														
22	j	94	116	152	71	3			x				>1			x						x				200	
69	j	100	122	158	72	3			x				>3				x					x				100	
110	j	103	125	161	68	3			x				>2				x					x				50	
220	j	93	115	151	78	3				x						x					x						Spacing every 50 mm very fractured major fracture // to datum
171	j	87	109	145	66	3				x							x				x						
276	j	110	132	168	86	3			x							x					x						
346	shr	94	116	152	73	3				x									x			x					
403	j	81	103	139	78	6				x							x				x						
520	j	84	106	142	68	6				x							x				x						
534	j	76	98	134	69	6				x							x				x						
550	shr	224	246	282	81	2					x						x					x					
563	shr	224	246	282	80	2				x							x					x					
762	j	91	113	149	82	3			x								x				x						
756	j	76	98	134	71	6				x							x				x					200	
764	j	81	103	139	62	3				x							x				x						
890	j	124	146	182	74	5			x								x				x					600	
893	j	73	95	131	59	6				x								x			x					400	
986	j	76	98	134	62	6				x								x			x						
1076	j	38	60	96	89	2			x								x				x						mixed
1088	j	39	61	97	86	2			x								x				x						
1092	j	274	296	332	76	3			x								x				x						
1190	j	86	108	144	62	6			x								x				x						
1231	j	89	111	147	76	3			x								x				x						
1266	j	79	101	137	48	6			x									x			x						
1274	j	86	108	144	68	6			x									x				x					
1376	j	83	105	141	62	6		x										x			x						
1411	j	83	105	141	68	6		x									x				x						
1434	j	168	190	226	73	1		x										x			x						
1519	j	96	118	154	36	4		x										x			x						
1529	j	84	106	142	89	3			x								x				x						
1544	j	82	104	140	79	3			x								x				x						
1558	j	161	183	219	87	1			x								x				x						
1572	j	80	102	138	84	3			x								x				x						
1593		82	104	140	82	3			x							x					x						
1621	j	84	106	142	73	3			x							x					x						
1472	j	203	225	261	83	1			x						x						x						
1682	j	78	100	136	72	6			x								x					x					
1880	j	73	95	131	81	6		x									x				x						
1753	j	32	54	90	26	?										x						x					
1824	j	193	215	251	62	1		x					>1			x					x						
1902	j	72	94	130	83	6	x									x					x					300	
1950	j	222	244	280	82	2	x										x				x					>150	
1958	j	218	240	276	81	2	x										x					x					
2032	j	253	275	311	83	?		x								x					x						
2135	j	35	57	93	79	2	x										x				x						
2192	j	38	60	96	89	2	x						>1			x					x						
2208	j	265	287	323	86	3	x										x				x						
2283	j	270	292	328	82	3	x										x				x						
2264	j	236	258	294	81	3	x										x						x			Singe contact with B/P	

#11 section 2 25m 299/8-10																									
2320	Shr	291	313	349	72	3		x			>1				x		x		3	silty clay	400mm				
2362	Shr	282	304	340	74	3		x			>1				x		x		3	silty clay					
2438	Shr	264	286	322	80	6		x			>1				x		x		4	silty clay	300mm				
2485	Shr	280	302	338	74	3		x			>1				x		x		2	silty clay					
2540	j	235	257	293	75	2	x							x		x					200mm	Contact			
2561	Shr	234	256	292	70	2	x				>3	50mm			x	x			3	staining					
2619	j	26	48	84	82	?	x				>3	>80mm			x	x									
2685	j	271	293	329	72	3	x				>2			x		x									
2892	j	286	308	344	70	3		x			>1		x				x								
2902	j	274	296	332	66	3	x							x		x					500mm				
2910	j	230	252	288	78	2		x			>1			x			x								
2986	Shr	222	244	280	72	2	x				>3			x		x				tight					
3051	j	218	240	276	73	2	x							x		x									
3070	j	214	236	272	82	2	x				>1				x	x									
3088	j	214	236	272	82	2	x				>1				x	x									
2911	j	40	62	98	52	?	x				>2		x			x									
2939	j	78	100	136	45	6	x				>2		x			x									
3231	j	86	108	144	42	6	x							x		x									
3242	Shr	232	254	290	66	2	x				>4	60mm			x		x		4mm	Staining	200-500mr	Repeatative fracturing either side			
3320	j	316	338	374	84	?	x				>1			x		x									
3521	j	275	297	333	78	3	x				>2			x		x									
3702	j	220	242	278	68	2	x				>1			x			x								
3772	j	45	67	103	64	?		x							x	x									
3818	j	88	110	146	52	4	x								x	x									
3904	Shr	72	94	130	78	?	x				>1				x		x		3mm	Staining					
4009	j	222	244	280	72	2	x				>2			x			x				400mm				
4037	j	264	286	322	89	3			x						x	x					50mm				
4194	j	265	287	323	90	3	x							x		x									
4208	j	224	246	282	78	2	x				>2			x			x				500mm				
4271	j	251	273	309	85	?	x				>1				x		x				100mm				
4359	j	86	108	144	76	3		x						x		x									
4389	j	206	228	264	76	?	x				>1			x		x									
4429	j	222	244	280	82	2	x							x		x					>300mm				
4490	j	220	242	278	84	2	x				>1			x		x					>300mm				
4738	j	76	98	134	82	3		x						x		x									

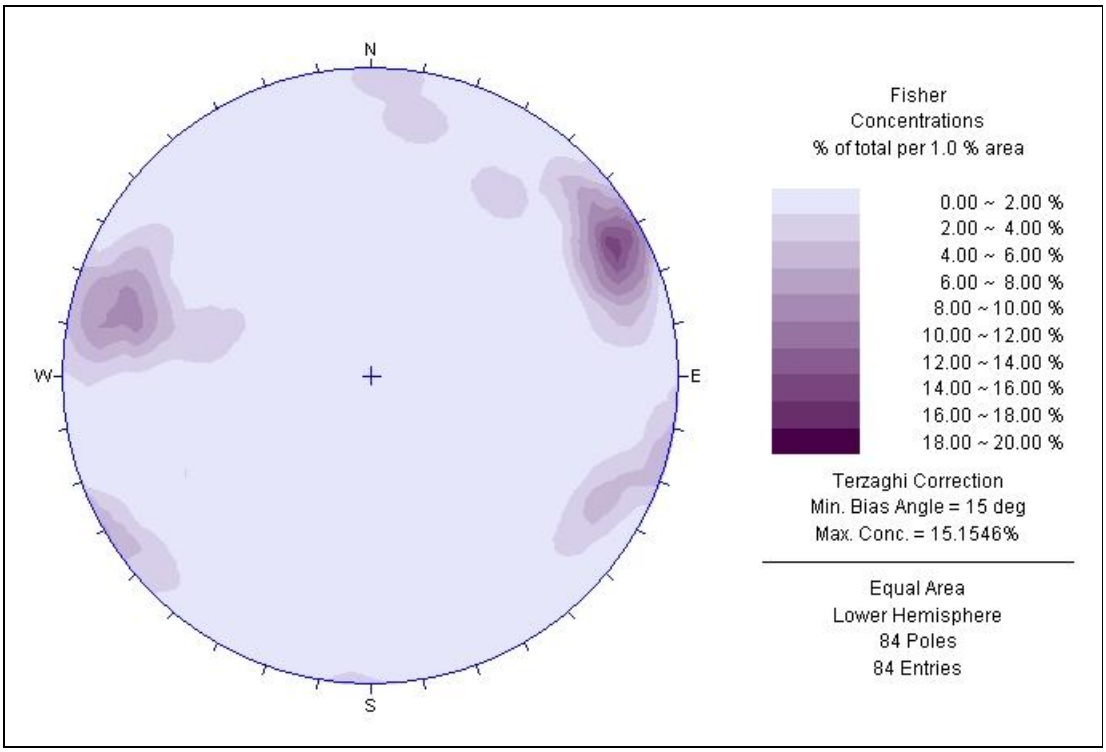

Scanline 11 Contour Plot – Pole Density Distribution

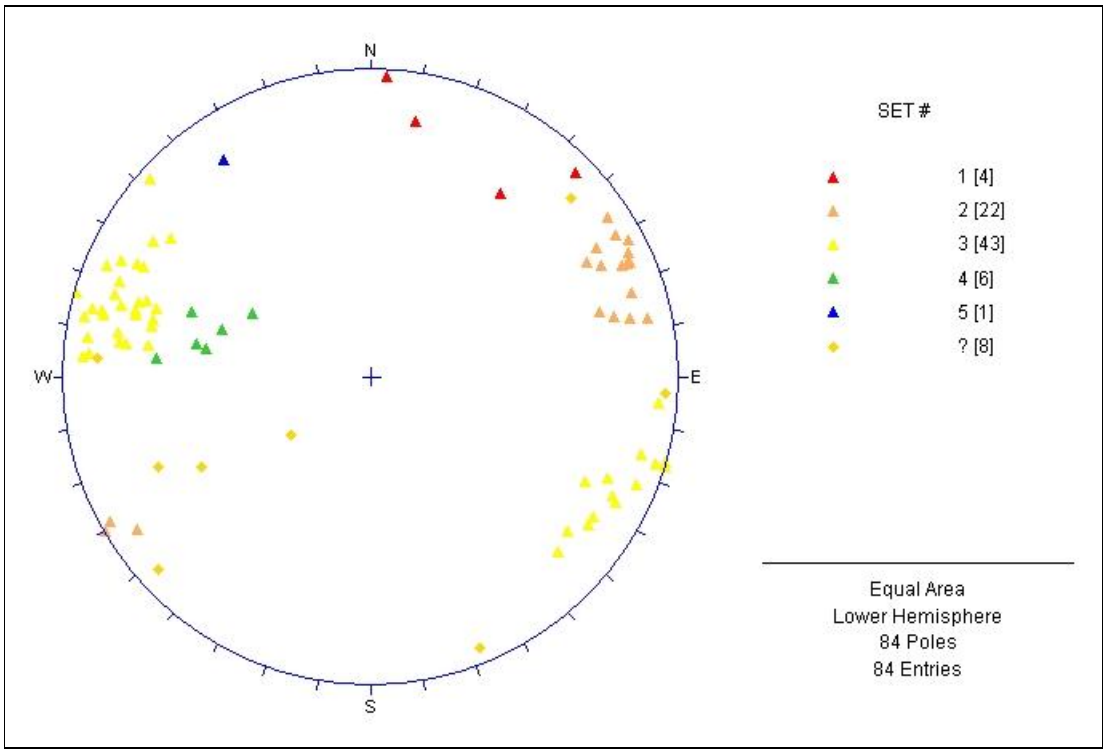

Scanline 11 Scatter Plot – Joint Sets

Distance along	Defect	Dip	Corrected	Correlated	Dip	Set #	Hardness						Persis	Aperture	Roughness					Spacing (mm)				Infill Thick~		Fracture	Notes
Datum (cm)	type	Direction	D/D	D/D			vh	h	mh	m	s	vs	tence (m)	(mm)	vr	r	sr	sm	sl	< .1	.1-1	1-5*	>5	ness (mm)	Discription	Spacing (mm)	
#12													<1 unless otherwise stated														
60	Contact with GG																										
262		282	304	340	77	3		x					>1				x				x						
281		97	119	155	84	3		x					>1				x				x						
178		318	340	376	60	5			x							x					x						
61		321	343	379	82	5			x							x					x						
389		71	93	129	81	1		x					>1		x						x						
298		296	318	354	83	5		x								x					x						
233		154	176	212	81	5		x								x					x						
318		308	330	366	58	5			x							x					x						
343		120	142	178	31	4		x									x				x						
411		131	153	189	28	4		x									x				x						
502		275	297	333	86	3		x									x					x		2mm	staining		iron staining on joint surfaces
392		323	345	381	64	5		x									x				x						
574		106	128	164	71	3		x								x					x						
681		80	102	138	80	1		x					>2				x				x					150mm	Series of smallter fractures further along stri
720		263	285	321	79	3			x				>2				x				x						
558		136	158	194	59	?		x								x					x						
463		172	194	230	82	1			x						x						x						Truncates #1 alternating Dip
746		274	296	332	81	3		x					>3	25mm			x				x						
754		283	305	341	80	3		x					>1				x				x						
872		270	292	328	80	3		x					>4	22mm	x						x					300-400	Major Outcrop
893		268	290	326	72	3		x					>2				x				x						
944		275	297	333	71	3		x					>2				x				x						
958		276	298	334	71	3		x					>2				x				x						
978		270	292	328	73	3		x					>2				x				x						
1006		280	302	338	79	3		x					>2			x					x						
1065		276	298	334	62	3		x					>2			x					x						
1222		254	276	312	73	6			x					>30mm			x				x						
1239		258	280	316	81	6			x								x				x					50mm	Change in composition and orientation, influenced by B/P
1264		253	275	311	76	6			x								x				x						
1282		282	304	340	72	3			x								x				x						
1311		269	291	327	82	3			x							x					x						
1378		347	9	45	86	1		x									x				x						
1378		265	287	323	86	3		x									x					x		#2	Staining	200	
1416		276	298	334	75	3		x									x				x						
1462		0	22	58	81	1		x									x				x						
1481		267	289	325	86	3		x					>3				x				x						
1487		349	11	47	87	1		x								x					x						
1628		78	100	136	79	3		x								x					x						
1620	Mixed B/P/GG			36													x				x						
1741		94	116	152	36	4		x					>2			x					x					80mm	

1741	271	293	329	72		3	x			x			x		
1644	352	14	50	83		1	x		>3		x		x		
1782	91	113	149	82		3	x		>2			x	x		
1803	87	109	145	81		3	x		>2			x	x		
1841	93	115	151	78		3	x		>2			x	x		
1868	91	113	149	80		3	x		>2			x	x		
1941	263	285	321	65		6	x		>2			x	x		
2010	272	294	330	77		3	x		>3			x	x		
1882	358	20	56	89		1	x			x				x	
2010	93	115	151	48		4	x		>1			x	x		<100
2178	57	79	115	61	?		x					x	x		
2241	262	284	320	71		3		x	>4		x		x		
2291	265	287	323	74		3		x	>1		x		x		
2384	260	282	318	63		6		x	>1		x		x		
2770	222	244	280	58		2		x	>3			x	x		
2654	265	287	323	72		3		x	>4			x		x	
2502	264	286	322	75		3		x	>1			x	x		
2520	267	289	325	68		6		x	>2			x	x		
2518	262	284	320	63		6		x	>1			x	x		<100
2468	261	283	319	56		6		x				x	x		
2458	174	196	232	84		1		x	>1			x	x		

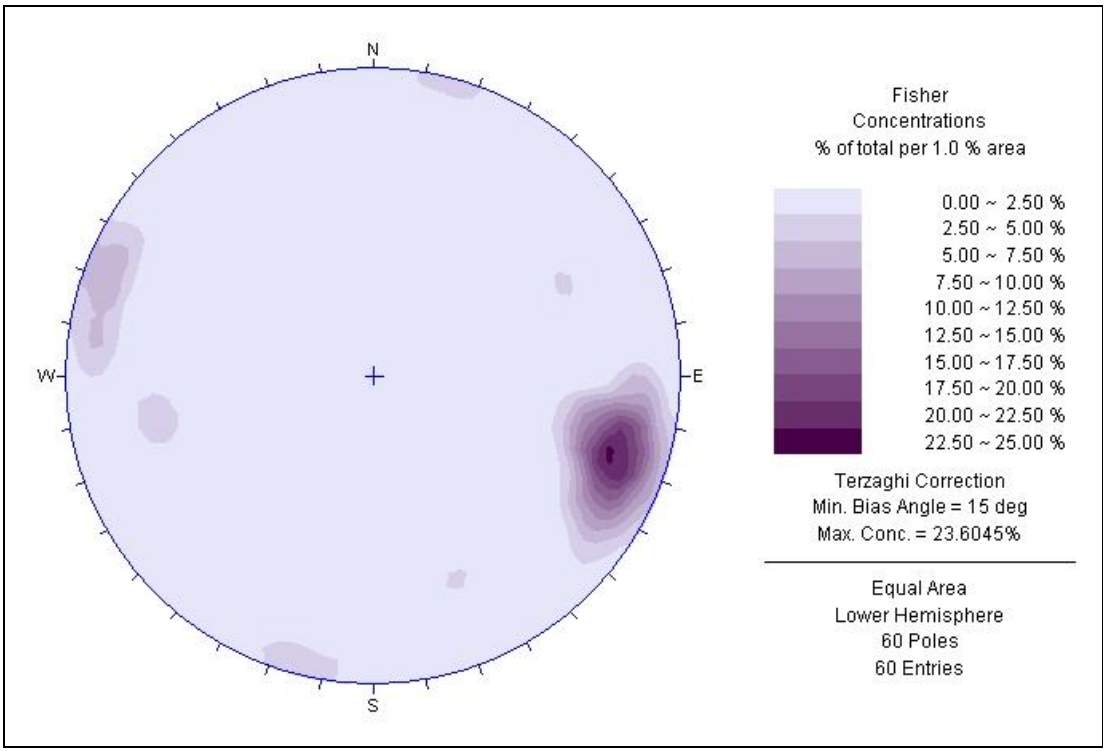

Scanline 12 Contour Plot – Pole Density Distribution

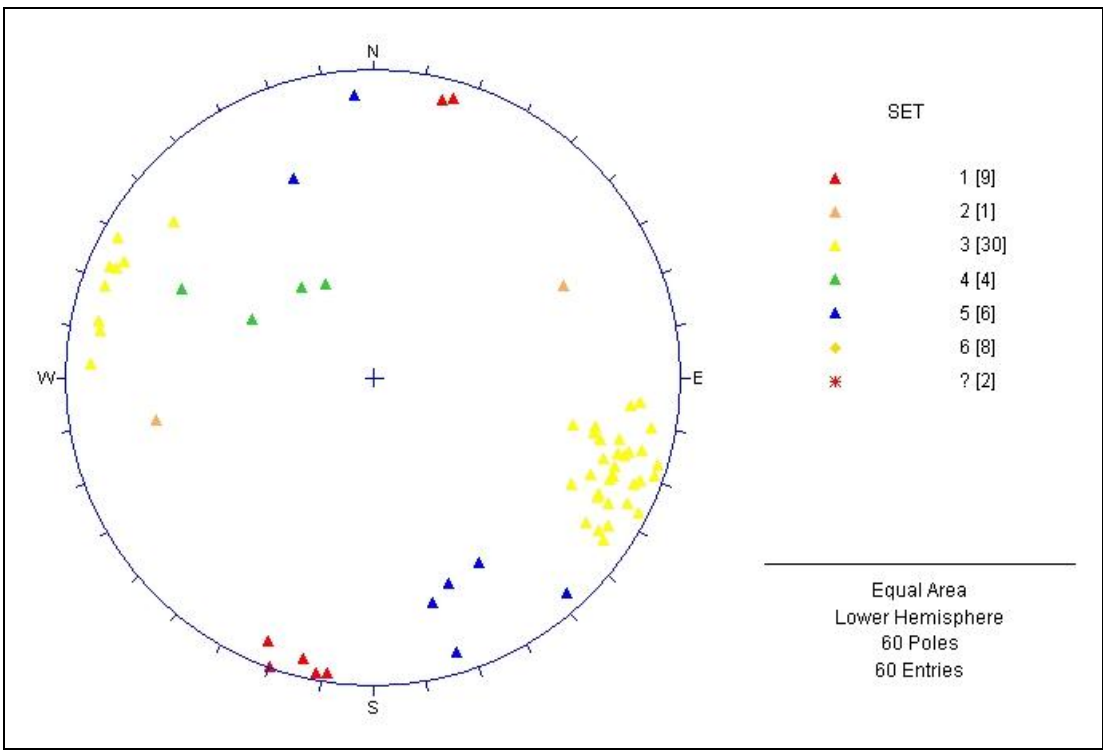

Scanline 12 Scatter Plot – Joint Sets

A3.2 Calculation of the Terzaghi Weighting Function

The geometric weighting function included in the Stereographic projection program "DIP's" version 5.050 (Hoek, 2002) is calculated the following way

When orientation measurements are made, a bias is introduced in favour of those features which are perpendicular to the direction of surveying. To illustrate this concept, three joints of identical spacing along a scanline are shown below.

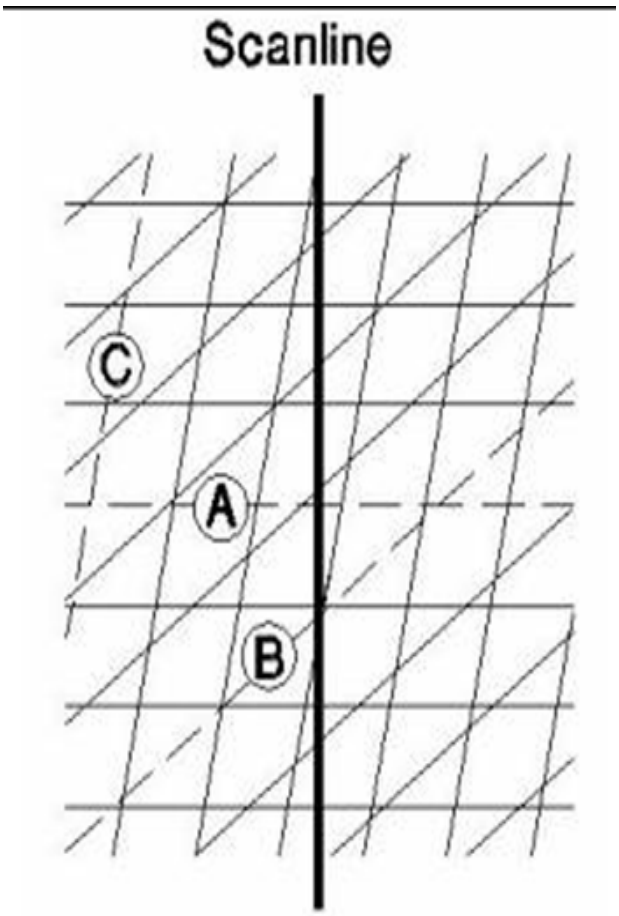

Measurements along the scanline record many more joints in Set A than in Set C, which will bias the density contour plot heavily in favour of Set A. To compensate for this bias, a geometrical weighting factor is calculated and applied to each feature measured. This weighting, W, can be applied to contour and rosette plots in DIPS, and is also used in the weighted mean vector calculations. The bias correction should only be used for planar features, and will not account properly for measurement bias in linear features such as acicular crystal fabric.

The geometric weighting factor, W, is calculated as follows:

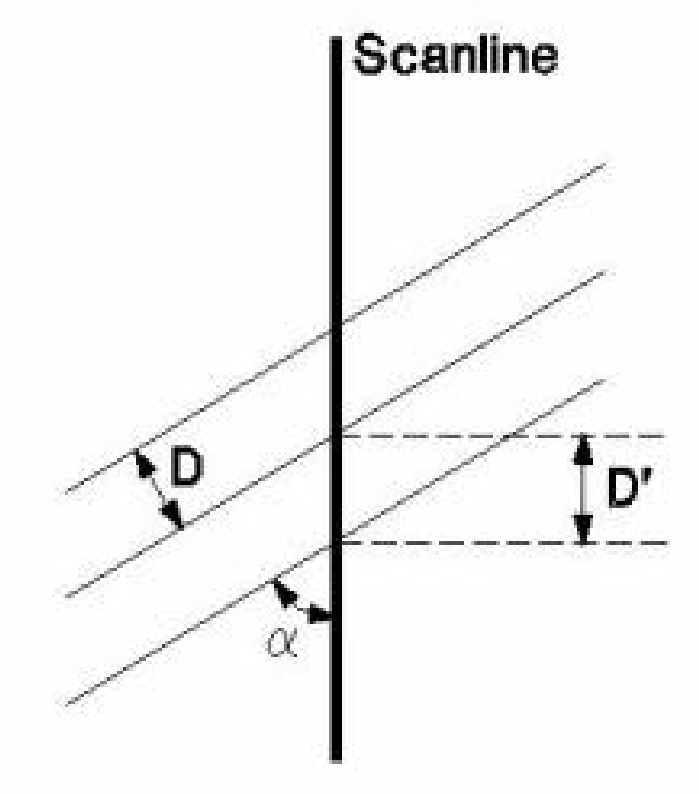

α = minimum angle between plane and traverse
D' = apparent spacing along traverse
D = D' sin α = D' (1/W) = true spacing of discontinuity set
R' = 1/D = 1/D' sin α = D' cosec α = true density of joint population
W = (1) cosec α = weighting applied to individual pole before density calculation

Since the weighting function tends to infinity as α approaches zero, a maximum limit for this weighting must be set to prevent unreasonable results. This maximum limit corresponds to a minimum angle, which can be between 0.1° and 89.9°. However, the recommended range is limited to 5° to 25°, and the default of 15° degrees being used during calculations.

APPENDIX IV

Summary of the graphical determination of kinematic failure mechanism;

Planar Failure
Toppling Failure
Wedge Failure

Section 1 – Scanline Traverses 1-6
Section 2 – Scanline Traverses 7-12

Planar Failure – Scanline 1

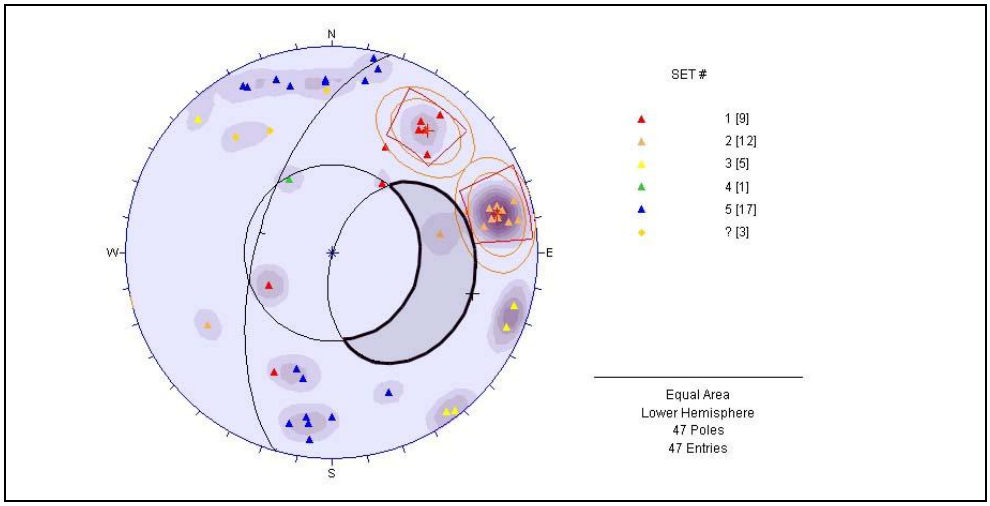

Planar Failure – Scanline 2

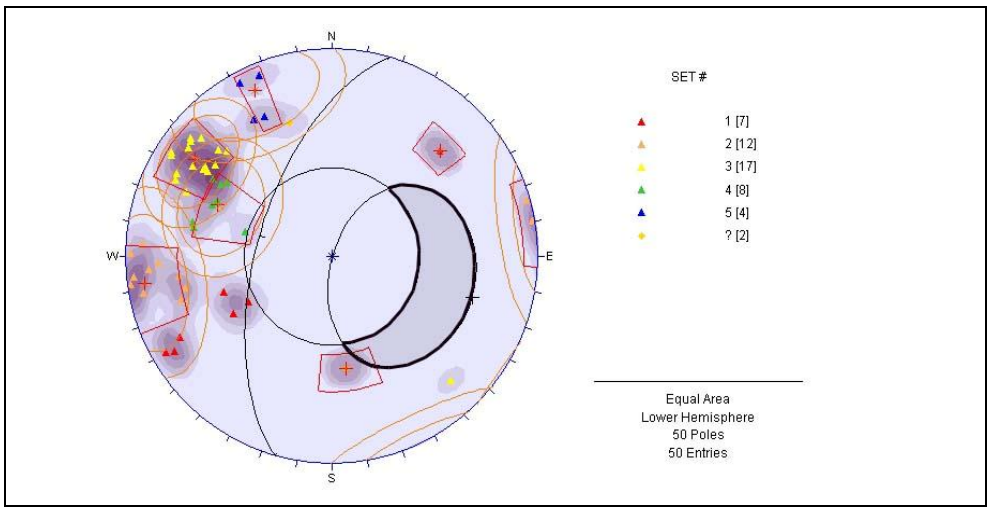

Planar Failure – Scanline 3

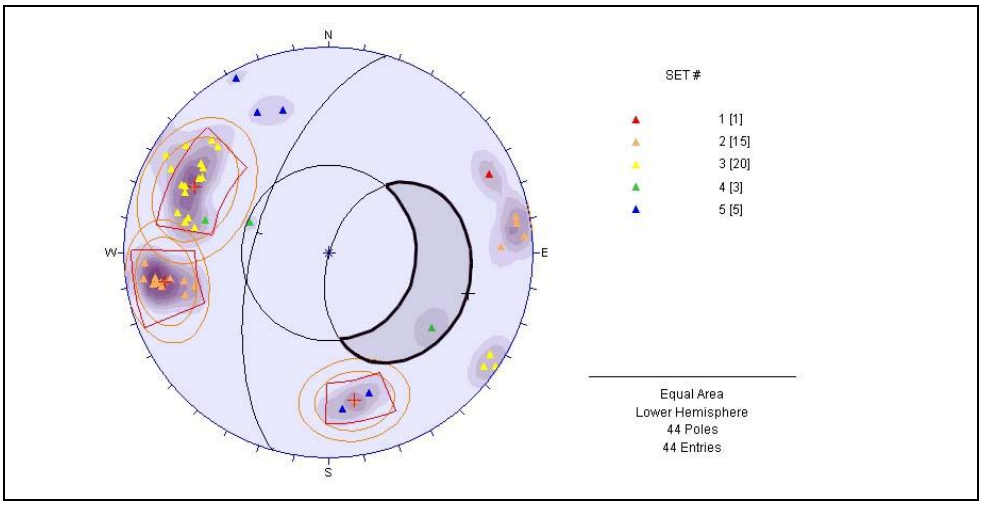

Planar Failure – Scanline 4

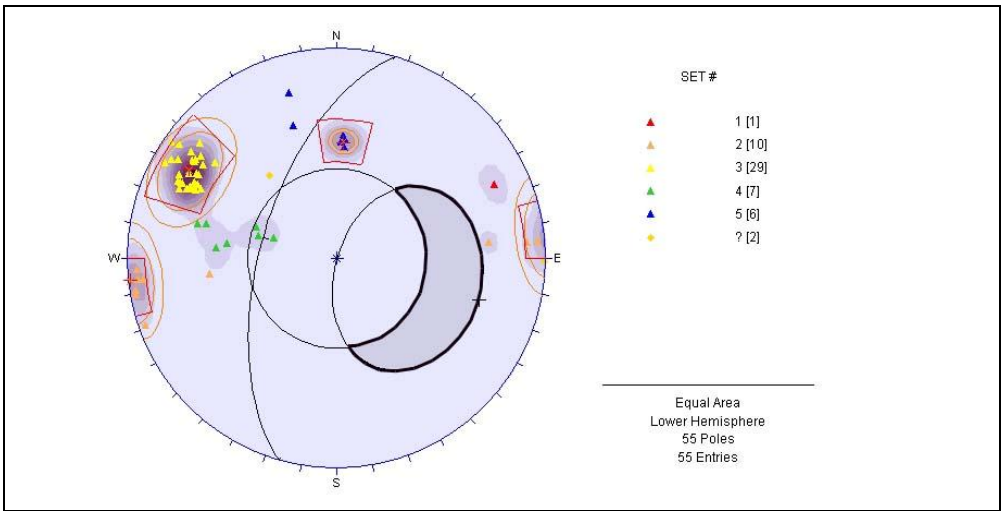

Planar Failure – Scanline 5

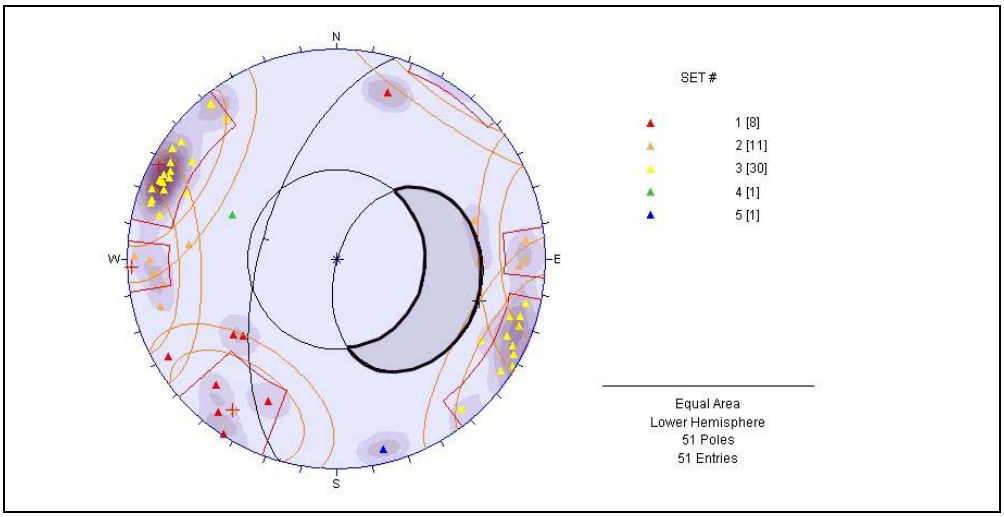

Planar Failure – Scanline 6

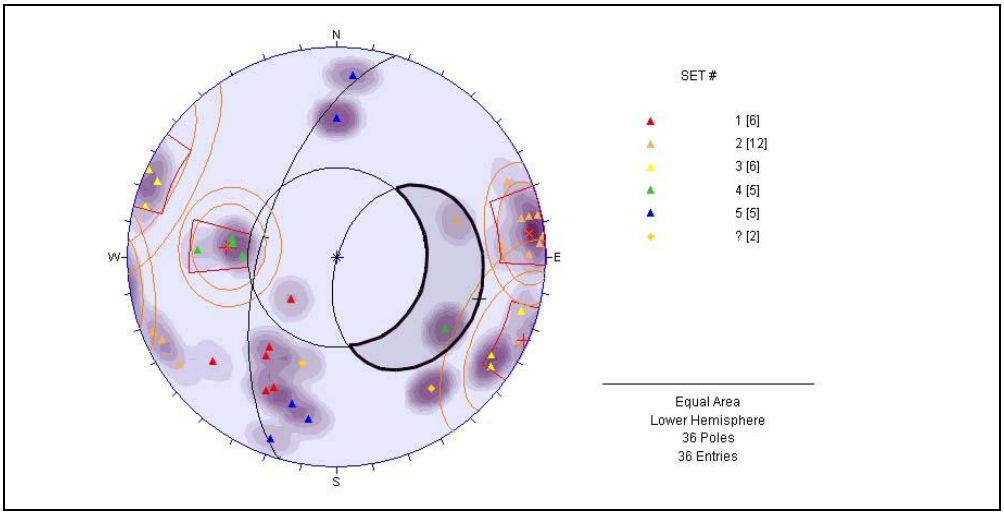

Planar Failure – Scanline 7

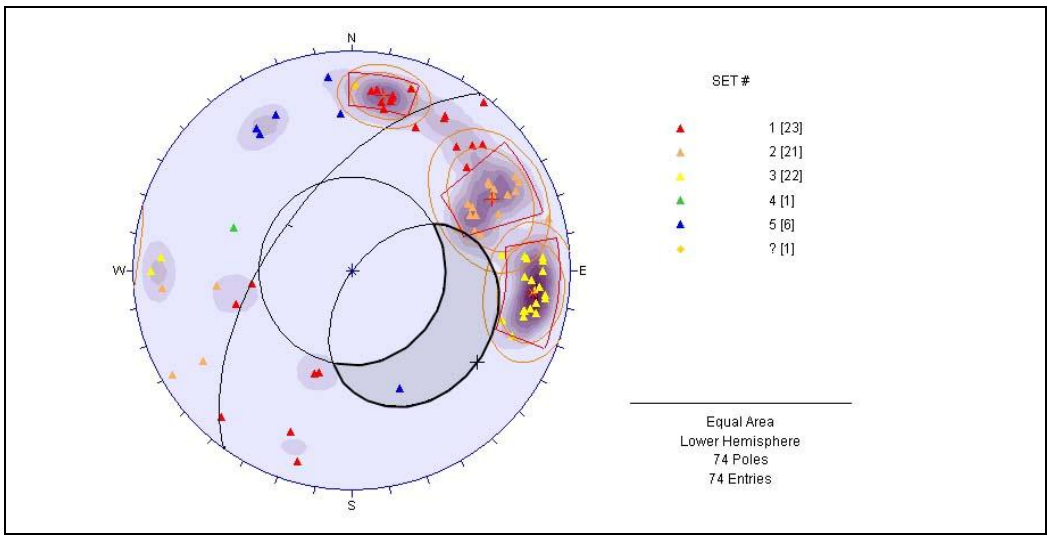

Planar Failure – Scanline 8

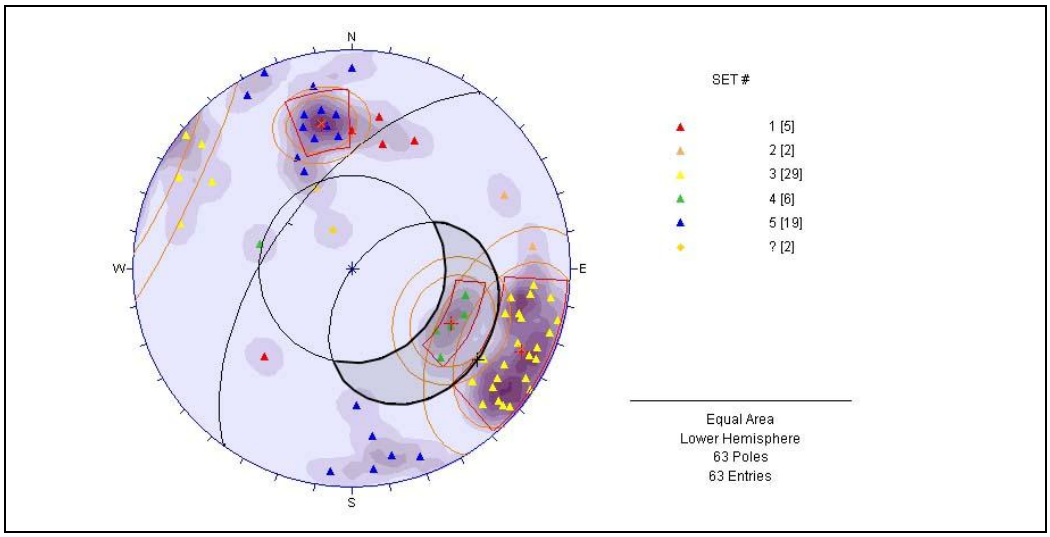

Planar Failure – Scanline 9

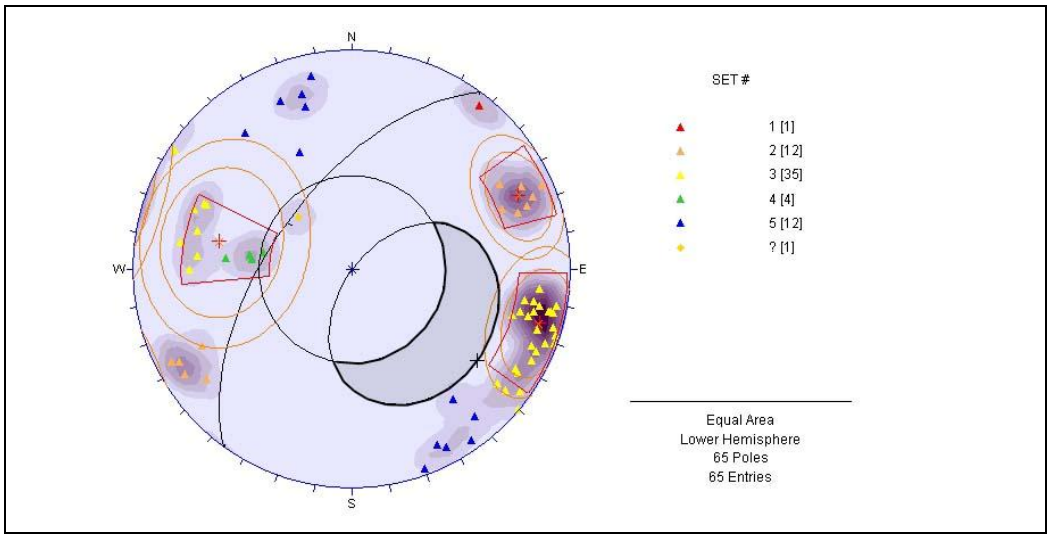

Planar Failure – Scanline 10

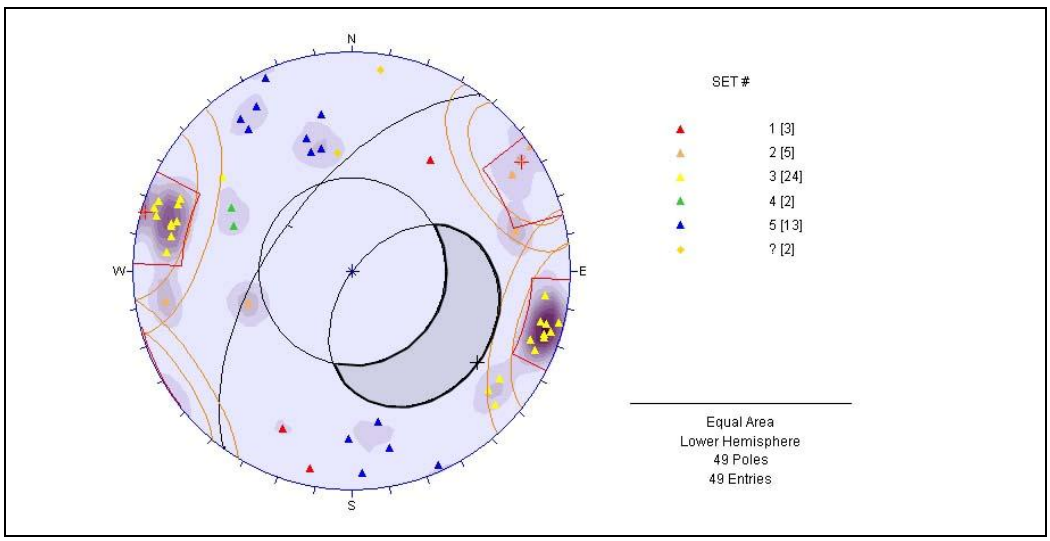

Planar Failure – Scanline 11

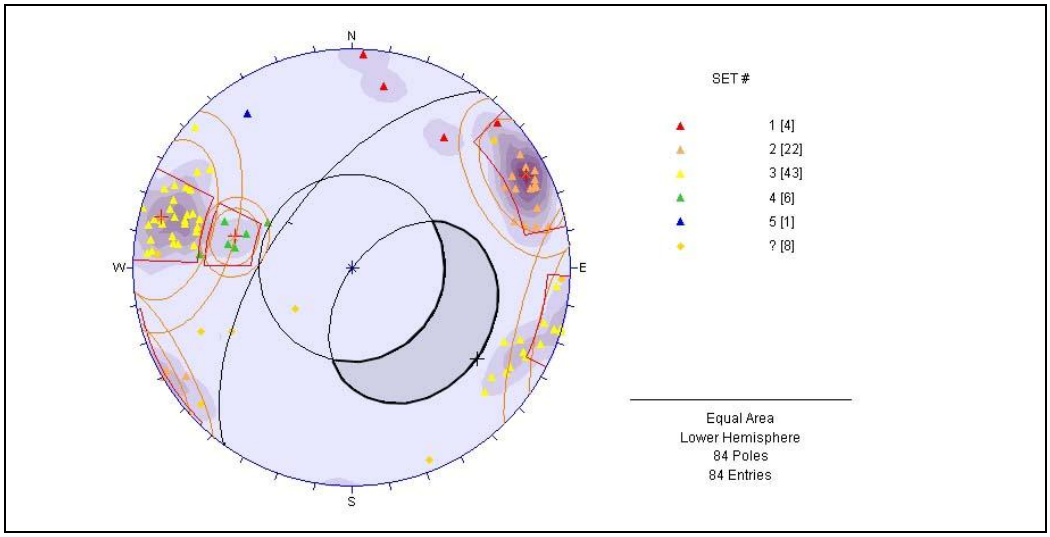

Planar Failure – Scanline 12

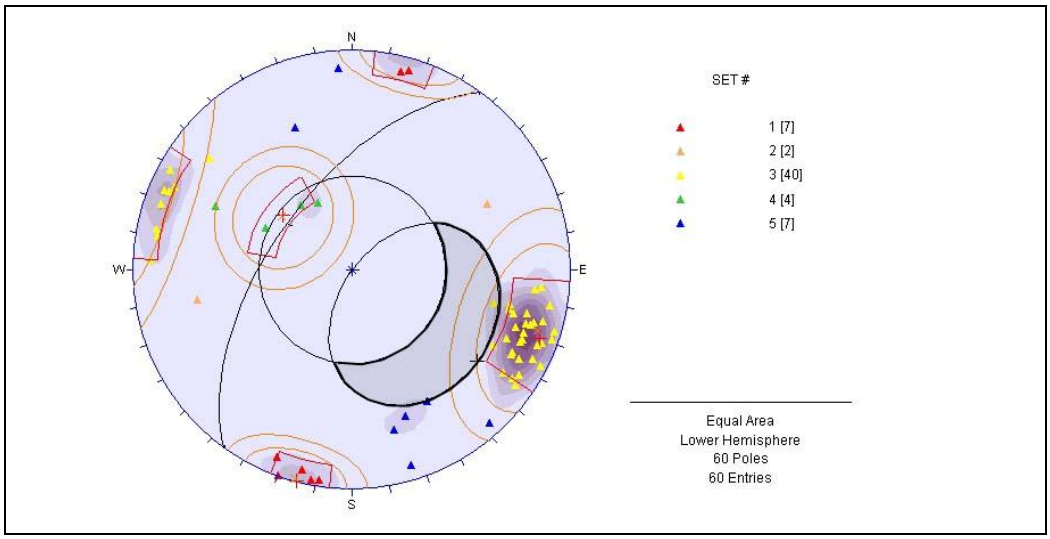

Toppling Failure – Scanline 1

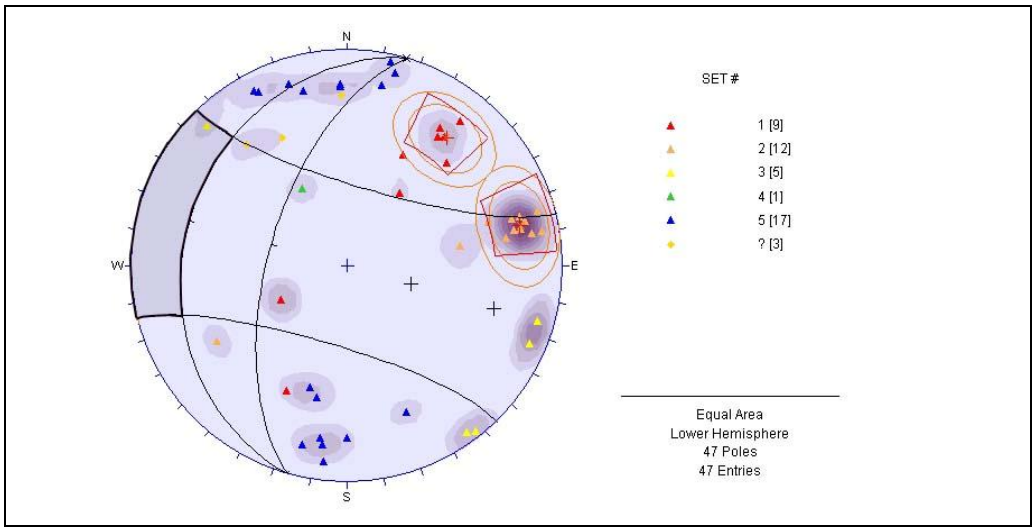

Toppling Failure – Scanline 2

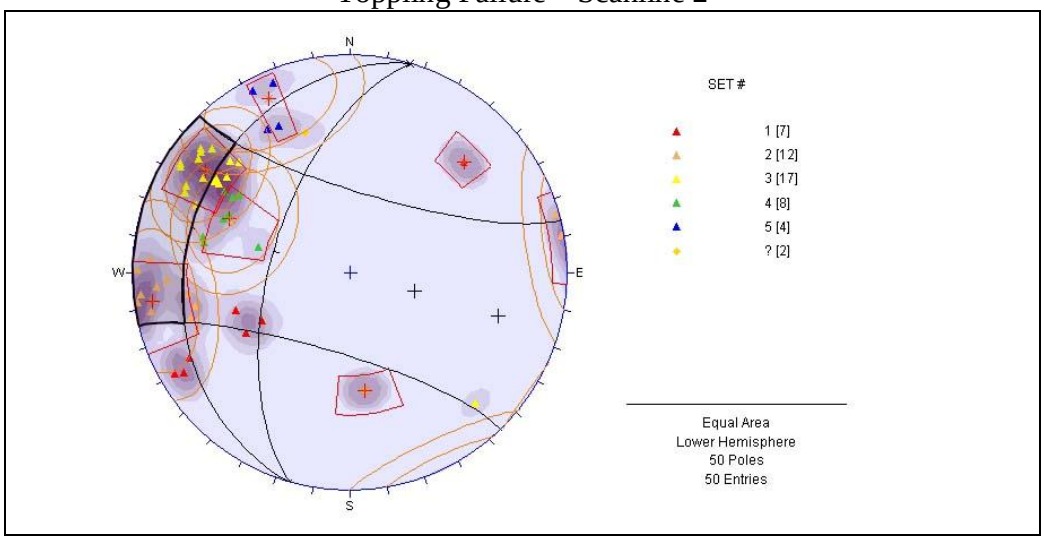

Toppling Failure – Scanline 3

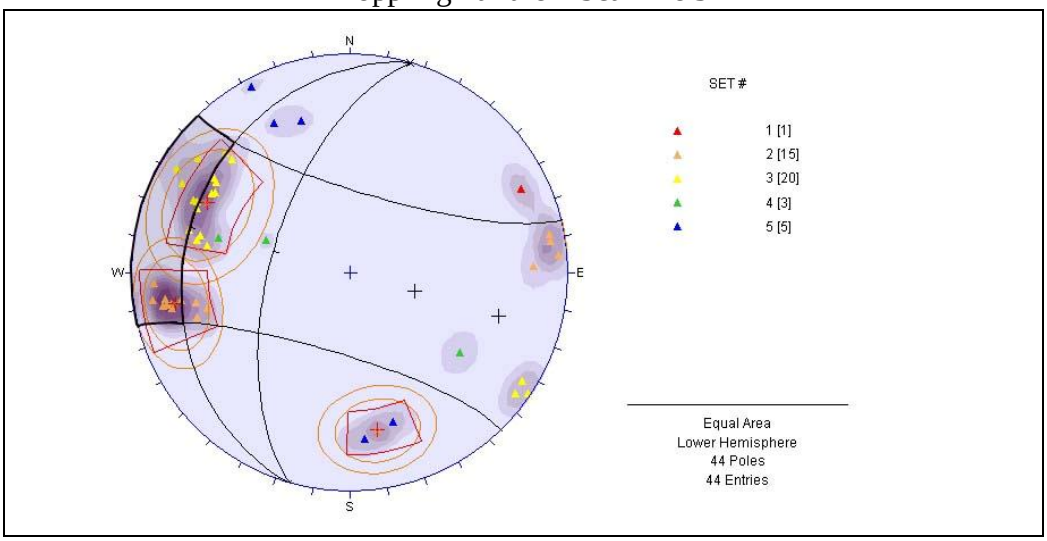

Toppling Failure – Scanline 4

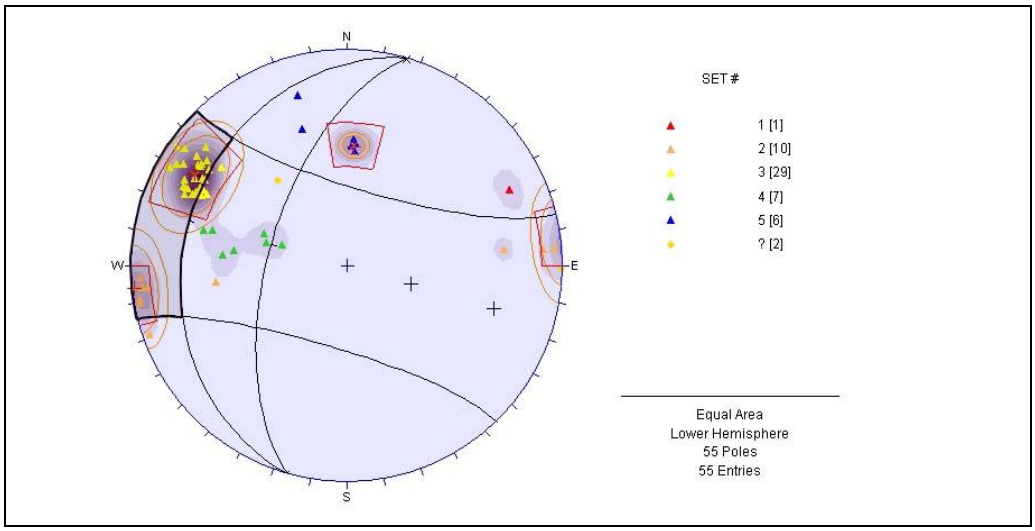

Toppling Failure – Scanline 5

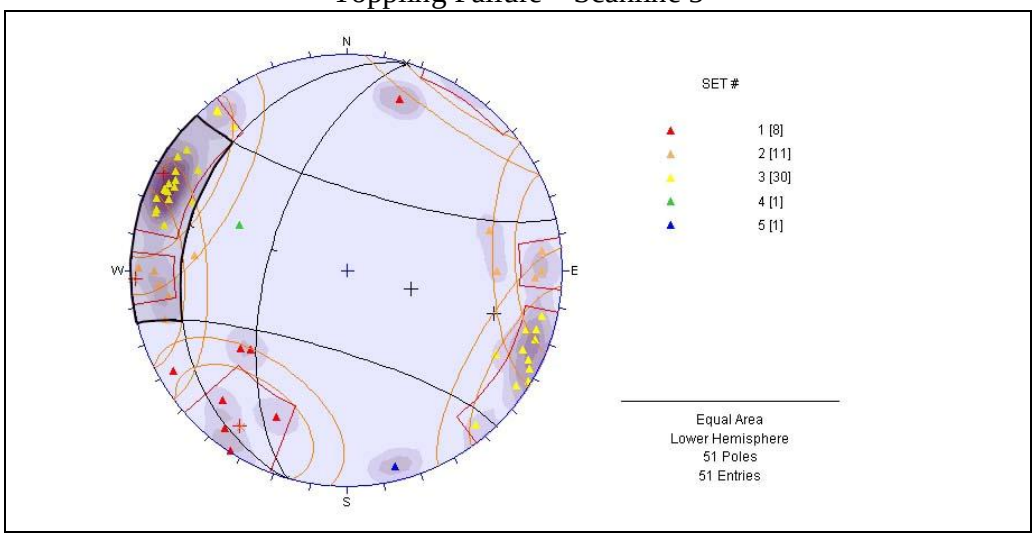

Toppling Failure – Scanline 6

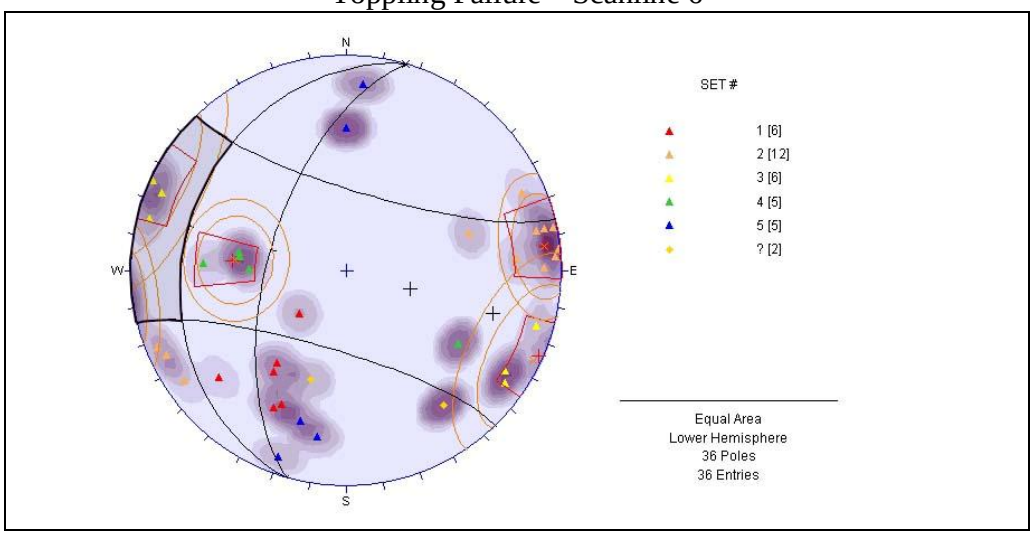

Toppling Failure – Scanline 7

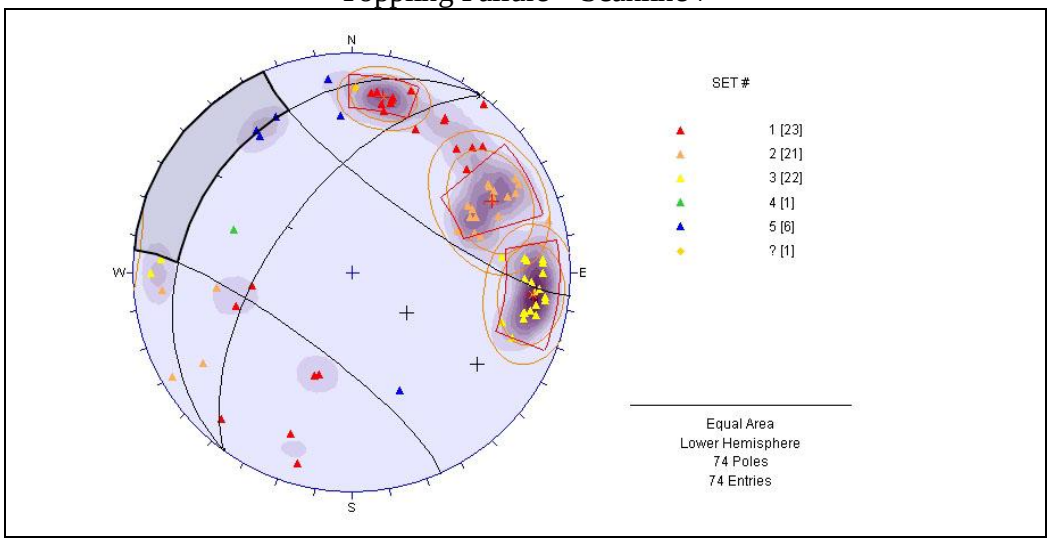

Toppling Failure – Scanline 8

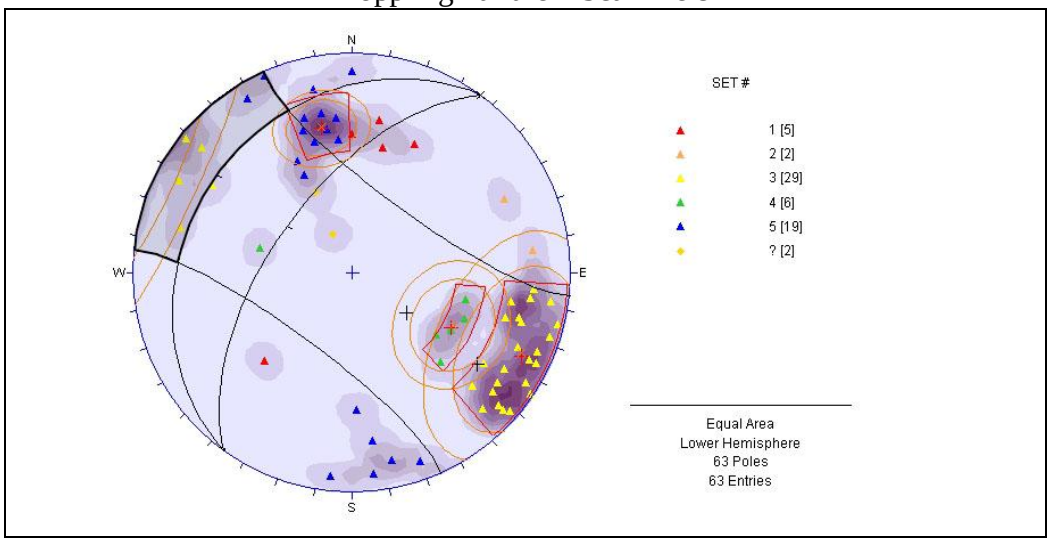

Toppling Failure – Scanline 9

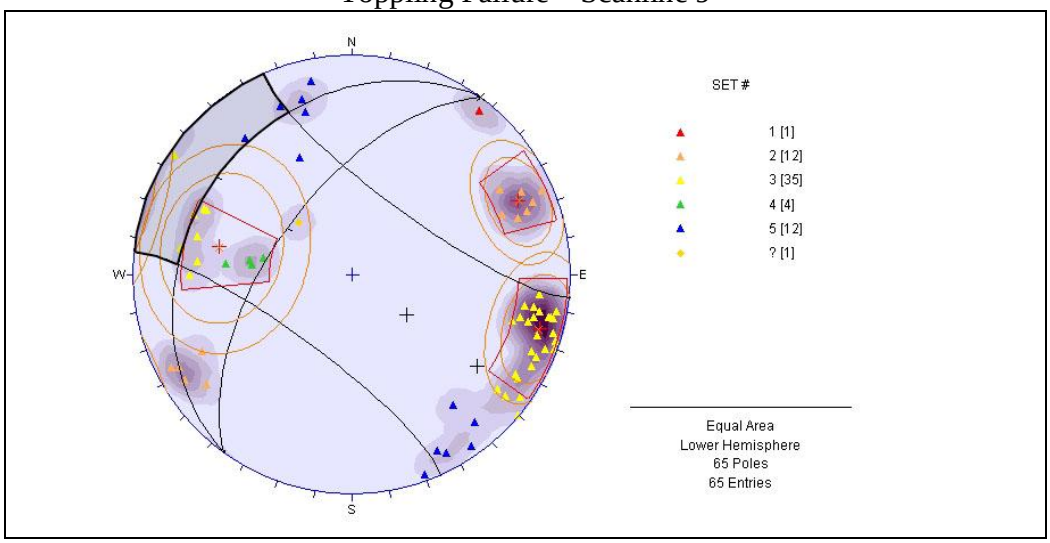

Toppling Failure – Scanline 10

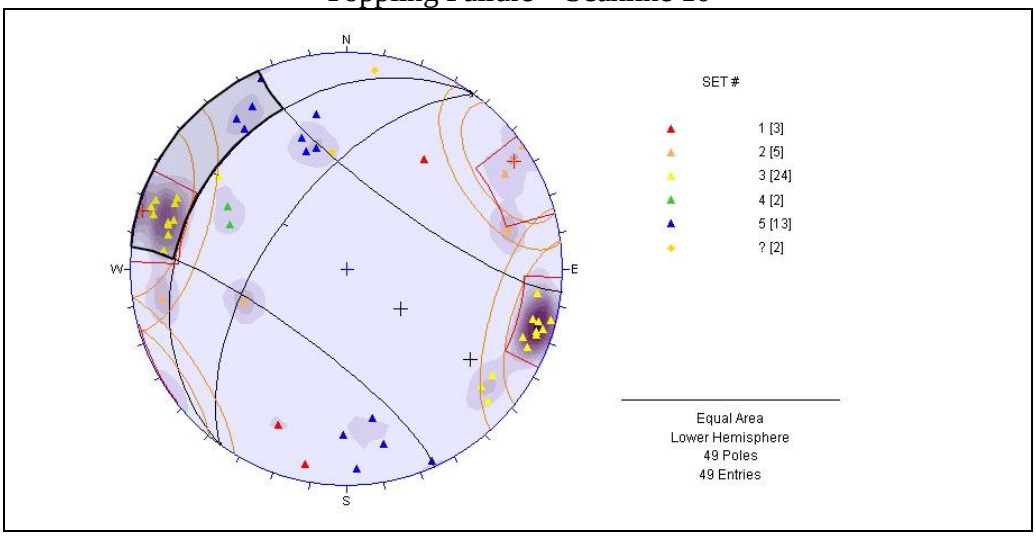

Toppling Failure – Scanline 11

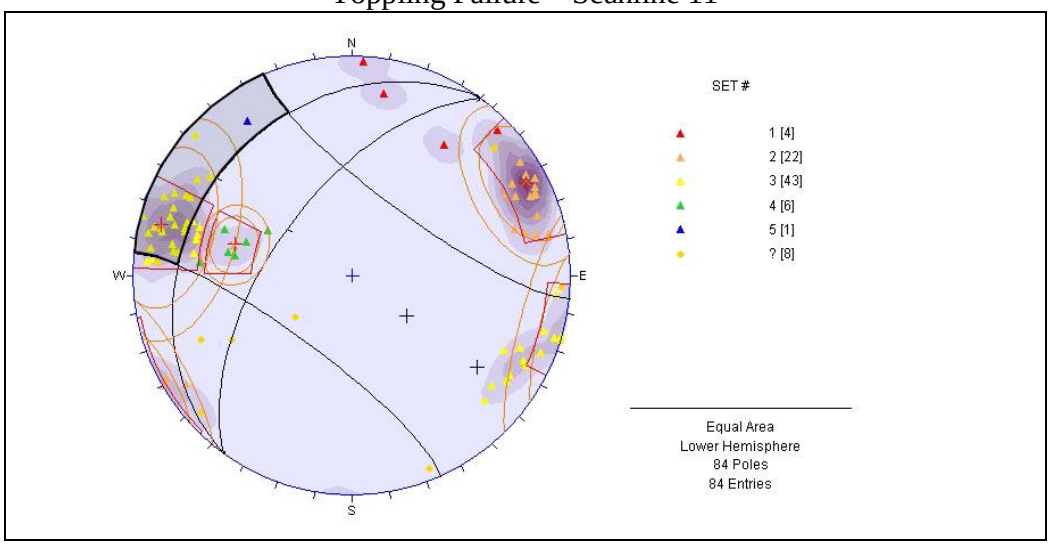

Toppling Failure – Scanline 12

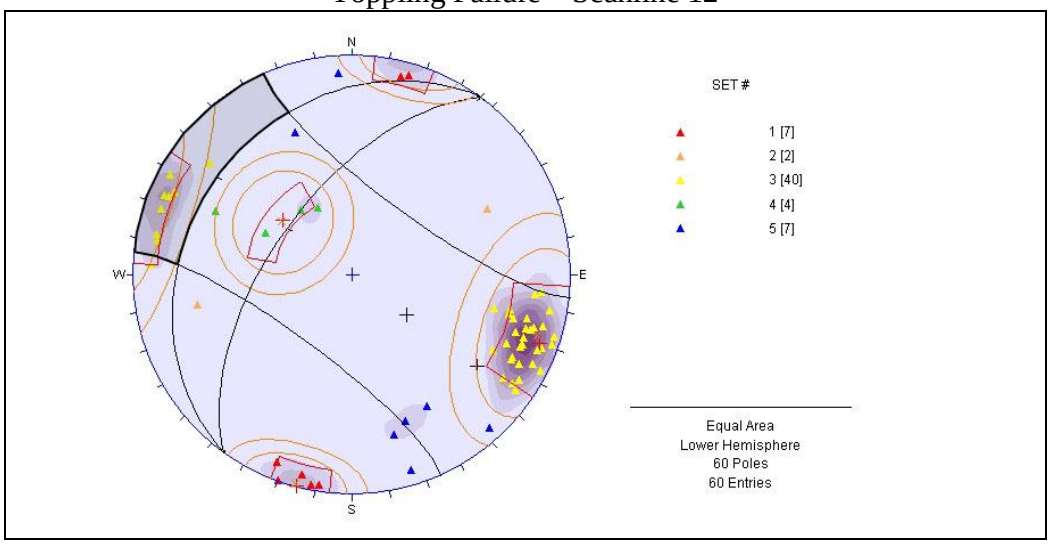

Wedge Failure – Scanline 1

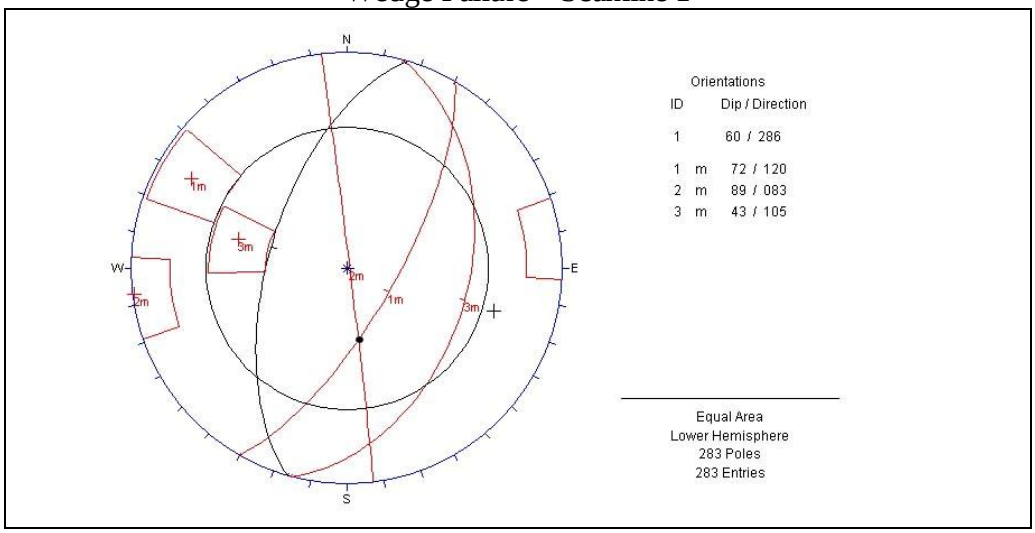

Wedge Failure – Scanline 2

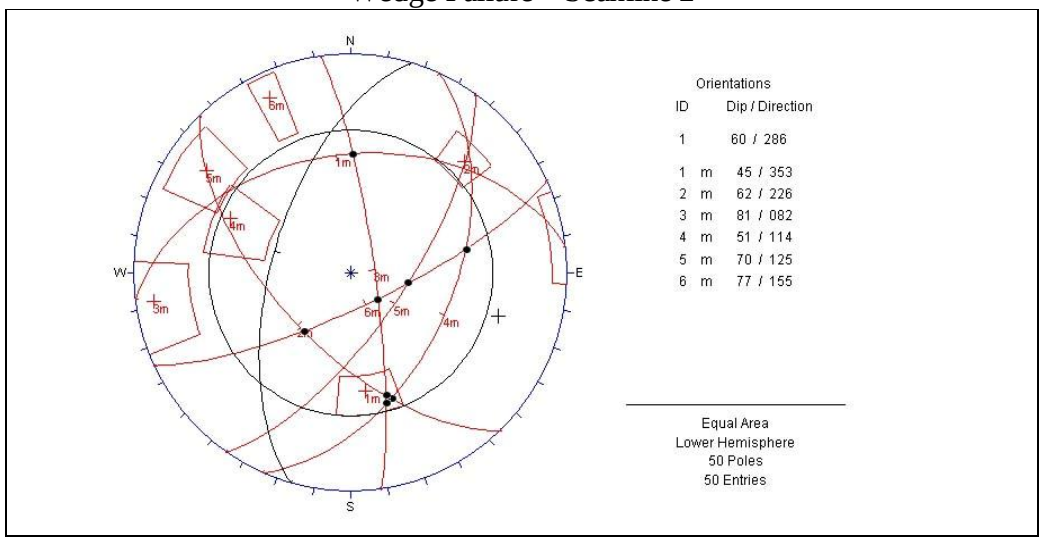

Wedge Failure – Scanline 3

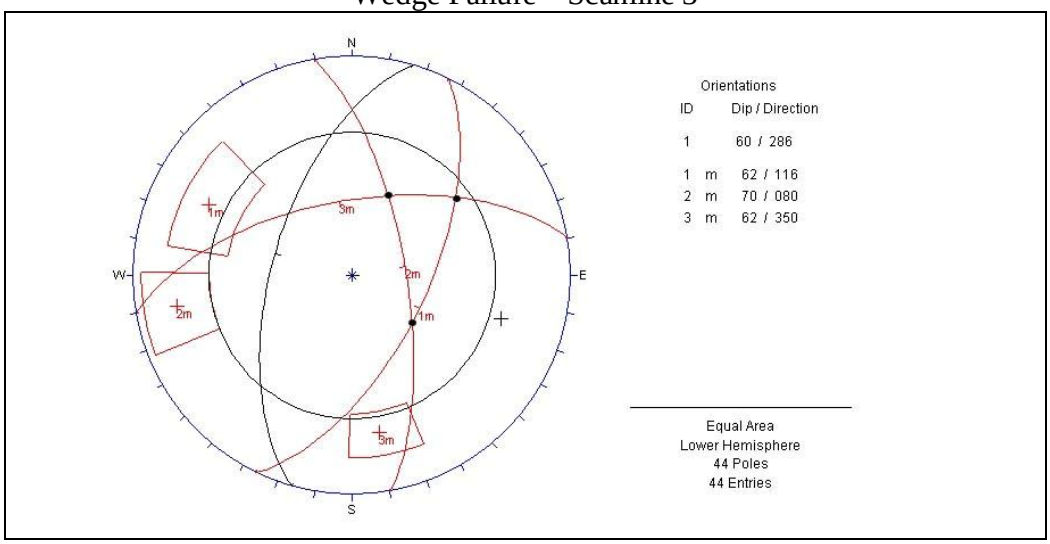

Wedge Failure – Scanline 4

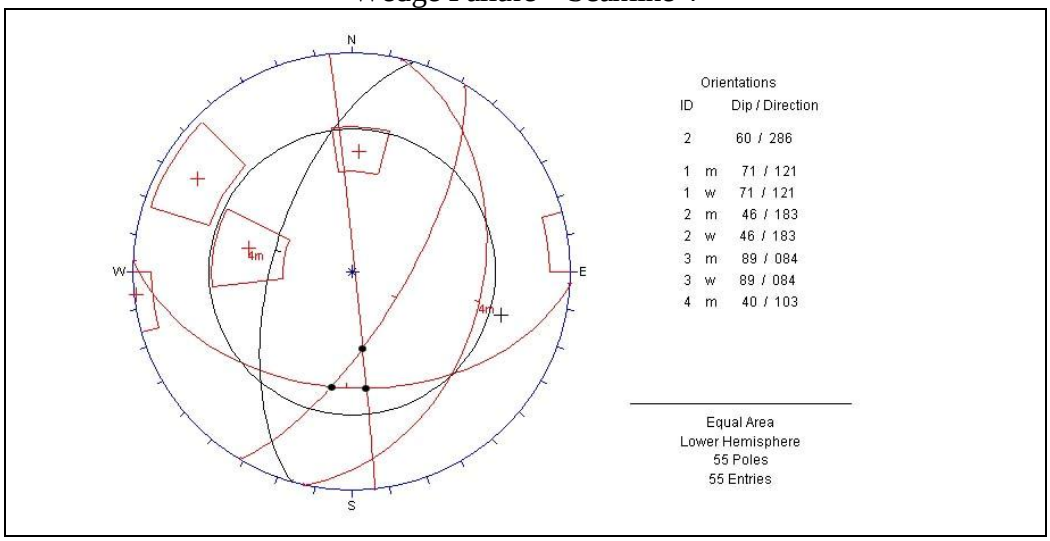

Wedge Failure – Scanline 5

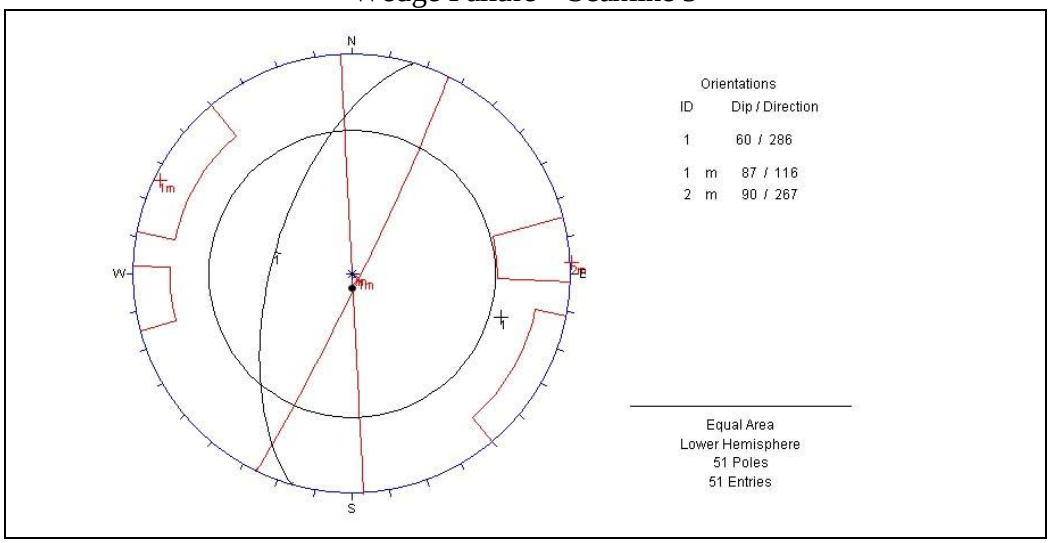

Wedge Failure – Scanline 6

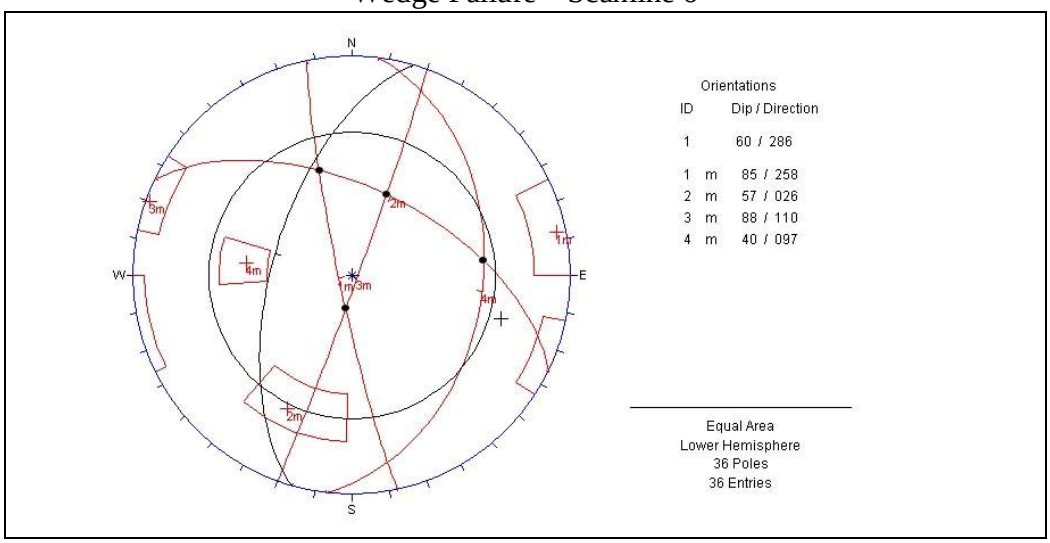

Wedge Failure – Scanline 7

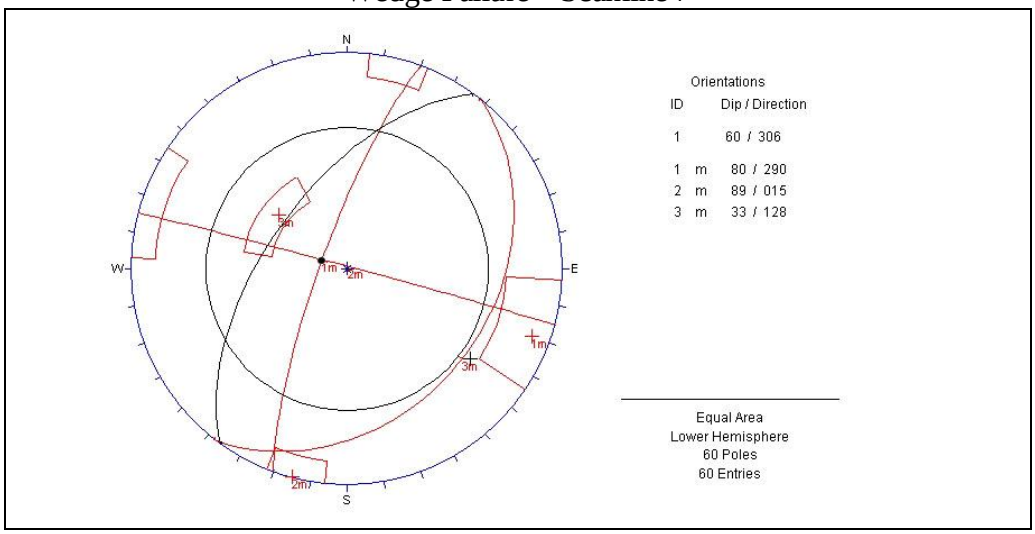

Wedge Failure – Scanline 8

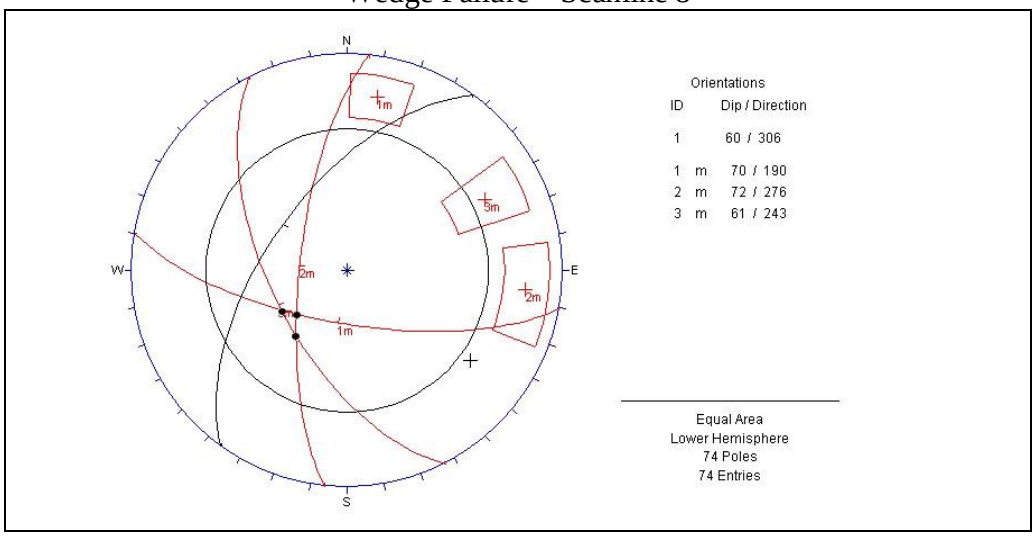

Wedge Failure – Scanline 9

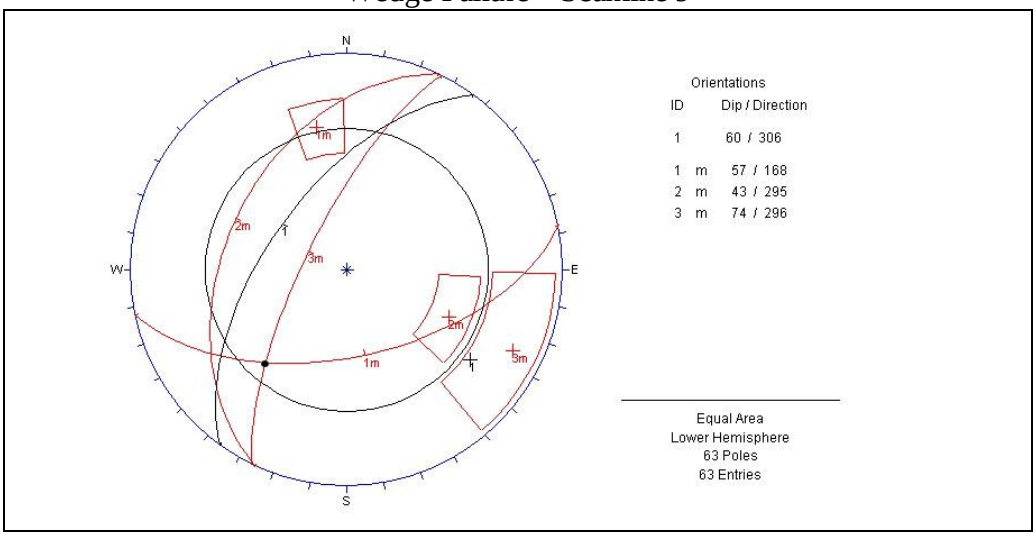

Wedge Failure – Scanline 10

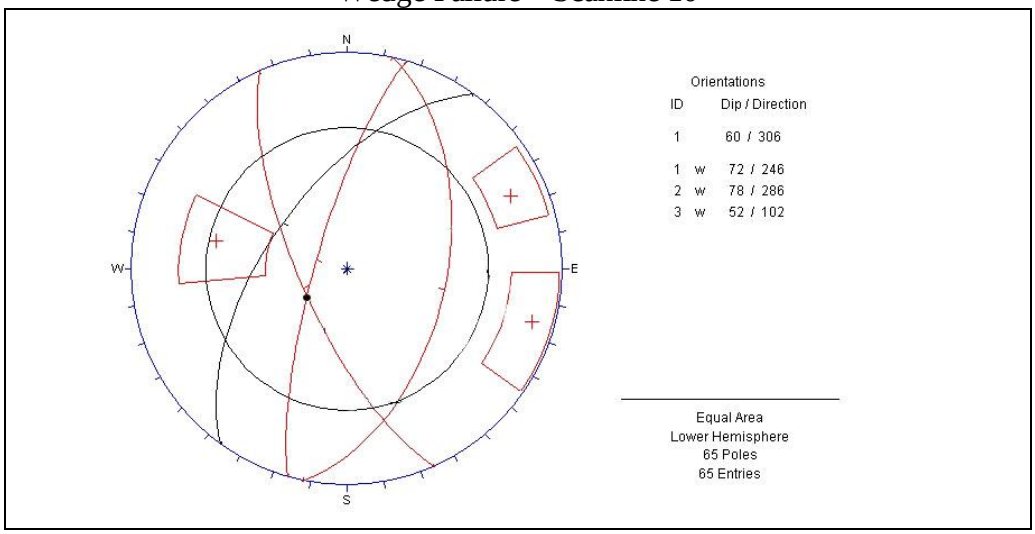

Wedge Failure – Scanline 11

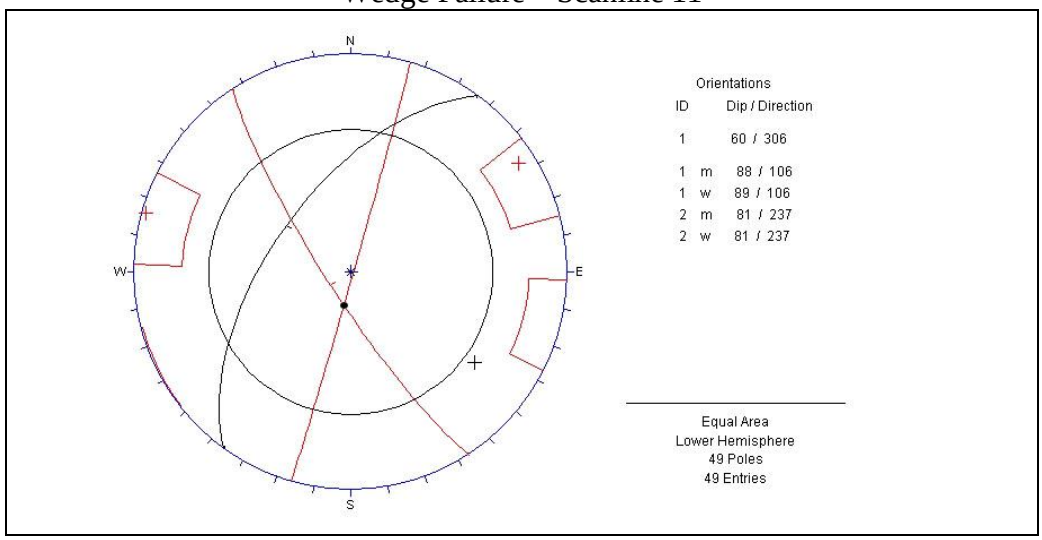

Wedge Failure – Scanline 12

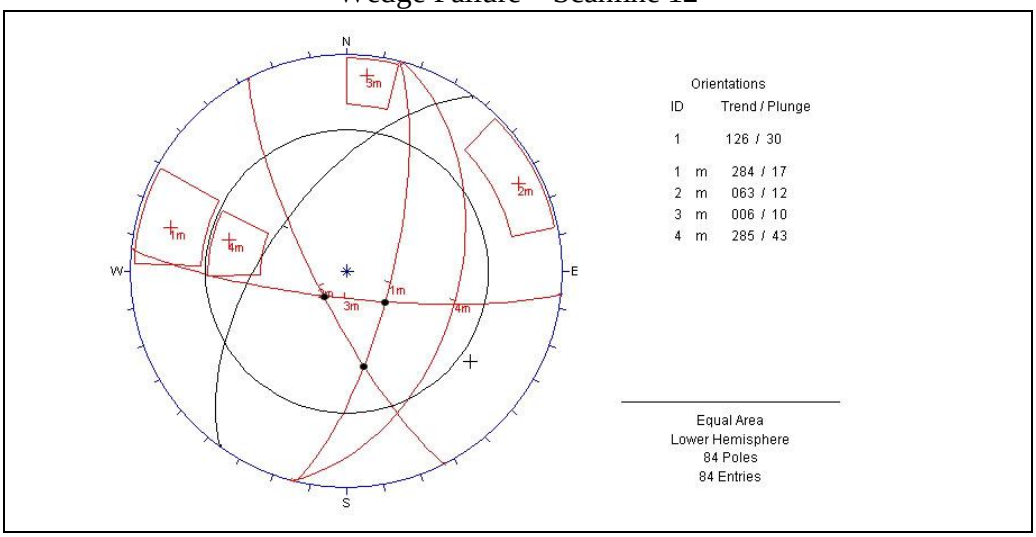

APPENDIX V

Provided in this appendix is a summary of the five exploratory drillhole logs commissioned during the duration of this project. Also provided are the full lithological and geotechnical logs for the following drill holes:-

- DH 1694
- DH 1697
- DH 1698
- DH 1715
- DH 1717

All Drillholes were logged by Adrian Field (geologist).

DH1694

BULLER COALFIELD

UPPER WAIMANGAROA PROJECT

Drillhole Number:	1694		
Location:	Cypress North Opencast		
Grid Reference:	326018.44 mE	711019.46 mN	
Surface Level:	711.46 m		
Total Depth:	82.50 m		
Period Drilled:	8/5/03 – 19/5/03		
Driller:	Alton Drilling Ltd	Drill Rig:	CS 1000
Logged By:	ABF		
Drilling Procedure:	Hole wash drilled in P size from ground surface through soft, weathered Kaiata Mudstone to 30.00 m, then cored in HQ size to TD.		
Drilling Fluid:	"Drill Pro" polymer fluid additive, to assist core recovery.		
Geophysical Sondes:	None run.		

Summary of Intersected Formations:

FORMATION	DEPTH FM	DEPTH TO	THICKNESS	R.L. TOP
Kaiata Mudstone	0	67.30	67.30	711.46
Brunner Coal Measures	67.30	82.50	15.20	644.16
Coal Seam	73.66	*78.35	*4.69	637.80
McKay Fault	79.30	79.90	0.60	632.16

* Coal seam floor faulted

Overburden Thickness: 73.66m

Downhole Ratio: 15.7

Remarks: Geotechnical and coal sampling hole.
VW piezometers set at 49.90 and 69.80 m b.g.l.
Coal seam thinned by faulting and only upper portion of seam present in this DH.

DH1697

BULLER COALFIELD

UPPER WAIMANGAROA PROJECT

Drillhole Number:	1697		
Location:	Cypress North Opencast		
Grid Reference:	326199.40 mE	711787.02 mN	
Surface Level:	767.12 m		
Total Depth:	98.00 m		
Period Drilled:	9/6/03 – 19/6/03		
Driller:	Alton Drilling Ltd	Drill Rig:	CS 1000
Logged By:	ABF		
Drilling Procedure:	Hole wash drilled in P size and cased in HW from ground surface through weathered basement granites to 19.70 m, then cored in HQ size through basement rock, [Berlins Porphyry (quartz-orthoclase-muscovite granite) and Hornfels Greenland Group] to TD.		
Drilling Fluid:	"Drill Pro" polymer fluid additive, to assist core recovery.		
Geophysical Sondes:	None run.		

Summary of Intersected Formations:

FORMATION	DEPTH FM	DEPTH TO	THICKNESS	R.L. TOP
Basement	0	98.00	98.00	767.12
Coal Seam	none			

Overburden Thickness:	N/A
Downhole Ratio:	N/A
Remarks:	Geotechnical hole drilled entirely in basement rock. VW piezometers installed and set at 47.70 and 94.90m b.g.l.

DH1698

BULLER COALFIELD

UPPER WAIMANGAROA PROJECT

Drillhole Number:	1698		
Location:	Cypress North Opencast		
Grid Reference:	326053.61 mE	711337.94 mN	
Surface Level:	799.11 m		
Total Depth:	120.10 m		
Period Drilled:	30/6/03 – 14/7/03		
Driller:	Alton Drilling Ltd	Drill Rig:	CS 1000
Logged By:	ABF		
Drilling Procedure:	Hole wash drilled in P size and cased in HW from ground surface through weathered basement granites to 20.00 m, then cored in HQ size through basement rock, [Berlins Porphyry and Hornfels Greenland Group], to TD.		
Drilling Fluid:	"Drill Pro" polymer fluid additive, to assist core recovery.		
Geophysical Sondes:	None run.		

Summary of Intersected Formations:

FORMATION	DEPTH FM	DEPTH TO	THICKNESS	R.L. TOP
Basement	0	120.10	120.10	799.11
Coal Seam	none			

Overburden Thickness: N/A

Downhole Ratio: N/A

Remarks: Geotechnical hole drilled entirely in basement rock;
VW piezometer set at 115.0m b.g.l.
Error made while grouting hole and HQ rods remain grouted in to 67m b.g.l.

DH1715

BULLER COALFIELD

UPPER WAIMANGAROA PROJECT

Drillhole Number:	1715		
Location:	Cypress North Opencast		
Grid Reference:	325814.92 mE	711106.19 mN	
Surface Level:	815.80 m		
Total Depth:	120.10 m		
Period Drilled:	30/7/03 - 3/8/03		
Driller:	Alton Drilling Ltd	Drill Rig:	CS 1000
Logged By:	ABF		
Drilling Procedure:	Hole wash drilled in P size and cased in HW from ground surface through weathered basement to 30.00 m, then cored in HQ size through basement rock, (Berlins Porphyry and hornfels Greenland Group), to TD.		
Drilling Fluid:	"Drill Pro" polymer fluid additive, to assist core recovery.		
Geophysical Sondes:	None run.		

Summary of Intersected Formations:

FORMATION	DEPTH FM	DEPTH TO	THICKNESS	R.L. TOP
Basement	0	126.90	126.90	815.80
Coal Seam	none			

Overburden Thickness:	N/A
Downhole Ratio:	N/A
Remarks:	Geotechnical hole drilled entirely in weathered and fractured basement rock.. VW piezometers installed at 63.05m and 124.00m b.g.l.

DH1717

BULLER COALFIELD

UPPER WAIMANGAROA PROJECT

Drillhole Number: 1717

Location: Cypress North Opencast

Grid Reference: 325662.89 mE 711236.50 mN

Surface Level: 752.78 m

Total Depth: 123.70 m

Period Drilled: 9/8/03 - 17/8/03

Driller: Alton Drilling Ltd Drill Rig: CS 1000

Logged By: ABF

Drilling Procedure: Hole wash drilled in P size and cased in HW from ground surface through fault zone to 5.50 m, then cored in HQ size through fault pug, Kaiata Mudstone and Brunner Coal Measures to TD.

Drilling Fluid: "Drill Pro" polymer fluid additive, to assist core recovery.

Geophysical Sondes: None run.

Summary of Intersected Formations:

FORMATION	DEPTH FM	DEPTH TO	THICKNESS	R.L. TOP
Weathered Basement	0	7.10	7.10	752.78
Mt William Fault	7.10	11.50	4.40	745.68
Kaiata Mudstone	11.50	96.04	84.54	741.28
Brunner Coal Measures	96.04	123.7	27.66	656.74
Coal Seam M3	107.05	107.88	0.83	645.73
Coal Seam	108.50	120.65	12.15	644.28

Overburden Thickness: 108.50m

Downhole Ratio: 8.9

Remarks: Geotechnical hole drilled through Mt William Fault zone.
VW piezometers installed at 69.05m and 104.10m b.g.l.

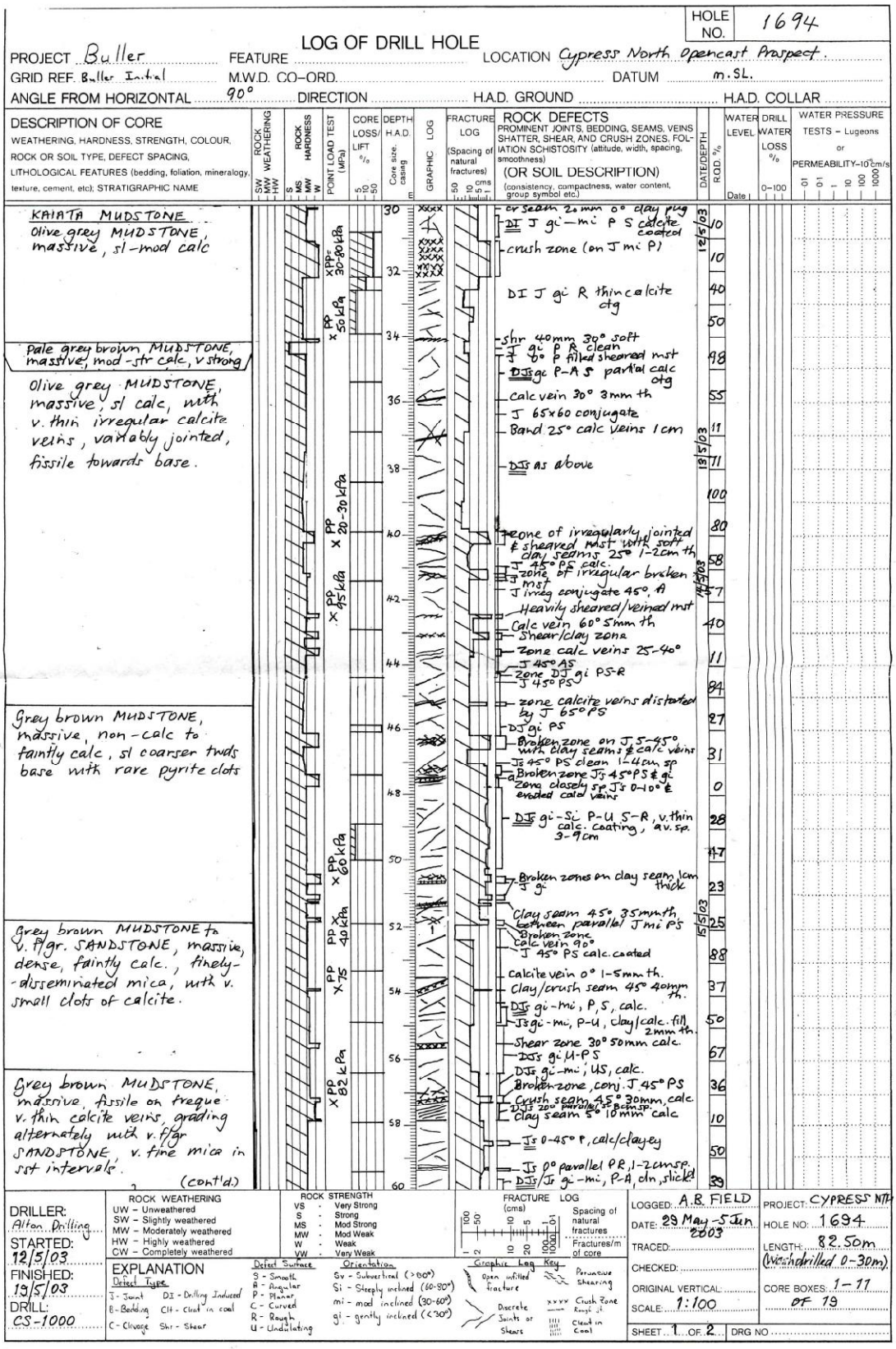

LOG OF DRILL HOLE

HOLE NO. 1694

PROJECT Buller FEATURE LOCATION Cypress North opencast Prospect.

GRID REF. Buller Initial M.W.D. CO-ORD. DATUM m.SL.

ANGLE FROM HORIZONTAL 90° DIRECTION H.A.D. GROUND H.A.D. COLLAR

DESCRIPTION OF CORE
WEATHERING, HARDNESS, STRENGTH, COLOUR, ROCK OR SOIL TYPE, DEFECT SPACING, LITHOLOGICAL FEATURES (bedding, foliation, mineralogy, texture, cement, etc); STRATIGRAPHIC NAME

ROCK WEATHERING: SW – MW – HW

ROCK HARDNESS: S – MS – MW – W

POINT LOAD TEST (MPa)

CORE LOSS/LIFT % 5 10 50

DEPTH H.A.D. m

Core size, casing

GRAPHIC LOG

FRACTURE LOG (Spacing of natural fractures) 50 10 5 – cms

ROCK DEFECTS
PROMINENT JOINTS, BEDDING, SEAMS, VEINS SHATTER, SHEAR, AND CRUSH ZONES. FOLIATION SCHISTOSITY (attitude, width, spacing, smoothness)
(OR SOIL DESCRIPTION)
(consistency, compactness, water content, group symbol etc.)

DATE/DEPTH

R.Q.D. % Date

WATER LEVEL

DRILL WATER LOSS % 0–100

WATER PRESSURE TESTS – Lugeons or PERMEABILITY–10⁻⁵cm/s 01 0.1 1 10 100 1000

KAIATA MUDSTONE
Olive grey MUDSTONE, massive, sl-mod calc

Pale grey brown MUDSTONE, massive, mod-str calc, v strong

Olive grey MUDSTONE, massive, sl calc, with v. thin irregular calcite veins, variably jointed, fissile towards base.

Grey brown MUDSTONE, massive, non-calc to faintly calc, sl coarser twds base with rare pyrite clots

Grey brown MUDSTONE to V. fgr. SANDSTONE, massive, dense, faintly calc., finely-disseminated mica, with v. small clots of calcite.

Grey brown MUDSTONE, massive, fissile on frequ v. thin calcite veins, grading alternately with v. f/gr SANDSTONE, v. fine mica in sst intervals. (cont'd.)

PP 30-80 kPa
PP 50 kPa
PP 20-30 kPa
PP 95 kPa
PP 60 kPa
PP 40 kPa
PP 75
PP 82 kPa

cr seam 2mm 0° clay plug
DI J gi–mi P S calcite coated
crush zone (on J mi P)
DI J gi R thin calcite ctg
shr 40mm 30° soft
J gi P R clean
J 90° P filled sheared mst
DJ sgc P-A S partial calc ctg
calc vein 30° 3mm th
J 65x60 conjugate
Band 25° calc veins 1cm
DJ as above
zone of irregularly jointed & sheared mst with soft clay seams 25° 1-2cm th
J 45° PS calc.
J zone of irregular broken mst
J irreg conjugate 45° A
Heavily sheared/veined mst
Calc vein 60° 5mm th
Shear/clay zone
Zone calc veins 25-40°
J 45° AS
Zone DJ gi PS-R
J 45° PS
zone calcite veins distorted by J 65° PS
DJ gi PS
Broken zone on J 5-45° with clay seams & calc veins
J 45° PS clean 1-4cm sp
Broken zone J 45° PS & gi
Zone closely sp J 0-10° & eroded calc veins
DJ gi-Si P-U, S-R, v. thin calc. coating, av. sp. 3-9cm
Broken zones on clay seam 1cm thick J gi
Clay seam 45° 35mm th between parallel J mi PS
Broken zone
Calc vein 90° J 45° PS calc. coated
Calcite vein 0° 1-5mm th.
Clay/crush seam 45° 40mm th.
DJ gi-mi, P, S, calc.
J sgi-mi, P-U, clay/calc. fill 2mm th.
Shear zone 30° 50mm calc.
DJ sgi U-P S
DJ gi-mi; US, calc.
Broken zone, conj. J 45° PS
Crush seam 45° 30mm calc.
DJ J 20° parallel J 8cm sp.
Clay seam 5° 10mm calc
J 0-45° P, calc/clayey
J 0° parallel PR, 1-2cm sp.
DJ J gi-mi, P-A, oln, slickl

DRILLER: Alton Drilling
STARTED: 12/5/03
FINISHED: 19/5/03
DRILL: CS-1000

ROCK WEATHERING
UW – Unweathered
SW – Slightly weathered
MW – Moderately weathered
HW – Highly weathered
CW – Completely weathered

ROCK STRENGTH
VS – Very Strong
S – Strong
MS – Mod Strong
MW – Mod Weak
W – Weak
VW – Very Weak

FRACTURE LOG (cms) 100 50 10 up 01 100 20 10 dn 01
Spacing of natural fractures
Fractures/m of core

EXPLANATION
Defect Types
J - Joint DI - Drilling Induced
B - Bedding Clt - Clout in coal
C - Clivage Shr - Shear

Defect Surface
S - Smooth
R - Angular
P - Planar
C - Curved
R - Rough
U - Undulating

Orientation
Sv - Subvertical (>80°)
Si - Steeply inclined (60-80°)
mi - mod inclined (30-60°)
gi - gently inclined (<30°)

Graphic Log Key
Open infilled fracture
Pervasive Shearing
Discrete Joints or Shears
xxxx Crush Zone Rough jt.
Clout in Coal

LOGGED: A.R FIELD
DATE: 29 May-5 Jun 2003
TRACED:
CHECKED:
ORIGINAL VERTICAL:
SCALE: 1:100
SHEET 1 OF 2

PROJECT: CYPRESS NTH
HOLE NO: 1694
LENGTH: 82.50m (Washdrilled 0-30m)
CORE BOXES: 1-17 OF 19
DRG NO

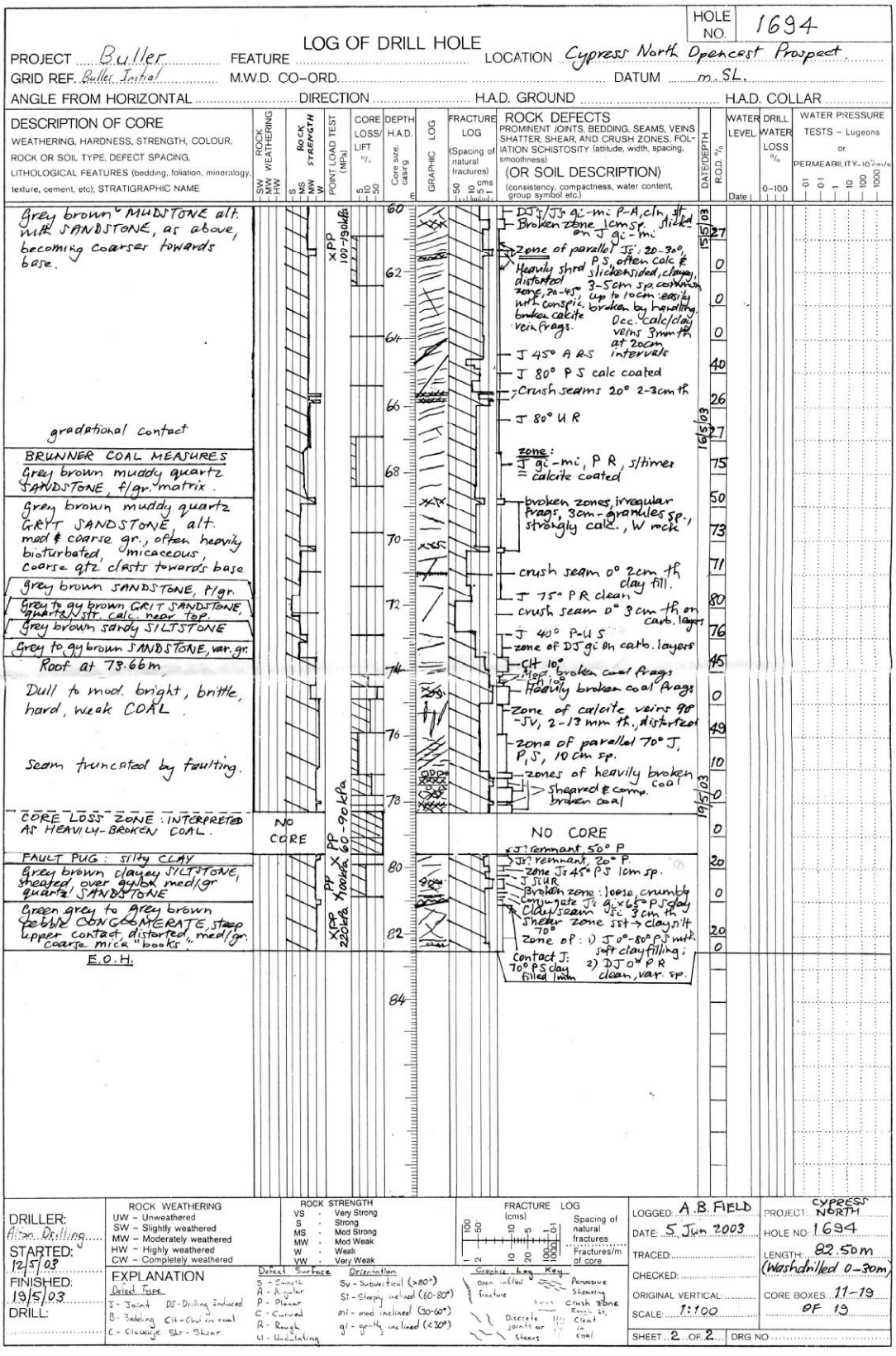
LOG OF DRILL HOLE
HOLE NO. 1694
PROJECT Buller
FEATURE
LOCATION Cypress North Opencast Prospect
GRID REF. Buller Initial
M.W.D. CO-ORD.
DATUM m.SL.
ANGLE FROM HORIZONTAL
DIRECTION
H.A.D. GROUND
H.A.D. COLLAR
DESCRIPTION OF CORE
WEATHERING, HARDNESS, STRENGTH, COLOUR, ROCK OR SOIL TYPE, DEFECT SPACING, LITHOLOGICAL FEATURES (bedding, foliation, mineralogy, texture, cement, etc); STRATIGRAPHIC NAME
ROCK WEATHERING
ROCK STRENGTH
POINT LOAD TEST (MPa)
CORE LOSS/ LIFT
DEPTH H.A.D.
GRAPHIC LOG
FRACTURE LOG (Spacing of natural fractures)
ROCK DEFECTS
PROMINENT JOINTS, BEDDING, SEAMS, VEINS SHATTER, SHEAR, AND CRUSH ZONES. FOLIATION SCHISTOSITY (attitude, width, spacing, smoothness)
(OR SOIL DESCRIPTION)
(consistency, compactness, water content, group symbol etc.)
DATE/DEPTH
R.Q.D. %
WATER LEVEL
DRILL WATER LOSS %
WATER PRESSURE TESTS - Lugeons or PERMEABILITY
Grey brown MUDSTONE alt. with SANDSTONE, as above, becoming coarser towards base.
gradational contact
BRUNNER COAL MEASURES
Grey brown muddy quartz SANDSTONE, f/gr. matrix.
Grey brown muddy quartz GRIT SANDSTONE, alt. med & coarse gr., often heavily bioturbated, micaceous, coarse qtz clasts towards base
Grey brown SANDSTONE, f/gr.
Grey to gy brown GRIT SANDSTONE, quartz, str. calc. near top.
Grey brown sandy SILTSTONE
Grey to gy brown SANDSTONE, var. gr.
Roof at 73.66m
Dull to mod. bright, brittle, hard, weak COAL.
Seam truncated by faulting.
CORE LOSS ZONE: INTERPRETED AS HEAVILY-BROKEN COAL.
FAULT PUG: silty CLAY
Grey brown clayey SILTSTONE, sheared, over gy/br med/gr quartz SANDSTONE
Green grey to grey brown pebble CONGLOMERATE, steep upper contact, distorted, med/gr coarse mica "books".
E.O.H.
NO CORE
PP 100-190kPa
PP 60-90kPa
PP 190kPa
XPP 220kPa
DJ gi-mi P-A, cln, slickensided
Broken zone 1cm sp. slicks on J gi-mi
Zone of parallel Js: 20-30°, P,S, often calc & slickensided, clayey, distorted zone, 30-45° to CA, 3-5cm sp, contains up to 10cm: easily with conspic. broken by hammering broken calcite vein frags. Occ. calc/clay veins 3mm th at 20cm intervals
J 45° A R S
J 80° P S calc coated
Crush seams 20° 2-3cm th
J 80° U R
zone: J gi-mi, P R, s/times = calcite coated
broken zones, irregular frags, 3cm-granules sp., strongly calc., W rock
crush seam 0° 2cm th clay fill.
J 75° P R clean
crush seam 0° 3cm th on carb. layer
J 40° P-U S
zone of DJ gi on carb. layers
CH 10° Mod. broken coal frags
Heavily broken coal frags
Zone of calcite veins 90° -SV, 2-13 mm th., distorted
zone of parallel 70° J, P,S, 10 cm sp.
zones of heavily broken coal
Sheared & comm. broken coal
NO CORE
SJ: remnant, 50° P
JS: remnant, 20° P
zone Js 45° P S 1cm sp.
J SUR
Broken zone: loose, crumbly conjugate Js & gi 65° P S clay
Clay seam Jsc 3cm th
Shear zone 55° → clay s/lt
zone of: 1) J 0°-80° P S with soft clay filling; 2) DJ 0° P R clean, var. sp.
contact J: 70° P S clay filled with
DRILLER: Alpin Drilling
STARTED: 12/5/03
FINISHED: 19/5/03
DRILL:
ROCK WEATHERING
UW - Unweathered
SW - Slightly weathered
MW - Moderately weathered
HW - Highly weathered
CW - Completely weathered
ROCK STRENGTH
VS - Very Strong
S - Strong
MS - Mod Strong
MW - Mod Weak
W - Weak
VW - Very Weak
FRACTURE LOG (cms)
Spacing of natural fractures
Fractures/m of core
EXPLANATION
Defect Type
J - Joint DJ - Drilling Induced
B - Bedding Clt - Clay in coal
C - Cleavage Shr - Shear
Defect Surface
S - Smooth
A - Angular
P - Planar
C - Curved
R - Rough
U - Undulating
Orientation
Sv - Subvertical (>80°)
Sl - Steeply inclined (60-80°)
mi - mod inclined (30-60°)
gi - gently inclined (<30°)
Graphic Log Key
Open infilled fracture
Pervasive Shearing
Crush Zone
Rough Sf.
Clean in coal
Discrete joints or Shears
LOGGED: A.B. FIELD
DATE: 5 Jun 2003
TRACED:
CHECKED:
ORIGINAL VERTICAL:
SCALE: 1:100
SHEET 2 OF 2
DRG NO
PROJECT: CYPRESS NORTH
HOLE NO: 1694
LENGTH: 82.50m (Washdrilled 0-30m)
CORE BOXES: 11-19
OF 19

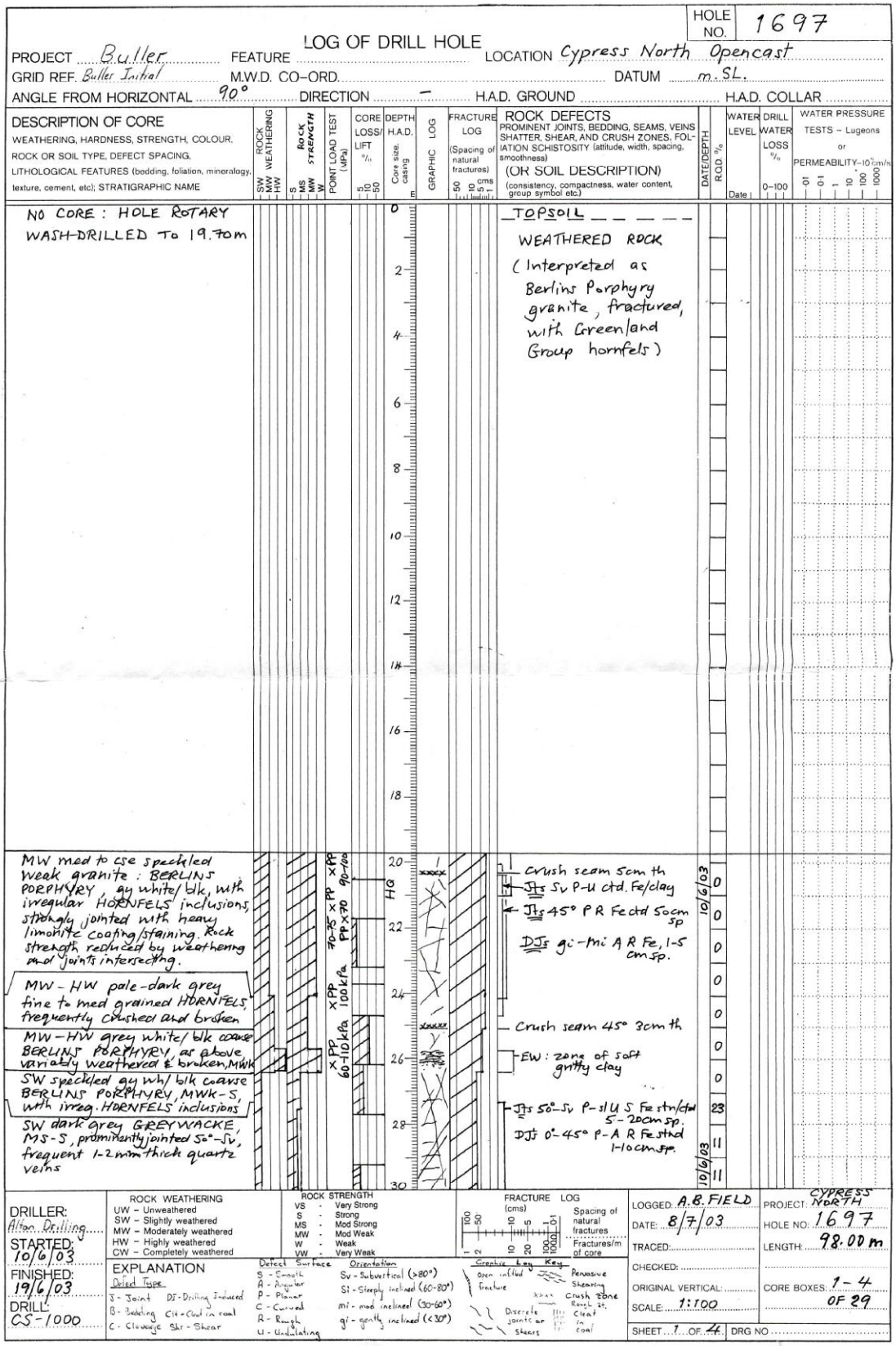

LOG OF DRILL HOLE

HOLE NO. 1697

PROJECT Buller FEATURE LOCATION Cypress North Opencast

GRID REF. Buller Initial M.W.D. CO-ORD. DATUM m.SL.

ANGLE FROM HORIZONTAL 90° DIRECTION – H.A.D. GROUND H.A.D. COLLAR

DESCRIPTION OF CORE
WEATHERING, HARDNESS, STRENGTH, COLOUR, ROCK OR SOIL TYPE, DEFECT SPACING, LITHOLOGICAL FEATURES (bedding, foliation, mineralogy, texture, cement, etc); STRATIGRAPHIC NAME

ROCK WEATHERING: SW MW HW | ROCK STRENGTH: S MS MW W | POINT LOAD TEST (MPa) 5 10 50 | CORE LOSS/LIFT % 10 50 | DEPTH H.A.D. m | Core size, casing | GRAPHIC LOG | FRACTURE LOG (Spacing of natural fractures) 50 10 5 1 cms

ROCK DEFECTS
PROMINENT JOINTS, BEDDING, SEAMS, VEINS SHATTER, SHEAR, AND CRUSH ZONES, FOLIATION SCHISTOSITY (attitude, width, spacing, smoothness)
(OR SOIL DESCRIPTION)
(consistency, compactness, water content, group symbol etc.)

DATE/DEPTH | R.Q.D. % | WATER LEVEL Date | DRILL WATER LOSS % 0–100 | WATER PRESSURE TESTS – Lugeons or PERMEABILITY–10⁻⁵cm/s 01 0.1 1 10 100 1000

NO CORE: HOLE ROTARY WASH-DRILLED TO 19.70m

TOPSOIL

WEATHERED ROCK (Interpreted as Berlins Porphyry granite, fractured, with Greenland Group hornfels)

MW med to cse speckled weak granite: BERLINS PORPHYRY, gy white/blk, with irregular HORNFELS inclusions, strongly jointed with heavy limonite coating/staining. Rock strength reduced by weathering and joints intersecting.

MW–HW pale-dark grey fine to med grained HORNFELS, frequently crushed and broken

MW–HW grey white/blk coarse BERLINS PORPHYRY, as above, variably weathered & broken, MWk

SW speckled gy wh/blk coarse BERLINS PORPHYRY, MWk–S, with irreg. HORNFELS inclusions

SW dark grey GREYWACKE, MS–S, prominently jointed 50°–Sv, frequent 1–2mm thick quartz veins

PP 70-75 x PP 90-100 | PP x PP 60-110 kPa 100 kPa | HG

Crush seam 5cm th
Jts Sv P-U ctd. Fe/clay
Jts 45° P R Fe ctd 50cm sp
DJs gi-mi A R Fe, 1-5 cm sp.
Crush seam 45° 3cm th
EW: zone of soft gritty clay
Jts 50–Sv P–sl U S Fe stn/ctd 5–200mm sp.
DJs 0–45° P–A R Fe stnd 1–10cm sp.

10/6/03 0 0 0 0 0 0 0 23
10/6/03 11 11

DRILLER: Alton Drilling
STARTED: 10/6/03
FINISHED: 19/6/03
DRILL: CS-1000

ROCK WEATHERING
UW – Unweathered
SW – Slightly weathered
MW – Moderately weathered
HW – Highly weathered
CW – Completely weathered

ROCK STRENGTH
VS – Very Strong
S – Strong
MS – Mod Strong
MW – Mod Weak
W – Weak
VW – Very Weak

FRACTURE LOG (cms) 100 50 10 1 0.1 — 5 10 20 100 1000 Spacing of natural fractures/m of core

EXPLANATION
Defect Type
J – Joint DS – Drilling Induced
B – Bedding Clt – Clast in coal
C – Cleavage Shr – Shear

Defect Surface
S – Smooth
A – Angular
P – Planar
C – Curved
R – Rough
U – Undulating

Orientation
Sv – Subvertical (>80°)
St – Steeply inclined (60–80°)
mi – mod inclined (30–60°)
gi – gently inclined (<30°)

Crenitic bag Key
Open infilled fracture
Pervasive Shearing
Crush zone
Rough, st. Clean in coal
Discrete joints or shears

LOGGED: A.B. FIELD
DATE: 8/7/03
TRACED:
CHECKED:
ORIGINAL VERTICAL:
SCALE: 1:100
SHEET 1 OF 4
DRG NO

PROJECT: CYPRESS NORTH
HOLE NO: 1697
LENGTH: 98.00m
CORE BOXES: 1–4 OF 29

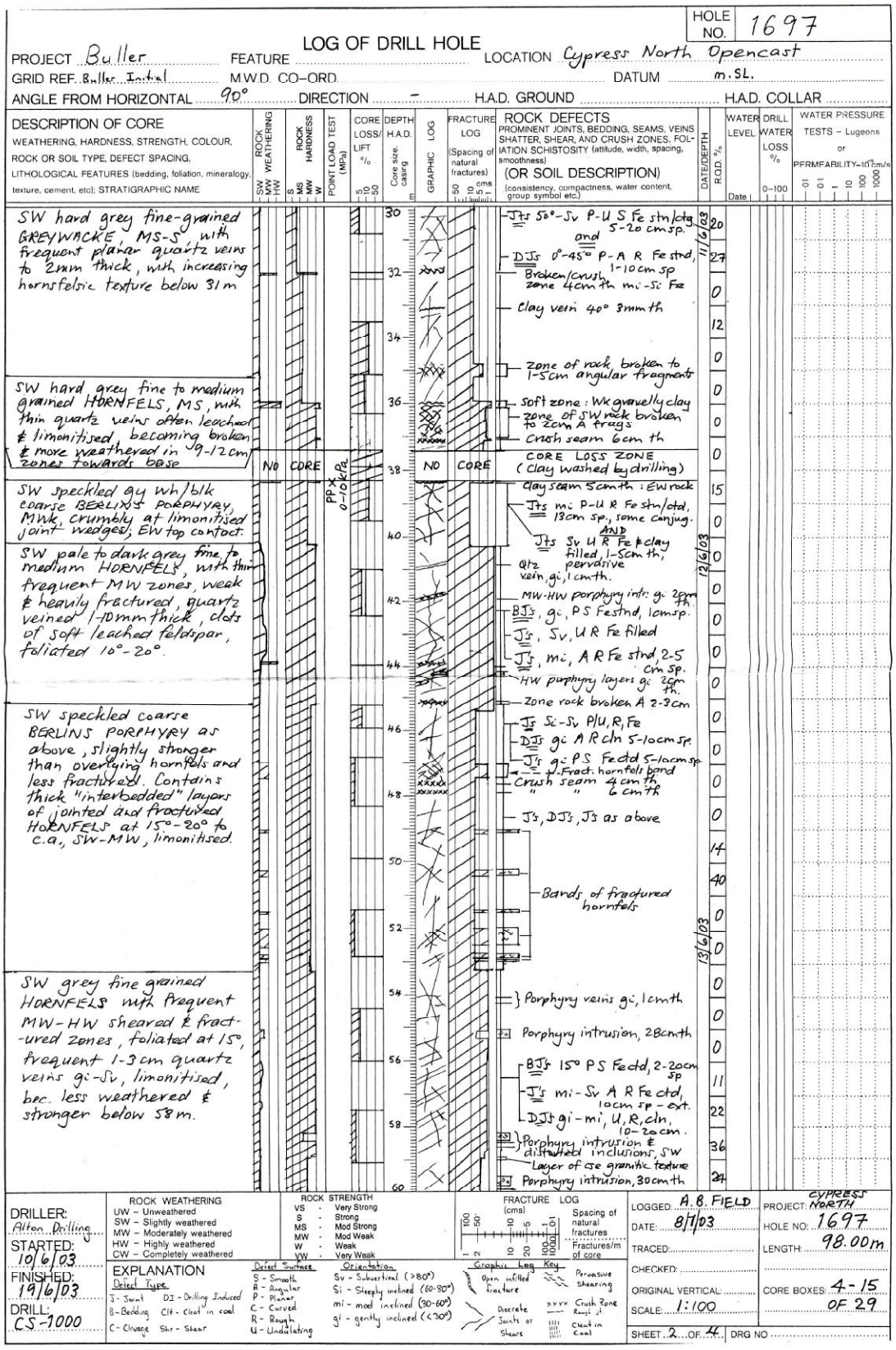
LOG OF DRILL HOLE
HOLE NO. 1697
PROJECT Buller
FEATURE
LOCATION Cypress North Opencast
GRID REF. Buller Initial
M.W.D. CO-ORD.
DATUM m.SL.
ANGLE FROM HORIZONTAL 90°
DIRECTION -
H.A.D. GROUND
H.A.D. COLLAR
DESCRIPTION OF CORE
WEATHERING, HARDNESS, STRENGTH, COLOUR, ROCK OR SOIL TYPE, DEFECT SPACING, LITHOLOGICAL FEATURES (bedding, foliation, mineralogy, texture, cement, etc); STRATIGRAPHIC NAME
ROCK WEATHERING
SW MW HW
ROCK HARDNESS
S MS MW W
POINT LOAD TEST (MPa)
CORE LOSS/ LIFT %
DEPTH H.A.D.
Core size, casing
GRAPHIC LOG
FRACTURE LOG
(Spacing of natural fractures)
ROCK DEFECTS
PROMINENT JOINTS, BEDDING, SEAMS, VEINS SHATTER, SHEAR, AND CRUSH ZONES. FOLIATION SCHISTOSITY (attitude, width, spacing, smoothness)
(OR SOIL DESCRIPTION)
(consistency, compactness, water content, group symbol etc.)
DATE/DEPTH
R.Q.D. %
WATER LEVEL
Date
DRILL WATER LOSS %
WATER PRESSURE TESTS – Lugeons or PERMEABILITY
SW hard grey fine-grained GREYWACKE, MS-S with frequent planar quartz veins to 2mm thick, with increasing hornsfelsic texture below 31 m
SW hard grey fine to medium grained HORNFELS, MS, with thin quartz veins often leached & limonitised, becoming broken & more weathered in 9-12cm zones towards base
NO CORE
PP x 0-10kPa
SW speckled gy wh/blk coarse BERLINS PORPHYRY, MWk, crumbly at limonitised joint wedges; EW top contact.
SW pale to dark grey fine to medium HORNFELS, with thin frequent MW zones, weak & heavily fractured, quartz veined 1-10mm thick, clots of soft leached feldspar, foliated 10°-20°.
SW speckled coarse BERLINS PORPHYRY as above, slightly stronger than overlying hornfels and less fractured. Contains thick "interbedded" layers of jointed and fractured HORNFELS at 15°-20° to c.a., SW-MW, limonitised.
SW grey fine grained HORNFELS with frequent MW-HW sheared & fractured zones, foliated at 15°, frequent 1-3cm quartz veins gi-Sv, limonitised, bec. less weathered & stronger below 58m.
Jts 50°-Sv P-U S Fe stn/ctg 5-20 cm sp. and
DJs 0°-45° P-A R Fe stnd, 1-10 cm sp
Broken/crush zone 4cm th mi-Si Fe
Clay vein 40° 3mm th
zone of rock broken to 1-5cm angular fragments
soft zone: Wk gravelly clay
zone of SW rock broken to 2cm A frags
Crush seam 6cm th
CORE LOSS ZONE (clay washed by drilling)
NO CORE
Clay seam 5cm th: EW rock
Jts mi P-U R Fe stn/ctd, 13cm sp., some conjug. AND
Jts Sv U R Fe & clay filled, 1-5cm th;
Qtz pervasive vein, gi, 1cm th.
MW-HW porphyry intr. gi 2cm th
BJs, gi, P S Fe stnd, 1cm sp.
Js, Sv, U R Fe filled
Js, mi, A R Fe stnd, 2-5 cm sp.
HW porphyry layers gi 2cm th.
Zone rock broken A 2-3cm
Js Si-Sv P/U, R, Fe
DJs gi A R cln 5-10cm sp.
Js gi P S Fe ctd 5-10cm sp.
Fract. hornfels bond
Crush seam 4cm th
" " 6cm th
Js, DJs, Js as above
Bands of fractured hornfels
Porphyry veins gi, 1cm th
Porphyry intrusion, 28cm th
BJs 15° P S Fe ctd, 2-20cm sp
Js mi-Sv A R Fe ctd, 10cm sp - ext.
DJs gi-mi, U, R, cln, 10-20cm.
Porphyry intrusion & diffuse inclusions, SW
Layer of ce granitic texture
Porphyry intrusion, 30cm th
11/6/03
12/6/03
13/6/03
ROCK WEATHERING
UW – Unweathered
SW – Slightly weathered
MW – Moderately weathered
HW – Highly weathered
CW – Completely weathered
ROCK STRENGTH
VS - Very Strong
S - Strong
MS - Mod Strong
MW - Mod Weak
W - Weak
VW - Very Weak
FRACTURE LOG (cms)
Spacing of natural fractures
Fractures/m of core
EXPLANATION
Defect Type
J - Joint DI - Drilling Induced
B - Bedding Clt - Cleat in coal
C - Cleavage Shr - Shear
Defect Surface
S - Smooth
R - Angular
P - Planar
C - Curved
R - Rough
U - Undulating
Orientation
Sv - Subvertical (>80°)
Si - Steeply inclined (60-80°)
mi - mod inclined (30-60°)
gi - gently inclined (<30°)
Graphic Log Key
Open infilled fracture
Pervasive Shearing
Discrete Joints or Shears
Crush Zone
Cleat in Coal
DRILLER: Alton Drilling
STARTED: 10/6/03
FINISHED: 19/6/03
DRILL: CS-1000
LOGGED: A.B. FIELD
DATE: 8/1/03
TRACED:
CHECKED:
ORIGINAL VERTICAL:
SCALE: 1:100
PROJECT: CYPRESS NORTH
HOLE NO: 1697
LENGTH: 98.00m
CORE BOXES: 4-15 OF 29
SHEET 2 OF 4
DRG NO

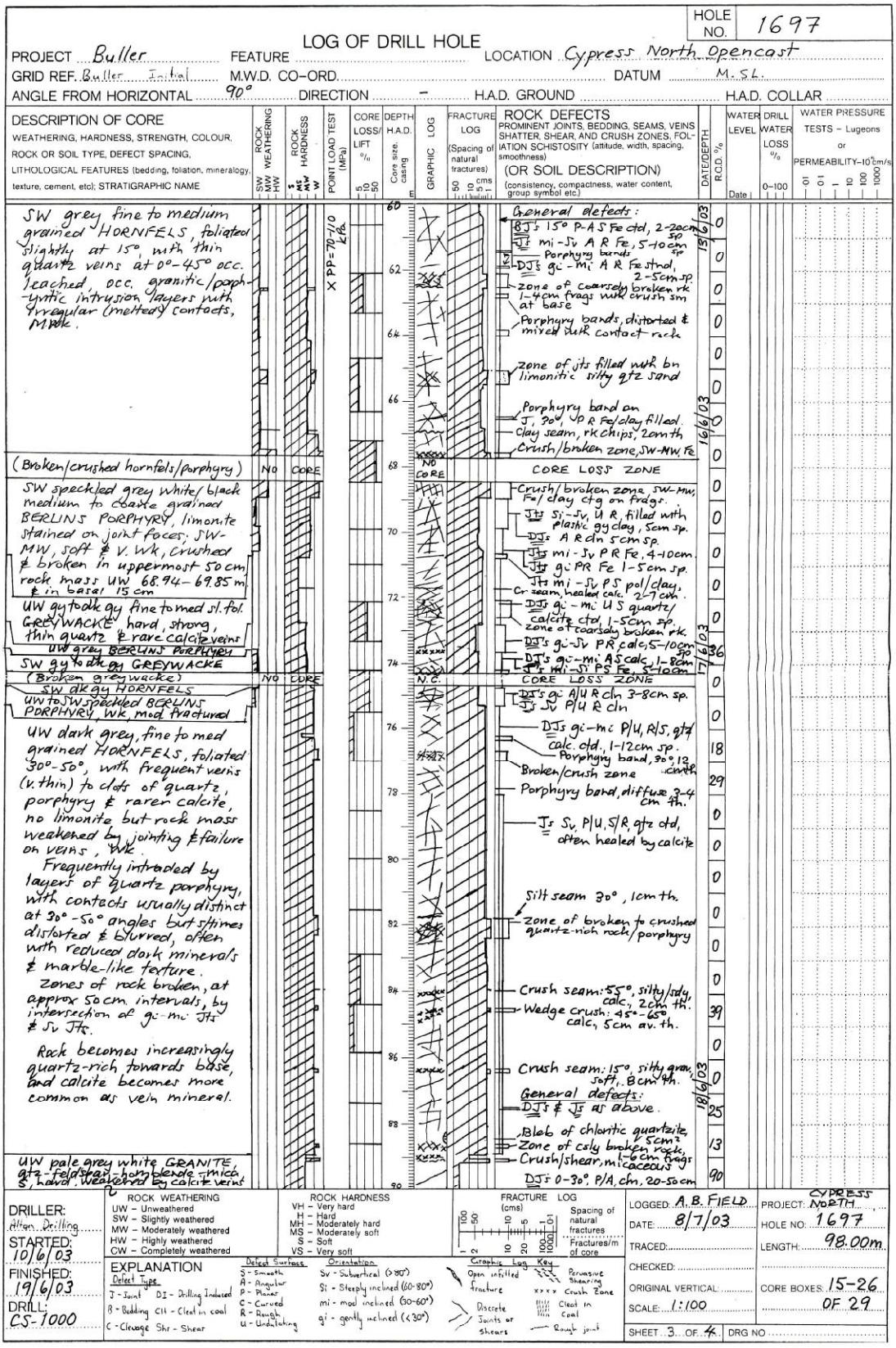
HOLE NO. 1697
LOG OF DRILL HOLE
PROJECT Buller FEATURE LOCATION Cypress North Opencast
GRID REF. Buller Initial M.W.D. CO-ORD. DATUM M.S.L.
ANGLE FROM HORIZONTAL 90° DIRECTION – H.A.D. GROUND H.A.D. COLLAR
DESCRIPTION OF CORE
WEATHERING, HARDNESS, STRENGTH, COLOUR, ROCK OR SOIL TYPE, DEFECT SPACING, LITHOLOGICAL FEATURES (bedding, foliation, mineralogy, texture, cement, etc); STRATIGRAPHIC NAME
ROCK WEATHERING
ROCK HARDNESS
POINT LOAD TEST (MPa)
CORE LOSS/ LIFT %
DEPTH H.A.D.
GRAPHIC LOG
FRACTURE LOG (Spacing of natural fractures)
ROCK DEFECTS PROMINENT JOINTS, BEDDING, SEAMS, VEINS SHATTER, SHEAR, AND CRUSH ZONES, FOLIATION SCHISTOSITY (attitude, width, spacing, smoothness)
(OR SOIL DESCRIPTION) (consistency, compactness, water content, group symbol etc.)
DATE/DEPTH
R.Q.D. %
WATER LEVEL
DRILL WATER LOSS %
WATER PRESSURE TESTS – Lugeons or PERMEABILITY–10⁻⁵cm/s
SW grey fine to medium grained HORNFELS, foliated slightly at 15°, with thin qtz veins at 0°–45° occ. leached, occ. granitic/porphyritic intrusion layers with irregular (melted) contacts, MWk.
X PP=70–110 kPa
General defects:
BJs 15° P-A S Fe ctd, 2-20cm sp
Js mi-Sv A R Fe, 5-10cm sp
Porphyry bands
DJs gi-mi A R Fe stnd, 2-5cm sp
zone of coarsely broken rk 1-4cm frags with crush sm at base
Porphyry bands, distorted & mixed with contact rock
zone of jts filled with bn limonitic silty qtz sand
Porphyry band on J, 20°, VO R Fe/clay filled
Clay seam, rk chips, 2cm th
Crush/broken zone, SW-MW, Fe
(Broken/crushed hornfels/porphyry) NO CORE
NO CORE
CORE LOSS ZONE
SW speckled grey white/black medium to coarse grained BERLINS PORPHYRY, limonite stained on joint faces; SW-MW, soft & V. Wk, crushed & broken in uppermost 50 cm rock mass UW 68.94–69.85 m & in basal 15 cm.
Crush/broken zone, SW-MW, Fe/clay ctg on frags.
Js Si-Sv, U R, filled with plastic gy clay, 5cm sp.
DJs A R dn 5cm sp.
Js mi-Sv P R Fe, 4-10cm.
Js gi PR Fe 1-5cm sp.
Js mi-Sv P S pol/clay, Cr seam, healed calc, 2-7 cm.
DJs gi-mi U S quartz/calcite ctd, 1-5cm sp.
zone of coarsely broken rk.
DJs gi-Sv P R calc, 5-10cm sp
DJs gi-mi A S calc, 1-8cm sp
Js mi-Sv P S Fe, 5-10cm
UW gy to dk gy fine to med sl. fol. GREYWACKE hard, strong, thin quartz & rare calcite veins
UW grey BERLINS PORPHYRY
SW gy to dk gy GREYWACKE
(Broken greywacke) NO CORE
N.C.
CORE LOSS ZONE
SW dk gy HORNFELS
UW to SW speckled BERLINS PORPHYRY, Wk, mod fractured
DJs gi A/U R cln 3-8cm sp.
Js Sv P/U R cln
UW dark grey, fine to med grained HORNFELS, foliated 30°–50°, with frequent veins (v. thin) to clots of quartz, porphyry & rarer calcite, no limonite but rock mass weakened by jointing & failure on veins, Wk.
Frequently intruded by layers of quartz porphyry, with contacts usually distinct at 30°–50° angles but sometimes distorted & blurred, often with reduced dark minerals & marble-like texture.
Zones of rock broken, at approx 50 cm intervals, by intersection of gi-mi Jts & Sv Jts.
DJs gi-mc P/U, R/S, qtz/calc. ctd., 1-12cm sp.
Porphyry band, 90°, 12 cm th
Broken/crush zone
Porphyry band, diffuse 3-4 cm th.
Js Sv, P/U, S/R, qtz ctd, often healed by calcite
Silt seam 30°, 1cm th.
zone of broken to crushed quartz-rich rock/porphyry
Crush seam: 55°, silty/sdy calc., 2cm th.
Wedge crush: 45°–65° calc, 5cm av. th.
Crush seam: 15°, silty grav, soft, 8cm th.
General defects:
DJs & Js as above.
Blob of chloritic quartzite, 5cm²
Zone of csly broken rock, 1–6cm frags
Crush/shear, micaceous
DJs 0–30°, P/A, cln, 20–50cm
Rock becomes increasingly quartz-rich towards base, and calcite becomes more common as vein mineral.
UW pale grey white GRANITE, qtz-feldspar-hornblende-mica, S, hard, weakened by calcite veins
ROCK WEATHERING
UW – Unweathered
SW – Slightly weathered
MW – Moderately weathered
HW – Highly weathered
CW – Completely weathered
ROCK HARDNESS
VH – Very hard
H – Hard
MH – Moderately hard
MS – Moderately soft
S – Soft
VS – Very soft
FRACTURE LOG (cms) Spacing of natural fractures Fractures/m of core
EXPLANATION
Defect Types
J - Joint DI - Drilling Induced
B - Bedding Cli - Cleat in coal
C - Cleavage Shr - Shear
Defect Surface
S - Smooth
A - Angular
P - Planar
C - Curved
R - Rough
U - Undulating
Orientation
Sv - Subvertical (>80°)
St - Steeply inclined (60-80°)
mi - mod inclined (30-60°)
gi - gently inclined (<30°)
Graphic Log Key
Open infilled fracture
Discrete Joints or Shears
Pervasive Shearing
xxxx Crush Zone
Cleat in Coal
Rough joint
DRILLER: Atlas Drilling
STARTED: 10/6/03
FINISHED: 19/6/03
DRILL: CS-1000
LOGGED: A.B. FIELD
DATE: 8/7/03
TRACED:
CHECKED:
ORIGINAL VERTICAL:
SCALE: 1:100
PROJECT: CYPRESS NORTH
HOLE NO: 1697
LENGTH: 98.00m
CORE BOXES: 15–26 OF 29
SHEET 3 OF 4
DRG NO

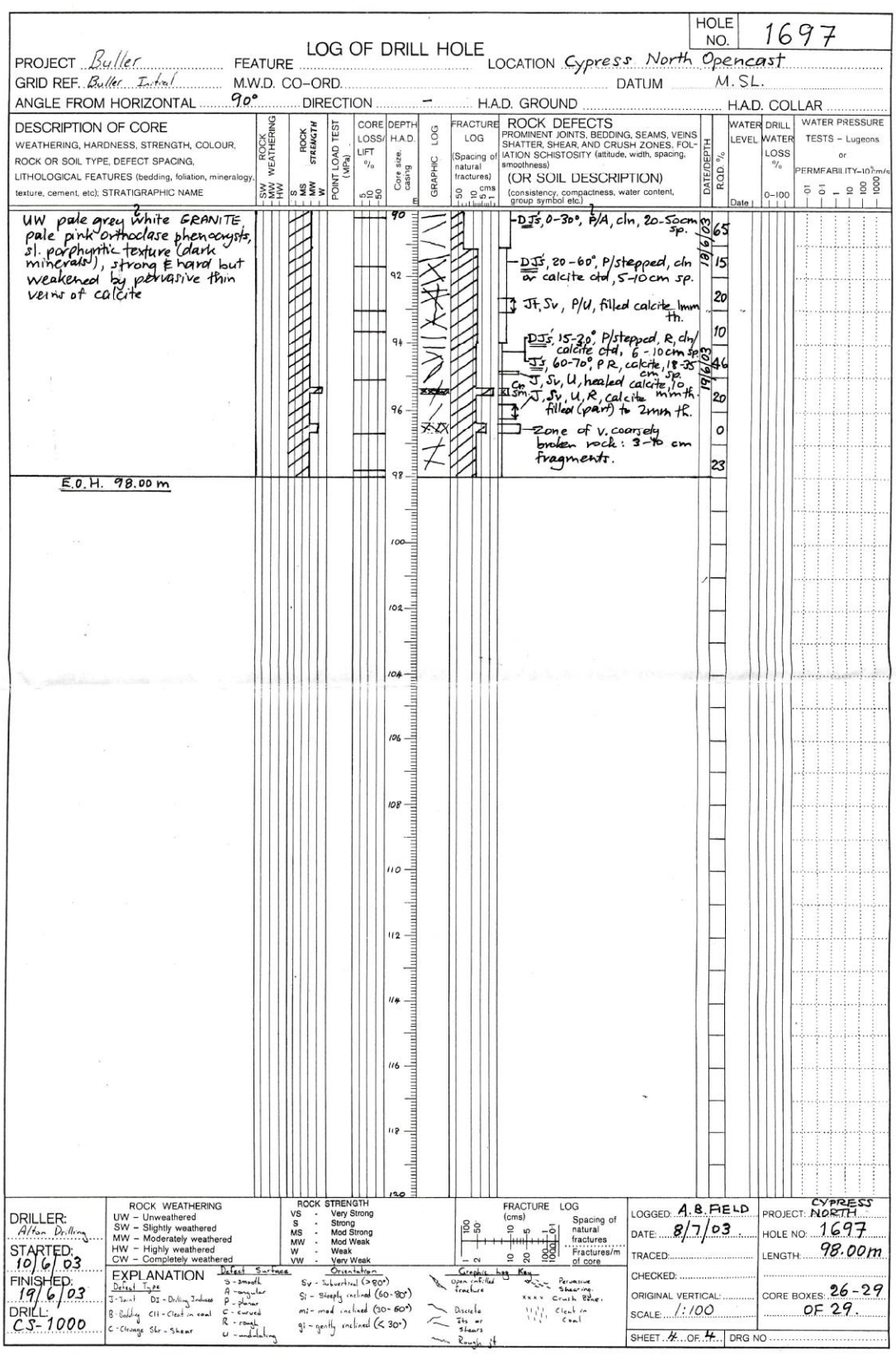

LOG OF DRILL HOLE

HOLE NO. 1697

PROJECT Buller FEATURE LOCATION Cypress North Opencast

GRID REF. Buller Initial M.W.D. CO-ORD. DATUM M.SL.

ANGLE FROM HORIZONTAL 90° DIRECTION – H.A.D. GROUND H.A.D. COLLAR

DESCRIPTION OF CORE
WEATHERING, HARDNESS, STRENGTH, COLOUR, ROCK OR SOIL TYPE, DEFECT SPACING, LITHOLOGICAL FEATURES (bedding, foliation, mineralogy, texture, cement, etc); STRATIGRAPHIC NAME

ROCK WEATHERING: SW MW HW
ROCK STRENGTH: S MS MW W
POINT LOAD TEST (MPa)
CORE LOSS/ LIFT %: 5 50
DEPTH H.A.D.: Core size, casing
GRAPHIC LOG
FRACTURE LOG (Spacing of natural fractures): 50 10 5 1 cms
ROCK DEFECTS PROMINENT JOINTS, BEDDING, SEAMS, VEINS SHATTER, SHEAR, AND CRUSH ZONES, FOLIATION SCHISTOSITY (attitude, width, spacing, smoothness) (OR SOIL DESCRIPTION) (consistency, compactness, water content, group symbol etc.)
DATE/DEPTH
RQD %
WATER LEVEL: Date
DRILL WATER LOSS %: 0–100
WATER PRESSURE TESTS – Lugeons or PERMEABILITY–10⁻⁷m/s: 01 0·1 1 10 100 1000

UW pale grey white GRANITE, pale pink orthoclase phenocrysts, sl. porphyritic texture (dark minerals), strong & hard but weakened by pervasive thin veins of calcite

90
92
94
96
98
100
102
104
106
108
110
112
114
116
118
120

DJs, 0-30°, P/A, cln, 20-50cm sp. — 19/6/03 — 65
DJs, 20-60°, P/stepped, cln or calcite ctd, 5-10cm sp. — 15
JF, Sv, P/U, filled calcite 1mm th. — 20
DJs, 15-30°, P/stepped, R, cln/ calcite ctd, 6-10cm sp. — 10
Js, 60-70°, P R, calcite, 18-35 cm sp. — 19/6/03 — 46
Cs 15mm J, Sv, U, healed calcite, 10 mm th.
J, Sv, U, R, calcite mm th. filled (paint) to 2mm th. — 20
Zone of V. coarsely broken rock: 3-10 cm fragments. — 0
23

E.O.H. 98.00 m

DRILLER: Alton Drilling
STARTED: 10/6/03
FINISHED: 19/6/03
DRILL: CS-1000

ROCK WEATHERING
UW – Unweathered
SW – Slightly weathered
MW – Moderately weathered
HW – Highly weathered
CW – Completely weathered

ROCK STRENGTH
VS - Very Strong
S - Strong
MS - Mod Strong
MW - Mod Weak
W - Weak
VW - Very Weak

FRACTURE LOG (cms): 100 50 10 5 1 0·1 — Spacing of natural fractures — Fractures/m of core

EXPLANATION
Defect Type: J - Joint, DJ - Drilling Induced, B - Bedding, Cli - Cleat in coal, C - Cleavage, Shr - Shear
Defect Surface: S - smooth, A - angular, P - planar, C - curved, R - rough, U - undulating
Orientation: Sv - Subvertical (>80°), Si - Steeply inclined (60-80°), mi - mod inclined (30-60°), gi - gently inclined (<30°)
Graphic log Key: Open infilled fracture, Discrete, Its or Shears, Rough, Pervasive Shearing, xxxx Crush Rbke., Cleat in Coal

LOGGED: A.B. FIELD
DATE: 8/7/03
TRACED:
CHECKED:
ORIGINAL VERTICAL:
SCALE: 1:100
SHEET 4 OF 4 DRG NO

PROJECT: CYPRESS NORTH
HOLE NO: 1697
LENGTH: 98.00m
CORE BOXES: 26-29 OF 29.

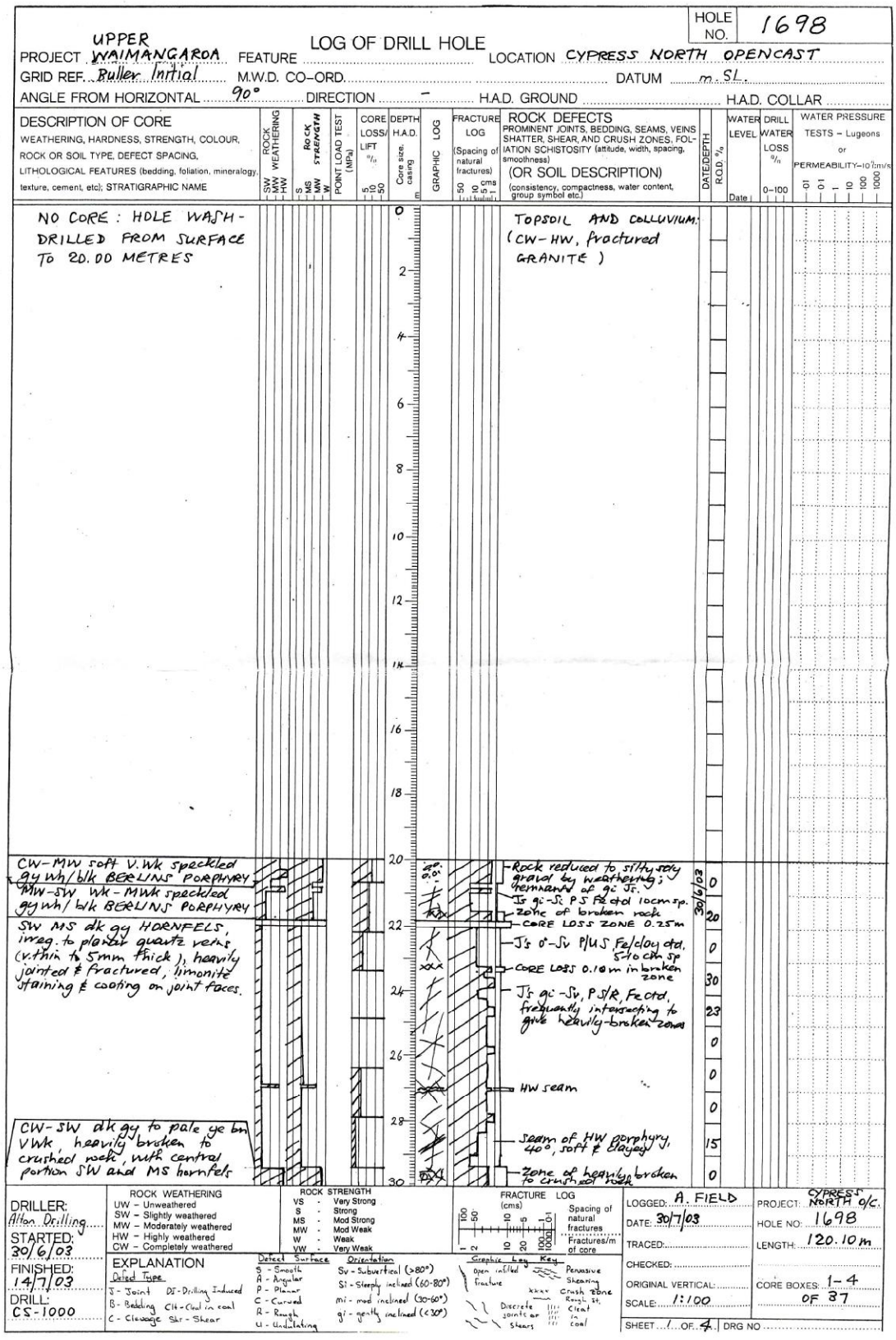
HOLE NO. 1698
LOG OF DRILL HOLE
PROJECT UPPER WAIMANGAROA FEATURE LOCATION CYPRESS NORTH OPENCAST
GRID REF. Buller Initial M.W.D. CO-ORD. DATUM m. SL.
ANGLE FROM HORIZONTAL 90° DIRECTION – H.A.D. GROUND H.A.D. COLLAR
DESCRIPTION OF CORE
WEATHERING, HARDNESS, STRENGTH, COLOUR, ROCK OR SOIL TYPE, DEFECT SPACING, LITHOLOGICAL FEATURES (bedding, foliation, mineralogy, texture, cement, etc); STRATIGRAPHIC NAME
ROCK WEATHERING
ROCK STRENGTH
POINT LOAD TEST (MPa)
CORE LOSS/ LIFT
DEPTH H.A.D.
Core size. casing
GRAPHIC LOG
FRACTURE LOG (Spacing of natural fractures)
ROCK DEFECTS PROMINENT JOINTS, BEDDING, SEAMS, VEINS SHATTER, SHEAR, AND CRUSH ZONES, FOLIATION SCHISTOSITY (attitude, width, spacing, smoothness)
(OR SOIL DESCRIPTION)
(consistency, compactness, water content, group symbol etc.)
DATE/DEPTH
R.Q.D. %
WATER LEVEL
DRILL WATER LOSS
WATER PRESSURE TESTS – Lugeons or PERMEABILITY–10⁻² cm/s
NO CORE : HOLE WASH-DRILLED FROM SURFACE TO 20.00 METRES
TOPSOIL AND COLLUVIUM: (CW–HW, fractured GRANITE)
CW–MW soft V.Wk speckled gy wh/blk BERLINS PORPHYRY
MW–SW Wk–MWk speckled gy wh/blk BERLINS PORPHYRY
SW MS dk gy HORNFELS, irreg. to planar quartz veins (v.thin to 5mm thick), heavily jointed & fractured, limonite staining & coating on joint faces.
CW–SW dk gy to pale ye bn VWk, heavily broken to crushed rock, with central portion SW and MS hornfels
Rock reduced to silty sdy gravel by weathering; remnants of qi Js.
Js qi–Sr P S Fe ctd 10cm sp.
zone of broken rock
CORE LOSS ZONE 0.25m
Js 0°–Sv P/U S Fe/cloy ctd. 5–10 cm sp
CORE LOSS 0.10m in broken zone
Js qi–Sv, P S/R Fe ctd, frequently intersecting to give heavily-broken zones
HW seam
seam of HW porphyry J, 40°, soft & clayey
zone of heavily broken to crushed rock
30/6/03
DRILLER: Alton Drilling
STARTED: 30/6/03
FINISHED: 14/7/03
DRILL: CS-1000
ROCK WEATHERING
UW – Unweathered
SW – Slightly weathered
MW – Moderately weathered
HW – Highly weathered
CW – Completely weathered
ROCK STRENGTH
VS – Very Strong
S – Strong
MS – Mod Strong
MW – Mod Weak
W – Weak
VW – Very Weak
FRACTURE LOG (cms)
Spacing of natural fractures
Fractures/m of core
EXPLANATION
Defect Type
J – Joint
B – Bedding
C – Cleavage
DI – Drilling Induced
Clt – Clay in coal
Shr – Shear
Defect Surface
S – Smooth
A – Angular
P – Planar
C – Curved
R – Rough
U – Undulating
Orientation
Sv – Subvertical (>80°)
St – Steeply inclined (60–80°)
mi – mod inclined (30–60°)
gi – gently inclined (<30°)
Graphic Log Key
open infilled fracture
Pervasive Shearing
Crush Zone
Rough Jt.
Clean
Discrete joints or shears
coal
LOGGED: A. FIELD
DATE: 30/7/03
TRACED:
CHECKED:
ORIGINAL VERTICAL:
SCALE: 1:100
PROJECT: CYPRESS NORTH o/c.
HOLE NO: 1698
LENGTH: 120.10m
CORE BOXES: 1–4 OF 37
SHEET 1 OF 4 DRG NO

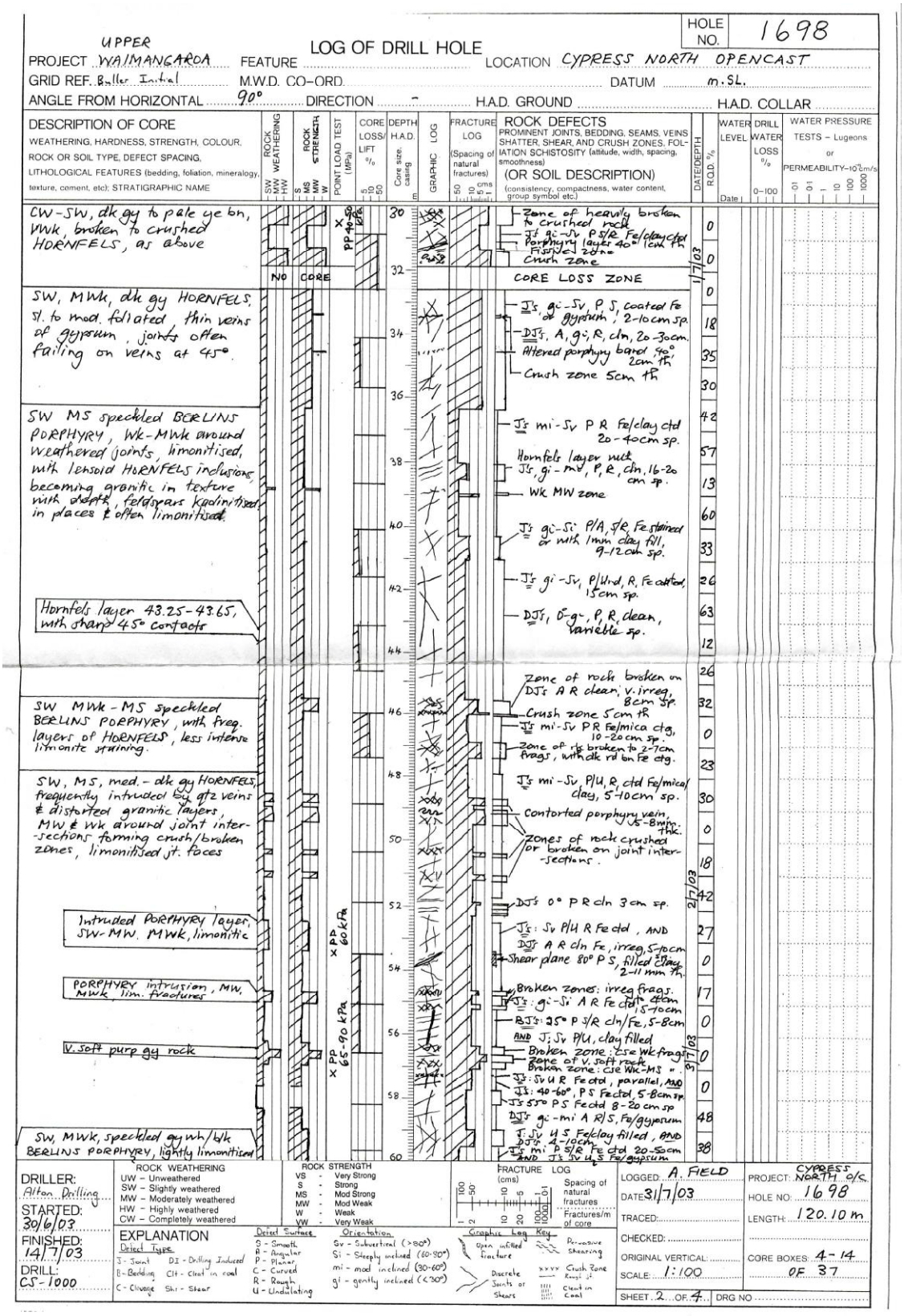
HOLE NO. 1698
LOG OF DRILL HOLE
PROJECT UPPER WAIMANGAROA FEATURE LOCATION CYPRESS NORTH OPENCAST
GRID REF. Buller Initial M.W.D. CO-ORD. DATUM m.SL.
ANGLE FROM HORIZONTAL 90° DIRECTION - H.A.D. GROUND H.A.D. COLLAR
DESCRIPTION OF CORE
WEATHERING, HARDNESS, STRENGTH, COLOUR, ROCK OR SOIL TYPE, DEFECT SPACING, LITHOLOGICAL FEATURES (bedding, foliation, mineralogy, texture, cement, etc); STRATIGRAPHIC NAME
ROCK WEATHERING
ROCK STRENGTH
POINT LOAD TEST (MPa)
CORE LOSS/ LIFT %
DEPTH H.A.D.
GRAPHIC LOG
FRACTURE LOG (Spacing of natural fractures)
ROCK DEFECTS
PROMINENT JOINTS, BEDDING, SEAMS, VEINS SHATTER, SHEAR, AND CRUSH ZONES. FOLIATION SCHISTOSITY (attitude, width, spacing, smoothness)
(OR SOIL DESCRIPTION)
(consistency, compactness, water content, group symbol etc.)
DATE/DEPTH
R.Q.D. %
WATER LEVEL
DRILL WATER LOSS %
WATER PRESSURE TESTS – Lugeons or PERMEABILITY–10⁻²cm/s
CW-SW, dk gy to pale ye bn, MWk, broken to crushed HORNFELS, as above
Zone of heavily broken to crushed rock
Jf gi-Sv P S/R Fe/clay ctd Porphyry layer 40° 1cm th
Fracture zone 20cm
Crush zone
NO CORE
CORE LOSS ZONE
SW, MWk, dk gy HORNFELS, sl. to mod. foliated, thin veins of gypsum, joints often failing on veins at 45°.
Js gi-Sv, P S, coated Fe or gypsum, 2-10cm sp.
DJs, A, gi, R, cln, 20-30cm.
Altered porphyry band 50° 2cm th
Crush zone 5cm th
SW MS speckled BERLINS PORPHYRY, Wk-MWk around weathered joints, limonitised, with lensoid HORNFELS inclusions becoming granitic in texture with depth, feldspars kaolinitised in places & often limonitised.
Js mi-Sv P R Fe/clay ctd 20-40cm sp.
Hornfels layer with Js, gi-mv, P, R, cln, 16-20 cm sp.
Wk MW zone
Js gi-Si P/A, S/R, Fe stained or with 1mm clay fill, 9-12cm sp.
Js gi-Sv, P/Und, R, Fe coated, 15cm sp.
DJs, 0-gi, P, R, clean, variable sp.
Hornfels layer 43.25-43.65, with sharp 45° contacts
Zone of rock broken on DJs A R clean, v. irreg, 8cm sp.
Crush zone 5cm th
Js mi-Sv P R Fe/mica ctg, 10-20cm sp.
Zone of rock broken to 2-7cm frags, with dk rd bn Fe ctg.
SW MWk-MS speckled BERLINS PORPHYRY, with freq. layers of HORNFELS, less intense limonite staining.
Js mi-Sv, P/U, R, ctd Fe/mica/clay, 5-10cm sp.
Contorted porphyry vein, 5-8mm thk.
SW, MS, med.-dk gy HORNFELS, frequently intruded by qtz veins & distorted granitic layers, MW & Wk around joint inter-sections forming crush/broken zones, limonitised jt. faces
Zones of rock crushed or broken on joint inter-sections.
DJs 0° P R cln 3cm sp.
Js: Sv P/U R Fe ctd, AND
DJs A R cln Fe, irreg, 5-10cm
Shear plane 80° P S, filled clay 2-11 mm th.
Intruded PORPHYRY layer, SW-MW, MWk, limonitic
Broken zones: irreg frags.
Js: gi-Si A R Fe ctd, 5-10cm
BJs: 25° P S/R cln/Fe, 5-8cm
AND Js: Sv P/U, clay filled
Broken zone: Core Wk frags
Zone of V. soft rock
Broken zone: Core Wk-MS "
PORPHYRY intrusion, MW, MWk, lim. fractures
V. soft purp gy rock
Js: Sv U R Fe ctd, parallel, AND
Js: 40-60°, P S Fe ctd, 5-8cm sp.
Js 55° P S Fe ctd 8-20 cm sp
DJs gi-mi A R/S, Fe/gypsum
Js: Sv U S Fe/clay filled, AND
DJs, 4-10cm
Js mi B S/R Fe ctd 20-50cm
AND Js Sv U S Fe/gypsum
SW, MWk, speckled gy wh/blk BERLINS PORPHYRY, lightly limonitised
PP 40-50 kPa
PP 60 kPa
PP 65-90 kPa
1/7/03
2/7/03
3/7/03
0 0 0 18 35 30 42 57 13 60 33 26 63 12 26 32 0 23 30 0 18 42 27 0 17 0 0 0 48 38
DRILLER: Alton Drilling
STARTED: 30/6/03
FINISHED: 14/7/03
DRILL: CS-1000
ROCK WEATHERING
UW – Unweathered
SW – Slightly weathered
MW – Moderately weathered
HW – Highly weathered
CW – Completely weathered
ROCK STRENGTH
VS - Very Strong
S - Strong
MS - Mod Strong
MW - Mod Weak
W - Weak
VW - Very Weak
FRACTURE LOG (cms)
Spacing of natural fractures
Fractures/m of core
EXPLANATION
Defect Types
J - Joint DI - Drilling Induced
B - Bedding Clt - Clest in coal
C - Cleavage Shr - Shear
Defect Surfaces
S - Smooth
P - Planar
C - Curved
R - Rough
U - Undulating
Orientation
Sv - Subvertical (>80°)
Si - Steeply inclined (60-80°)
mi - mod inclined (30-60°)
gi - gently inclined (<30°)
Graphic Log Key
Open infilled fracture
Pervasive Shearing
Discrete Joints or Shears
Crush Zone Rough jt
Clest in Coal
LOGGED: A. FIELD
DATE: 31/7/03
TRACED:
CHECKED:
ORIGINAL VERTICAL:
SCALE: 1:100
PROJECT: CYPRESS NORTH O/C
HOLE NO: 1698
LENGTH: 120.10 m
CORE BOXES: 4-14
OF 37
SHEET 2 OF 4
DRG NO

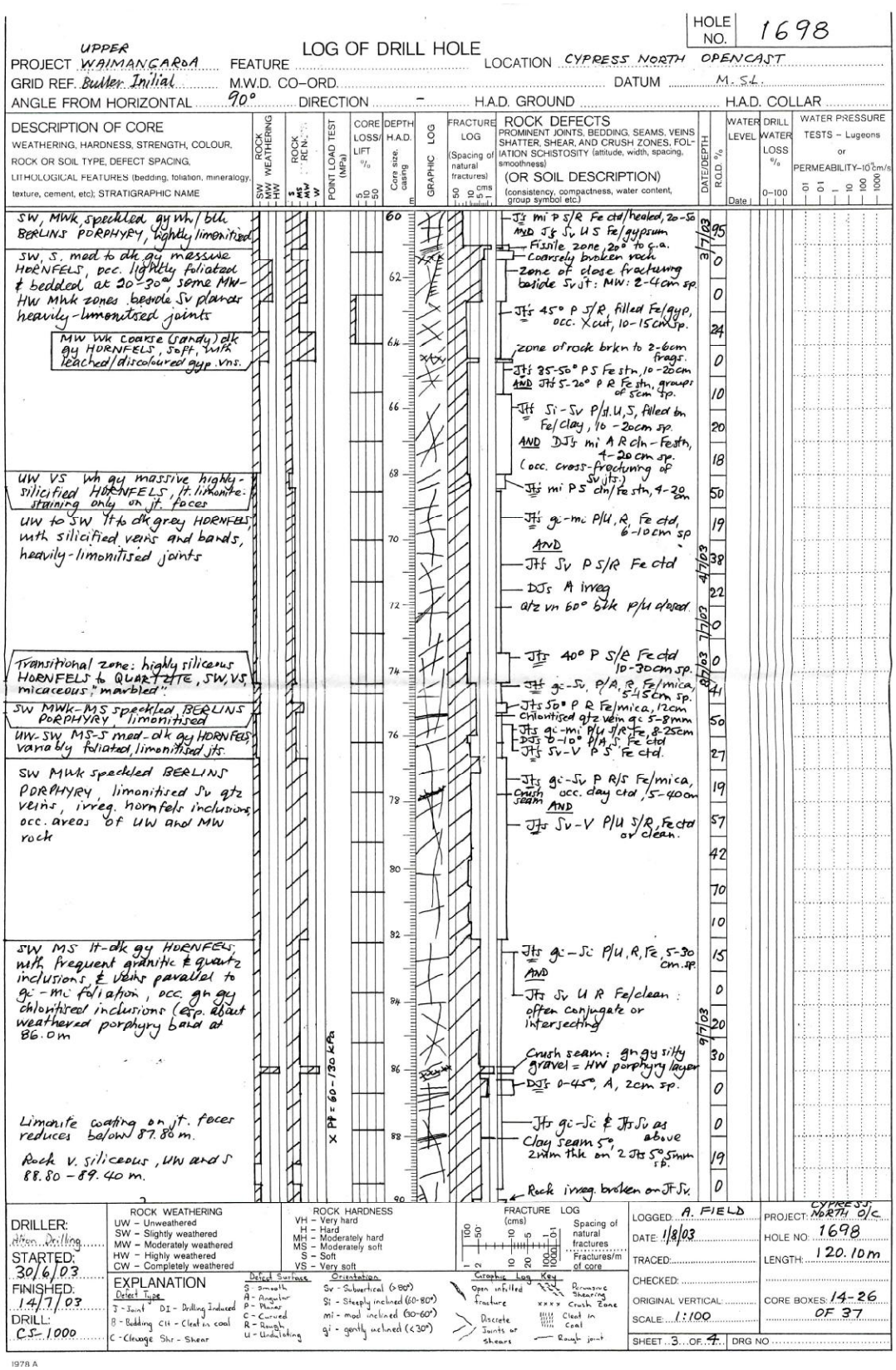
HOLE NO. 1698
LOG OF DRILL HOLE
PROJECT UPPER WAIMANGAROA FEATURE LOCATION CYPRESS NORTH OPENCAST
GRID REF. Butler Initial M.W.D. CO-ORD. DATUM M.S.L.
ANGLE FROM HORIZONTAL 90° DIRECTION - H.A.D. GROUND H.A.D. COLLAR
DESCRIPTION OF CORE
WEATHERING, HARDNESS, STRENGTH, COLOUR, ROCK OR SOIL TYPE, DEFECT SPACING, LITHOLOGICAL FEATURES (bedding, foliation, mineralogy, texture, cement, etc); STRATIGRAPHIC NAME
ROCK WEATHERING
ROCK RETN.
POINT LOAD TEST (MPa)
CORE LOSS/ LIFT %
DEPTH H.A.D.
Core size, casing
GRAPHIC LOG
FRACTURE LOG (Spacing of natural fractures)
ROCK DEFECTS
PROMINENT JOINTS, BEDDING, SEAMS, VEINS SHATTER, SHEAR, AND CRUSH ZONES; FOLIATION SCHISTOSITY (attitude, width, spacing, smoothness)
(OR SOIL DESCRIPTION)
(consistency, compactness, water content, group symbol etc.)
DATE/DEPTH
R.Q.D. %
WATER LEVEL Date
DRILL WATER LOSS %
WATER PRESSURE TESTS - Lugeons or PERMEABILITY
SW, MWk, speckled gy Wh/ blk BERLINS PORPHYRY, lightly limonitised
SW, S, med to dk gy massive HORNFELS, occ. lightly foliated & bedded at 20-30°, some MW-HW MWk zones beside Sv planar heavily-limonitised joints
MW Wk coarse (sandy) dk gy HORNFELS, SoFt, with leached/discoloured gyp. vns.
UW VS Wh gy massive highly-silicified HORNFELS, jt. limonite-staining only on jt. faces
UW to SW It to dk grey HORNFELS with silicified veins and bands, heavily-limonitised joints
Transitional zone: highly siliceous HORNFELS to QUARTZITE, SW, VS, micaceous, "marbled".
SW MWk-MS speckled BERLINS PORPHYRY limonitised
UW-SW MS-S med-dk gy HORNFELS variably foliated, limonitised jts.
SW MWk speckled BERLINS PORPHYRY, limonitised Sv qtz veins, irreg. hornfels inclusions occ. areas of UW and MW rock
SW MS It-dk gy HORNFELS with frequent granitic & quartz inclusions & veins parallel to gi-mi foliation, occ. gn gy chloritised inclusions (esp. about weathered porphyry band at 86.0m
Limonite coating on jt. faces reduces below 87.80 m.
Rock V. siliceous, UW and S 88.80 - 89.40 m.
x PI = 60-130 kPa
Jr mi P S/R Fe ctd/healed, 20-50 AND Jfs Sv U S Fe/gypsum
Fissile zone, 20° to c.a.
Coarsely broken rock
Zone of close fracturing beside Sv jt: MW: 2-4cm sp.
Jfs 45° P S/R, filled Fe/gyp, occ. X cut, 10-15cm sp.
zone of rock brkn to 2-6cm frags.
Jfs 35-50° P S Fe stn, 10-20cm AND Jfs 5-20° P R Fe stn, groups of 5cm sp.
Jfs Si-Sv P/U, U, S, filled bn Fe/clay, 10-20cm sp. AND DJs mi A R cln-Fe stn, 4-20 cm sp. (occ. cross-fracturing of Sv jts.)
Jfs mi P S cln/Fe stn, 4-20cm
Jfs gc-mc P/U, R, Fe ctd, 6-10cm sp AND
Jfs Sv P S/R Fe ctd
DJs A irreg
qtz vn 60° bik P/U closed
Jfs 40° P S/R Fe ctd 10-30cm sp.
Jfs gc-Sv, P/A, R, Fe/mica, 5-15cm sp.
Jfs 50° P R Fe/mica, 12cm
chloritised qtz vein qc 5-8mm
Jfs gc-mi P/U S/R Fe, 8-25cm
DJs 5-10° P/A, S, Fe ctd
Jfs Sv-V P S Fe ctd.
Jfs gc-Sv P R/S Fe/mica, Crush seam occ. clay ctd, 5-40cm AND
Jfs Sv-V P/U S/R, Fe ctd or clean.
Jfs gc-Sc P/U, R, Fe, 5-30 cm sp. AND
Jfs Sv U R Fe/clean: often conjugate or intersecting
Crush seam: gn gy silty gravel = HW porphyry layer
DJs 0-45°, A, 2cm sp.
Jfs gc-Sc & Jfs Sv as above
Clay seam 5° 2mm thk on 2 Jfs 5° 5mm sp.
Rock irreg. broken on Jf Sv.
3/7/03
4/7/03
7/7/03
8/7/03
9/7/03
DRILLER: Atlas Drilling
STARTED: 30/6/03
FINISHED: 14/7/03
DRILL: CS-1000
ROCK WEATHERING
UW - Unweathered
SW - Slightly weathered
MW - Moderately weathered
HW - Highly weathered
CW - Completely weathered
ROCK HARDNESS
VH - Very hard
H - Hard
MH - Moderately hard
MS - Moderately soft
S - Soft
VS - Very soft
FRACTURE LOG (cms)
Spacing of natural fractures
Fractures/m of core
EXPLANATION
Defect Type
J - Joint DI - Drilling Induced
B - Bedding Clt - Cleat in coal
C - Cleavage Shr - Shear
Defect Surface
S - Smooth
A - Angular
P - Planar
C - Curved
R - Rough
U - Undulating
Orientation
Sv - Subvertical (>80°)
Si - Steeply inclined (60-80°)
mi - mod inclined (30-60°)
gi - gently inclined (<30°)
Graphic Log Key
Open infilled fracture
Discrete Joints or shears
Recessive Shearing
xxxx Crush Zone
Cleat in Coal
Rough joint
LOGGED: A. FIELD
DATE: 1/8/03
TRACED:
CHECKED:
ORIGINAL VERTICAL:
SCALE: 1:100
SHEET 3 OF 4
DRG NO
PROJECT: CYPRESS NORTH O/C
HOLE NO: 1698
LENGTH: 120.10m
CORE BOXES: 14-26 OF 37
1978 A

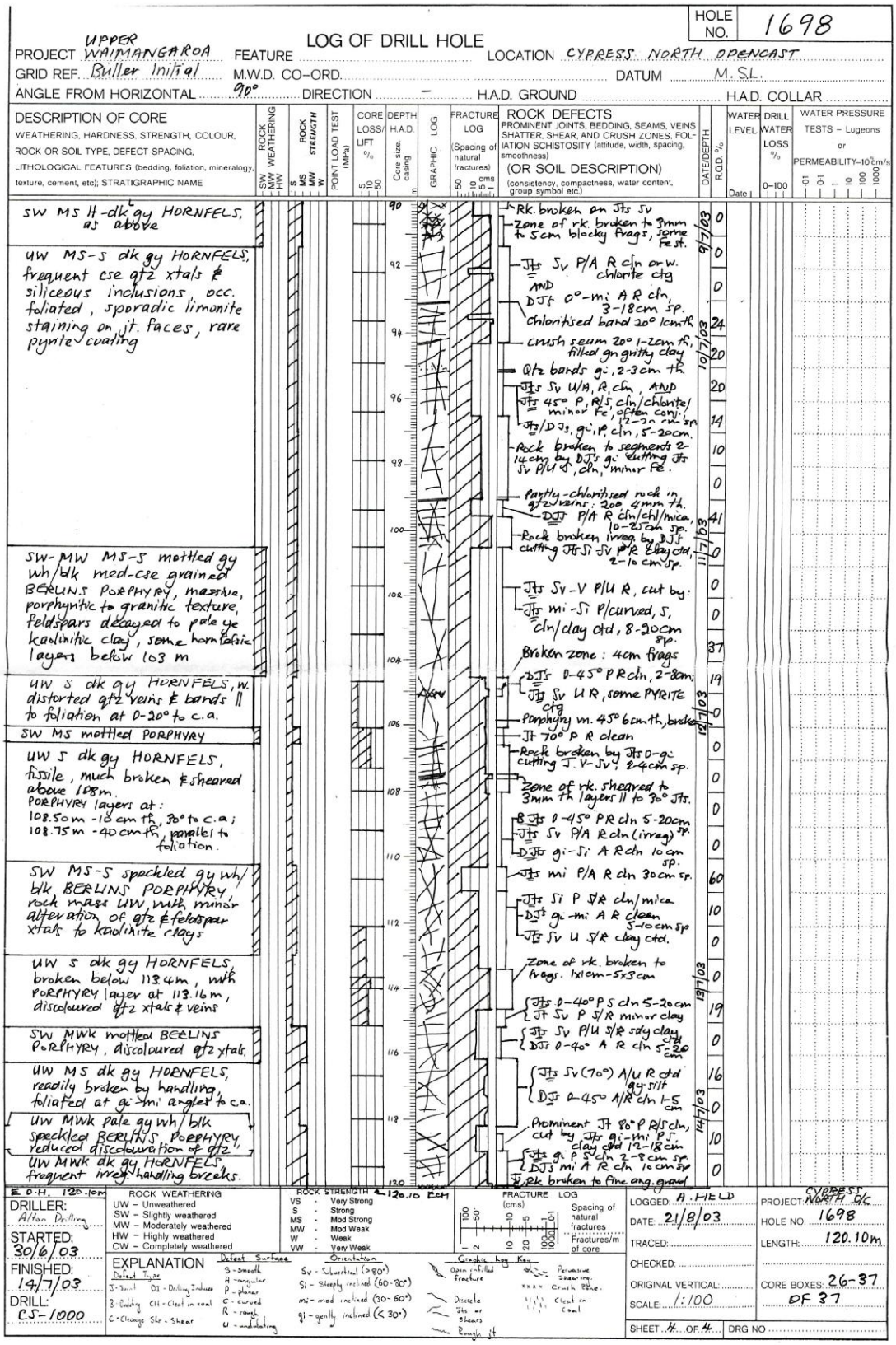
HOLE NO. 1698
LOG OF DRILL HOLE
PROJECT UPPER WAIMANGAROA FEATURE LOCATION CYPRESS NORTH OPENCAST
GRID REF. Buller Initial M.W.D. CO-ORD. DATUM M.S.L.
ANGLE FROM HORIZONTAL 90° DIRECTION – H.A.D. GROUND H.A.D. COLLAR
DESCRIPTION OF CORE
WEATHERING, HARDNESS, STRENGTH, COLOUR, ROCK OR SOIL TYPE, DEFECT SPACING, LITHOLOGICAL FEATURES (bedding, foliation, mineralogy, texture, cement, etc); STRATIGRAPHIC NAME
ROCK WEATHERING SW MW HW
ROCK STRENGTH S MS MW W
POINT LOAD TEST (MPa)
CORE LOSS/ LIFT %
DEPTH H.A.D.
GRAPHIC LOG
FRACTURE LOG (Spacing of natural fractures)
ROCK DEFECTS
PROMINENT JOINTS, BEDDING, SEAMS, VEINS SHATTER, SHEAR, AND CRUSH ZONES, FOLIATION SCHISTOSITY (attitude, width, spacing, smoothness)
(OR SOIL DESCRIPTION)
(consistency, compactness, water content, group symbol etc.)
DATE/DEPTH
R.Q.D. %
WATER LEVEL Date
DRILL WATER LOSS %
WATER PRESSURE TESTS – Lugeons or PERMEABILITY-10⁻³cm/s
SW MS lt-dk gy HORNFELS, as above
UW MS-S dk gy HORNFELS, frequent cse qtz xtals & siliceous inclusions, occ. foliated, sporadic limonite staining on jt. faces, rare pyrite coating
SW-MW MS-S mottled gy wh/dk med-cse grained BERLINS PORPHYRY, massive, porphyritic to granitic texture, feldspars decayed to pale ye kaolinitic clay, some hornfelsic layers below 103 m
UW S dk gy HORNFELS, w. distorted qtz veins & bands ∥ to foliation at 0-20° to c.a.
SW MS mottled PORPHYRY
UW S dk gy HORNFELS, fissile, much broken & sheared above 108m. PORPHYRY layers at: 108.50m -18 cm th, 30° to c.a; 108.75m -40 cm th, parallel to foliation.
SW MS-S speckled gy wh/blk BERLINS PORPHYRY, rock mass UW, with minor alteration of qtz & feldspar xtals to kaolinite clays
UW S dk gy HORNFELS, broken below 113.4m, with PORPHYRY layer at 113.16m, discoloured qtz xtals & veins
SW MWk mottled BERLINS PORPHYRY, discoloured qtz xtals.
UW MS dk gy HORNFELS, readily broken by handling, foliated at gi-mi angles to c.a.
UW MWk pale gy wh/blk speckled BERLINS PORPHYRY, reduced discolouration of qtz
UW MWk dk gy HORNFELS, frequent irreg. handling breaks.
Rk. broken on Jts Sv
Zone of rk. broken to 3mm to 5cm blocky frags, some Fe st.
Jts Sv P/A R cln or w. chlorite ctg AND DJs 0°-mi A R cln, 3-18cm sp. chloritised band 20° lcm th
crush seam 20° 1-2cm th, filled gn gritty clay
Qtz bands gi, 2-3cm th.
Jts Sv U/R, R, cln, AND Jts 45° P, R/S cln/chlorite/minor Fe, often conj. 12-20 cm sp.
Jts/D Js, gi, lP, cln, 5-20cm.
Rock broken to segments 2-10cm by DJs gi cutting Jts Sv P/U Js, cln, minor Fe.
partly-chloritised rock in qtz veins: 200 4mm th.
DJs P/A R cln/chl/mica, 10-25cm sp.
Rock broken irreg by DJs cutting Jts Si Sv P/R clay ctd, 2-10 cm sp.
Jts Sv-V P/U R, cut by: Jts mi-Si P/curved, S, cln/clay ctd, 8-20cm sp.
Broken zone: 4cm frags
DJs 0-45° P R cln, 2-8cm
Jts Sv U R, some PYRITE ctg
Porphyry vn. 45° 6cm th, broken
Jt 70° P R clean
Rock broken by Jts 0-gi cutting J. V-Sv, 2-4cm sp.
Zone of rk. sheared to 3mm th layers ∥ to 30° Jts.
B Jts 0-45° P R cln 5-20cm
Jts Sv P/A R cln (irreg) sp.
D Js gi-Si A R cln 10 cm sp.
Jts mi P/A R cln 30cm sp.
Jts Si P S/R cln/mica
DJs gi-mi A R clean 5-10 cm sp
Jts Sv U S/R clay ctd.
Zone of rk. broken to frags. 1x1cm-5x3cm
Jts 0-40° P S cln 5-20cm
Jt Sv P S/R minor clay
Jts Sv P/U S/R sdy clay ctd
DJs 0-40° A R cln 5-20 cm
Jts Sv (70°) A/U R ctd gy silt
DJs 0-45° A/R cln 1-5 cm
Prominent Jt 80° P R/S cln, cut by Jts gi-mi P S, clay ctd 12-18cm
Js gi P S cln 2-8cm sp.
DJs mi A R cln 10 cm Sv
Jt, Rk broken to fine ang. gravel
E.O.H. 120.10m
DRILLER: Allan Drilling
STARTED: 30/6/03
FINISHED: 14/7/03
DRILL: CS-1000
ROCK WEATHERING
UW – Unweathered
SW – Slightly weathered
MW – Moderately weathered
HW – Highly weathered
CW – Completely weathered
ROCK STRENGTH
VS - Very Strong
S - Strong
MS - Mod Strong
MW - Mod Weak
W - Weak
VW - Very Weak
2 120.10 EOH
FRACTURE LOG (cms) Spacing of natural fractures Fractures/m of core
EXPLANATION
Defect Type
J - Joint D1 - Drilling Induced
B - Bedding Cli - Clast in coal
C - Cleavage Slr - Shear
Defect Surface
S - smooth
A - angular
P - planar
C - curved
R - rough
U - undulating
Orientation
Sv - Subvertical (>80°)
Si - Steeply inclined (60-80°)
mi - mod inclined (30-60°)
gi - gently inclined (<30°)
Graphic Log Key
Open infilled fracture
Discrete Jts or Shears
Rough jt
Pervasive Shearing
Crush Zone
Clast in Coal
LOGGED: A. FIELD
DATE: 21/8/03
TRACED:
CHECKED:
ORIGINAL VERTICAL:
SCALE: 1:100
SHEET 4 OF 4
DRG NO
PROJECT: CYPRESS NORTH OC
HOLE NO: 1698
LENGTH: 120.10m
CORE BOXES: 26-37 OF 37

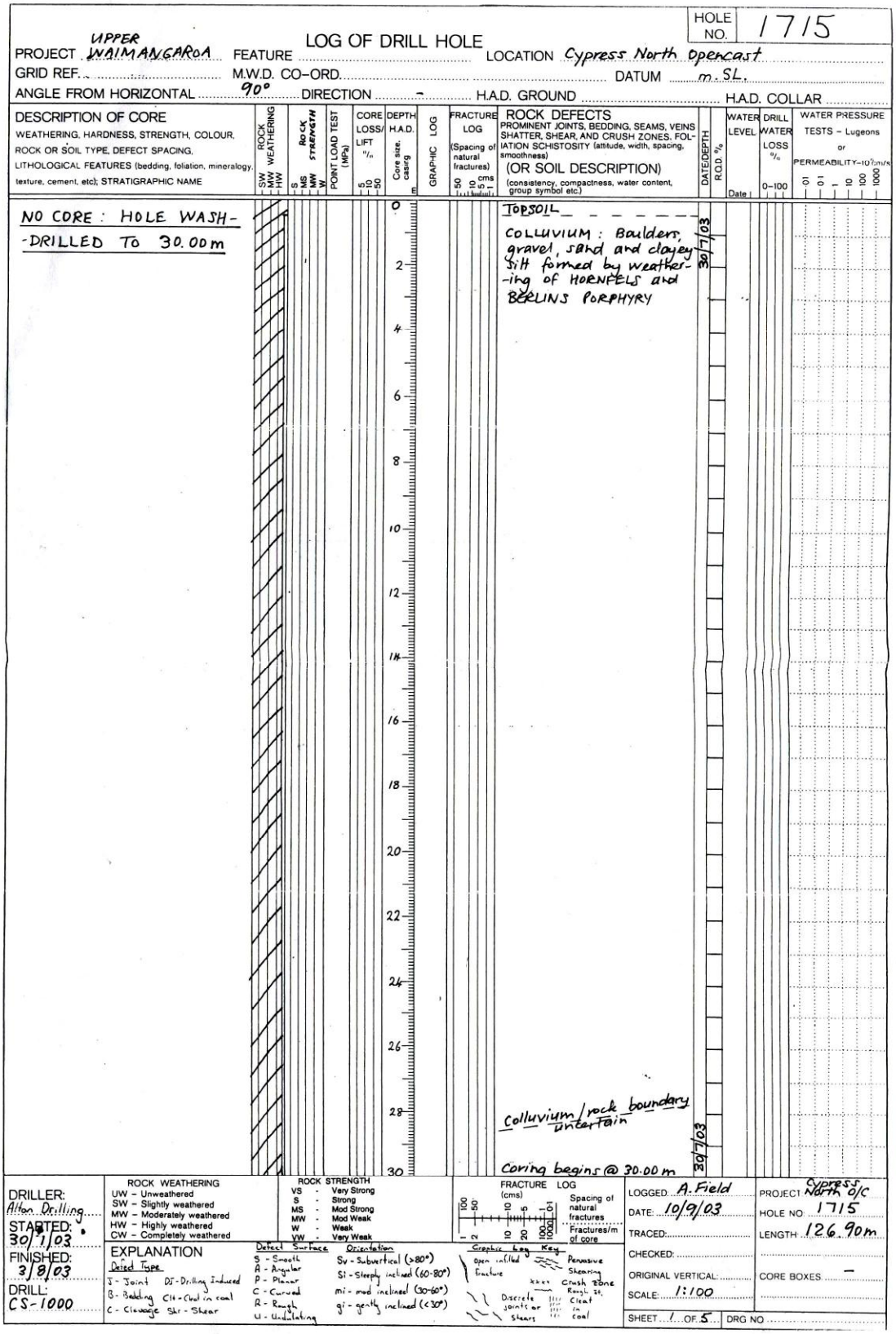

LOG OF DRILL HOLE

HOLE NO. 1715

PROJECT UPPER WAIMANGAROA FEATURE LOCATION Cypress North opencast

GRID REF. M.W.D. CO-ORD. DATUM m.SL.

ANGLE FROM HORIZONTAL 90° DIRECTION - H.A.D. GROUND H.A.D. COLLAR

DESCRIPTION OF CORE
WEATHERING, HARDNESS, STRENGTH, COLOUR, ROCK OR SOIL TYPE, DEFECT SPACING, LITHOLOGICAL FEATURES (bedding, foliation, mineralogy, texture, cement, etc); STRATIGRAPHIC NAME

ROCK WEATHERING: SW – MW – HW

ROCK STRENGTH: S – MS – MW – W

POINT LOAD TEST (MPa): 5 – 50

CORE LOSS/LIFT %: 5 – 50

DEPTH H.A.D. Core size, casing

GRAPHIC LOG

FRACTURE LOG (Spacing of natural fractures): 50 – 10 – cms

ROCK DEFECTS
PROMINENT JOINTS, BEDDING, SEAMS, VEINS SHATTER, SHEAR, AND CRUSH ZONES, FOLIATION SCHISTOSITY (attitude, width, spacing, smoothness)
(OR SOIL DESCRIPTION)
(consistency, compactness, water content, group symbol etc.)

DATE/DEPTH

R.Q.D. %

WATER LEVEL Date

DRILL WATER LOSS % 0–100

WATER PRESSURE TESTS – Lugeons or PERMEABILITY–10⁻⁵cm/s: .01 – .01 – 1 – 10 – 100 – 1000

NO CORE : HOLE WASH-
-DRILLED TO 30.00m

0 TOPSOIL

COLLUVIUM : Boulders, gravel, sand and clayey silt formed by weathering of HORNFELS and BERLINS PORPHYRY

30/7/03

2 4 6 8 10 12 14 16 18 20 22 24 26 28 30

Colluvium/rock boundary uncertain

30/7/03

Coring begins @ 30.00 m

DRILLER: Alton Drilling
STARTED: 30/7/03
FINISHED: 3/8/03
DRILL: CS-1000

ROCK WEATHERING
UW – Unweathered
SW – Slightly weathered
MW – Moderately weathered
HW – Highly weathered
CW – Completely weathered

ROCK STRENGTH
VS – Very Strong
S – Strong
MS – Mod Strong
MW – Mod Weak
W – Weak
VW – Very Weak

FRACTURE LOG (cms): 100 – 50 – 10 – up – 0.1 – 10 – 20 – 100 – 1000 – cv
Spacing of natural fractures
Fractures/m of core

EXPLANATION
Defect Type
J - Joint DI - Drilling Induced
B - Bedding Clt - Clay in coal
C - Cleavage Shr - Shear

Defect Surface
S - Smooth
A - Angular
P - Planar
C - Curved
R - Rough
U - Undulating

Orientation
Sv - Subvertical (>80°)
St - Steeply inclined (60-80°)
mi - mod inclined (30-60°)
gi - gently inclined (<30°)

Graphic Log Key
open infilled fracture
Permissive Shearing
Crush Zone
Rough jt.
Clean
in coal
Discrete joints or Shears

LOGGED: A. Field
DATE: 10/9/03
TRACED:
CHECKED:
ORIGINAL VERTICAL:
SCALE: 1:100
SHEET 1 OF 5

PROJECT Cypress North O/C
HOLE NO. 1715
LENGTH 126.90m
CORE BOXES –
DRG NO

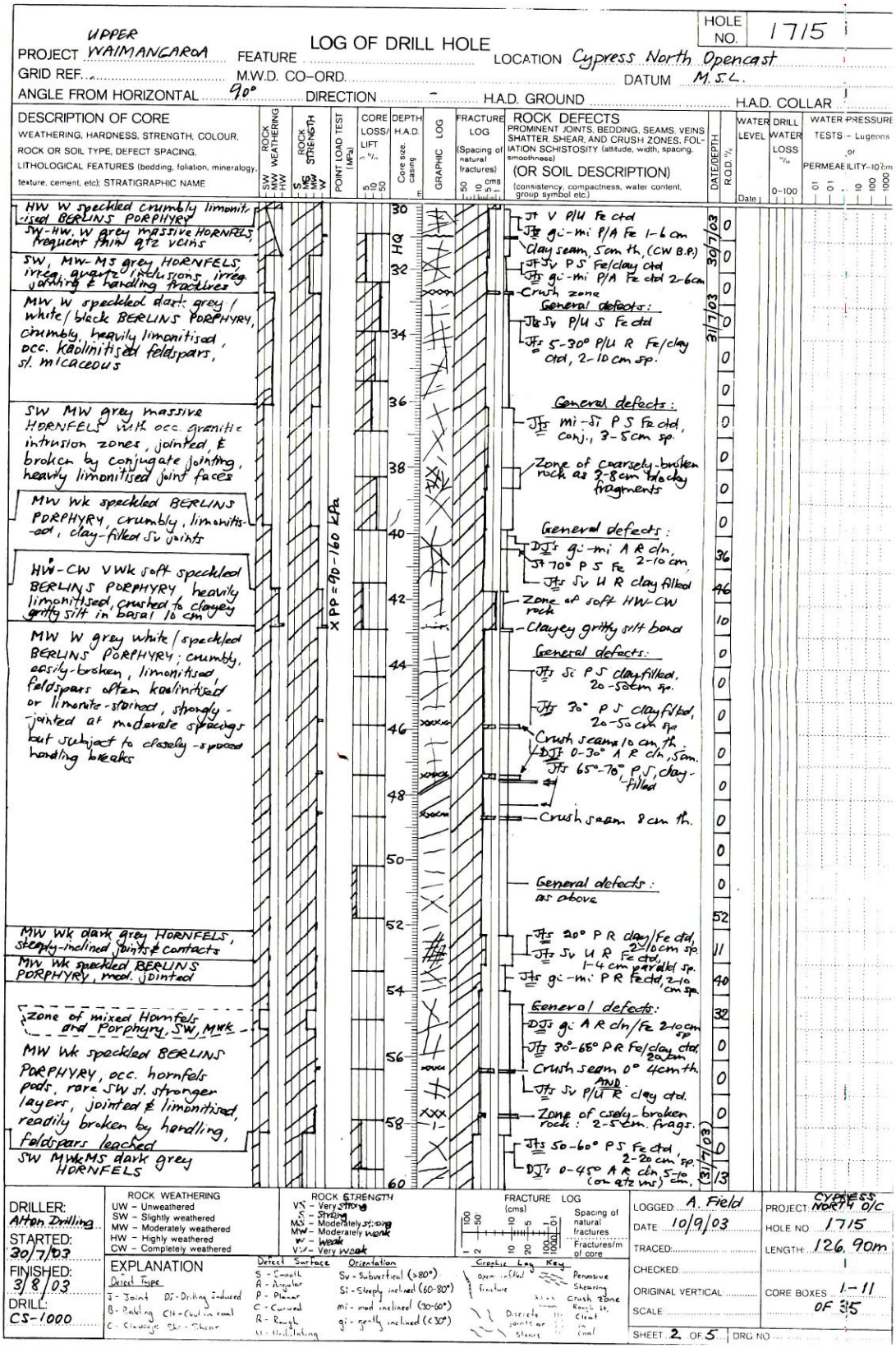
LOG OF DRILL HOLE
HOLE NO. 1715
PROJECT UPPER WAIMANGAROA FEATURE LOCATION Cypress North Opencast
GRID REF. M.W.D. CO-ORD. DATUM M.S.L.
ANGLE FROM HORIZONTAL 90° DIRECTION - H.A.D. GROUND H.A.D. COLLAR
DESCRIPTION OF CORE
WEATHERING, HARDNESS, STRENGTH, COLOUR, ROCK OR SOIL TYPE, DEFECT SPACING, LITHOLOGICAL FEATURES (bedding, foliation, mineralogy, texture, cement, etc); STRATIGRAPHIC NAME
ROCK WEATHERING
ROCK STRENGTH
POINT LOAD TEST (MPa)
CORE LOSS/ LIFT
DEPTH H.A.D.
GRAPHIC LOG
FRACTURE LOG (Spacing of natural fractures)
ROCK DEFECTS
PROMINENT JOINTS, BEDDING, SEAMS, VEINS SHATTER, SHEAR, AND CRUSH ZONES, FOLIATION SCHISTOSITY (attitude, width, spacing, smoothness)
(OR SOIL DESCRIPTION)
(consistency, compactness, water content, group symbol etc.)
DATE/DEPTH
R.Q.D. %
WATER LEVEL
DRILL WATER LOSS
WATER PRESSURE TESTS - Lugeons or PERMEABILITY - m/s
HW W speckled crumbly limonitised BERLINS PORPHYRY
SW-HW, W grey massive HORNFELS frequent thin qtz veins
SW, MW-MS grey HORNFELS, irreg. quartz inclusions, irreg. jointing & handling fractures
MW W speckled dark grey / white / black BERLINS PORPHYRY, crumbly, heavily limonitised, occ. kaolinitised feldspars, sl. micaceous
SW MW grey massive HORNFELS with occ. granitic intrusion zones, jointed & broken by conjugate jointing, heavily limonitised joint faces
MW Wk speckled BERLINS PORPHYRY, crumbly, limonitised, clay-filled Sv joints
HW-CW VWk soft speckled BERLINS PORPHYRY heavily limonitised, crushed to clayey gritty silt in basal 10 cm
MW W grey white / speckled BERLINS PORPHYRY; crumbly, easily-broken, limonitised, feldspars often kaolinitised or limonite-stained, strongly-jointed at moderate spacings but subject to closely-spaced handling breaks
MW Wk dark grey HORNFELS, steeply-inclined joints & contacts
MW Wk speckled BERLINS PORPHYRY, mod. jointed
zone of mixed Hornfels and Porphyry, SW, MWk
MW Wk speckled BERLINS PORPHYRY, occ. hornfels pods, rare SW sl. stronger layers, jointed & limonitised, readily broken by handling, feldspars leached
SW MWk MS dark grey HORNFELS
X PP = 90-160 kPa
HQ
Jt V P/U Fe ctd
Jfs gi-mi P/A Fe 1-6 cm
clay seam, 5cm th. (CW B.P.)
JFs Sv P S Fe/clay ctd
Jfs gi-mi P/A Fe ctd 2-6cm
Crush zone
General defects:
Jfs Sv P/U S Fe ctd
Jfs 5-30° P/U R Fe/clay ctd, 2-10 cm sp.
General defects:
Jfs mi-Si P S Fe ctd, conj., 3-5cm sp.
Zone of coarsely-broken rock as 2-8cm blocky fragments
General defects:
DJfs gi-mi A R c/n, 2-10 cm
Jfs 70° P S Fe
Jfs Sv U R clay filled
Zone of soft HW-CW rock
Clayey gritty silt band
General defects:
Jfs Si P S clay-filled, 20-50cm sp.
Jfs 30° P S clay filled, 20-50 cm sp.
Crush seams 10 cm th.
DJfs 0-30° A R c/n, 5cm.
Jfs 65°-70° P S, clay-filled
Crush seam 8 cm th.
General defects:
as above
Jfs 20° P R clay/Fe ctd, 2-10cm sp.
Jfs Sv U R Fe ctd, 1-4 cm parallel sp.
Jfs gi-mi P R Fe ctd, 2-10 cm sp.
General defects:
DJfs gi A R c/n/Fe 2-10cm sp.
Jfs 30°-65° P R Fe/clay ctd, 20cm
Crush seam 0° 4cm th.
AND:
Jfs Sv P/U R clay ctd.
Zone of csely-broken rock: 2-5cm frags.
Jfs 50-60° P S Fe ctd, 2-20 cm sp.
DJfs 0-45° A R c/n 5-10 cm. (on qtz vns)
30/7/03
31/7/03
31/7/03
ROCK WEATHERING
UW - Unweathered
SW - Slightly weathered
MW - Moderately weathered
HW - Highly weathered
CW - Completely weathered
ROCK STRENGTH
VS - Very Strong
S - Strong
MS - Moderately strong
MW - Moderately weak
W - Weak
VW - Very weak
FRACTURE LOG (cms)
Spacing of natural fractures
Fractures/m of core
EXPLANATION
Defect Type
J - Joint DI - Drilling Induced
B - Parting CH - Clast in rock
C - Cleavage Shr - Shear
Defect Surface
S - Smooth
A - Angular
P - Planar
C - Curved
R - Rough
U - Undulating
Orientation
Sv - Subvertical (>80°)
Si - Steeply inclined (60-80°)
mi - mod inclined (30-60°)
gi - gently inclined (<30°)
Graphic Log Key
Open infilled
Fracture
Pervasive Shearing
Crush Zone
Broken rock etc.
Discrete joints or shears
Clast
Coal
DRILLER: Alton Drilling
STARTED: 30/7/03
FINISHED: 3/8/03
DRILL: CS-1000
LOGGED: A. Field
DATE 10/9/03
TRACED:
CHECKED:
ORIGINAL VERTICAL
SCALE:
PROJECT: CYPRESS NORTH O/C
HOLE NO 1715
LENGTH: 126.90m
CORE BOXES 1-11 OF 35
SHEET 2 OF 5
DRG NO

LOG OF DRILL HOLE

HOLE NO. 1715

PROJECT: UPPER WAIMANGAROA
FEATURE: ...
LOCATION: Cypress North Opencast
GRID REF.: Buller Inlier
M.W.D. CO-ORD.: ...
DATUM: M.S.L.
ANGLE FROM HORIZONTAL: 90°
DIRECTION: –
H.A.D. GROUND: ...
H.A.D. COLLAR: ...

DESCRIPTION OF CORE (weathering, hardness, strength, colour, rock or soil type, defect spacing, lithological features (bedding, foliation, mineralogy, texture, cement, etc); stratigraphic name)	ROCK DEFECTS (prominent joints, bedding, seams, veins, shatter, shear, and crush zones, foliation, schistosity (attitude, width, spacing, smoothness)) (OR SOIL DESCRIPTION)
SW MWk-MS dark grey massive HORNFELS, jointed with variable spacing, limonitic coating on joint faces, often with contorted qtz veins. Occasional 8-12cm thick intrusions of MW-HW PORPHYRY, VWk, slt. crumbly, with leached feldspars. Becomes paler and greenish-grey below 65.7m	Jts 50-60° P S Fe ctd, 2-20cm. DJs 0-45° A R cln, 5-10cm. Zone of parallel Jts 55° @ 5cm sp., Fe ctd. Jts Sv U S Fe ctd. Zone of rock broken to 1-5 cm frags. **General defects:** 50-60° Jts & DJs, as above. Crush seam 45° 8mm th, sl. clayey. Irregular weathered porphyry intrusions. **General defects as above.** Zone of coarsely broken rock, 1x4cm frags. Weathered porphyry layer
SW MS med to dark grey massive HORNFELS, with thin contorted qtz veins occ. replaced by gypsum, becomes coarse grained 70.7-71.3m, broken zones about MW porphyry layers	Jts gi P/A R Fe ctd, 3-8 cm. Jts Sv U/P qtz/gypsum filled (pervasive). Jts 0-20° A R Fe stained 20-30 cm sp. Jts 55-65° P S Fe stnd
SW-MW, MWk med to dk grey massive HORNFELS, heavily fractured in zones, limonitised jts.	Jts Si-Sv P/U S/R Fe ctd 10-20cm sp. Jts 0°-mi A R Fe, 2-8cm sp. Freq. zones rock broken to 4cm frags
SW MS dk grey massive HORNFELS, occ. "foliated" at 60°, freq. intruded by bands of MW Wk BERLINS PORPHYRY (50%), limonitised jt. faces.	Jts Si P R Fe ctd 5-10cm sp. Jts Sv U R Fe ctd. DJs 0-mi A R cln/Fe, 3-10 cm. Coarsely broken zone 2-5cm. Finely broken zone 1-2cm incl. 40°
MW Wk grey/white speckled BERLINS PORPHYRY mod. fractured & crushed, variably limonitised, feldspars leached, occ. crush zones: fine qtz gravel to coarse sand	NO CORE – CORE LOSS IN FINELY BROKEN / CRUSHED ROCK. **General defects:** Jts Sv P/U S Feox filled 1-3 mm. Jts mi-Si P/A R, Fe ctd, 2-5cm sp. Core loss zone in crushed rock
SW-MW Hornfels	Crush seam gi 3cm th. Jt 50° P S. Fe/clay/mica ctd.
SW-MW, MWk grey/white BERLINS PORPHYRY, limonitised, feldspars often kaolinitised, mica & clay also coating jt. faces, mod. jtd. & fractured, occ. MS zones, with small oval pods of hornfels becoming more frequent below 83.9 m.	**General defects:** Jts Sv-V P/U S, Fe/clay/mica ctd. Jts mi-Si P/U S/R, " ctd, 10-20cm sp. DJs 0°-mi A R cln/Fe stn, 5-10cm sp. Rock crushed & broken in 5cm slabs. Zone of MW broken rock in 5cm tabular frags

Core size: HQ. Depth (H.A.D., m): 62, 64, 66, 68, 70, 72, 74, 76, 78, 80, 82, 84, 86, 88, 90

Date/Depth: 31/7/03; 1/8/03; 2/8/03

R.Q.D. %: 34, 0, 20, 0, 0, 0, 0, 0, 0, 0, 0, 0, 0, 0, 0, 0, 0, 0, 0, 0, 11, 12, 0, 0, 0, 0, 0, 0, 0

DRILLER: Aitken Drilling
STARTED: 30/7/03
FINISHED: 3/8/03
DRILL: CS-1000

ROCK WEATHERING
UW – Unweathered
SW – Slightly weathered
MW – Moderately weathered
HW – Highly weathered
CW – Completely weathered

ROCK STRENGTH
VS – Very strong
S – Strong
MS – Moderately strong
MW – Moderately weak
W – Weak
VW – Very weak

FRACTURE LOG (cms): 100, 50, 10, 5, 1, 0.1 – Spacing of natural fractures; 1, 2, 10, 20, 100, 1000 – Fractures/m of core

EXPLANATION

Defect Type: J – Joint; DI – Drilling Induced; B – Bedding; Clt – Cleat in coal; C – Cleavage; Shr – Shear

Defect Surface: S – Smooth; A – Angular; P – Planar; C – Curved; R – Rough; U – Undulating

Orientation: Sv – Subvertical (>80°); Si – Steeply inclined (60-80°); mi – mod inclined (30-60°); gi – gently inclined (<30°)

Graphic Log Key: Open infilled fracture; Pervasive Shearing; xxxx Crush Zone; Discrete Joints or Shears; Cleat in Coal; Rough joint

LOGGED: A. Field
DATE: 12/9/03
TRACED: ...
CHECKED: ...
ORIGINAL VERTICAL: ...
SCALE: 1:100
SHEET 3 OF 5
PROJECT: CYPRESS NORTH O/C
HOLE NO: 1715
LENGTH: 126.90m
CORE BOXES: 11 – 21 OF 35
DRG NO: ...

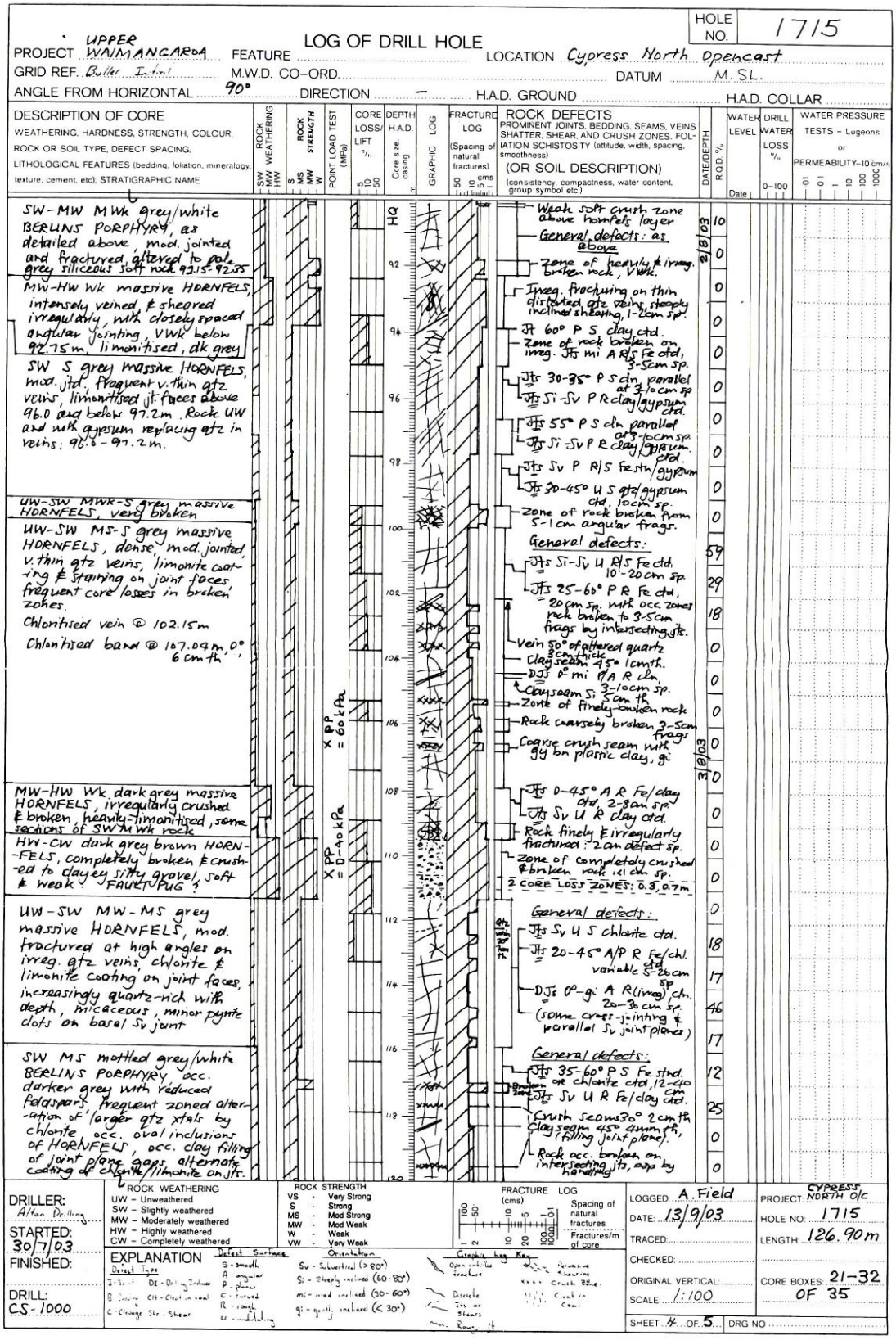
LOG OF DRILL HOLE
HOLE NO. 1715
PROJECT UPPER WAIMANGAROA FEATURE
LOCATION Cypress North Opencast
GRID REF. Buller I-Int M.W.D. CO-ORD.
DATUM M.S.L.
ANGLE FROM HORIZONTAL 90° DIRECTION —
H.A.D. GROUND H.A.D. COLLAR
DESCRIPTION OF CORE
WEATHERING, HARDNESS, STRENGTH, COLOUR, ROCK OR SOIL TYPE, DEFECT SPACING, LITHOLOGICAL FEATURES (bedding, foliation, mineralogy, texture, cement, etc), STRATIGRAPHIC NAME
ROCK WEATHERING
ROCK STRENGTH
POINT LOAD TEST (MPa)
CORE LOSS/ LIFT
DEPTH H.A.D.
Core size casing
GRAPHIC LOG
FRACTURE LOG (Spacing of natural fractures)
ROCK DEFECTS
PROMINENT JOINTS, BEDDING, SEAMS, VEINS SHATTER, SHEAR, AND CRUSH ZONES. FOLIATION SCHISTOSITY (attitude, width, spacing, smoothness)
(OR SOIL DESCRIPTION)
(consistency, compactness, water content, group symbol etc.)
DATE/DEPTH
R.Q.D.
WATER LEVEL
DRILL WATER LOSS
WATER PRESSURE TESTS – Lugeons or PERMEABILITY
SW-MW MWk grey/white BERLINS PORPHYRY, as detailed above, mod. jointed and fractured, altered to pale grey siliceous soft rock 92.15-92.35
MW-HW Wk massive HORNFELS, intensely veined & sheared irregularly, with closely spaced angular jointing, VWk below 92.75m, limonitised, dk grey
SW S grey massive HORNFELS, mod. jtd., frequent v. thin qtz veins, limonitised jt faces above 96.0 and below 97.2m. Rock UW and with gypsum replacing qtz in veins: 96.0-97.2m.
UW-SW MWk-S grey massive HORNFELS, very broken
UW-SW MS-S grey massive HORNFELS, dense, mod. jointed, v. thin qtz veins, limonite coating & staining on joint faces, frequent core losses in broken zones.
Chloritised vein @ 102.15m
Chloritised band @ 107.09m, 0° 6cm th.
MW-HW Wk dark grey massive HORNFELS, irregularly crushed & broken, heavily limonitised, some sections of SW MWk rock
HW-CW dark grey brown HORNFELS, completely broken & crushed to clayey silty gravel, soft & weak FAULT/PUG ?
UW-SW MW-MS grey massive HORNFELS, mod. fractured at high angles on irreg. qtz veins, chlorite & limonite coating on joint faces, increasingly quartz-rich with depth, micaceous, minor pyrite dots on basal Sv joint
SW MS mottled grey/white BERLINS PORPHYRY, occ. darker grey with reduced feldspars, frequent zoned alteration of larger qtz xtals by chlorite, occ. oval inclusions of HORNFELS, occ. clay filling of joint plane gaps, alternate coating of chlorite/limonite on jts.
X PP = 60 kPa
X PP = 0-40 kPa
Weak soft crush zone above hornfels layer
General defects: as above
Zone of heavily & irreg. broken rock, VWk.
Irreg. fracturing on thin distorted qtz veins, steeply inclined shearing, 1-2cm sp.
Jt 60° P S clay ctd.
Zone of rock broken on irreg. Jts mi A R/S Fe ctd, 3-5cm sp.
Jts 30-35° P S cln, parallel at 3-10cm sp
Jts Si-Sv P R clay/gypsum ctd.
Jts 55° P S cln parallel at 3-10cm sp.
Jts Si-Sv P R clay/gypsum ctd.
Jts Sv P R/S Fe stn/gypsum ctd.
Jts 30-45° U S qtz/gypsum ctd, 10cm sp.
Zone of rock broken from 5-1cm angular frags.
General defects:
Jts Si-Sv U R/S Fe ctd. 10-20cm sp.
Jts 25-60° P R Fe ctd, 20cm sp. with occ zones rock broken to 3-5cm frags by intersecting jts.
Vein 30° of altered quartz & chlorite
Clay seam 45° 1cm th.
Djs 0° mi P/A R cln.
Clay seam Si 3-10cm sp.
Clay seam Si 5cm th.
Zone of finely broken rock
Rock coarsely broken 2-5cm frags
Coarse crush seam with gg on plastic clay, gi
Jts 0-45° A R Fe/clay ctd, 2-8cm sp.
Jts Sv U R clay ctd.
Rock finely & irregularly fractured 2cm defect sp.
Zone of completely crushed & broken rock 1cl cln sp.
2 CORE LOSS ZONES: 0.3, 0.7m
General defects:
Jts Sv U S chlorite ctd.
Jts 20-45° A/P R Fe/chl. ctd variable 5-20cm sp
Djs 0°-gi A R(irreg) cln. 20-30cm sp.
(some cross-jointing & parallel Sv joint planes)
General defects:
Jts 35-60° P S Fe stnd. or chlorite ctd, 12-40cm
Jts Sv U R Fe/clay ctd.
Crush seams 30° 2cm th
Clay seam 45° 2mm th, (filling joint plane).
Rock occ. broken on intersecting jts, easy by handling
DRILLER: Alton Drilling
STARTED: 30/7/03
FINISHED:
DRILL: CS-1000
ROCK WEATHERING
UW – Unweathered
SW – Slightly weathered
MW – Moderately weathered
HW – Highly weathered
CW – Completely weathered
ROCK STRENGTH
VS - Very Strong
S - Strong
MS - Mod Strong
MW - Mod Weak
W - Weak
VW - Very Weak
FRACTURE LOG (cms) Spacing of natural fractures Fractures/m of core
EXPLANATION
Defect Type
Defect Surface
Orientation
Graphic Log Key
LOGGED: A. Field
DATE: 13/9/03
TRACED:
CHECKED:
ORIGINAL VERTICAL:
SCALE: 1:100
SHEET 4 OF 5
DRG NO
PROJECT: CYPRESS NORTH O/C
HOLE NO: 1715
LENGTH: 126.90m
CORE BOXES: 21-32 OF 35

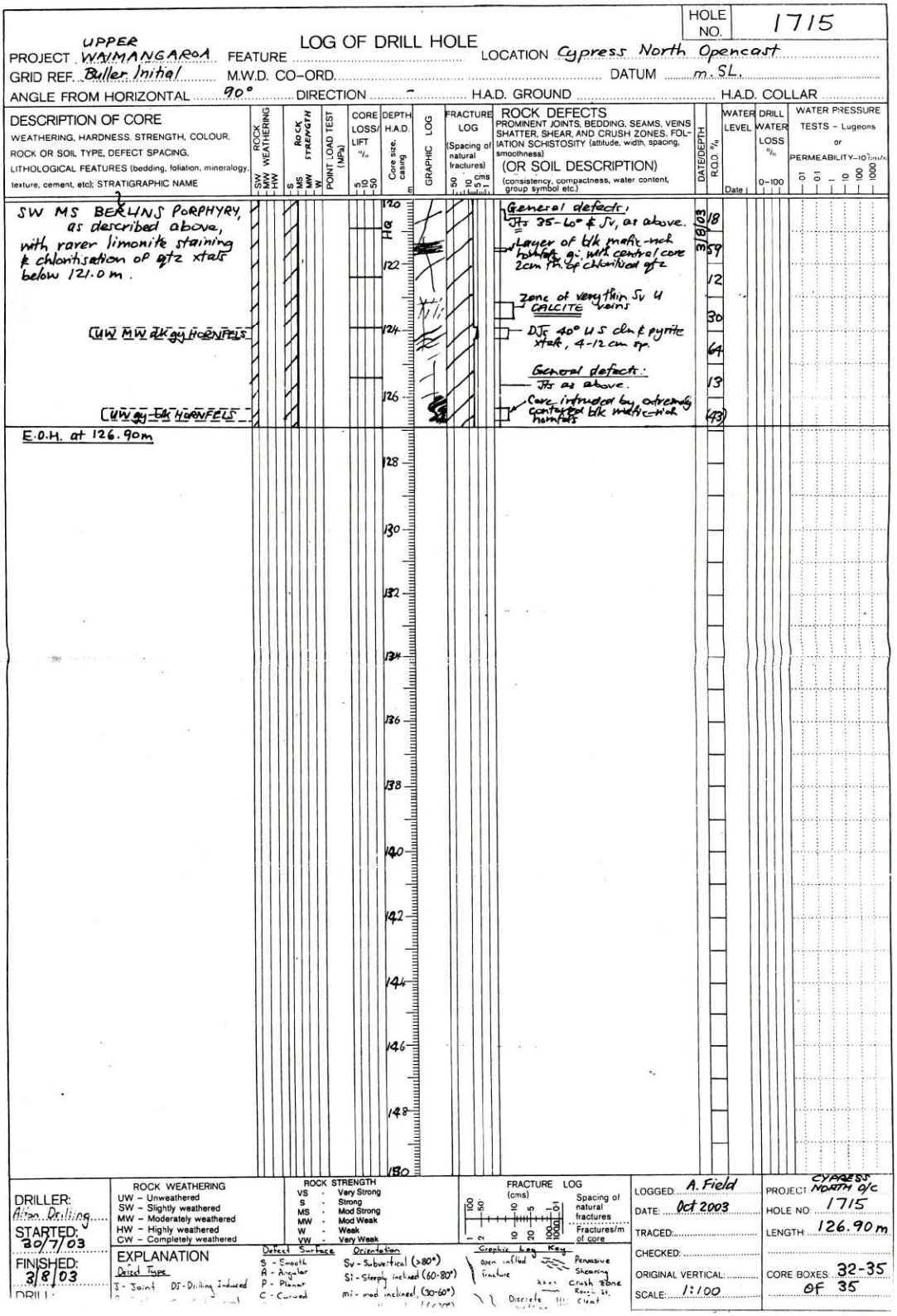

LOG OF DRILL HOLE

HOLE NO. 1715

PROJECT UPPER WAIMANGAROA FEATURE LOCATION Cypress North Opencast

GRID REF. Buller Initial M.W.D. CO-ORD. DATUM m.SL.

ANGLE FROM HORIZONTAL 90° DIRECTION - H.A.D. GROUND H.A.D. COLLAR

DESCRIPTION OF CORE
WEATHERING, HARDNESS, STRENGTH, COLOUR, ROCK OR SOIL TYPE, DEFECT SPACING, LITHOLOGICAL FEATURES (bedding, foliation, mineralogy, texture, cement, etc); STRATIGRAPHIC NAME

ROCK WEATHERING: SW – SW – HW

ROCK STRENGTH: S – MS – MW – W

POINT LOAD TEST (MPa)

CORE LOSS/LIFT %

DEPTH H.A.D. m

Core size, casing

GRAPHIC LOG

FRACTURE LOG (Spacing of natural fractures) cms

ROCK DEFECTS
PROMINENT JOINTS, BEDDING, SEAMS, VEINS SHATTER, SHEAR, AND CRUSH ZONES, FOLIATION SCHISTOSITY (attitude, width, spacing, smoothness)
(OR SOIL DESCRIPTION)
(consistency, compactness, water content, group symbol etc.)

DATE/DEPTH

R.Q.D. %

WATER LEVEL Date

DRILL WATER LOSS %

WATER PRESSURE TESTS – Lugeons or PERMEABILITY – 10^{-3} cm/s

SW MS BERLINS PORPHYRY, as described above, with rarer limonite staining & chloritisation of qtz xtals below 121.0 m.

CUW MW dk gy HORNFELS

CUW gy-blk HORNFELS

E.O.H. at 126.90m

General defects:
JTs 35-40° & Sv, as above.

Layer of blk mafic-rich hornfels, qz. vnlt central core 2cm th. & chloritised qtz

Zone of very thin Sv & CALCITE veins

DJs 40° U S clay & pyrite stain, 4-12 cm op.

General defects:
JTs as above.

Core intruded by extremely contorted blk mafic-rich hornfels

3/8/03 18 59 12 30 64 13 (43)

DRILLER: Allen Drilling
STARTED: 30/7/03
FINISHED: 3/8/03

ROCK WEATHERING
UW – Unweathered
SW – Slightly weathered
MW – Moderately weathered
HW – Highly weathered
CW – Completely weathered

ROCK STRENGTH
VS – Very Strong
S – Strong
MS – Mod Strong
MW – Mod Weak
W – Weak
VW – Very Weak

FRACTURE LOG (cms) Spacing of natural fractures Fractures/m of core

EXPLANATION
Defect Type
J – Joint DJ – Drilling Induced

Defect Surface
S – Smooth
A – Angular
P – Planar
C – Curved

Orientation
Sv – Subvertical (>80°)
St – Steeply inclined (60-80°)
mi – mod inclined (30-60°)

Graphic Log Key
Open infilled fracture
Pervasive Shearing
Crush Zone
Discrete Clay

LOGGED: A. Field
DATE: Oct 2003
TRACED:
CHECKED:
ORIGINAL VERTICAL:
SCALE: 1:100

PROJECT: CYPRESS NORTH O/C
HOLE NO: 1715
LENGTH: 126.90m
CORE BOXES: 32-35
OF 35

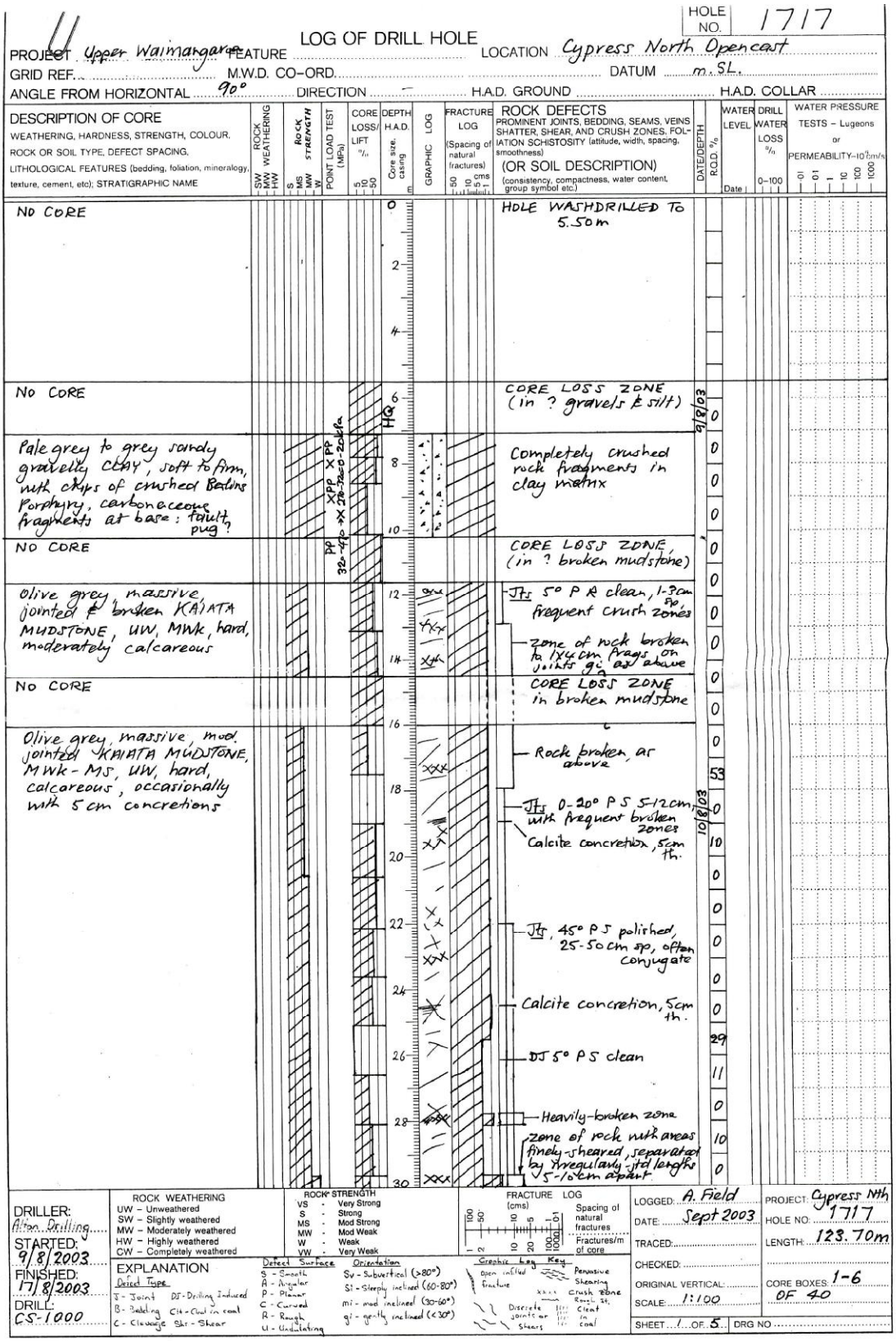
HOLE NO. 1717
LOG OF DRILL HOLE
PROJECT Upper Waimangaroa FEATURE LOCATION Cypress North Opencast
GRID REF. M.W.D. CO-ORD. DATUM m.SL.
ANGLE FROM HORIZONTAL 90° DIRECTION – H.A.D. GROUND H.A.D. COLLAR
DESCRIPTION OF CORE
WEATHERING, HARDNESS, STRENGTH, COLOUR, ROCK OR SOIL TYPE, DEFECT SPACING, LITHOLOGICAL FEATURES (bedding, foliation, mineralogy, texture, cement, etc); STRATIGRAPHIC NAME
ROCK WEATHERING SW MW HW
ROCK STRENGTH S MS MW W
POINT LOAD TEST (MPa)
CORE LOSS/ LIFT %
DEPTH H.A.D. Core size, casing m
GRAPHIC LOG
FRACTURE LOG (Spacing of natural fractures) cms
ROCK DEFECTS PROMINENT JOINTS, BEDDING, SEAMS, VEINS, SHATTER, SHEAR, AND CRUSH ZONES. FOLIATION SCHISTOSITY (attitude, width, spacing, smoothness)
(OR SOIL DESCRIPTION) (consistency, compactness, water content, group symbol etc.)
DATE/DEPTH
R.Q.D. %
WATER LEVEL Date
DRILL WATER LOSS %
WATER PRESSURE TESTS – Lugeons or PERMEABILITY–10⁻²cm/s
NO CORE
HOLE WASHDRILLED TO 5.50m
NO CORE
CORE LOSS ZONE (in ? gravels & silt)
9/8/03
Pale grey to grey sandy gravelly CLAY, soft to firm, with chips of crushed Basins Porphyry, carbonaceous fragments at base: fault gug?
XPP XPP
32-42° → X 28-36° to 2cm fa
Completely crushed rock fragments in clay matrix
NO CORE
CORE LOSS ZONE (in ? broken mudstone)
Olive grey, massive, jointed & broken KAIATA MUDSTONE, UW, MWk, hard, moderately calcareous
Jts 5° P R clean, 1-3cm sp, frequent crush zones
zone of rock broken to 1x4 cm frags on joints gi as above
NO CORE
CORE LOSS ZONE in broken mudstone
Olive grey, massive, mod jointed KAIATA MUDSTONE, MWk-MS, UW, hard, calcareous, occasionally with 5cm concretions
Rock broken as above
Jts 0-20° P S 5-12cm, with frequent broken zones
10/8/03
Calcite concretion, 5cm th.
Jts, 45° P S polished, 25-50cm sp, often conjugate
Calcite concretion, 5cm th.
DJ 5° P S clean
Heavily-broken zone
zone of rock with areas finely-sheared, separated by irregularly-jtd lengths 5-10cm apart
DRILLER: Alton Drilling
STARTED: 9/8/2003
FINISHED: 17/8/2003
DRILL: CS-1000
ROCK WEATHERING
UW – Unweathered
SW – Slightly weathered
MW – Moderately weathered
HW – Highly weathered
CW – Completely weathered
ROCK STRENGTH
VS - Very Strong
S - Strong
MS - Mod Strong
MW - Mod Weak
W - Weak
VW - Very Weak
FRACTURE LOG (cms) Spacing of natural fractures
Fractures/m of core
EXPLANATION
Defect Type
J - Joint DI - Drilling Induced
B - Bedding Clt - Clvd in coal
C - Cleavage Shr - Shear
Defect Surface
S - Smooth
A - Angular
P - Planar
C - Curved
R - Rough
U - Undulating
Orientation
Sv - Subvertical (>80°)
St - Steeply inclined (60-80°)
mi - mod inclined (30-60°)
gi - gently inclined (<30°)
Graphic Log Key
Open infilled fracture
Pervasive Shearing
Crush Zone
Bands Sh.
Discrete joints or shears
Cleat in coal
LOGGED: A. Field
DATE: Sept 2003
TRACED:
CHECKED:
ORIGINAL VERTICAL:
SCALE: 1:100
SHEET 1 OF 5
DRG NO
PROJECT: Cypress Nth
HOLE NO: 1717
LENGTH: 123.70m
CORE BOXES: 1-6 OF 40

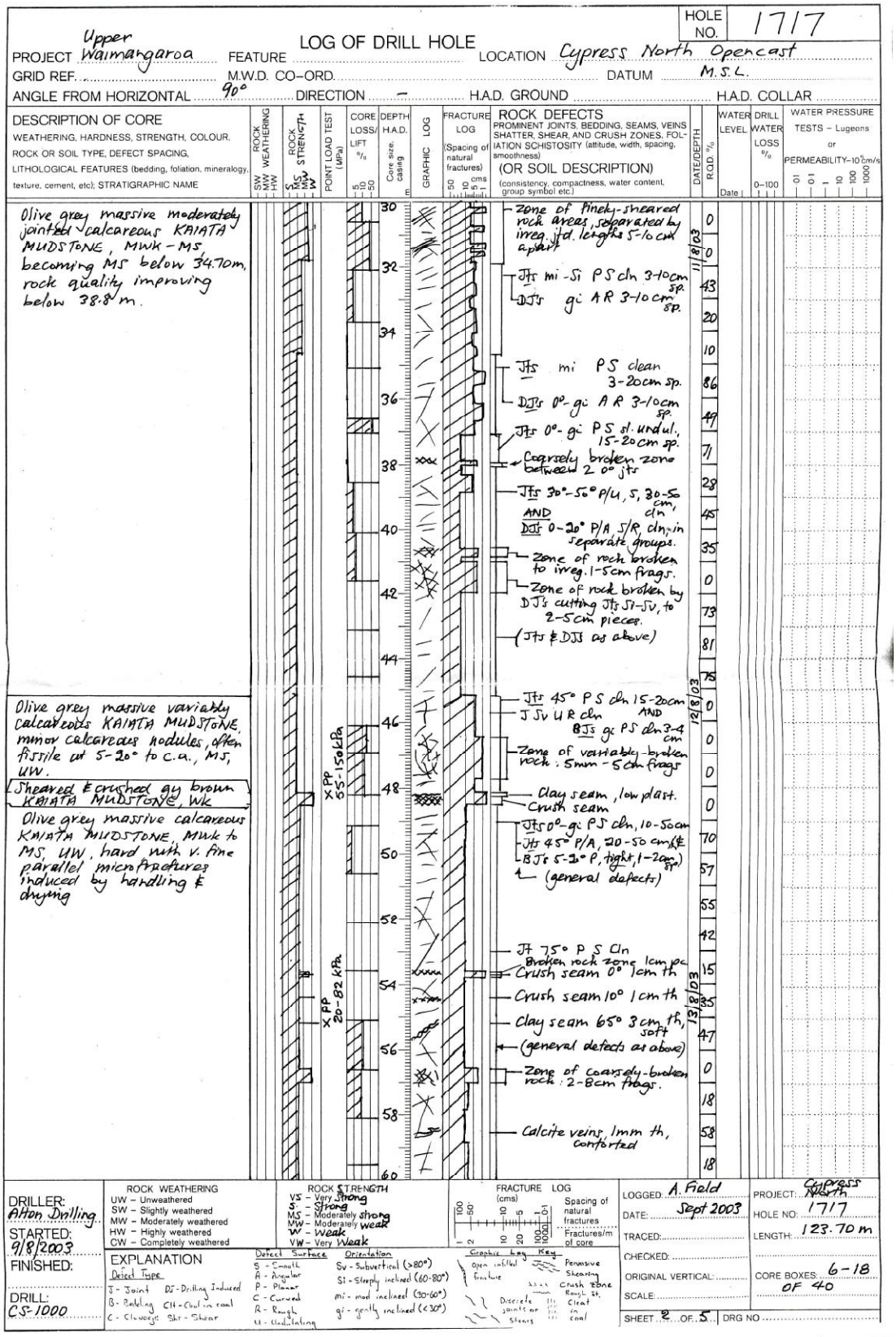
HOLE NO. 1717
LOG OF DRILL HOLE
PROJECT Upper Waimangaroa
FEATURE
LOCATION Cypress North Opencast
GRID REF.
M.W.D. CO-ORD.
DATUM M.S.L.
ANGLE FROM HORIZONTAL 90°
DIRECTION –
H.A.D. GROUND
H.A.D. COLLAR
DESCRIPTION OF CORE
WEATHERING, HARDNESS, STRENGTH, COLOUR, ROCK OR SOIL TYPE, DEFECT SPACING, LITHOLOGICAL FEATURES (bedding, foliation, mineralogy, texture, cement, etc); STRATIGRAPHIC NAME
ROCK WEATHERING
SW MW HW
ROCK STRENGTH
MS W
POINT LOAD TEST (MPa)
CORE LOSS/ LIFT %
DEPTH H.A.D.
Core size, casing
GRAPHIC LOG
FRACTURE LOG
(Spacing of natural fractures) cms
ROCK DEFECTS
PROMINENT JOINTS, BEDDING, SEAMS, VEINS SHATTER, SHEAR, AND CRUSH ZONES, FOLIATION SCHISTOSITY (attitude, width, spacing, smoothness)
(OR SOIL DESCRIPTION)
(consistency, compactness, water content, group symbol etc.)
DATE/DEPTH
RQD %
WATER LEVEL
DRILL WATER LOSS %
WATER PRESSURE TESTS – Lugeons or PERMEABILITY–10⁻⁵cm/s
Olive grey massive moderately jointed calcareous KAIATA MUDSTONE, MW-MS becoming MS below 34.70m, rock quality improving below 38.8m.
Olive grey massive variably calcareous KAIATA MUDSTONE, minor calcareous nodules, often fissile at 5-20° to c.a., MS, UW.
Sheared & crushed grey brown KAIATA MUDSTONE, Wk
Olive grey massive calcareous KAIATA MUDSTONE, MW to MS, UW, hard with v. fine parallel microfractures induced by handling & drying
Zone of finely-sheared rock areas, separated by irreg. jtd. lengths 5-10cm apart
Jts mi-Si PS cln 3-10cm sp.
DJs gi AR 3-10cm sp.
Jts mi PS clean 3-20cm sp.
DJs 0°-gi AR 3-10cm sp.
Jts 0°-gi PS sl. undul., 15-20cm sp.
Coarsely broken zone between 2 0° jts
Jts 30°-50° P/U, S, 30-50 cm, cln AND DJs 0-20° P/A S/R cln, in separate groups.
Zone of rock broken to irreg. 1-5cm frags.
Zone of rock broken by DJ's cutting Jts SI-SV, to 2-5cm pieces. (Jts & DJs as above)
Jts 45° PS cln 15-20cm AND JSv UR cln
BJs gi PS cln 3-4 cm sp.
Zone of variably-broken rock: 5mm-5cm frags
Clay seam, low plast.
Crush seam
Jts 50°-gi PS cln, 10-50cm
Jts 45° P/A, 20-50 cm sp.
BJs 5-20° P, tight, 1-2cm sp.
(general defects)
Jt 75° P S Cln
Broken rock zone 1cm pc
Crush seam 0° 1cm th
Crush seam 10° 1cm th
Clay seam 65° 3cm th, soft
(general defects as above)
Zone of coarsely-broken rock: 2-8cm frags.
Calcite veins, 1mm th, contorted
PP 55-150kPa
PP 20-82 kPa
11/8/03
12/8/03
13/8/03
DRILLER: Alton Drilling
STARTED: 9/8/2003
FINISHED:
DRILL: CS-1000
ROCK WEATHERING
UW – Unweathered
SW – Slightly weathered
MW – Moderately weathered
HW – Highly weathered
CW – Completely weathered
ROCK STRENGTH
VS – Very Strong
S – Strong
MS – Moderately strong
MW – Moderately weak
W – Weak
VW – Very Weak
FRACTURE LOG (cms)
Spacing of natural fractures
Fractures/m of core
EXPLANATION
Defect Type
J – Joint DJ – Drilling Induced
B – Bedding CH – Chalk in coal
C – Cleavage Shr – Shear
Defect Surface
S – Smooth
A – Angular
P – Planar
C – Curved
R – Rough
U – Undulating
Orientation
Sv – Subvertical (>80°)
St – Steeply inclined (60-80°)
mi – mod. inclined (30-60°)
gi – gently inclined (<30°)
Graphic Log Key
Open infilled fracture
Pervasive Shearing
Crush Zone
Bands sh. Clear in coal
Discrete joint or shears
LOGGED: A. Field
DATE: Sept 2003
TRACED:
CHECKED:
ORIGINAL VERTICAL:
SCALE:
SHEET 2 OF 5
DRG NO
PROJECT: Cypress North
HOLE NO: 1717
LENGTH: 123.70 m
CORE BOXES: 6-18 OF 40

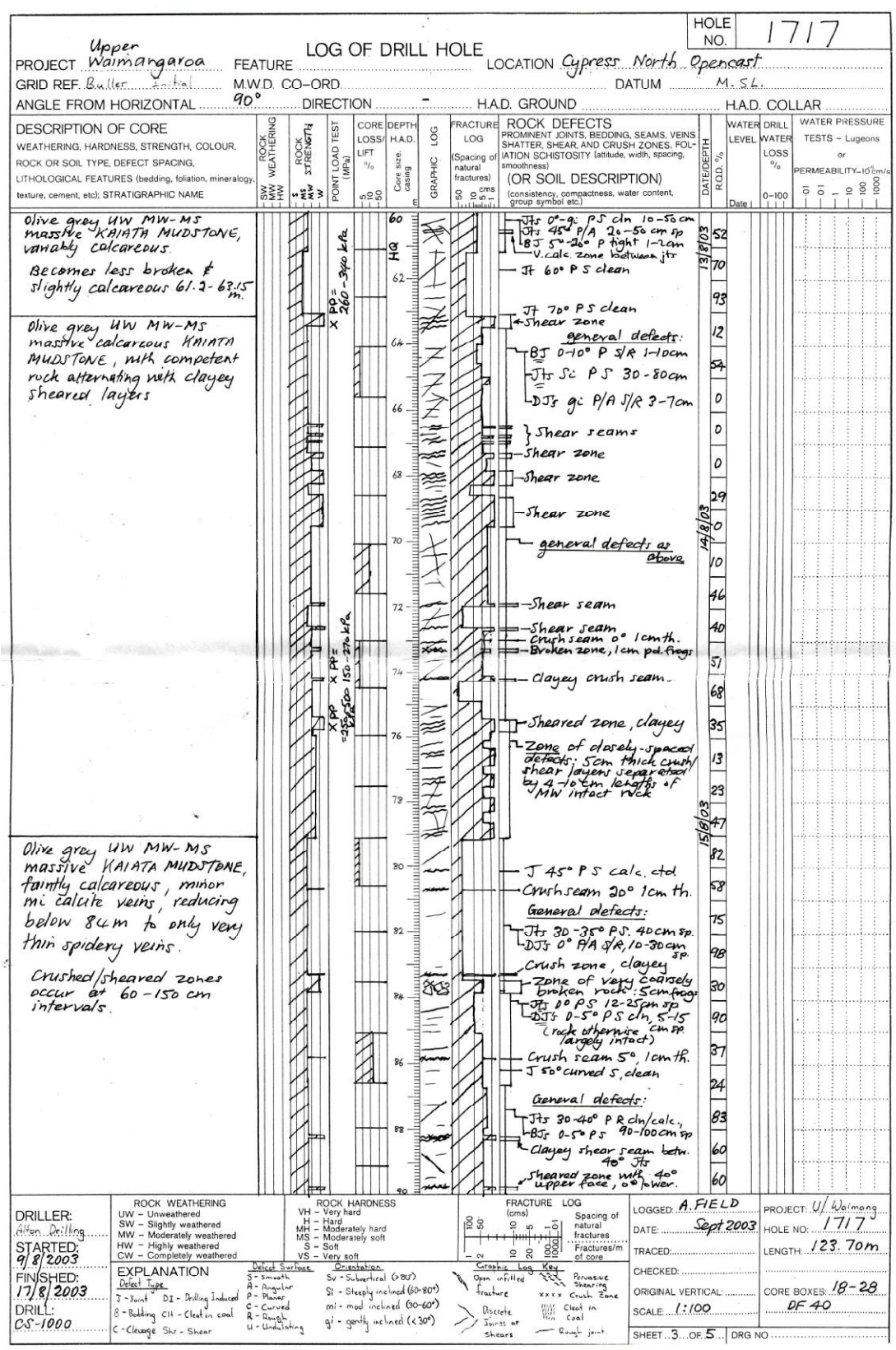
HOLE NO. 1717
LOG OF DRILL HOLE
PROJECT Upper Waimangaroa
FEATURE
LOCATION Cypress North Opencast
GRID REF. Buller 1:50 000
M.W.D. CO-ORD.
DATUM M.S.L.
ANGLE FROM HORIZONTAL 90°
DIRECTION -
H.A.D. GROUND
H.A.D. COLLAR
DESCRIPTION OF CORE
WEATHERING, HARDNESS, STRENGTH, COLOUR, ROCK OR SOIL TYPE, DEFECT SPACING, LITHOLOGICAL FEATURES (bedding, foliation, mineralogy, texture, cement, etc); STRATIGRAPHIC NAME
ROCK WEATHERING
ROCK STRENGTH
POINT LOAD TEST (MPa)
CORE LOSS/ LIFT %
DEPTH H.A.D.
GRAPHIC LOG
FRACTURE LOG (Spacing of natural fractures)
ROCK DEFECTS
PROMINENT JOINTS, BEDDING, SEAMS, VEINS SHATTER, SHEAR, AND CRUSH ZONES. FOLIATION SCHISTOSITY (attitude, width, spacing, smoothness)
(OR SOIL DESCRIPTION)
(consistency, compactness, water content, group symbol etc.)
DATE/DEPTH
R.Q.D. %
WATER LEVEL
DRILL WATER LOSS %
WATER PRESSURE TESTS – Lugeons or PERMEABILITY
Olive grey UW MW-MS massive KAIATA MUDSTONE, variably calcareous.
Becomes less broken & slightly calcareous 61.2 - 63.15 m.
Olive grey UW MW-MS massive calcareous KAIATA MUDSTONE, with competent rock alternating with clayey sheared layers
Olive grey UW MW-MS massive KAIATA MUDSTONE, faintly calcareous, minor mi calcite veins, reducing below 8cm to only very thin spidery veins.
Crushed/sheared zones occur at 60 - 150 cm intervals.
Jts 0°-9° PS cln 10-50 cm
Jts 45° P/A 20-50 cm sp
BJ 5°-20° P tight 1-2cm
V. calc. zone between jts
Jt 60° P S clean
Jt 70° P S clean
Shear zone
general defects:
BJ 0-10° P S/R 1-10cm
Jts Sc P S 30-80cm
DJs gc P/A S/R 3-7cm
Shear seams
Shear zone
Shear zone
Shear zone
general defects as above
Shear seam
Shear seam
Crush seam 0° 1cm th.
Broken zone, 1cm pd. frags
Clayey crush seam.
Sheared zone, clayey
Zone of closely-spaced defects; 5cm thick crush/shear layers separated by 4-10cm lengths of MW intact rock
J 45° P S calc. ctd.
Crush seam 20° 1cm th.
General defects:
Jts 30-35° P S. 40cm sp.
DJs 0° P/A S/R, 10-30cm sp.
Crush zone, clayey
Zone of very coarsely broken rock: 5cm frags
Jts 10° P S 12-25cm sp
DJs 0-5° P S cln, 5-15 (rock otherwise cm fr. largely intact)
Crush seam 5°, 1cm th.
J 50° curved S, clean
General defects:
Jts 30-40° P R cln/calc.,
BJs 0-5° P S 90-100cm sp
Clayey shear seam betw. 40° Jts
Sheared zone with 40° upper face, 0° lower.
X PP = 260 - 340 kPa
X PP = 150 - 270 kPa
X PP = 250 - 300 kPa
13/8/03
14/8/03
15/8/03
DRILLER: Alton Drilling
STARTED: 9/8/2003
FINISHED: 17/8/2003
DRILL: CS-1000
ROCK WEATHERING
UW – Unweathered
SW – Slightly weathered
MW – Moderately weathered
HW – Highly weathered
CW – Completely weathered
ROCK HARDNESS
VH – Very hard
H – Hard
MH – Moderately hard
MS – Moderately soft
S – Soft
VS – Very soft
FRACTURE LOG (cms)
Spacing of natural fractures
Fractures/m of core
EXPLANATION
Defect Type
J - Joint DI - Drilling Induced
B - Bedding Clt - Cleat in coal
C - Cleavage Shr - Shear
Defect Surface
S - Smooth
A - Angular
P - Planar
C - Curved
R - Rough
U - Undulating
Orientation
Sv - Subvertical (>80°)
St - Steeply inclined (60-80°)
mi - mod inclined (30-60°)
gi - gently inclined (<30°)
Graphic Log Key
Open infilled fracture
Pervasive shearing
xxxx Crush Zone
Discrete joints or shears
Cleat in coal
Rough joint.
LOGGED: A. FIELD
DATE: Sept 2003
TRACED:
CHECKED:
ORIGINAL VERTICAL:
SCALE: 1:100
PROJECT: U/ Waimang.
HOLE NO: 1717
LENGTH: 123.70m
CORE BOXES: 18-28
DF 40
SHEET 3 OF 5
DRG NO

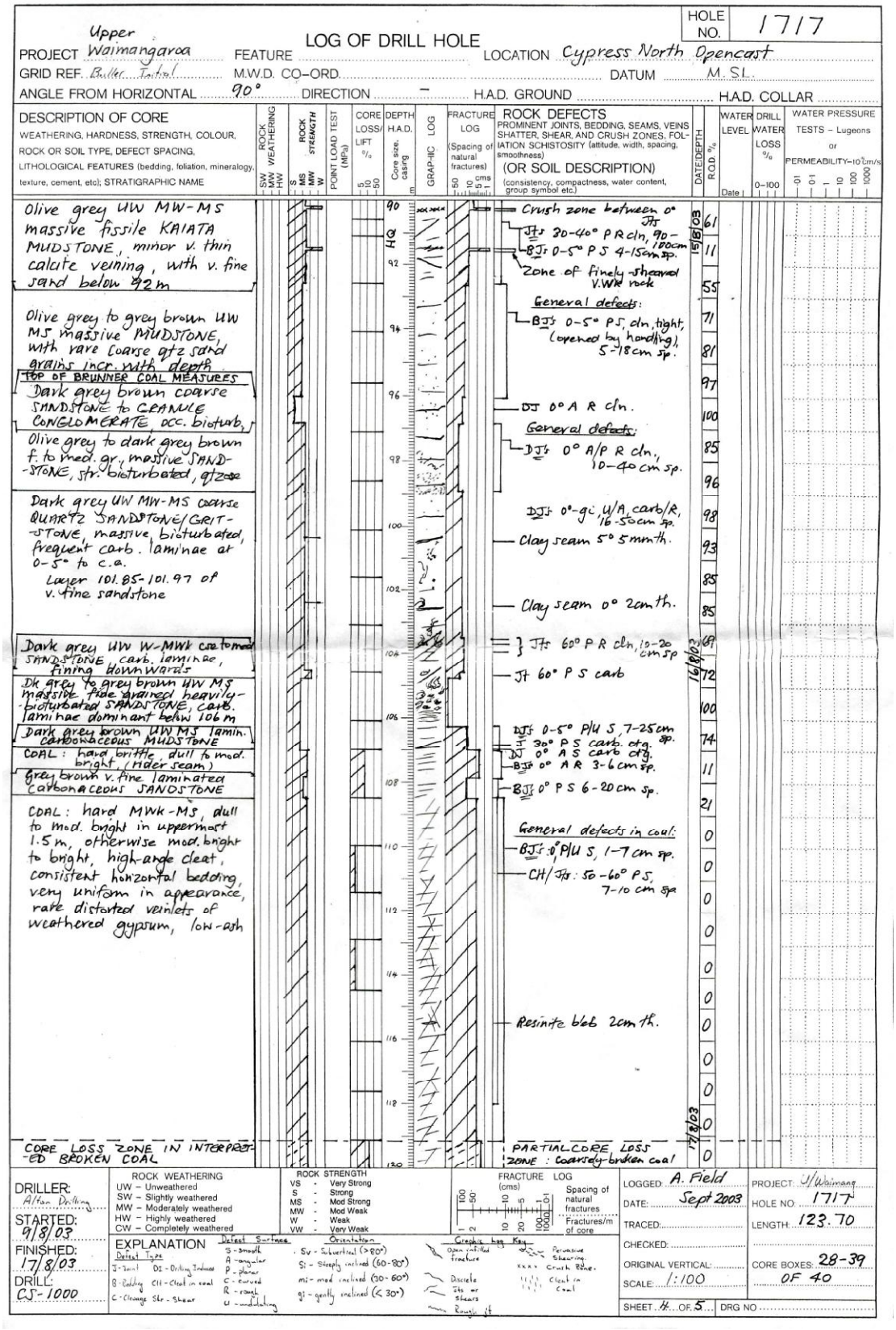
LOG OF DRILL HOLE
HOLE NO. 1717
PROJECT Upper Waimangaroa
FEATURE
LOCATION Cypress North Opencast
GRID REF. Buller Total
M.W.D. CO-ORD.
DATUM M.S.L.
ANGLE FROM HORIZONTAL 90°
DIRECTION –
H.A.D. GROUND
H.A.D. COLLAR
DESCRIPTION OF CORE
WEATHERING, HARDNESS, STRENGTH, COLOUR, ROCK OR SOIL TYPE, DEFECT SPACING, LITHOLOGICAL FEATURES (bedding, foliation, mineralogy, texture, cement, etc); STRATIGRAPHIC NAME
ROCK WEATHERING
SW MW HW
ROCK STRENGTH
S MS MW W
POINT LOAD TEST (MPa)
CORE LOSS/ LIFT %
DEPTH H.A.D.
Core size, casing
GRAPHIC LOG
FRACTURE LOG
(Spacing of natural fractures)
ROCK DEFECTS
PROMINENT JOINTS, BEDDING, SEAMS, VEINS SHATTER, SHEAR, AND CRUSH ZONES. FOLIATION SCHISTOSITY (attitude, width, spacing, smoothness)
(OR SOIL DESCRIPTION)
(consistency, compactness, water content, group symbol etc.)
DATE/DEPTH
R.Q.D. %
WATER LEVEL
DRILL WATER LOSS %
WATER PRESSURE TESTS – Lugeons or PERMEABILITY–10⁻²cm/s
Olive grey UW MW-MS massive fissile KAIATA MUDSTONE, minor v. thin calcite veining, with v. fine sand below 92 m
Olive grey to grey brown UW MS massive MUDSTONE, with rare coarse qtz sand grains incr. with depth
TOP OF BRUNNER COAL MEASURES
Dark grey brown coarse SANDSTONE to GRANULE CONGLOMERATE, occ. bioturb.
Olive grey to dark grey brown f. to med. gr., massive SANDSTONE, str. bioturbated, qtz-ss
Dark grey UW MW-MS coarse QUARTZ SANDSTONE/GRITSTONE, massive, bioturbated, frequent carb. laminae at 0-5° to c.a.
Layer 101.85-101.97 of v. fine sandstone
Dark grey UW W-MWk coarse SANDSTONE, carb. laminae, fining upwards
Dk grey to grey brown UW MS massive tide dominated heavily-bioturbated SANDSTONE, carb. laminae dominant below 106 m
Dark grey brown UW MS lamin. carbonaceous MUDSTONE
COAL: hard brittle, dull to mod. bright, (Older seam)
Grey brown v. fine laminated carbonaceous SANDSTONE
COAL: hard MWk-MS, dull to mod. bright in uppermost 1.5 m, otherwise mod. bright to bright, high-angle cleat, consistent horizontal bedding, very uniform in appearance, rate distorted veinlets of weathered gypsum, low-ash
CORE LOSS ZONE IN INTERPRETED BROKEN COAL
Crush zone between 0° Jts
Jts 30-40° P R cln, 90-100cm
BJs 0-5° P S 4-15cm sp.
Zone of finely sheared V.Wk rock
General defects:
BJs 0-5° P S, cln, tight, (opened by handling), 5-18cm sp.
DJ 0° A R cln.
General defects:
DJs 0° A/P R cln., 10-40 cm sp.
DJs 0°-gc U/A, carb/R, 16-50cm sp.
Clay seam 5° 5mm th.
Clay seam 0° 2cm th.
} Jts 60° P R cln, 10-20 cm sp
Jt 60° P S carb
DJs 0-5° P/U S, 7-25cm sp.
J 30° P S carb. ctg.
DJ 0° A S carb ctg.
BJs 0° A R 3-6cm sp.
BJs 0° P S 6-20 cm sp.
General defects in coal:
BJs 0° P/U S, 1-7 cm sp.
CH/Jts: 50-60° P S, 7-10 cm sp.
Resinite blob 2cm th.
PARTIAL CORE LOSS ZONE: coarsely-broken coal
16/8/03
17/8/03
DRILLER: Alfon Drilling
STARTED: 9/8/03
FINISHED: 17/8/03
DRILL: CS-1000
ROCK WEATHERING
UW – Unweathered
SW – Slightly weathered
MW – Moderately weathered
HW – Highly weathered
CW – Completely weathered
ROCK STRENGTH
VS – Very Strong
S – Strong
MS – Mod Strong
MW – Mod Weak
W – Weak
VW – Very Weak
FRACTURE LOG (cms)
Spacing of natural fractures
Fractures/m of core
EXPLANATION
Defect Type
J-Joint DI-Drilling Induced
B-Bedding CH-Clast in coal
C-Cleavage Shr-Shear
Defect Surface
S-smooth
A-angular
P-planar
C-curved
R-rough
U-undulating
Orientation
Sv-Subvertical (>80°)
Si-Steeply inclined (60-80°)
mi-mod inclined (30-60°)
gi-gently inclined (<30°)
Graphic Log Key
Open infilled fracture
Discrete Jts or Shears
Pervasive Shearing
Crush Zone
Clast in Coal
LOGGED: A. Field
DATE: Sept 2003
TRACED:
CHECKED:
ORIGINAL VERTICAL:
SCALE: 1:100
PROJECT: U/Waimang
HOLE NO: 1717
LENGTH: 123.70
CORE BOXES: 28-39 OF 40
SHEET 4 OF 5
DRG NO

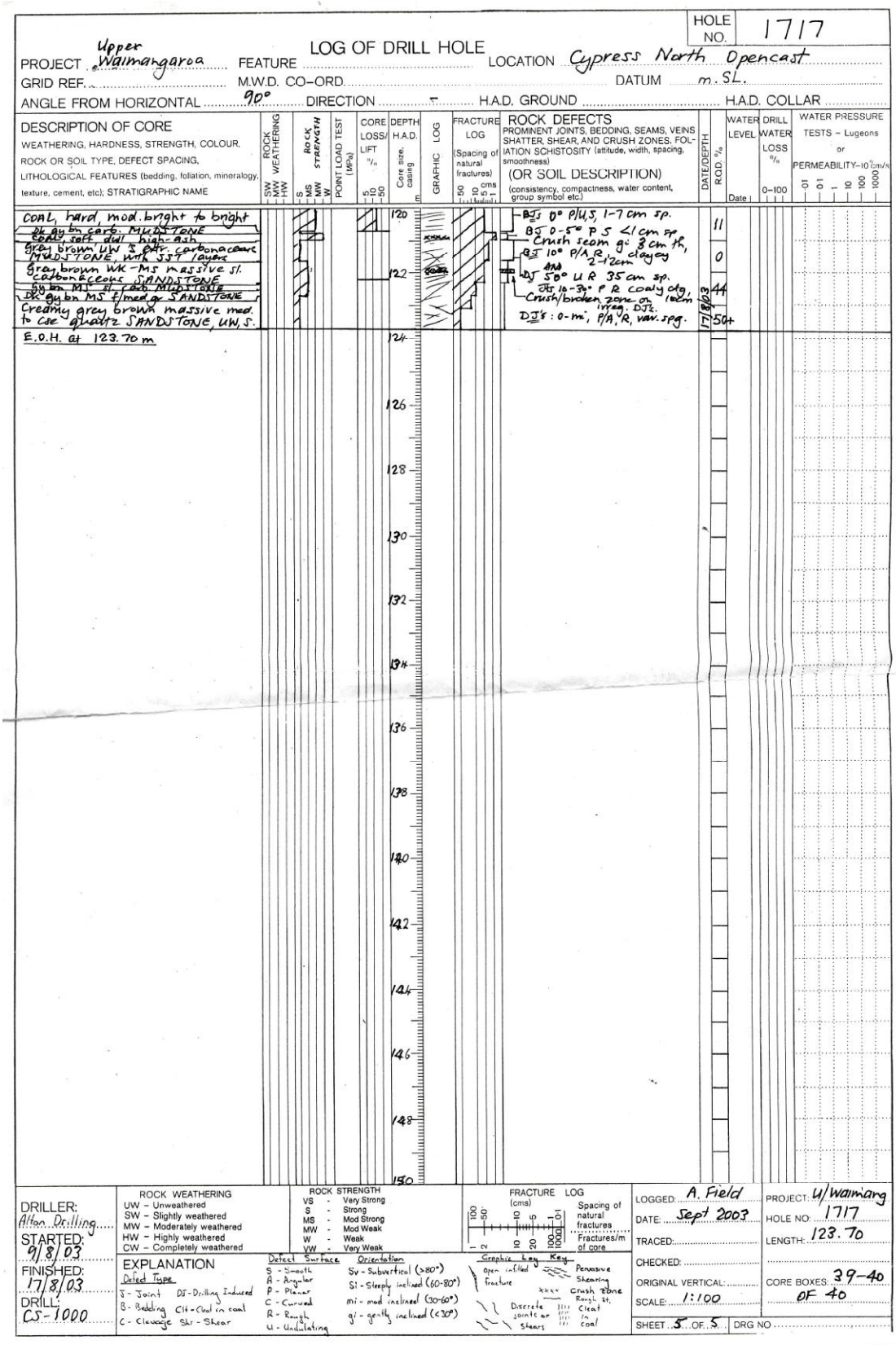

HOLE NO. 1717

LOG OF DRILL HOLE

PROJECT Upper Waimangaroa FEATURE LOCATION Cypress North Opencast

GRID REF. M.W.D. CO-ORD. DATUM m.SL.

ANGLE FROM HORIZONTAL 90° DIRECTION H.A.D. GROUND H.A.D. COLLAR

DESCRIPTION OF CORE
WEATHERING, HARDNESS, STRENGTH, COLOUR, ROCK OR SOIL TYPE, DEFECT SPACING, LITHOLOGICAL FEATURES (bedding, foliation, mineralogy, texture, cement, etc); STRATIGRAPHIC NAME

ROCK WEATHERING: SW – MW – HW
ROCK STRENGTH: S – MS – MW – W
POINT LOAD TEST (MPa): 5 – 10 – 50
CORE LOSS/LIFT %: 10 – 50
DEPTH H.A.D. m: Core size, casing
GRAPHIC LOG
FRACTURE LOG (Spacing of natural fractures): 50 – 10 – 0 cms

ROCK DEFECTS
PROMINENT JOINTS, BEDDING, SEAMS, VEINS SHATTER, SHEAR, AND CRUSH ZONES; FOLIATION SCHISTOSITY (attitude, width, spacing, smoothness)
(OR SOIL DESCRIPTION)
(consistency, compactness, water content, group symbol etc.)

DATE/DEPTH
R.Q.D. %
WATER LEVEL Date
DRILL WATER LOSS %/m: 0–100
WATER PRESSURE TESTS – Lugeons or PERMEABILITY–10⁻⁵ m/s: .01 – 0.1 – 1 – 10 – 100 – 1000

COAL, hard, mod. bright to bright
DK GY bn carb. MUDSTONE
COAL, soft, dull, high ash
Grey brown UW & ltly. carbonaceous MUDSTONE, with SST layers
Grey brown WK–MS massive sl. carbonaceous SANDSTONE
DK GY bn MS f/med gr SANDSTONE
DK GY bn MS f/med gr SANDSTONE
Creamy grey brown massive med. to coe. quartz SANDSTONE, UW, S.

E.O.H. @ 123.70 m

BJs 0° P/U,S, 1-7 cm sp.
BJ 0-5° P S <1 cm sp.
Crush seam gi 3 cm th, clayey
BJ 10° P/A,R, 2-12cm
DJ 50° U R 35 cm sp.
Jt. 10-30° P R coaly clg, Crush/broken zone on 10cm irreg. DJs.
DJs: 0-mi, P/A,R, var. spg.

17/8/03 11 0 44 150+

120 122 124 126 128 130 132 134 136 138 140 142 144 146 148 150

ROCK WEATHERING
UW – Unweathered
SW – Slightly weathered
MW – Moderately weathered
HW – Highly weathered
CW – Completely weathered

ROCK STRENGTH
VS – Very Strong
S – Strong
MS – Mod Strong
MW – Mod Weak
W – Weak
VW – Very Weak

FRACTURE LOG (cms): 100 – 50 – 10 – 1 – 0.1 — Spacing of natural fractures — Fractures/m of core

EXPLANATION
Defect Type
J - Joint DI - Drilling Induced
B - Bedding Clt - Clast in coal
C - Cleavage Shr - Shear

Defect Surface
S - Smooth
A - Angular
P - Planar
C - Curved
R - Rough
U - Undulating

Orientation
Sv - Subvertical (>80°)
St - Steeply inclined (60-80°)
mi - mod inclined (30-60°)
gi - gently inclined (<30°)

Graphic Log Key
open infilled fracture
Pervasive Shearing
Crush Zone
Rough, Sl. Clean
Discrete joints or shears
Fracture in coal

DRILLER: Alton Drilling
STARTED: 9/8/03
FINISHED: 17/8/03
DRILL: CS-1000

LOGGED: A. Field
DATE: Sept 2003
TRACED:
CHECKED:
ORIGINAL VERTICAL:
SCALE: 1:100

PROJECT: U/waimarg
HOLE NO: 1717
LENGTH: 123.70
CORE BOXES: 39-40 OF 40

SHEET 5 OF 5 DRG NO

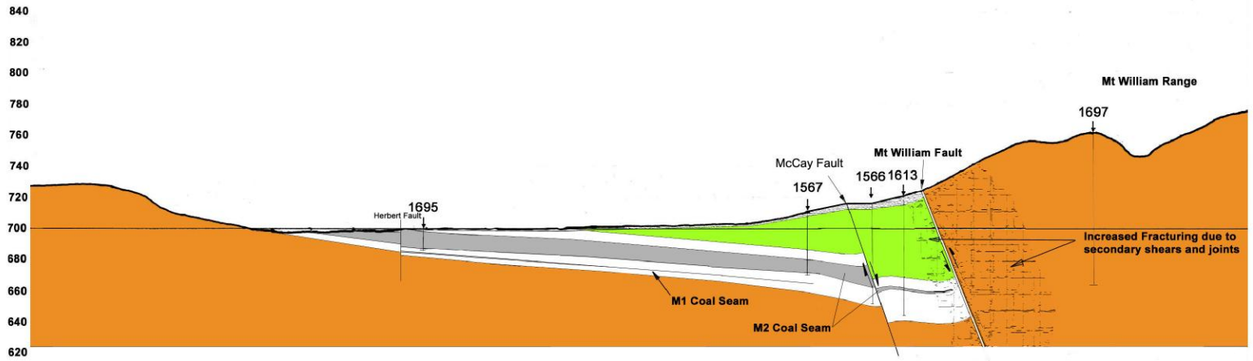

Cross Section A - A`
Upper Extent of the Cypress North Block

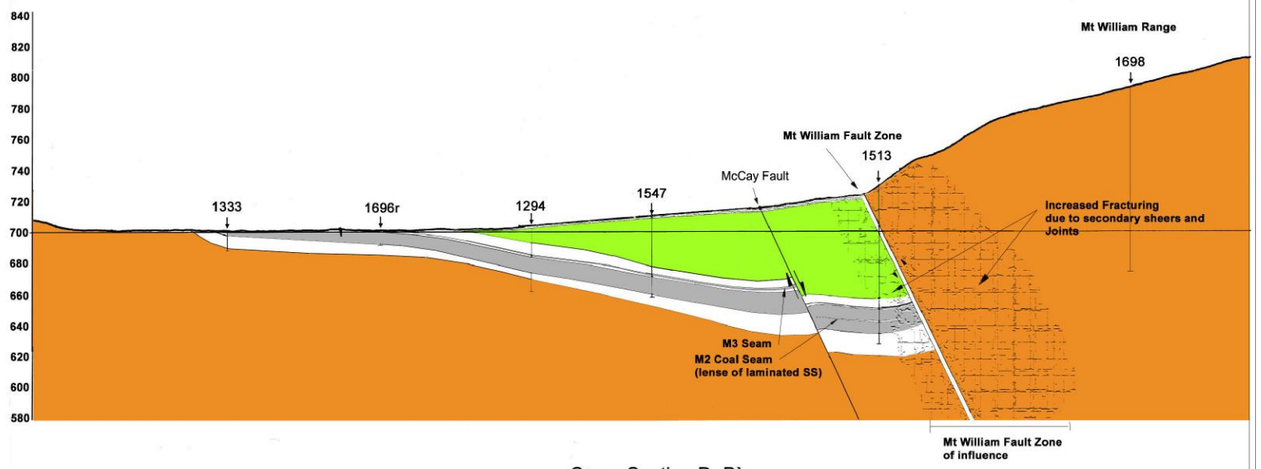

Cross Section B- B`
Middle to Upper Extent of Cypress North Block

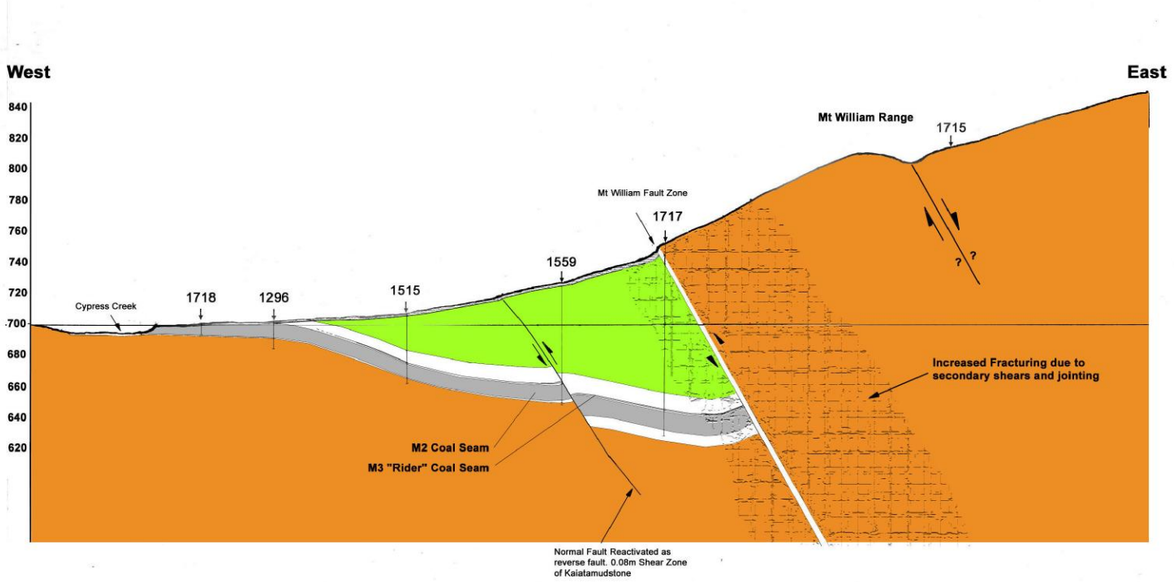

Cross Section C-C`
Southern Extent of Cypress North Basin

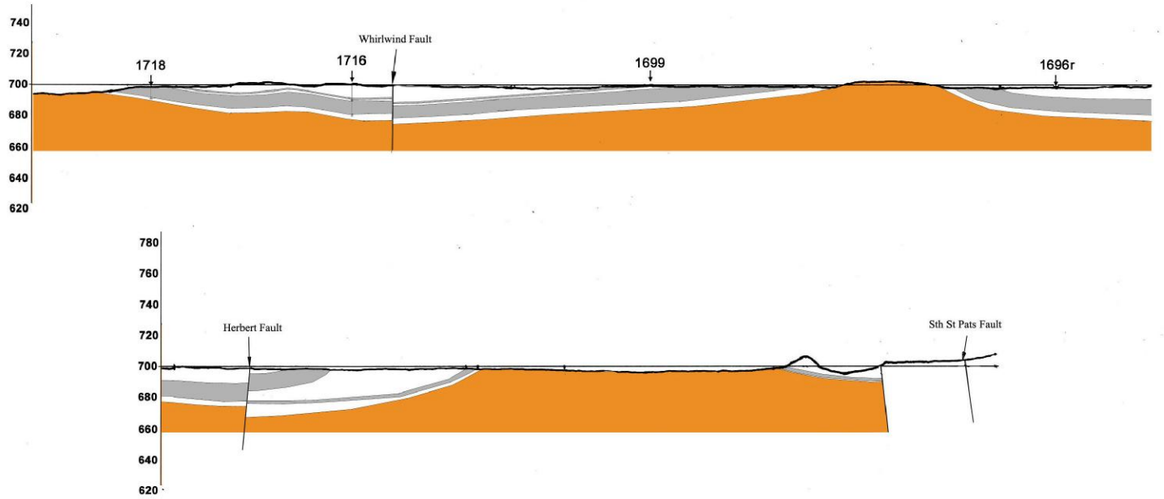

Cross Sections D-D" D"-D

Legend

- Kaiata Mudstone
- Coal Seam
- Brunner Coal Measures
- Basement lithologies - Berlins Porphyry Greenland Group Hornfels

1697 - Drillhole Location
- Fault
- Zone of Influence
- Coluvium Debris

Cross Sectional Views
Cypress North Basin
Upper Waimangaroa Sector

Figure 1.6

January 2004 Scale 1 : 1000

Compiled and Drafted by T.N.R. Pehi

325 250 325 500 325 750 326 000 326 250

712 250 712 000 711 750 711 500 711 250

Herbert Fault
St Pats Stream
Stn St Pats Fault
Whirlwind Fault
Cypress North Block Basin
McCrae Fault
Mt William Fault Zone
Cypress Creek

A A' B B' C C' D D'

U D

1201 1200 1615 1467 1291 1614 1695 1545 1465 1464 1333 1543 1567 1613 1697 1463 1696r 1563 1694 1514 1294 1565 1547 1462 1564 1699 1551 1513 1461 1387 1716 1554 1562 1698 1718 1296 1466 1515 1460 1717 1559 1292 1561 1715 1197

Geology

Description	Formation	Age
Massive, micaceous silty mudstone. Sandy interbeds near basal contact	Kaiata Formation	Mid - late Eocene
Quartzose sandstones and conglomerates, mudstones, shales, mudstones and bituminous coal seams (M1,M2,M3)	Brunner Coal Measures	Eocene (lower Tertiary)
Interfingered Basement Lithologies - biotite hornfels metasediments granite-granodiorite	Greenland Group Berlins Porphyry	Ordovician Cretaceous

Legend

Structural

- Lithological Contact
- Bedding, Dip and Strike (14)
- Coal Seam Exposure
- Joint (vertical)
- Joint, Dip and Dip Direction (75)
- Fault (minor <10m Throw)
- Fault (Major >10m Throw)
- Inferred Fault Trace

Geomophological

- Escarpment (minor)
- Escarpment (major)

Topographical

- 700 Contour (20m interval)
- Stream / Creek
- 741.8 Spot Heights

A Cross Sections (Figure 1.6 Map Pocket)

⊙1292 Borehole (geotechnical and core quality)

Full Internal Grid:
Buller Meridional Circuit : 711 000

Height Datum: Mean Sea Level

Map 1

Geological Map

Proposed Cypress Opencast Mine
Cypress North Block
Upper Waimangaroa Sector
Buller Coalfield

April 2004 Scale 1:2000

Compiled and Draughted : T.N.R.Pehi
University of Canterbury

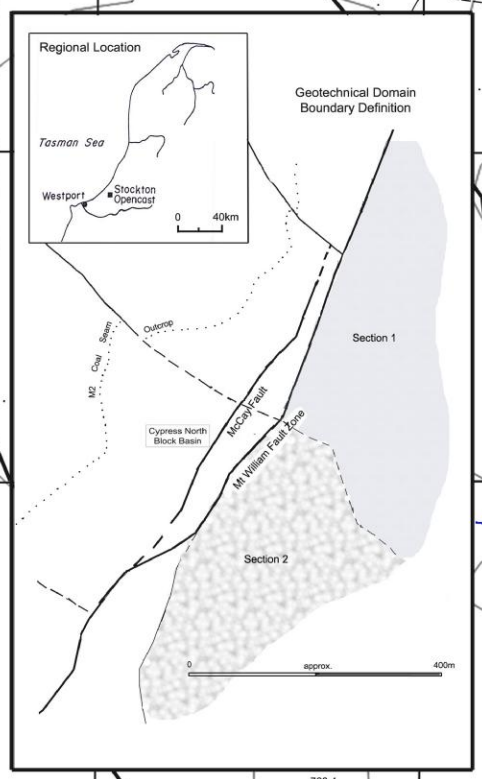

325 250 325 500 325 750 326 000 326 250

712 250 712 000 711 750 711 500 711 250 711 000

Herbert Fault
Sth St Pats Fault
St Pats Stream
McCay Fault
Mt William Fault Zone
Whirlwind Fault
Cypress Creek
Cypress North Block Basin

1201 1615 1200 1467 1614 1291 1695 1545 1465 1464 1613 1567 1333 1543 1566 1697 1463 1696r 1563 1694 1514 1294 1565 1547 1462 1564 1513 1699 1551 1461 1387 1716 1554 1562 1698 1718 1296 1466 1515 1460 1717 1559 1292 1561 1715 1197

Poles to Defects
Apparent Frequency Plots
From Scanline Survey Traverses

1 2 3 4 5 6 7 8 9 10 11 12

Legend

Structural

- Lithological Contact
- Bedding, Dip and Strike
- Coal Seam Exposure
- Joint (vertical)
- Joint, Dip and Dip Direction
- Dominant Fracture Pattern of Discontinuities
- Fault (minor <10m Throw)
- Fault (Major >10m Throw)
- Inferred Fault Trace
- Fault Zone Deformation (inferred initial zone of deformation)
- Scanline Locations
- 1292 Borehole (geotechnical and core quality)

Geomophological

- Escarpment (minor)
- Escarpment (major)

Topographical

- 700 Contour (20m interval)
- Stream / Creek
- 741.8 Spot Heights

Full Internal Grid:
Buller Meridional Circuit : 711 000

Height Datum: Mean Sea Level

Map 2

Engineering Geological Plan

Proposed Cypress Opencast Mine
Cypress North Block
Upper Waimangaroa Sector
Buller Coalfield

April 2004 Scale 1:2000

Compiled and Draughted : T.N.R.Pehi
University of Canterbury